Title
Genetic and biochemical analysis of the spliceosomal GTPase Snu114

Author
Brenner, Tamara J

Publication Date
2005

Peer reviewed|Thesis/dissertation

Genetic and Biochemical Analysis of the Spliceosomal GTPase Snu114

by

Tamara J. Brenner

DISSERTATION

Submitted in partial satisfaction of the requirements for the degree of

DOCTOR OF PHILOSOPHY

in

Biochemistry and Molecular Biology

in the

GRADUATE DIVISION

of the

UNIVERSITY OF CALIFORNIA, SAN FRANCISCO

Date University Librarian

Degree Conferred:.....

ACKNOWLEDGEMENTS

I have many people to thank for helping me scientifically through graduate school and for ensuring that I enjoyed myself while I was here.

Clearly, this thesis would not exist without Christine Guthrie. One of the reasons that I came to the lab was that she asks deep, probing, interesting questions—the kinds that make science worthwhile. I have learned much from Christine about communicating science in its many forms, and about interpreting data and creating models. I have appreciated the confidence that Christine places in the members of the lab; she really cares about our opinions and treats us as her peers. Thanks also to Christine for her generosity and her hospitality in hosting the lab at Priest Lake every year. For the past few years, John Abelson has been a second PI in the lab. I have enjoyed his enthusiasm for science and his extensive knowledge of splicing and biochemistry.

The Guthrie lab has been a wonderful home for me. People in the Guthrie lab are not just smart and interesting, but also remarkably friendly and warm. I have found common interests with many people: a love of the outdoors, an appreciation of good food, an interest in current events, and a fondness for soccer. I have always loved being in lab and talking with people, and I will greatly miss everybody.

The splicers of my early years—Cathy Collins, Amy Kistler, and Stephen Rader—provided me with a lot of advice as I was getting started. Maki Inada also helped me during the early years, especially with genetics. Fortunately for me, she stayed around long enough for many discussions about science and life, and she kept me laughing in the process.

Thanks to the lab backpackers—Maki, Jeff, Gregg, and Megan—for many trips, including adventures in Banff, Idaho, and the Sierras. I have learned much from Jeff Pleiss due to his knowledge of GTPases, his expertise in troubleshooting, and his general wisdom. For the first several years of grad school, Gregg Whitworth and I sat next to each other. I will remember him for the motto, "Go home and publish," our mantra for success in grad school. Gregg is full of creative ideas, many of which were well before their time. Megan Bergkessel is notable not just for her enthusiasm for science, but also for her ability to enjoy so many activities outside of lab, including printmaking, climbing, hiking, and traveling.

Tommaso Villa and I have sat next to each other since moving to Mission Bay, and as a result, we've spent a lot of time talking with each other. Tommaso has had the privilege of looking at almost every piece of data that I have produced for the past three years, and he's been remarkably generous with his time in helping me think about what my experiments mean and what I should do next. He's also one person I can count on to know the reference for something that I need to cite. Alan Kutach taught me a lot of techniques: how to pour polyacrylamide gels, how to do a western, how to clone. Since Alan works on Prp8, our projects have intersected and overlapped over the years, and we've spent a lot of time contemplating what our proteins are doing at the heart of the spliceosome.

I've also enjoyed interacting with the transporters, both scientifically and socially. Mette Lund's history as a splicer gives her insight into many issues beyond her current work in the transport field. Anne de Bruyn Kops has the courage to speak up when conversations between the splicers are unclear. Additionally, her stories about her son

Tristan have provided hours of entertainment. I appreciate Karen Kim's candor and willingness to disagree with the common viewpoint, and I've enjoyed her enthusiasm for knitting. Thanks to Pascal Preker for mentoring me when I was a rotation student.

In the past two years, several postdocs have joined the lab. Tracy Kress is notable for her cheerfulness and thoughtfulness. Quinn Mitrovich pays great attention to detail and ensures that everyone's models are rational. Gwen Wilmes and I share a love of fiction and for the past two years have both had boyfriends living in Boston. I am excited that Corina Maeder, who just joined the lab, will carry on the Snu114 torch, and I have confidence that she will find success along the way. Our newest graduate student, Alex Plocik, impressed me beginning with our discussions while he was preparing his bioreg proposal. I wish him luck in his goal of graduating from the Guthrie lab in record time.

I want to thank friends outside of lab—Meg Byrne and Avi Kar, Monica Schwartz, Miri VanHoven, and Mercedes Paredes—for keeping me entertained and happy throughout grad school. Thanks to Susanna Mlynarczyk-Evans for years of partnership in teaching; I have learned much from our collaborations. I am also grateful to the wonderful folks at SEP for getting me excited about science education.

My pre-grad school advisors, Liz Vallen (of Swarthmore) and Steve DiNardo (of the University of Pennsylvania) deserve much credit for getting me into grad school in the first place. They showed me that science is fun, and their confidence in my scientific abilities inspired me to continue.

I've always appreciated the support and confidence that my family places in me. My dad, who is a scientist, helped cultivate my interest in science when I was in high school by helping me find internships in laboratories at the University of Minnesota. He

has continued to give me advice about what it takes to succeed as a scientist. My mother taught me the value of education, and now I hope to help educate others. As we were growing up, my desire to emulate my big brother Jonathan always pushed me to work hard. Additionally, we have enjoyed many outdoor adventures together over the years.

And finally, thanks to Mike Springer for everything—for taking me hiking, for cooking good food, for making me laugh. Mike loves science, and has given me copious good ideas for experiments, talks, and papers. It's hard to imagine what grad school would have been like without his constant support.

Genetic and Biochemical Analysis of the Spliceosomal GTPase Snu114

Tamara J. Brenner

ABSTRACT

Proteins that use the energy of NTP hydrolysis are thought to mediate the large number of conformational changes that are necessary for spliceosome assembly, activation, and recycling. Snu114, an essential and conserved U5 snRNP protein, is homologous to EF-G, the GTPase that induces translocation of tRNA on the ribosome. This raises the intriguing possibility that Snu114 may similarly couple the hydrolysis of GTP with conformational changes in the spliceosome. Based on the EF-G homology, domains III-V of Snu114 are predicted to undergo a large rearrangement following GTP hydrolysis.

To investigate Snu114 activity in *Saccharomyces cerevisiae*, I generated conditionally lethal alleles of the protein. The allele *snu114-60*, which truncates the 70 carboxy-terminal amino acids, is synthetically lethal with mutations in factors required for spliceosome activation, including the core U5 snRNP protein *PRP8* and the ATPases *PRP28* and *BRR2*, which release U1 and U4 from the spliceosome. When spliceosomes are assembled *in vitro* at the non-permissive temperature, *snu114-60* blocks the release of U4 snRNA. We propose that activation of the spliceosome is dependent on GTP hydrolysis by Snu114, which leads to a rearrangement between the C-terminus of the protein and Prp8. This, in turn, would activate the ATPases Prp28 and Brr2.

A second class of *SNU114* mutations greatly reduces the formation of the U5 snRNP and U5•U4/U6 tri-snRNPs. In these mutants, the interaction between Snu114 and Prp8 is reduced, and the total levels of Prp8 are decreased. These mutations fall within

conserved motifs in the GTPase domain and in small clusters within each of domains III-V. We predict that these mutations either directly affect GTP binding/hydrolysis, or impact a rearrangement of the protein resulting from changes in nucleotide binding. We propose that Snu114 must bind GTP in order to interact productively with Prp8 and that this GTP-bound heterodimer is required in turn to assemble the U5 snRNP. This strategy would ensure that Snu114 is bound to GTP when it joins the spliceosome; subsequent GTP hydrolysis would then lead to spliceosome activation.

TABLE OF CONTENTS

LIST OF TABLES

LIST OF FIGURES

PROLOGUE

PROLOGUE

Pre-mRNA transcripts must be processed to achieve competency for nuclear export and translation. One predominant form of processing is splicing, where non-coding sequences, or introns, must be excised in order to produce a functional protein. In humans, almost all transcripts contain introns. Although the number of intron-containing genes in the budding yeast *Saccharomyces cerevisiae* is much smaller, a majority of these genes encode proteins that are either abundant or of regulatory importance (Ares et al. 1999). Because the process by which introns are removed is well conserved between yeast and humans, yeast provide an excellent model system for studying the mechanism of pre-mRNA splicing.

Three sequence elements are required for the removal of an intron: the 5' and 3' intron/exon junctions and the branchpoint, a consensus sequence within the intron located just upstream of the 3' splice site (Figure 1A). Pre-mRNA splicing occurs via two phosphoryl trans-esterification reactions (Figure 1B) (Moore et al. 1993). In the first chemical reaction, the 2' hydroxyl of a conserved adenosine in the branchpoint sequence of the intron attacks the 5' splice site phosphate, creating a branched lariat intermediate and excising the upstream exon. In the second reaction, the 3' hydroxyl of the cleaved upstream exon attacks the phosphate at the 3' splice site, ligating the exons and releasing the lariat intron. These two reactions are catalyzed by the spliceosome, a macromolecular complex that consists of five small nuclear RNAs (snRNAs) and over 100 proteins (Burge et al. 1998; Jurica and Moore 2003). The snRNAs are packaged with proteins into snRNPs (small nuclear ribonucleoprotein particles). Some of the snRNPs interact with each other in the absence of transcript. The U4 and U6 snRNAs are

extensively base paired within the U4/U6 di-snRNP (Figure 1C), and the U5 snRNP interacts with this complex to form the U4/U6•U5 tri-snRNP. The snRNPs assemble dynamically onto each intron.

The snRNAs recognize conserved sequences that define the exon/intron boundaries and the branchpoint sequence (Nilsen 1998). At each intron, U1 snRNA base pairs with the 5' splice site, and U2 snRNA base pairs with the branchpoint sequence (Figure 1D) (Staley and Guthrie 1998; Brow 2002). Following addition of the tri-snRNP to this complex, extensive reorganization of the spliceosome occurs. The U1/5' splice site and the U4/U6 duplexes are unwound, releasing U1 and U4 snRNPs from tight association with the spliceosome (Figure 1E). This allows formation of the catalytic core, in which U2 and U6 snRNAs interact extensively with each other, U6 base pairs with the 5' splice site, and U2 remains bound to the branch site sequence (Figure 1F) (Madhani and Guthrie 1992; Field and Friesen 1996). This arrangement juxtaposes the attacking adenosine of the branchpoint sequence with the 5' splice site, facilitating the first chemical reaction.

After the first chemical step the 5' and 3' exons are no longer physically attached through their phosphate backbone, yet these molecules must be held together to allow for the second chemical step. The conserved loop of U5 snRNA, a core spliceosomal component, can be crosslinked to the 5' exon throughout splicing and to the 3' exon following the first step (Wyatt et al. 1992; Sontheimer and Steitz 1993; Newman et al. 1995). This suggests that U5 tethers the 5' exon to the spliceosome after it has been cleaved from the intron (Newman 1997). Additionally, alteration of the sequence of the conserved loop of U5 snRNA can affect 5' splice site usage (Newman and Norman 1992;

Cortes et al. 1993). The U5 snRNA can be crosslinked to Prp8, which is the largest protein component of the spliceosome (Dix et al. 1998; Urlaub et al. 2000). Prp8 interacts biochemically and genetically with all sites of chemistry on the pre-mRNA transcript, suggesting that it cooperates with U5 at the catalytic center of the spliceosome (Grainger and Beggs 2005). Prp8 has been hypothesized to stabilize the RNA structure of the spliceosome and to help retain the 5' exon between the chemical reactions (Collins and Guthrie 2000). Following the two chemical steps of splicing, the mRNA is released and the spliceosome is disassembled (Staley and Guthrie 1998).

Many critical spliceosomal rearrangements are energy dependent. U5 snRNP contains two ATPases, Prp28 and Brr2, which are thought to cause the release of U1 and U4, respectively, from the spliceosome (Laggerbauer et al. 1998; Raghunathan and Guthrie 1998a; Staley and Guthrie 1999; Stevens et al. 2001). Prp28 and Brr2 are members of the DExH/D-box family of RNA-dependent helicases. In yeast, six additional members of this family interact transiently with the spliceosome, and each is required for a distinct stage of splicing (Staley and Guthrie 1998). DExH/D-box helicases are found in a myriad of cellular processes involving RNA metabolism (Tanner and Linder 2001; Rocak and Linder 2004). These proteins are believed to use the energy of ATP hydrolysis to disrupt RNA-RNA and RNA-protein interactions, destabilizing transient interactions and promoting the formation of productive complexes (Rocak and Linder 2004).

In 1997, the first—and only—spliceosomal GTPase was identified (Fabrizio et al. 1997). Snu114 (called U5-116 kDa in humans) is an essential protein in yeast. A component of U5 snRNP, Snu114 binds tightly to Prp8 (Achsel et al. 1998), suggesting

that it, too, may function at the core of the spliceosome. Snu114 is intriguing not only because it is the sole GTPase in the spliceosome, but because it is homologous over almost its entire sequence to the ribosomal translocase elongation factor G (EF-G) (Fabrizio et al. 1997). This suggests a potential connection between some of the RNA rearrangements that occur on the spliceosome and the ribosome.

Mechanism and regulation of GTPases

GTPases are involved in numerous cellular processes, including cell proliferation and development, vesicular and nucleocytoplasmic trafficking, sensory perception, and translation (Bourne et al. 1990; Scheffzek et al. 1998). GTPases can be categorized as belonging to one of three major families: the small monomeric GTPases, which include Ras, Rho, and Ran; the heterotrimeric GTPases; and the translational GTPases (Bourne et al. 1990; Bourne et al. 1991; Sprang 1997). A GTPase can be found at almost every stage of translation (Rodnina et al. 2000; Sprinzl et al. 2000; Kapp and Lorsch 2004): initiation (IF2 in prokaryotes/eIF2 and eIF5B in eukaryotes), delivery of tRNA to the ribosome (EF-Tu/EF1A), translocation of peptidyl-tRNA from the A-site to the P-site (EF-G/EF2), and release of the completed peptide (RF3/eRF3).

Most GTPases are considered to function as switches (Bourne et al. 1990). In the GTP-bound state they are able to bind to downstream effectors, while they are unable to interact with effector molecules when bound to GDP. For example, the small GTPase Ras interacts with and activates the Raf protein kinase—and thus the MAP kinase signaling cascade—only when bound to GTP (Takai et al. 2001). GDP-bound Ras cannot interact with Raf. In heterotrimeric G proteins, an extracellular signal is transmitted via a transmembrane protein to the α subunit (Bourne et al. 1991; Sprang

1997). This causes the α subunit to exchange GDP for GTP and consequently to dissociate from the βγ heterodimer. The liberated α subunit can bind to downstream effectors such as adenylate cyclase. Again, signaling can persist only as long as the α subunit remains in the GTP-bound form.

The nucleotide binding domain is structurally conserved among all GTPases (Bourne et al. 1991; Sprang 1997; Vetter and Wittinghofer 2001). Within this domain, five motifs (G1-G5) interact with the nucleotide (Table 1 and Figure 2). The guanosine ring is bound by residues in the G4 and G5 motifs, which impose a strong specificity for this nucleotide. Residues in the G1 motif (GKT) bind to the α and β phosphates of the nucleotide, while residues in the G2 and G3 motifs interact primarily with the γ phosphate and the Mg^{2+} cofactor. The conformations of the G2 and G3 motifs, which are also known as Switch I and Switch II, are dramatically altered upon GTP hydrolysis and loss of the γ phosphate (Figure 3) (Sprang 1997; Vetter and Wittinghofer 2001). The change underlies the basis of how GTPases work. Effector molecules bind specifically to the G2 and G3 motifs in the GTP-conformation and therefore can only interact with a G protein that is bound to GTP.

The rates of both GTP hydrolysis and nucleotide exchange are intrinsically slow in all GTPases (Bourne et al. 1991). Thus, both of these critical activities are dependent on extrinsic factors: GTPase activating proteins (or GAPs) and guanine exchange factors (GEFs; also called guanine nucleotide releasing proteins). GAPs and GEFs can accelerate the rates of GTP hydrolysis and nucleotide exchange by up to five orders of magnitude (Sprang 1997; Vetter and Wittinghofer 2001).

GTP hydrolysis occurs via the nucleophilic attack of a water molecule on the γ phosphate (Sprinzl et al. 2000). In small GTPases and heterotrimeric GTPases, the transition state is stabilized by a conserved glutamine within the G3 motif (Scheffzek et al. 1998). In the ribosomal GTPases, this glutamine is replaced by histidine, which also appears to be essential for catalysis (Sprinzl et al. 2000). In all cases that are understood, catalysis additionally depends on an arginine residue, which both neutralizes the negative charge of the transition state and stabilizes the G3 glutamine (Bourne 1995; Scheffzek et al. 1998). For small GTPases, this arginine is provided by the GAP. Thus, two proteins create the active site of the enzyme (Scheffzek et al. 1998). The catalytic arginine of heterotrimeric GTPases is found in *cis* within the α subunit (Scheffzek et al. 1998). Correspondingly, heterotrimeric GTPases possess a faster intrinsic rate of GTP hydrolysis than the other families of GTPases (seconds, as opposed to minutes) (Bourne et al. 1990; Bourne 1995). Nonetheless, GAPs can accelerate the rate of hydrolysis by stabilizing the transition state (Scheffzek et al. 1998; Vetter and Wittinghofer 2001). The GAP for most of the ribosomal GTPases is the ribosome itself (Rodnina et al. 2000; Mohr et al. 2002). While particular domains of the ribosome, including the L7/L12 dimer and the sarcin-ricin loop, have been implicated, the exact mechanism of this activation is unclear (Mohr et al. 2002; Andersen et al. 2003; Savelsbergh et al. 2003; Savelsbergh et al. 2005).

Because the concentration of cellular GTP is approximately ten-fold higher than GDP, release of GDP by GEFs leads to GTP binding (Bourne et al. 1991). Although the mechanism of different GEFs varies, in general they function by destabilizing residues that bind to the nucleotide and to Mg^{2+} (Sprang 1997; Sprang and Coleman 1998; Vetter

and Wittinghofer 2001). While EF-Tu has a well-characterized GEF, EF-Ts, a GEF for EF-G has not been identified. It has commonly been thought that the affinity of EF-G for GDP is low enough to allow spontaneous release, thus obviating the need for a GEF (Kaziro 1978; Bourne et al. 1991).

Ribosomal GTPases

Unlike the small and heterotrimeric GTPases, the ribosomal GTPases contain multiple structural domains. Interdomain movements can be responsible for effecting the difference between GTP and GDP binding. In a well-characterized example, GTP-bound EF-Tu delivers aminoacylated tRNA to the ribosome (Rodnina et al. 2000). Cognate codon-anticodon interactions facilitate a conformational rearrangement of the ribosome that induces GTP hydrolysis (Pape et al. 1998). GTP hydrolysis causes a rearrangement of the G2 and G3 motifs, leading to a large movement of domains II and III of the protein and consequently disrupting the tRNA binding site (see Figure 3) (Berchtold et al. 1993; Kjeldgaard et al. 1993). GDP-bound EF-Tu then dissociates from the ribosome, leaving tRNA behind.

Detailed kinetic studies showed that GTP hydrolysis by EF-G precedes translocation of tRNA and mRNA on the ribosome, suggesting that a better analogy for its function is that of a motor, rather than a switch (Rodnina et al. 1997). EF-G contains five major domains (AEvarsson et al. 1994; Czworkowski et al. 1994), and structural studies have shown that domains III-V can rotate with respect to domains I (G domain) and II (Jorgensen et al. 2003). It is believed that GTP hydrolysis and the resulting movement of the G2 and G3 motifs is converted into a movement of domains III-V. Cryo-EM structures of EF-G before and after translocation showed that the tip of domain

IV moves by 40Å (Figure 4) (Stark et al. 2000). Either deleting domain IV or preventing the movement of domain IV by tethering domains I and V together abolishes translocation without affecting GTP hydrolysis (Rodnina et al. 1997; Peske et al. 2000). Thus, the conformational rearrangement of the protein is essential for its function.

Remarkably, the crystal structure of EF-G strongly resembles that of EF-Tu complexed with tRNA (Figure 5): domains I (G domain) and II are homologous to EF-Tu, and domains III, IV, and V structurally mimic the shape of tRNA acceptor stem, anticodon loop, and T stem, respectively (AEvarsson et al. 1994; Czworkowski et al. 1994; Nissen et al. 1995). Chemical probing and crystallographic studies of EF-G bound to ribosomes stalled at various stages of translocation have shown that EF-G binds to the ribosome in a similar location as EF-Tu-tRNA and undergoes a large conformational change upon GTP hydrolysis and translocation, resulting in domain IV reaching into the decoding center (Wilson and Noller 1998; Stark et al. 2000).

Snu114: The unknown GTPase

The homology between EF-G and Snu114 suggested several hypotheses. First, GTP hydrolysis by Snu114 could lead to a conformational rearrangement of the spliceosome, likely as a result of interdomain movements of the protein. Second, the nucleotide status of Snu114 is probably tightly regulated. Third, the C-terminal domains of Snu114 could structurally mimic an RNA component of the spliceosome. An attractive candidate was the conserved stem-loop of U5 snRNA (Staley and Guthrie 1998).

When I joined the lab, we knew very little about Snu114. We knew that it interacted tightly with Prp8 and that it could be crosslinked to U5 snRNA (Achsel et al.

1998; Dix et al. 1998). Fabrizio *et al.* (1997) had found that mutations in the GTPase domain eliminated viability and that genetic depletion of the protein inhibited splicing. Several studies had implicated Snu114 in the second step of splicing. Adding antibodies against U5-116 kDa to HeLa extract inhibited the second step (Fabrizio et al. 1997). U5-116 could be crosslinked to an artificial hairpin in pre-mRNA at multiple locations downstream of the branch point sequence; this crosslink was dependent on the completion of the first chemical step (Liu et al. 1997). Liu *et al.* (1997) therefore proposed that Snu114 was involved in scanning the intron in search of the 3' splice site. Another group (Chiara et al. 1997) similarly found that U5-116 crosslinked to pre-mRNA between the branch point sequence and 3'ss, although this crosslink was detected in both pre-spliceosomal and spliceosomal complexes. Staley and Guthrie (1998) had also proposed a function for Snu114 between the first and second steps of splicing. Based on the hypothesis that the C-terminal domains of Snu114 were a mimic of U5 snRNA, they had speculated that the protein could reposition U5 snRNA at the catalytic center of the spliceosome and thus align the two exons for the second chemical step. However, strong evidence that Snu114 functioned at the second step—and not at other stages of splicing—was lacking.

Fundamentally, I was intrigued by the idea that the spliceosome had co-opted a ribosomal GTPase. What processes during splicing are similar enough to translation that this protein could be useful? What conformational changes in the spliceosome could Snu114 be modulating? What is the nucleotide status of Snu114 at different stages of splicing, and what is the impact of changing the nucleotide status? More simply, at what stages of splicing does Snu114 function?

I took a genetic approach to identifying the role of Snu114 during splicing, which I describe in Chapter 1. I wanted to determine how mutations in the protein affect splicing, so I first generated conditionally lethal alleles that were either temperature-sensitive or cold-sensitive. Random mutagenesis of *SNU114* also allowed me to identify regions of the protein that are important for its function. In particular, I identified a large number of mutations within conserved motifs in the GTPase domain and in small clusters within each of domains III-V. Additionally, the allele *snu114-60*, which truncates the C-terminal domain (IVb), causes conditional growth defects. All of the mutations inhibited splicing prior to the first step. I then analyzed genetic interactions between *snu114* alleles and alleles of other splicing factors in order to better determine when the protein is required during splicing. Most strikingly, *snu114-60* is synthetically lethal with mutations in factors involved in spliceosome activation, including *PRP28*, *BRR2*, and *PRP8*, implicating the C-terminus in Snu114 in this transition. Additionally, I found genetic interactions between *snu114* alleles and mutations in factors involved in snRNP biogenesis, including *BRR1* and *SAD1*.

In Chapter 2, I biochemically characterize some of the *snu114* alleles that I had generated in Chapter 1. As a follow-up to the genetic interactions that had suggested roles for Snu114 during snRNP biogenesis and spliceosome activation, *in vitro* analyses confirmed that Snu114 is involved with these processes. The allele *snu114-60* blocks release of U4 from the spliceosome, while mutations in the GTPase domain inhibit interaction with Prp8 and formation of U5 snRNP. Together, the data suggest that the nucleotide-binding status of Snu114 regulates several early stages of splicing. We propose that Snu114 must be bound to GTP in order to bind Prp8 and form U5 snRNP.

After tri-snRNP joins the spliceosome, GTP hydrolysis is triggered, leading to spliceosome activation.

Table 1. Sequences in the G1-G4 motifs of a few members of each of the three main classes of GTPases.

	Protein	G1 P-loop	G2 Switch I	G3 Switch II	G4 Nucleoside
Translation Factors					
Ec	IF2	**GHVDHGKTS**	GGTITQH	**FLDTPGHA**	**AVNKID**
Ec	EF-Tu	**GHVDHGKTT**	RGITINT	**HVDGPGHA**	**FLNKCD**
Sc	EF2	**AHVDHGKST**	RGITIKS	**LIDSPGHV**	**VINKVD**
Sc	SNU114	**GPLHSGKTS**	RGLSIKL	**FLDAPGHV**	**VINKLD**
Small GTPases					
Hs	RAS	**GAGGVGKSA**	YDPTIEDSY	**ILDTAGQE**	**VGNKCD**
Sc	RHO1	**GDGACGKTC**	YVPTVFENY	**LWDTAGQE**	**VGCKVD**
Hs	RAB4	**GNAGTGKSC**	SNHTIGVEF	**IWDTAGQE**	**CGNKKD**
Sc	CDC42	**GDGAVGKTC**	YVPTVFDNY	**LFDTAGQE**	**VGTQID**
Sc	ARF1	**GLGGAGKTT**	TIPTIGFNV	**VWDVGGQD**	**FANKQD**
Heterotrimeric G proteins (α subunit)					
Sc	GPA1	**GAGESGKSTV**	RIKTTGITE	**VLDAGGQR**	**FLNKID**
Sc	GPA2	**GAGESGKSTV**	RQMTSGIFD	**IYDVGGQR**	**FLNKID**
Hs?	G_s	**GAGESGKST**	RVLTSGIFE	**MFDVGGQR**	**FLNKQD**

Conserved residues are shown in bold. Amino acids in the G2 motif are not conserved between different subclasses of GTPases. The G5 motif is not well conserved and therefore is not included here. Ec = *E. coli*; Sc = *S. cerevisiae*; Hs = *H. Sapiens*. Sequences were compiled from SGD, Bourne *et al* (1991), and Sprang (1997).

Figure 1. Overview of pre-mRNA splicing. **A:** The intronic consensus sequences of yeast: the 5' splice site, the branchpoint sequence, and the 3' splice site. Absolutely conserved residues are in larger font. **B:** Splicing occurs via two phosphoryl transfer reactions. **C:** The U4 and U6 snRNAs are extensively base-paired within the U4/U6 di-snRNP. **D:** U1 snRNA base pairs with the 5' splice site and U2 snRNA base pairs with the branchpoint sequence of the intron, forming the pre-spliceosome. **E:** Stages of spliceosome assembly. **F:** Model of the catalytic core of the spliceosome prior to the first chemical step. U2 snRNA (blue) and U6 snRNA (red) form extensive base pairs with each other, and also interact with the branchpoint sequence and 5' splice site of the intron (black). The conserved loop of the U5 snRNA (purple) interacts with the 5' exon, tethering it to the spliceosome. Reproduced and adapted from Collins and Guthrie (2000)

A

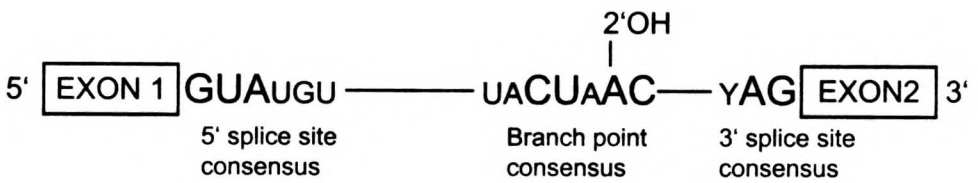
2'OH
5' EXON 1 GUAUGU UACUAAC YAG EXON2 3'
5' splice site consensus
Branch point consensus
3' splice site consensus

B

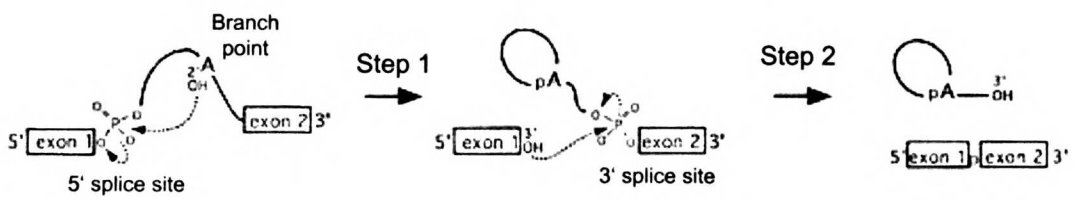
Branch point
Step 1
Step 2
5' exon 1
exon 2 3'
5' splice site
3' splice site

C

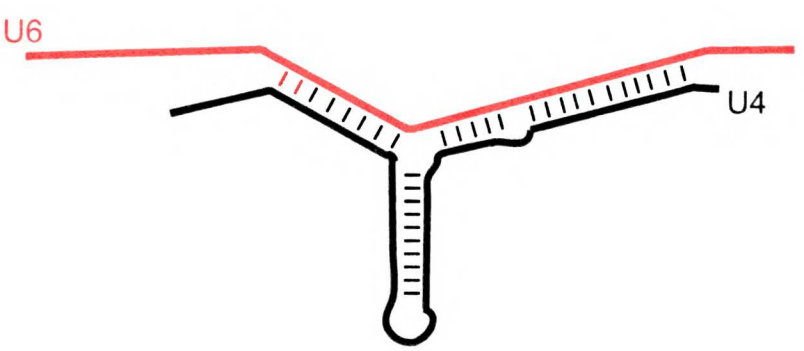
U6
U4

D

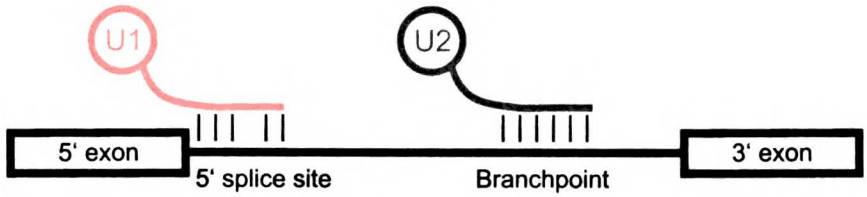
U1
U2
5' exon
3' exon
5' splice site
Branchpoint

E

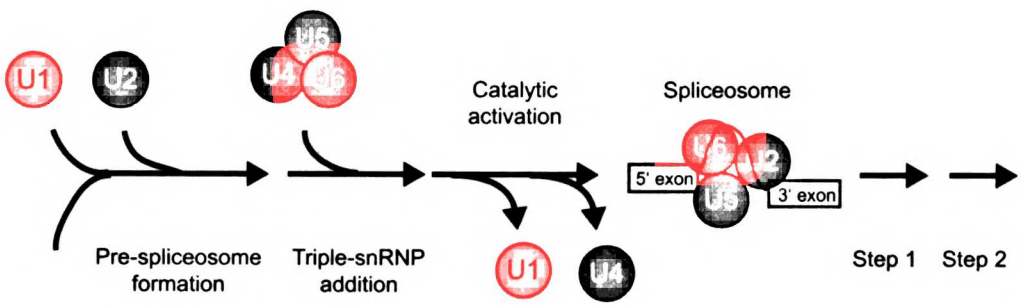
U1
U2
U6
U4
U5
Catalytic activation
Spliceosome
5' exon
3' exon
Pre-spliceosome formation
Triple-snRNP addition
U1
U4
Step 1
Step 2

F

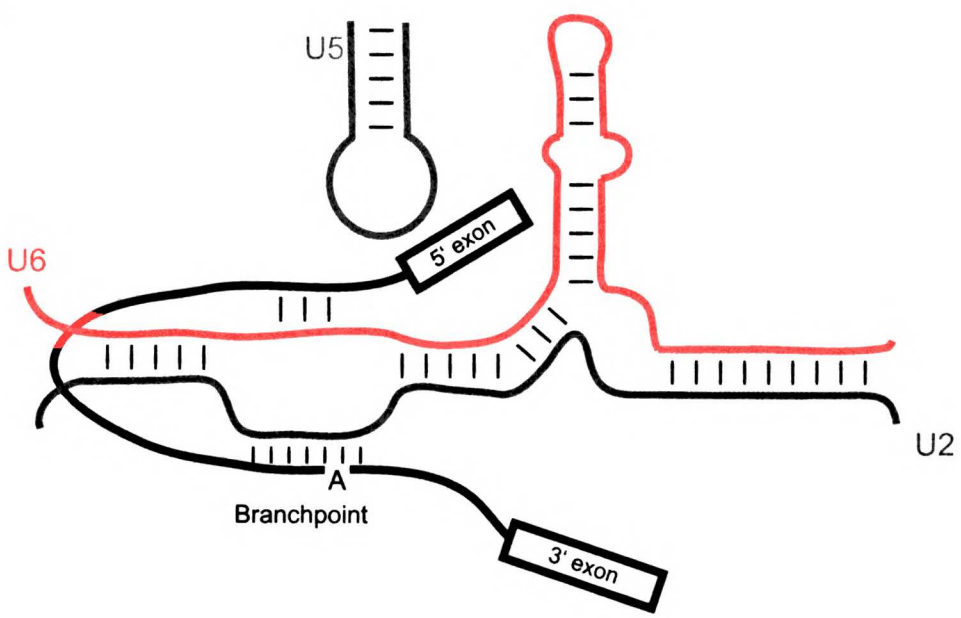
U5
5' exon
U6
U2
A
Branchpoint
3' exon

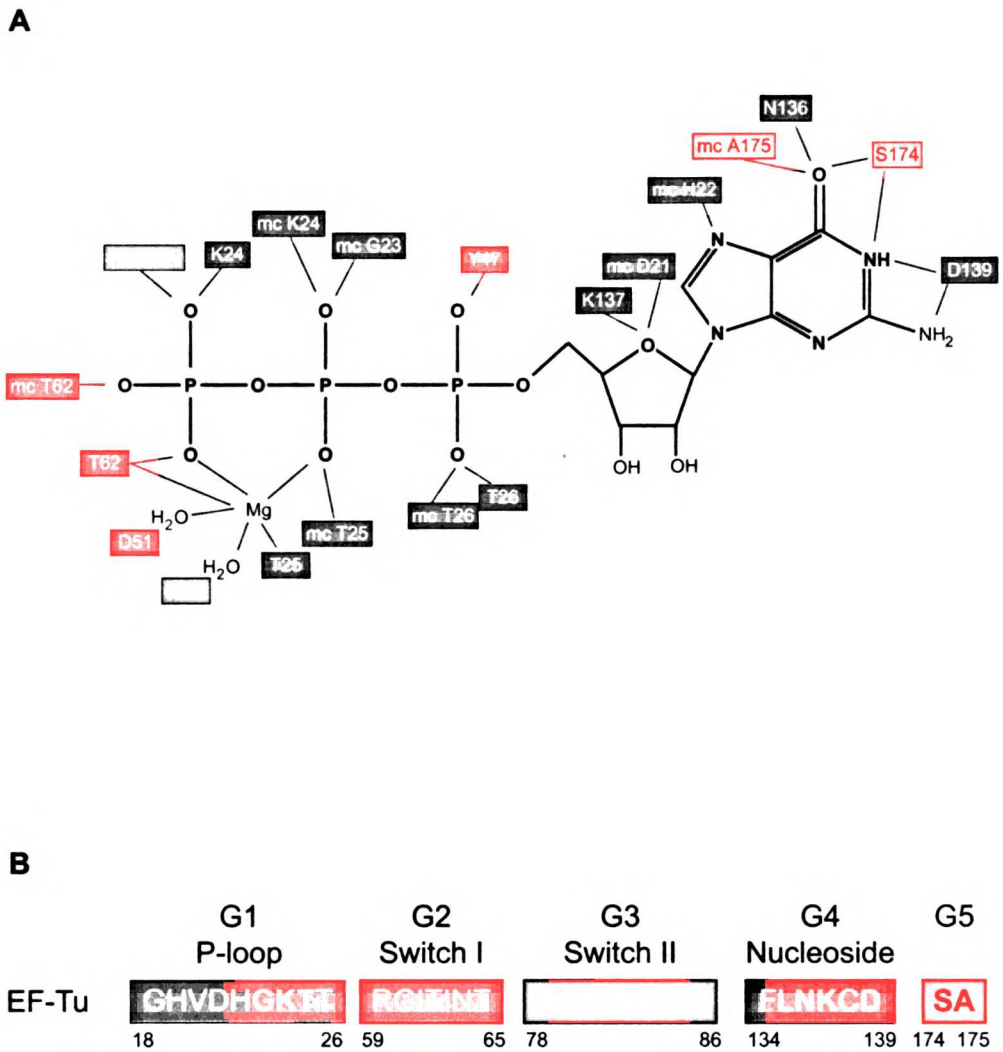

Figure 2. The guanine nucleotide binding site. **A:** Scheme of the GTP binding site based on the structure of *T. thermophilus* EF-Tu bound to GppNHp (Berchtold et al. 1993). Color code: G1 motif (P-loop), blue; G2 motif (Switch I), red; G3 motif(Switch II), purple; G4 motif (Nucleoside), green; G5 motif, yellow. mc = main chain atoms. **B:** Sequence of the nucleoside binding site in EF-Tu from *T. thermophilus*. Residues in motifs G1-G4 that are conserved throughout the GTPase superfamily are shown in yellow; the amino acids SA in the G5 motif are also well-conserved. Amino acids in A and B correspond to the sequence of *T. thermophilus* EF-Tu. Figure was adapted from Sprinzl *et al.* (2000)

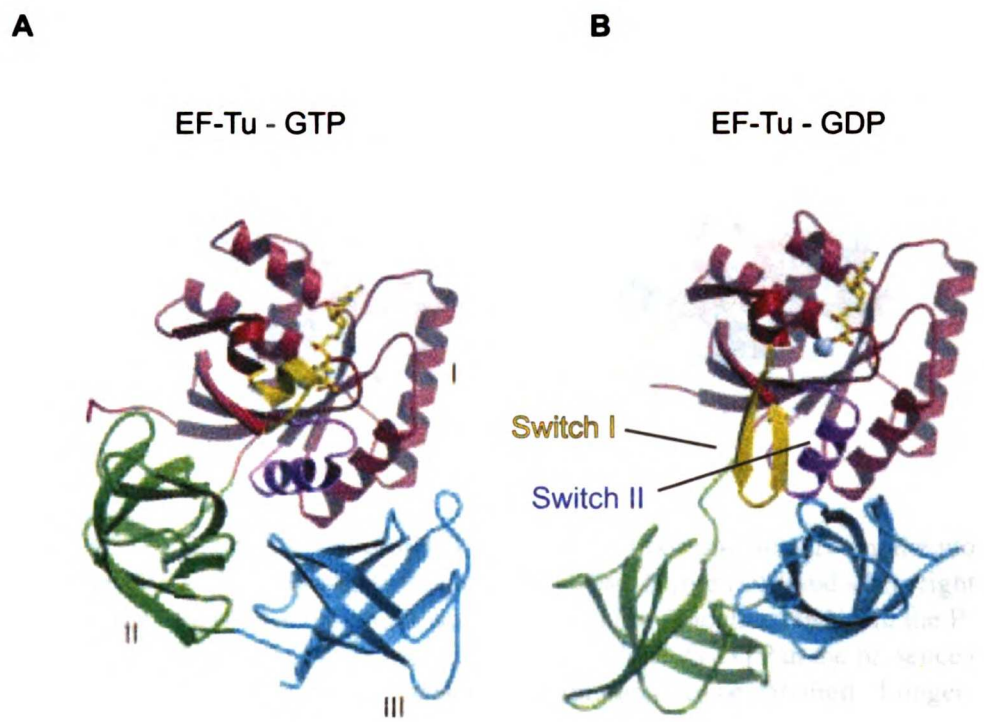

Figure 3. Changes in the Switch I and Switch II motifs upon GTP hydrolysis, as illustrated by the structures of EF-Tu. **A:** EF-Tu from *Thermus aquaticus* bound to GDPNP. **B:** EF-Tu from *Escherichia coli* bound to GDP. Color code: domain I: red; domain II: green; domain III: blue. Switch I (G2) is yellow and Switch II (G3) is purple. In the transition from bound GTP to GDP, Switch I changes from an α helix to two β sheets, and the orientation of Switch II is altered. This leads to a rearrangement of domains II and III. Nucleotides are shown in ball-and-stick models and Mg2+ ions are shown as grey balls. Reproduced from Andersen et al. (2003).

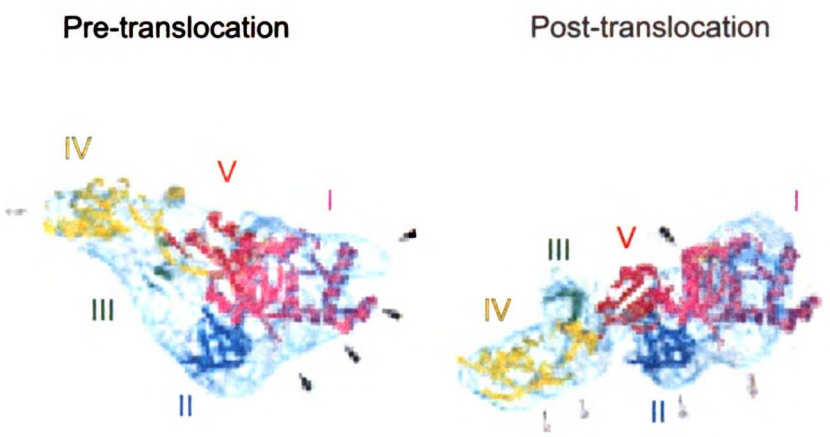

Figure 4. The fitted structure of EF-G bound to the ribosome, illustrating the movement of domains III-V. The cryo-EM structures are shown before (left) and after (right) translocation. Pre-translocation ribosomes, containing deacylated tRNA in the P site and peptidyl tRNA in the A site, were incubated with EF-G-GTP in the presence of thiostrepton, which allowed pre-translocation complexes to be captured. Longer incubation led to the formation of post-translocation complexes. The density of EF-G was then fitted to the known crystal structure (AEvarsson et al. 1994; Czworkowski et al. 1994), allowing movement of domains III-V relative to domains I-II. Color code: domain I, magenta; domain II, blue; domain III (only partially defined), green; domain IV, yellow; domain V, red. Arrowheads indicate contacts with the ribosome. Figure reproduced from Stark et al. (2000).

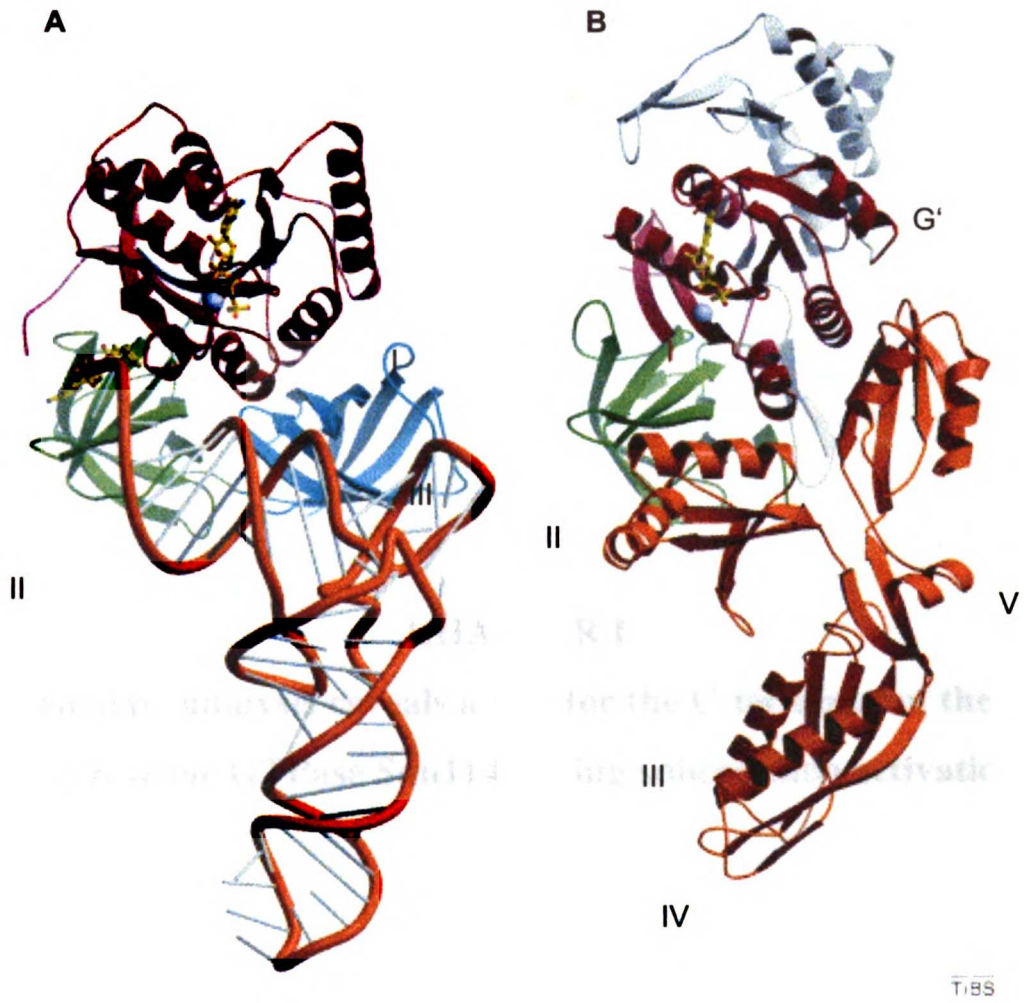

Figure 5. Structures of the ternary complex of EF-Tu and EF-G. **A:** EF-Tu-GDPNP from *Thermus aquaticus* in complex with yeast Phe-tRNA. Domain I is red, domain II is green, and domain III is blue. tRNA is shown in orange. **B:** EF-G-GDP from *Thermus thermophilus*. Domain I is red, domain II is green, and domains III-V are orange. The G' insertion within domain I is grey. GDPNP in **A** and GDP in **B** are shown in ball-and stick-model, as are the terminal A base and the amino acid of the CCA-end of the aa-tRNA in **A**. Reproduced from Andersen *et al.* (2003).

CHAPTER I

Genetic analysis reveals a role for the C-terminus of the *S. cerevisiae* GTPase Snu114 during spliceosome activation

Chapter I

Genetic analysis reveals a role for the C-terminus of the *S. cerevisiae* GTPase Snu114 during spliceosome activation

ABSTRACT

Snu114 is the only GTPase required for mRNA splicing. As a homolog of elongation factor G, it contains three domains (III-V) predicted to undergo a large rearrangement following GTP hydrolysis. To assess the functional importance of the domains of Snu114, we used random mutagenesis to create conditionally lethal alleles. We identified three main classes: 1) mutations that are predicted to affect GTP binding and hydrolysis, 2) mutations that are clustered in 10-20 amino acid stretches in each of domains III-V, and 3) mutations that result in deletion of up to 70 amino acids from the C-terminus. Representative mutations from each of these classes blocked the first step of splicing *in vivo* and *in vitro*. The growth defects caused by most alleles were synthetically exacerbated by mutations in *PRP8*, a U5 snRNP protein that physically interacts with Snu114, as well as in genes involved in snRNP biogenesis, including *SAD1* and *BRR1*. The allele *snu114-60*, which truncates the C-terminus, was synthetically lethal with factors required for activation of the spliceosome, including the DExD/H-box ATPases *BRR2* and *PRP28*. We propose that GTP hydrolysis results in a rearrangement between Prp8 and the C-terminus of Snu114 that leads to release of U1 and U4, thus activating the spliceosome for catalysis.

INTRODUCTION

Pre-mRNA splicing is catalyzed by the spliceosome, a large dynamic complex composed of five small nuclear RNAs (snRNAs) and over 80 proteins (BURGE *et al.*

1998; JURICA and MOORE 2003). The chemistry of splicing comprises two sequential trans-esterification reactions (MOORE *et al.* 1993). In the first reaction, the 5' splice site is cleaved and a branched lariat structure is formed within the intron. In the second reaction, the 3' splice site is cleaved and the two exons are joined together. During the splicing cycle, the RNA and protein components of the spliceosome undergo numerous rearrangements, which must be highly coordinated in order to ensure fidelity of the process (STALEY and GUTHRIE 1998). Most of these rearrangements appear to be energy dependent, and are correlated with the activity of individual ATPases of the DExD/H-box family. Eight known DExD/H-box proteins are required for the splicing cycle, and mutations in these proteins inhibit the ATP-dependent steps of splicing (STALEY and GUTHRIE 1998). Additionally, splicing requires one GTPase, Snu114, which is an essential protein in *S. cerevisiae* (FABRIZIO *et al.* 1997). Notably, Snu114 is homologous to the ribosomal translocase elongation factor G (EF-G in prokaryotes/EF2 in eukaryotes), leading to the hypothesis that Snu114 may similarly use the energy of GTP hydrolysis to drive rearrangements of the spliceosome (FABRIZIO *et al.* 1997).

Snu114 is packaged with other proteins and the U5 snRNA to form U5 snRNP (small ribonucleoprotein particle). Prior to formation of the spliceosome, U5 snRNP interacts with the U4/U6 di-snRNP, in which U4 and U6 snRNAs are extensively base paired, thus forming U4/U6·U5 tri-snRNP (reviewed in BURGE *et al.* 1998). According to the canonical model of spliceosome assembly, the tri-snRNP is then recruited to the pre-spliceosome, in which U1 snRNA is base paired with the 5' splice site and U2 snRNA is base paired with the branchpoint sequence, an intronic consensus sequence near the 3' splice site. Although the addition of tri-snRNP forms the complete

spliceosome, this complex is catalytically inert. Activation requires that the U1/5' splice site interaction and the base pairing between U4 and U6 be disrupted, such that U1 and U4 are no longer stably associated with the spliceosome. In contrast to the stepwise pathway of spliceosome assembly, recent evidence suggests that a holospliceosome containing all five snRNPs interacts as a complex with each intron (STEVENS *et al.* 2002). Nonetheless, ordered rearrangements of the snRNPs must occur prior to catalysis.

Rearrangements that occur during the early stages of spliceosome activation are regulated by several components of the U5 snRNP (BROW 2002). The Prp28 ATPase is required to unwind the U1/5' splice site duplex, possibly by destabilizing protein components of U1 snRNP (CHEN *et al.* 2001b; STALEY and GUTHRIE 1999), and the Brr2 ATPase is required to unwind the U4/U6 duplex (KIM and ROSSI 1999; LAGGERBAUER *et al.* 1998; RAGHUNATHAN and GUTHRIE 1998a). Presumably, the activities of Prp28 and Brr2 must be tightly regulated in order to ensure that catalytic activation does not occur prematurely. Genetic studies have suggested that the activities of these ATPases are modulated by Prp8, which is a large (280 kDa), well-conserved U5 snRNP protein (COLLINS and GUTHRIE 2000; KUHN and BROW 2000; KUHN *et al.* 1999). Prp8 is believed to inhibit the activities of Prp28 and Brr2 until spliceosome formation has occurred (KUHN *et al.* 2002). The mechanism by which Prp8 inhibits the ATPases is as yet unknown.

A strong physical interaction between Prp8 and Snu114 suggests that Snu114 may also play a regulatory role during spliceosome activation. Treatment of U5 snRNP from human cell extract with high concentrations of chaotropic salts disrupts the complex, but Prp8 (U5-220kD in human) and Snu114 (U5-116kD in human) remain associated as a

heterodimer (ACHSEL *et al.* 1998). Indeed, deletion of the N-terminal 120 amino acids of Snu114, which comprise the only domain that is not found in EF-G, causes a temperature-sensitive block to growth and inhibits the release of U1 and U4 from the spliceosome (BARTELS *et al.* 2002). Similarly, a mutation in Snu114 that is predicted to convert GTP binding to XTP binding inhibits U1 and U4 release, and also decreases cellular levels of U5 and tri-snRNP (BARTELS *et al.* 2003). While the N-terminal and GTPase domains have been implicated in spliceosome activation, previous studies have not addressed a function for the other domains of Snu114.

We used a two-step strategy to elucidate the timing and mechanism of Snu114 activity. First, we generated conditionally lethal alleles of Snu114 by random mutagenesis. We identified mutations in all domains of the protein, including clusters of mutations in domains III-V and mutations within the GTPase domain. We also found that deletion of the C-terminal 70 amino acids (*snu114-60*) causes a growth defect at 16° and 37°. Second, we analyzed synthetic interactions between *snu114* alleles and mutants of other proteins that function at distinct stages of splicing. We found strong genetic interactions between the *snu114* alleles and mutations in factors involved in snRNP formation and spliceosome activation. In particular, synthetically lethal interactions with *snu114-60* demonstrate a critical function for the C-terminus of the protein during spliceosome activation.

MATERIALS AND METHODS

Strains and plasmids: Yeast strains are listed in Table 1 and plasmids are listed in Table 2. All strains are isogenic with BY4743 (GIAEVER *et al.* 2002), which is an S288C derivative, unless otherwise noted. Heterozygous diploids with *KanMX* deletions of

SNU114, *SUB2*, *PRP22*, *PRP43*, *BRR2*, *PRP28*, and *SNU66* and haploids with *KanMX* deletions of *ISY1*, *SNT209*, and *BRR1* were obtained from Research Genetics (GIAEVER *et al.* 2002). A *PRP8* deletion strain was created by transforming a WT diploid with the *PRP8::LYS2 SacI/ApaI* fragment from pJU224 (UMEN and GUTHRIE 1996); integrants were confirmed by PCR. *sad1-1* (BSY387) (LYGEROU *et al.* 1999), *prp2-1* (SS304) and *prp19-1* (ts87) (VIJAYRAGHAVAN *et al.* 1989) strains were back-crossed twice to *snu114::KanMX* strains; *prp5-1* (SPJ 5.41) (VIJAYRAGHAVAN *et al.* 1989) was crossed once to a *snu114::KanMX* strain. yTB136 was derived from GLS618 (RADER and GUTHRIE 2002), and yTV161 was derived from yS79 [MAT α sister of yS78 (WANG and GUTHRIE 1998)]. yTB2 was created by sporulating YPF5 (FABRIZIO *et al.* 1997).

*Eco*RI/*Bgl*II sites were inserted immediately following the AUG start codon of SNU114 by PCR amplifying pTB1 (pRS316/SNU114) (FABRIZIO *et al.* 1997) with the primer pairs oTB1 (5'-GGGAACAAAAGCTGGGTACCGGGC-3')/ oTB2 (5'-GGAAGC**GAATTC**CATTTTGCTATGTTAGGAGCTATTG-3') and oTB3 (5'-CCGACC**GAATTCAGATCT**GAAGGTGACGATTTATTCGATGA-3')/ oTB4 (5'-ATCCTCTCCGGAATGTTAGCCAT-3'). The oTB1/oTB2 PCR product was digested with *Kpn*I and *Eco*RI and inserted into the same sites of pRS316. The resulting plasmid and the oTB3/oTB4 PCR product were digested with *Eco*RI and *Bam*HI and ligated together. The 4.73 kb *Bsp*EI-*Nsi*I fragment of the resulting plasmid was ligated with the 3.62 kb *Bsp*EI/*Nsi*I fragment of pTB1 to create pTB3. The *SNU114*-containing *Xho*I/*Sac*I fragments of pTB1 and pTB3 were inserted into the same sites in pRS314 to create pTB2 and pTB4, respectively.

A single myc epitope was placed immediately after the start codon of SNU114

by inserting the annealed oligos oKD140 (5'-AATTCCCAGAACAAAAATTGATTTCTGAAGAAGATTTGAATA-3') and oKD141 (5'-GATCTATTCAAATCTTCTTCAGAAATCAATTTTTGTTCTGGG-3'), which have overhanging *Eco*RI/*Bgl*II sites, into the same sites of pTB4. The resulting plasmid was named pTB19. pTB19 was transformed into yTB2, the plasmid pTB1 was lost by passage on 5-FOA media, and the presence of the myc epitope was confirmed by Western blotting with the 9E10 antibody (BAbCO). The yeast strain carrying pTB19 grew at the same rate as the strain with pTB1 at 16°, 25°, 30°, and 37°.

The *snu114-50* mutations E910G and C928R were separated by digesting pRS314/*snu114-50* and pTB19 with *Pst*I and *Nde*I and inserting the 356 bp fragment from each plasmid into the 7.89 kb fragment of the other plasmid.

In order to remove the myc tag and/or the restriction sites from the N-terminus of *snu114* alleles, the following restriction enzymes were used to clone the *snu114* mutations into pTB2: *Bsp*EI and *Bst*BI (*snu114-12* and *snu114-14*), *Bst*BI and *Sac*I (*snu114-30* and *snu114-50*), *Bst*BI and *Pst*I (*snu114-40*), and *Pst*I and *Sac*I (*snu114-60*). Plasmids pRS314/*SNU114* and pRS314/*snu114-12*, *-14*, *-15*, *-30*, *-40*, *-50*, and *-60* were named pTB95-102. The *snu114* alleles were moved from pRS314 (pTB95-102) to pRS315 (pTB106-113) by transforming the PCR-amplified *LEU2* marker from pRS315 with *Hin*dIII-cut pRS314/*snu114* plasmids into a WT strain. Plasmids were recovered from LEU2+ transformants.

Mutagenesis of *SNU114*: *SNU114* was PCR amplified in two fragments. Fragment 1 was amplified with oTB7 (5'-CTTGCCAACGGCTGACGATTGC-3'; 67 bp upstream of start AUG) and oTB8 (5'-CAAACAGTCCATATACAGCTCTCC-3'; 1965 bp

downstream of start AUG). Fragment 2 was amplified with oTB9 (5'-CCGCGACGTTGTACTCTGTAAAG-3'; 1720 bp downstream of start AUG) and oTB10 (5'-CCAGTGAATTGTAATACGACTCAC-3'; 3270 bp downstream of start AUG). Mutagenesis was performed under standard PCR conditions, using the natural error rate of Taq DNA polymerase. PCR reactions (100 μl volume) contained 1X Taq buffer (Roche), 200 μM each dNTP, 400 nM each oligo, 2.5 units of Taq (Roche), and 10 ng plasmid DNA. The PCR cycling parameters were the following: 2 min at 94°; ten cycles of: 1 min at 94°, 1 min at 55°, 2 min at 72°; and 4 min at 72°. After every ten cycles of PCR amplification, reactions were diluted 1:100. Two separate sets of reactions were performed (Set A/B and Set C). For set A, a total of 20 PCR cycles were performed, and an additional 10 cycles gave set B. For set C, a total of 40 cycles using Taq were performed, followed by an additional 10 cycles using Expand Taq. At least two independent PCR reactions were performed for each set. pTB19 (pRS314/*myc-SNU114*) was the template for sets A and B and pTB4 (pRS314/*SNU114*) was the template for Set C. Fragment 1 PCR products were transformed with the *Eco*RI/*Bst*BI-cut vector of pTB19 or pTB4, and Fragment 2 PCR products were transformed with the *Bst*BI/*Nde*I-cut vector of pTB19 or pTB4. PCR products and gapped vectors were transformed into yTB2. Transformants were selected on SD-TRP media at 25° and replica plated to 5-FOA media at 25°. Lethality on 5-FOA was 8-13% for Fragment 1 and 2-4% for Fragment 2, depending on the number of PCR cycles. Strains were then tested for conditional lethality by replica plating to YPD and incubating at 16° for 3 days, 25° for 1-2 days, and 37° for 1 day. Approximately 25,000 colonies were screened for each fragment. Plasmids from strains that were growth impaired at 37° or 16° were

recovered and transformed into yTB2 and yTB13. Plasmids that conferred conditional growth defects were sequenced by the Biomolecular Resource Center DNA sequencing facility at the University of California, San Francisco. The NCBI BLAST alignment server (http://www.ncbi.nlm.nih.gov/blast/bl2seq/wblast2.cgi) was used to identify mutations in the recovered *snu114* alleles.

The mutations K146I and T147N were created using the QuikChange site-directed mutagenesis method (Stratagene) with the template pTB2. The mutations P216N and H218R were created using site-directed mutagenesis of the template pTB19. Mutations were confirmed by sequencing and were subcloned into fresh plasmids.

Integration of *snu114* alleles: An integrating *snu114-12* plasmid (pTB126) was made by inserting the 3.3 kb *Pvu*II fragment of pTB107 into the *Pvu*II-cut vector of pRS306. Integrating *snu114-40* and *snu114-60* plasmids (pTB130 and pTB132) were created by ligating the 4.25 kb *Nhe*I/*Ngo*MIV fragment of pTB126 with the 3.63 kb *Nhe*I/*Ngo*MIV fragments of pTB111 and pTB113. Integrating plasmids pTB126, pTB130, and pTB132 were linearized with *Nhe*I (pTB126) or *Eco*47III (pTB130/132), transformed into yTB128, and selected on SD-URA media at 25°. Following growth on 5-FOA, transformants were streaked to YPD and grown at 16°, 25°, and 37° to select for ts or ts/cs integrants.

Primer extensions: For primer extensions, the following strains were grown in liquid YPD media to OD 0.5-1.0: yTB128 (*SNU114*), yTB165 (*snu114-60*), and yTB171 (*snu114-12*), all grown at 25°; and yTB23 carrying either pTB106 (*SNU114*) or pTB111 (*snu114-40*), grown at 30°. Cells were spun down, resuspended in YPD media pre-incubated at 37° or 16°, and grown in water baths at either 37° or 16°; 10 mL aliquots

were removed at the indicated times. Cultures were diluted during the time-course to maintain an OD between 0.5 and 1.0. *prp16-2* (yS79 (WANG and GUTHRIE 1998) +BHM110) was shifted to 37° for three hours as a control for a mutant that blocks the second step of splicing. RNA was isolated (SCHMITT *et al.* 1990), and primer extension were performed as described (BOORSTEIN and CRAIG 1989). 10 ug RNA were used per reaction. The following oligos were used: U3: 5'-CCAAGTTGGATTCAGTGGCTC-3', RPS17/RP51: 5'- CTTAGAAGCACGCTTGACGG-3', PGK1: 5'-ATCTTGGGTGGTGTTCC-3'; U14: 5'-ACGATGGGTTCGTAAGCGTACTCCTACCGT-3'. Data were quantitated by phosphorimager analysis (Molecular Dynamics).

***In vitro* splicing assays:** Liquid cultures of yTB23 in which pTB1 had been replaced by pTB106 (*SNU114*), pTB107 (*snu114-12*), pTB111 (*snu114-40*), or pTB113 (*snu114-60*) were grown at 30° to OD 1.2-1.4. Splicing extracts were prepared and actin pre-mRNA was spliced as described (UMEN and GUTHRIE 1995). Extracts were pre-incubated for 20 minutes at 37° or on ice in the presence of splicing buffer components (2.5 mM MgCl2, 60 mM potassium phosphate pH 7, 3% PEG 8000) prior to addition of radiolabeled actin and ATP (final concentrations 0.5 nM and 2 mM, respectively). Splicing reactions were performed at 25°.

Testing genetic interactions: In order to test genetic interactions, we created strains deleted for *SNU114* (*snu114::KanMX*) in combination with deletion or mutation of a second gene. Deletions were covered by WT plasmids marked with *URA3*. Plasmids containing mutant alleles of *snu114* (and in some cases, of a second gene) were

transformed, and the ability to lose the *URA3*-marked WT plasmid(s) on 5-FOA was tested.

The following strains (mutant allele/WT allele) were transformed with pTB106-113: yTB102/yTB23 (*snu66Δ*), yTB103/yTB105 (*brr2-1*), yTB106/yTB107 (*prp28-1*), yTB117/yTB118 (*prp5-1*), yTB133/yTB23 (*brr1D*), yTB139/yTB23 (*snt309Δ*), yTB142/yTB143 (*sad1-1*), yTB144/yTB145 (*prp19-1*), and yTB146/yTB145 (*prp2-1*). The strains yTB111/yTB15 (*isy1Δ*) were transformed with pTB95-102. yTB108 (*prp8Δ*) was transformed either with combinations of pTB95-102 and pJU204, pAK338, pJU206, and pCC18 or pTB106-113 and pCC11 and pCC121. yTB134 (*prp22Δ*) was transformed with pTB106-113 and pTB115-117. yTB135 (*prp43Δ*) was transformed with pTB106-113 and pTB118-121. yTB136 (*prp24Δ*) was transformed with pTB106-113 and pPR113, pSR53, pSR70, and pSR39. yTB148 (*sub2Δ*) was transformed with pTB106-113 and pAK354-356. yTV161 (*prp16Δ*) was transformed with pTB106-113 and pSB58, BHM108-110, and BHM115. Additionally, *snu114ΔN* (BARTELS *et al.* 2002) was cloned into pRS315 and transformed into yTB23, yTB102, yTB103, and yTB105-107. In all cases, corresponding empty vectors were also transformed as negative controls. Transformants were selected on the appropriate selective media at 25°. Between four and 14 transformants were streaked to 5-FOA-containing media and incubated at 25° for up to six days. If no colonies grew on 5-FOA, the combination of alleles was considered synthetically lethal. Viable strains were streaked to YPD media at 25°. Liquid cultures of each strain in duplicate were grown overnight at 25° and diluted to OD 0.1. Ten-fold serial dilutions were grown on YPD plates at 16° for eight days and 25°, 30°, and 37° for up to four days. For *prp8* strains, six 5-fold serial dilution were made; the middle three

dilutions are shown in Figure 8. For weak genetic interactions, we cannot distinguish between synthetic enhancement and additive enhancement.

A high number of transformants of *snu114-12*, *snu114-14*, and *snu114-15* in combination with *prp28-1* or *snu66Δ* (and *snu114-50* with *snu66Δ*) were either not viable on 5-FOA or produced very few colonies. For example, for the combination of *snu114-12* and *snu66Δ*, 4/14 transformants were not viable on 5-FOA, and 9/14 transformants produced only a small number of colonies on 5-FOA. To avoid the possibility that the viable colonies represented suppressors or revertants, we crossed integrated *snu114-12* (yTB171), *snu114-40* (yTB163), *snu114-60* (yTB165), and *SNU114* (yTB28) to *snu66::KanMX* (yTB100) and *prp28-1* (yEJS51) (STRAUSS and GUTHRIE 1991) strains and dissected tetrads. Genotypes of the spores were determined by replica plating to G418-containing media (for *snu66::KanMX*) and to YPD plates that were incubated at 16° and 37° (for the other ts/cs mutations).

Sequence alignment and structure modeling: An alignment between Snu114 and Eft1 (*S. cerevisiae* EF2) was created using ClustalW (THOMPSON *et al.* 1994) and was modified by hand, and the structure of Snu114 was modeled on the structure of apo-EF2 (PDB code 1N0V) and sordarin-bound EF2 (PDB code 1N0U) using the program MODELLER (SALI and BLUNDELL 1993). Structures were visualized with PyMOL (DELANO 2002). Coordinates of the models are available upon request.

The alignment of domain IVb was shaded using BOXSHADE (version 3.2; K. Hofmann and M. Baron). Swiss-Prot accession numbers are as follows: Snu114 from *S. cerevisiae* (P36048), *S. pombe* (O94316), *A. thaliana* (Q9LNC5), *H. sapiens* (Q15029), *C. elegans* (Q23463), *D. melanogaster* (Q9VAX8); EF2 from *S. cerevisiae* (P32324), *H.*

sapiens (P13639), *C. elegans* (P29691); EF-G from *T. thermophilus* (P13551), *E. coli* (P02996).

RESULTS

Modeling the structure of Snu114: In order to analyze how mutations in Snu114 might affect its function, we used the program MODELLER (SALI and BLUNDELL 1993) to model the structure of Snu114 onto the crystal structure of *S. cerevisiae* EF2 (JORGENSEN *et al.* 2003), which was possible because of the high sequence similarity between the two proteins (26% identity, 46% similarity). By homology with EF2, Snu114 contains five structural domains (Figure 1A), as well as a 120 amino acid N-terminal extension that is not conserved in EF2 and thus could not be modeled. The C-terminus of the protein (IVb) folds back onto domain IVa, and so is considered part of domain IV. For clarity, we refer to the two portions of domain IV as IVa and IVb. Figures 1B and 1C show the structure of Snu114 modeled onto nucleotide-free EF2, and Figure 1D shows the structure of Snu114 modeled onto EF2 bound to the translation inhibitor sordarin, which is believed to block EF2 on the ribosome in a post-translocation state (JORGENSEN *et al.* 2003). The two structures demonstrate the flexibility of the protein. In particular, domains I and II appear as a rigid body, while domain III rotates around a linker between domains II and III, and domains IV and V rotate as a rigid unit.

Screen for conditionally lethal alleles of *SNU114*: To generate conditionally lethal alleles of *SNU114*, we used the error-prone polymerase Taq to amplify the gene in two pieces: fragment 1 spans domains N, I, and II, and fragment 2 spans domains III-V (Figure 1A). Each fragment was transformed in combination with an appropriately gapped plasmid containing *SNU114* and the *TRP1* marker into a yeast strain in which the

chromosomal copy of *SNU114* was deleted and wild-type *SNU114* was present on a counterselectable *URA3*-marked plasmid (MUHLRAD *et al.* 1992). For each fragment, we screened approximately 25,000 transformants. When colonies were replica-plated to 5-FOA-containing media to select against the *WT SNU114* plasmid, >87% of the colonies were viable. We then screened for colonies that were unable to grow at 37° or 16°. From the transformation of mutagenized fragment 1, we isolated 37 thermal-sensitive (ts) strains and one strain that was both cold-sensitive (cs) and ts. Mutagenesis of fragment 2 yielded 54 ts and three cs/ts strains. Plasmids were recovered from 20 ts strains for each of the fragments and from all of the cs/ts strains, and were retransformed into the starting strain. Five of the plasmids from fragment 1 did not retest and were discarded. The remaining plasmids were sequenced.

The sequenced alleles contained an average of two mutations per gene, with a range of one to six mutations (Tables 3 and 4). Despite the presence of multiple mutations per allele, many of the mutations clustered within small stretches of highly conserved amino acids, highlighting regions that are important for Snu114 function (Figure 1A). Individual amino acids within these clusters were often mutated in multiple independent clones.

Fragment 1 mutations: Domain I contains the conserved motifs, G1-G5, which are present in all GTPases and are necessary for GTP binding and hydrolysis (BOURNE *et al.* 1991). Of the sixteen alleles from fragment 1 that were sequenced, six contain a mutation in the G1 motif, and four contain a mutation in the G3 motif. Concomitant with the PCR mutagenesis, we designed two mutations in the G1 motif of *SNU114* that are expected to decrease nucleotide binding (OGG *et al.* 1998); these mutations, K146I

(*snu114-15*) and T147N, confer a ts growth phenotype (Table 5). In order to study single point mutations in the G3 motif of *SNU114* that are predicted to affect GTP hydrolysis, we created the individual mutations P216N (*snu114-12*) and H218R, which had arisen in combination with other mutations during PCR mutagenesis. Each of these mutations alone causes a ts growth defect (Table 5).

While the structure of the G domain of most GTPases is similar, an insertion termed the G" domain is found in EF2 and Snu114, but not in the other translational GTPases (ÆVARSSON 1995). Although no function has been assigned to this domain, it has been postulated to act as a guanine exchange factor (GEF), since EF2 is not known to have an extrinsic GEF (ÆVARSSON *et al.* 1994; CZWORKOWSKI *et al.* 1994). In Snu114, a single mutation in this domain, L381P (*snu114-14*), causes slow growth and a weak ts/cs phenotype.

Fragment 2 mutations: Over half of the mutations identified in domains III-V are found within three 10-20 amino acid stretches, which are underlined in Figure 1A and highlighted in Figures 1C and 1D. The 23 sequenced fragment 2 alleles contain a total of 49 mutations. 13 of the mutations fall within a short stretch of domain III (residues 645-664), eight mutations are within a small region of domain IVa (residues 842-851), and seven mutations are clustered in domain V (residues 909-928). While a majority of the alleles that arose from mutagenesis of fragment 2 contain multiple mutations, six alleles contain a single point mutation. Four of these mutations, including *snu114-30*, are in the domain III cluster, and one, *snu114-40*, is in the domain IVa cluster. That single amino acid changes cause a conditional growth defect emphasizes the functional significance of these regions. Furthermore, in comparing Snu114, EF2, and EF-G, the amino acid cluster

in domain III contains the most conserved stretch of amino acids outside of domain I (CAMMARANO *et al.* 1992). As shown in Figures 1C and 1D, the clusters in domain III and V are in close proximity to each other and to the G3 motif. The cluster of residues in domain IVa forms a helix that faces domain IVb.

In addition to the mutations in domains III, IVa, and V, an additional class of mutations was found in domain IVb. Domain IVb is larger in Snu114 than in its homologs: the domain is 76 residues in Snu114, but only 44 residues in yeast EF2 and 20 residues in *E. coli* EF-G (Figure 1E). In comparison with EF2, Snu114 domain IVb has several insertions as well as a C-terminal extension. Only three sets of mutations were found in this domain, and all result in early truncation of the protein. The weak ts allele *snu114-62* causes a deletion of 23 amino acids, while the ts/cs alleles *snu114-60* and *snu114-61* result in the deletion of 70 and 68 amino acids, respectively (Table 4).

The severity of the growth defect of the C-terminal deletions was affected by the presence of a myc epitope that had been placed at the N-terminus of the gene prior to mutagenesis. Although *myc-snu114-60* and *snu114-61* have similar deletions, the growth defect of *myc-snu114-60* is much stronger. The allele *snu114-61* also contains mutations in domains II and IV and does not contain the myc epitope, perhaps due to homologous recombination with chromosomal *SNU114*. We tested whether any of these differences could suppress the growth defect of *myc-snu114-60*, and found that removing the myc epitope from this allele greatly reduces the severity of the growth defect at both high and low temperatures (Figure 2A). The presence or absence of the myc epitope did not affect the growth phenotype of the other *snu114* alleles that were further characterized.

Where possible, we focused subsequent experiments on a set of alleles with single mutations in each of the domains that were identified above as important. For the work described below, we used the alleles *snu114-15* (G1 motif), *snu114-12* (G3 motif), *snu114-14* (G" domain), *snu114-30* (domain III), *snu114-40* (domain IVa), *snu114-50* (domain V) (*snu114-50* contains two mutations, because the single mutations did not cause a growth phenotype [Table 5]), and *snu114-60* (truncation of domain IVb) (see Tables 3 and 4). All alleles are ts. *snu114-14* and *snu114-60* are only weakly ts as well as weakly cs (Figure 2B).

***snu114* mutants exhibit *in vivo* and *in vitro* splicing defects:** We tested whether a subset of the *snu114* mutations inhibit splicing. To monitor *in vivo* splicing, we purified RNA from cells that had been shifted to the non-permissive temperature for various times, and performed primer extensions on the intron-containing transcripts U3 and *RPS17/RP51*. U3 is a nucleolar snoRNA, and *RPS17* encodes a ribosomal protein. Mutations that block the first chemical step of splicing are expected to increase the level of precursor mRNA, while mutations that affect the second step of splicing should cause an accumulation of lariat intermediate. Strains containing integrated *snu114-12* allele grow slowly even at 25°, and show a constitutive accumulation of U3 precursor (Figure 3A). The level of pre-U3 in *snu114-60* cells, which are both ts and cs, increases following a shift to either 37° or 16° (Figures 3B and 3C). Primer extension of the less stable *RPS17* transcript reveals that shifting *snu114-40* to 37° causes a rapid increase in pre-mRNA, as well as a rapid and dramatic decrease in the level of mature mRNA (Figure 3D). While primer extension with U3 only allows the differentiation of precursor from mature RNA, the lariat intermediate of *RPS17* can be resolved. In contrast to the

second step mutant *prp16-2* (BURGESS and GUTHRIE 1993), none of the *snu114* mutants that we tested accumulate lariat intermediate (Figure 3D and data not shown). Together, pre-mRNA accumulation and a lack of lariat intermediate accumulation show that the *snu114* mutants block splicing at or before the first chemical step.

The data from *in vitro* splicing in extracts made from *snu114* mutant strains grown at the permissive temperature were consistent with the *in vivo* splicing data. To monitor splicing *in vitro*, radiolabeled actin pre-mRNA was incubated with extracts that had been pre-incubated either at 37° or on ice. The splicing intermediates and products were then separated by PAGE and visualized by phosphorimaging. The *snu114-12* extract splices poorly even at 25°, consistent with a constitutive defect (Figure 4A). Splicing in both *snu114-40* and *snu114-60* extracts can be inactivated by pre-incubation at high temperature (Figure 4B and 4C). While the kinetics of splicing in *snu114-60* extract at 16° *in vitro* are slow, they are not strongly inhibited (data not shown). For all *snu114* alleles, the levels of all splicing intermediates are decreased in the mutant extracts, indicating an early block to splicing.

Genetic interactions of *snu114* mutants: Inhibition of the first step of splicing can arise for many reasons, including defects in snRNP levels, defects in U1 or U2 addition, defects in tri-snRNP addition, and defects in activation of the spliceosome. Synthetic enhancement has proven to be a powerful tool for elucidating functions of and interactions between factors of large multicomponent complexes (DOYE and HURT 1995; GUARENTE 1993). To gain an understanding of the timing of Snu114 function(s), we examined genetic interactions between the *snu114* alleles and mutations or deletions of 16 splicing factors known to be required at different stages of splicing (Figure 5). We

tested each combination for viability and for conditional growth defects. Taking into consideration changes in growth rates at 16°, 25°, 30°, and 37°, the overall strength of synthetic enhancement for each interaction was rated on a scale of 0 to 5, where 0 indicates no interaction and 5 indicates a synthetically lethal interaction (Table 6). Interactions that were synthetically lethal or synthetically sick are summarized in Figure 5 (black stars and grey stars, respectively).

Interactions with ATPases: Each of the eight spliceosomal DExD/H box ATPases acts at a clearly defined and distinct stage of splicing (STALEY and GUTHRIE 1998). Strikingly, mutations in the ATPases Prp28 and Brr2, which are needed for activation of the spliceosome, exhibit strong genetic interactions with *snu114* mutations. Although *snu114-60* has only a weak conditional growth defect, it is inviable in combination with *prp28-1*, a cs mutation of Prp28 that disrupts the exchange of U1 for U6 at the 5' splice site (STALEY and GUTHRIE 1999) (Figure 6A). *prp28-1* is also synthetically sick in combination with mutations in domain I (*snu114-12*, *snu114-14*, and *snu114-15*); (data not shown). *brr2-1*, a cs mutation that decreases the U4/U6 unwinding activity of Brr2 (RAGHUNATHAN and GUTHRIE 1998a), is synthetically lethal with *snu114-60* at 16° and 37° (Figures 6A and 7B). In contrast to *prp28-1*, *brr2-1* only interacts strongly with *snu114-60*, although *snu114-14* and *snu114-40* enhance the cs growth defect (Figure 7B and data not shown).

snu114-60 is not synthetically lethal with any of the other ATPase mutations that were tested (Figure 6A and data not shown). The growth defects of the other *snu114* alleles are moderately enhanced by mutations in Sub2, which functions during U2 snRNP addition (KISTLER and GUTHRIE 2001; LIBRI *et al.* 2001; ZHANG and GREEN 2001), in

Prp2, which acts immediately before the first chemical step (KIM and LIN 1996), and in Prp22, which helps to disassemble the post-catalytic spliceosome (COMPANY *et al.* 1991). Mutations in Prp5, Prp16, and Prp43, which are involved in U2 addition, second step catalysis, and spliceosome recycling, respectively, exhibit no genetic interactions with *snu114* alleles (ARENAS and ABELSON 1997; RUBY *et al.* 1993; SCHWER and GUTHRIE 1991). Together, the pattern of genetic interactions with the spliceosomal ATPases suggests that Snu114, and especially domain IVb, is specifically involved in spliceosome activation.

Interactions with *PRP8* alleles: Distinct mutations of the core U5 protein Prp8 affect several stages of spliceosome assembly and both steps of splicing. While none of the *snu114* mutations have strong genetic interactions with *prp8-101*, which inhibits the second step of splicing (UMEN and GUTHRIE 1995), many of the alleles have synthetic interactions with *prp8* mutations that cause earlier splicing defects (Figures 6B and 7A). The mutations *prp8-1* and *prp8-brr* impair the formation of U5 and tri-snRNP (BROWN and BEGGS 1992; COLLINS 2001) and exhibit strong genetic interactions with *snu114* mutations. Notably, *prp8-1* and *prp8-brr* are synthetically lethal with *snu114-40* and *snu114-60*, indicating that Snu114 domain IV is important for interacting with Prp8 during snRNP formation. Additionally, many of the *snu114* mutations are synthetically sick or lethal in combination with *prp8-201*, an allele that affects spliceosome activation (KUHN *et al.* 1999).

Interactions with factors involved in tri-snRNP addition, snRNP biogenesis, and snRNP recycling: Because *snu114* mutations cause a block prior to the first step of splicing, we also tested genetic interactions with factors that are involved in addition of

tri-snRNP to the spliceosome and in snRNP biogenesis and recycling. In mammalian extract, depletion of either of the tri-snRNP proteins Snu66 or Sad1 inhibits tri-snRNP addition (MAKAROVA *et al.* 2001). In yeast, deletion of *SNU66* causes a cs growth defect and inhibits the first step of splicing (GOTTSCHALK *et al.* 1999; STEVENS *et al.* 2001), and the ts allele *sad1-1* blocks splicing and decreases the formation of U4/U6 di-snRNP (LYGEROU *et al.* 1999). Deletion of *SNU66* is synthetically lethal with *snu114-60*, and enhances the growth defects of *snu114-12*, *-14*, *-15*, and *–50* (Figures 6A and 8 and data not shown). All of the *snu114* alleles are synthetically lethal or sick in combination with *sad1-1*.

The recycling factor Prp24 assists in the base pairing of U4 and U6 snRNAs (RAGHUNATHAN and GUTHRIE 1998b). It has also been proposed to influence spliceosome activation, as alleles of *prp24* are synthetically lethal with *prp28-1* and with U4-cs1, a mutation in U4 that blocks spliceosome activation (KUHN and BROW 2000; STRAUSS and GUTHRIE 1991). The ts mutation *prp24-RRM3sub*, which is believed to disrupt the ability of Prp24 to bind RNA (VIDAVER *et al.* 1999), enhances the growth defect of *snu114-60.* However, none of the other *snu114* mutations exhibit genetic interactions with *prp24* mutations.

Deletion of the non-essential gene *BRR1* causes a cs growth defect, affects the processing of newly transcribed snRNAs, and causes a decrease in snRNA and snRNP levels (INADA 2004; NOBLE and GUTHRIE 1996). The deletion of *BRR1* is synthetically lethal with *snu114-60* at 16° and 37°, and the combination of *brr1Δ* with the other *snu114* mutations impairs growth at 30° (Figure 7C and data not shown).

Interactions with the NTC: Lastly, we tested components of the NTC (prp-nineteen complex), a complex that interacts with the spliceosome immediately prior to the first step of catalysis (CHAN *et al.* 2003; TARN *et al.* 1993). *prp19-1*, a ts mutation that blocks the first step of splicing (VIJAYRAGHAVAN *et al.* 1989), enhances the growth defects of all of the *snu114* alleles. Notably, Prp19 is an E3 ubiquitin ligase, and the *prp19-1* mutation decreases its enzymatic activity (OHI *et al.* 2003). Deletions of the non-essential NTC proteins *ISY1* and *SNT309* (CHEN *et al.* 2001a; CHEN *et al.* 1998; DIX *et al.* 1999) do not interact genetically with the *snu114* alleles.

DISCUSSION

Snu114 is a GTPase with homology to the ribosomal translocase EF-G, suggesting that it may mediate conformational rearrangements in the spliceosome. Based on comparison with EF-G, Snu114 can be divided into five structural domains (I-V), as well as a non-conserved N-terminal domain. In this study, we screened for conditionally lethal alleles of Snu114. We recovered a large number of mutations within the GTPase domain and in three small clusters of amino acids in domains III-V. Additionally, we found that *snu114-60*, which causes an almost complete deletion of the C-terminal domain IVb, causes a conditional growth defect. Domain IVb is larger in Snu114 than in its ribosomal homologs, suggesting that this domain may be important for an interaction specific to splicing. *snu114-60* is synthetically lethal with mutations in *prp8* and in other factors involved in activation of the spliceosome. We propose that domain IVb interacts with Prp8 to influence the activities of the DExD/H box ATPases Prp28 and Brr2 during spliceosome activation.

Structural interpretations: Studies of EF-G and EF2 indicate that GTP hydrolysis causes a substantial movement of domain IV with respect to domains I and II (JORGENSEN *et al.* 2003; STARK *et al.* 2000); (see Figures 1C and 1D). This conformational rearrangement of EF-G/EF2 is predicted to drive movement of tRNA within the ribosome (RODNINA *et al.* 2000). By analogy, GTP hydrolysis by Snu114 may cause rearrangements of the spliceosome.

All members of the GTPase superfamily share a similar architecture of the G domain and contain conserved motifs (G1-G5) that interact with GTP/GDP (BOURNE *et al.* 1991; SPRANG 1997). Our screen for conditionally lethal alleles of Snu114 identified mutations in the G1 and G3 motifs, which are predicted to cause defects in GTP binding and hydrolysis (ANBORGH *et al.* 1989; SIGAL *et al.* 1986; ZEIDLER *et al.* 1995). In multidomain G proteins, the GTP/GDP binding status is communicated to other domains via rearrangements of the G2 and G3 motifs (SPRANG 1997). The clusters of mutations that we identified in domains III and V are located near points of contact with the G3 motif (Figures 1C and 1D). Although the G2 motif is disordered in all EF-G/EF2 structures, comparison with the structure of the GTPase EF-Tu suggests that it is also close to the domain III cluster (LAURBERG *et al.* 2000). Therefore, the mutations that we found in domains III and V may impair a conformational rearrangement of the protein that normally results from GTP hydrolysis.

Domain IV of EF-G is necessary for transmitting a rearrangement within the protein, arising from GTP hydrolysis, into a conformational change of the ribosome, as deletion of IVa or IVa+IVb decreases translocation by ~2000-fold without affecting GTP hydrolysis (MARTEMYANOV and GUDKOV 1999; RODNINA *et al.* 1997; SAVELSBERGH *et*

al. 2000). Notably, deletion of six amino acids in EF-G that correspond to the cluster of mutant amino acids that we identified in Snu114 domain IVa, including *snu114-40*, causes a 300-fold reduction in translocation of the ribosome (SAVELSBERGH *et al.* 2000). Thus, the mutations in Snu114 domain IVa may prevent the transmission of a conformational rearrangement that normally results from GTP hydrolysis or nucleotide exchange. Studies of EF-G/EF2 have not directly addressed the role of domain IVb alone (although this domain is only 20 amino acids in *E. coli*). Based on our finding that deletion of domain IVb (*snu114-60*) causes a conditional growth defect and a splicing defect, we predict that domain IVb could be an interaction domain that communicates conformational changes of Snu114 to other splicing factors.

The βαββαβ structure of domains III, IVa, and V of EF-G is characteristic of the RNA recognition motif (RRM) (ÆVARSSON *et al.* 1994; LAURBERG *et al.* 2000; MURZIN 1995). In RRM domains, hydrophobic residues in two of the β-sheets interact directly with RNA (VARANI and NAGAI 1998). In our mutagenesis of Snu114, we found very few mutations in residues that would be predicted to interact with RNA; thus, our data does not provide evidence for a direct interaction between Snu114 and RNA through the RRM motifs. However, it is possible that we failed to obtain such mutations because they cause lethality or because our screen was not saturating.

Biochemistry and genetics suggest that Snu114 functions during spliceosome activation: We have found that mutations in Snu114 block splicing prior to the first chemical step both *in vivo* and *in vitro*. A first step block to splicing could reflect defects at a number of stages, including snRNP biogenesis and stability, tri-snRNP addition to the spliceosome, and spliceosome activation. In fact, we found that *snu114* mutants

exhibit genetic interactions with splicing mutants that affect each of these stages (Figure 5). However, *snu114* mutants do not interact genetically with any factors that function after the first step of catalysis, in agreement with the biochemical data showing a first step block.

A number of proteins that we tested affect multiple stages of splicing. For example, Prp24 and Sad1 are both implicated in tri-snRNP addition/reorganization as well as in formation of U4/U6 snRNP (KUHN and BROW 2000; LYGEROU *et al.* 1999; MAKAROVA *et al.* 2001; RAGHUNATHAN and GUTHRIE 1998b). The snRNP biogenesis factor *BRR1* exhibits genetic interactions not only with snRNP biogenesis factors, but also with factors that affect spliceosome assembly. Interestingly, *brr1Δ* and the *snu114* alleles are synthetically lethal with many of the same mutations, including *prp24-RRM3sub*, *sub2* mutations, *sad1-1*, and *snu66Δ* (INADA 2004). The genetic interactions observed between *snu114* mutations and *prp24-RRM3sub*, *sad1-1*, and *brr1Δ* could arise because a) all of the proteins are involved in addition and rearrangement of tri-snRNP, b) the function of Snu114 during spliceosome activation is particularly sensitive to low levels of snRNPs, or c) Snu114 is also necessary for snRNP biogenesis. However, *snu114-60*, which has the strongest interactions with *prp24*, *sad1*, and *brr1* mutants, contains wildtype snRNP levels (T.J.B. and C.G., unpublished data).

Snu114 alleles exhibit strong genetic interactions with factors involved in spliceosome activation, including *prp28-1*, *brr2-1*, and *prp8-201* (KUHN *et al.* 1999; RAGHUNATHAN and GUTHRIE 1998a; STALEY and GUTHRIE 1999). We also found strong genetic interactions with deletion of *SNU66* and mutation of *SAD1*, factors involved in tri-snRNP addition (MAKAROVA *et al.* 2001). All of these genetic interactions may be

related, as mutations that block spliceosome activation, including *prp28-1* and *brr2-1*, decrease the interaction of tri-snRNP with the spliceosome (RAGHUNATHAN and GUTHRIE 1998a; STALEY and GUTHRIE 1999), indicating that rearrangements within the tri-snRNP are necessary for its stable association with the spliceosome. Together, these genetic interactions strongly implicate Snu114 in spliceosome activation.

The N- and C- terminal domains of Snu114 are involved in similar functions: Snu114 contains a 120 amino acid N-terminal domain that is not found in EF-G/EF2. Previous studies showed that deletion of this domain (*snu114ΔN*) causes a ts growth defect and a block to the release of U1 and U4 from the spliceosome (BARTELS *et al.* 2002). Similar to the biochemical phenotype of *snu114ΔN*, genetic interactions suggest that *snu114-60* causes defects in spliceosome activation. Furthermore, we found that the presence of a 15 amino acid epitope tag at the N-terminus of Snu114 is synthetically lethal with *snu114-60* at 16° and 37° (Figure 2A), which suggests that the N-terminal domain and domain IVb are both necessary for the same process. If the N- and C-termini are involved in the same function, we predicted that they would exhibit the same genetic interactions. Similarly to *snu114-60*, *snu114ΔN* is synthetically lethal with *prp28-1* and *snu66Δ* and sick with *brr2-1* (T.J.B. and C.G., unpublished data). We conclude that both domains are necessary for tri-snRNP addition/spliceosome activation. It is possible that the N-terminal domain is necessary for the activation of GTPase activity, while the C-terminal domain is necessary to transmit a conformational change driven by GTP hydrolysis. Alternatively, it is possible that both domains must interact with other factors, such as Prp8, in order for a conformational change in Snu114 to be transmitted.

A model for the activity of Snu114: Snu114 and Prp8 physically interact with each other, and both proteins can be crosslinked to U5 snRNA (ACHSEL *et al.* 1998; DIX *et al.* 1998). Thus, interactions between Snu114, Prp8, and U5 snRNA form the core of U5 snRNP. Domain IVa/IVb of Snu114 may be particularly important for this interaction, as *snu114-40* and *snu114-60* are synthetically lethal with *prp8-1* and *prp8-brr*.

Synthetic lethality between *snu114-60* and mutations in factors involved in spliceosome activation indicates a pivotal role for domain IVb in this process. Previous genetic data have suggested that an allosteric interaction between Prp8 and the ATPases Prp28 and Brr2 regulates the timing of spliceosome activation (KUHN and BROW 2000; KUHN *et al.* 2002). The mutations *prp28-1* and *brr2-1* are synthetically lethal with the U4-cs1 mutation, which increases the base pairing between U4 and U6 snRNAs and inhibits the release of U1 and U4 from the spliceosome (KUHN *et al.* 1999; LI and BROW 1996). A large number of *prp8* alleles, including *prp8-201*, can suppress the cold-sensitivity of U4-cs1, and a subset of these *prp8* alleles can suppress *prp28-1* or *brr2-1*. Thus, it has been hypothesized that Prp8 inhibits the activity of the ATPases until spliceosome formation has occurred, while certain mutations of *prp8* may relax this inhibition.

Based on the strong genetic interactions between *SNU114* and *PRP8*, *PRP28*, and *BRR2*, we suggest that Snu114 may regulate Prp8's inhibition of Prp28 and Brr2 (Figure 9). We hypothesize that Snu114 is bound to GTP when tri-snRNP binds to the spliceosome. GTP hydrolysis could be triggered by interactions with U1 snRNP, since Snu114 and the U1 proteins Prp39 and Prp40 interact with neighboring regions of Prp8, according to yeast-two-hybrid analyses (ABOVICH and ROSBASH 1997; DIX *et al.* 1998;

GRAINGER and BEGGS 2005; VAN NUES and BEGGS 2001). Thus, successful interaction with the spliceosome would induce GTP hydrolysis by Snu114 and a concomitant structural rearrangement of domains III-V with relation to the N-terminus. In particular, this may modify the interaction between domain IVb and Prp8, which in turn could alter the conformation of Prp8 and lead to the unwinding of the U1/5' splice site duplex by Prp28 and the U4/U6 duplex by Brr2. It is possible that Prp8 sequesters the RNA helices, and an altered conformation of Prp8 would allow Brr2 and Prp28 access to their substrates. Alternatively, Prp8 could inhibit the ATPase activity of Prp28 and Brr2 via direct physical interactions with the DExD/H-box proteins, and altering the conformation of Prp8 could relieve the inhibition by severing these associations (KUHN and BROW 2000; KUHN *et al.* 2002).

Previous biochemical studies support the model that Snu114 hydrolyzes GTP during spliceosome activation. A mutation that is expected to convert the nucleotide-specificity of Snu114 from GTP to XTP causes a temperature-sensitive block to U1 and U4 release, which can be partially overcome by addition of XTP (BARTELS *et al.* 2003). Non-hydrolyzable XTP did not stimulate snRNA release, suggesting that GTP hydrolysis, and not just GTP binding, is important (BARTELS *et al.* 2003).

For most GTPases, GTPase activating proteins (GAPs) are necessary to stimulate GTP hydrolysis. The ribosome itself serves as the GAP for EF-G and elongation factor Tu (EF-Tu), which delivers aminoacyl tRNA to the ribosome (MOHR *et al.* 2002). In the case of EF-Tu, a cognate codon:anti-codon interaction is required to trigger GTP hydrolysis (RODNINA *et al.* 2005). Because the structure of EF-Tu bound to aminoacyl-tRNA resembles EF-G (NISSEN *et al.* 1995), and because EF-G and Snu114 are

homologous, it is tempting to speculate that interactions between spliceosomal components and Snu114 domain IV, which would correspond to the anticodon arm of tRNA, may be necessary to trigger GTPase activity. Just as GTP hydrolysis by EF-Tu functions as a checkpoint to ensure that the appropriate aminoacyl tRNA is retained in the ribosome, GTP hydrolysis by Snu114 after addition of tri-snRNP could serve as a checkpoint to ensure proper formation of the spliceosome. It will be informative to investigate what components of the spliceosome function as a GAP for Snu114. Additionally, we are interested in testing whether mutations in domain IV of Snu114 directly affect GTP binding and hydrolysis.

A link to ubiquitination: Strong genetic interactions between Snu114 and proteins that are involved in ubiquitin metabolism suggest that a cycle of ubiquitination could affect splicing. In a large-scale proteomics study, Snu114 was one of only three splicing proteins, including Sad1, that were found to be ubiquitinated (PENG *et al.* 2003). Interestingly, Sad1, which has strong genetic interactions with Snu114, contains a ubiquitin hydrolase domain (COSTANZO *et al.* 2000). Prp19, which we also found to interact genetically with Snu114, is a member of the U-box family of E3 ubiquitin ligases (HATAKEYAMA *et al.* 2001). The *prp19-1* mutation specifically disrupts the fold of the U-box domain and greatly decreases ubiquitin ligase activity *in vitro* (OHI *et al.* 2003). Lastly, the Snu114-interacting protein Prp8 contains a Jab/MPN domain, which is typically associated with ubiquitin removal (MAYTAL-KIVITY *et al.* 2002; VERMA *et al.* 2002). Thus, the genetic interactions with *sad1-1*, *prp19-1*, and *prp8* mutants could reflect the requirement for a cycle of ubiquitination and de-ubiquitination of Snu114. Currently, the timing of Snu114 ubiquitination is not known. One possibility is that after

U5 snRNP is released from the post-catalytic spliceosome in complex with the NTC (MAKAROV *et al.* 2002), ubiquitination of Snu114 by Prp19 induces dissociation of the two particles. Ubiquitin removal by Sad1 during the following round of spliceosome assembly could promote tri-snRNP binding or spliceosome activation. The particularly strong genetic interactions between *sad1-1* and *snu114* mutations suggests that de-ubiquitination of Snu114 is essential for splicing. Ubiquitination of Snu114 may also affect its interactions with Prp8, as Prp8 is predicted to bind ubiquitin via its Jab/MPN domain. We are most interested in determining when during splicing Snu114 is ubiquitinated, and how this is affected by mutations in *PRP19*, *SAD1*, and *PRP8*.

ACKNOWLEDGEMENTS

We thank Beate Schwer, Patrizia Fabrizio, Scott Stevens, and Dave Brow for strains and plasmids, Jean Beggs for communicating results prior to publication, Marcy Diaz for assistance with genetic crosses, and Michael Dinglasan and Jorge Mendoza for excellent technical assistance. Thanks to John Abelson, Elizabeth Blackburn, Hiten Madhani, Mike Springer, Miri VanHoven, and members of the Guthrie lab for discussions and comments on the manuscript. T.J.B. is a Howard Hughes Medical Institute predoctoral fellow. C.G. is an American Cancer Society Research Professor of Molecular Genetics. This work was supported by National Institutes of Health Grant GM21119.

LITERATURE CITED

ABOVICH, N., and M. ROSBASH, 1997 Cross-intron bridging interactions in the yeast commitment complex are conserved in mammals. Cell **89:** 403-412.

ACHSEL, T., K. AHRENS, H. BRAHMS, S. TEIGELKAMP and R. LUHRMANN, 1998 The human U5-220kD protein (hPrp8) forms a stable RNA-free complex with several U5-specific proteins, including an RNA unwindase, a homologue of ribosomal

elongation factor EF-2, and a novel WD-40 protein. Mol. Cell. Biol. **18:** 6756-6766.

ÆVARSSON, A., 1995 Structure-based sequence alignment of elongation factors Tu and G with related GTPases involved in translation. J. Mol. Evol. **41:** 1096-1104.

ÆVARSSON, A., E. BRAZHNIKOV, M. GARBER, J. ZHELTONOSOVA, Y. CHIRGADZE et al., 1994 Three-dimensional structure of the ribosomal translocase: elongation factor G from Thermus thermophilus. EMBO J. **13:** 3669-3677.

ANBORGH, P. H., R. H. COOL, M. JACQUET, G. PARLATO and A. PARMEGGIANI, 1989 Structure-function relationships of the GTP-binding domain of Elongation Factor Tu, pp. 67-75 in *The guanine-nucleotide binding proteins: common structural and functional properties*, edited by L. BOSCH, B. KRAAL and A. PARMEGGIANI. Plenum Press, New York.

ARENAS, J. E., and J. N. ABELSON, 1997 Prp43: An RNA helicase-like factor involved in spliceosome disassembly. Proc. Natl. Acad. Sci. U S A **94:** 11798-11802.

BARTELS, C., C. KLATT, R. LUHRMANN and P. FABRIZIO, 2002 The ribosomal translocase homologue Snu114p is involved in unwinding U4/U6 RNA during activation of the spliceosome. EMBO Rep. **3:** 875-880.

BARTELS, C., H. URLAUB, R. LUHRMANN and P. FABRIZIO, 2003 Mutagenesis suggests several roles of Snu114p in pre-mRNA splicing. J. Biol. Chem. **278:** 28324-28334.

BOORSTEIN, W. R., and E. A. CRAIG, 1989 Primer extension analysis of RNA. Methods Enzymol. **180:** 347-369.

BOURNE, H. R., D. A. SANDERS and F. MCCORMICK, 1991 The GTPase superfamily: conserved structure and molecular mechanism. Nature **349:** 117-127.

BROW, D. A., 2002 Allosteric cascade of spliceosome activation. Annu. Rev. Genet. **36:** 333-360.

BROWN, J. D., and J. D. BEGGS, 1992 Roles of PRP8 protein in the assembly of splicing complexes. EMBO J. **11:** 3721-3729.

BURGE, C. B., T. H. TUSCHL and P. A. SHARP, 1998 Splicing of precursors to mRNAs by the spliceosomes, pp. 525-560 in *RNA World II*, edited by R. F. GESTELAND, T. R.

CECH and J. F. ATKINS. Cold Spring Harbor Laboratory Press, Cold Spring Harbor, NY.

BURGESS, S. M., and C. GUTHRIE, 1993 A mechanism to enhance mRNA splicing fidelity: the RNA-dependent ATPase Prp16 governs usage of a discard pathway for aberrant lariat intermediates. Cell **73:** 1377-1391.

CAMMARANO, P., P. PALM, R. CRETI, E. CECCARELLI, A. M. SANANGELANTONI et al., 1992 Early evolutionary relationships among known life forms inferred from elongation factor EF-2/EF-G sequences: phylogenetic coherence and structure of the archaeal domain. J. Mol. Evol. **34:** 396-405.

CHAN, S. P., D. I. KAO, W. Y. TSAI and S. C. CHENG, 2003 The Prp19p-associated complex in spliceosome activation. Science **302:** 279-282.

CHEN, C. H., W. Y. TSAI, H. R. CHEN, C. H. WANG and S. C. CHENG, 2001a Identification and characterization of two novel components of the Prp19p-associated complex, Ntc30p and Ntc20p. J. Biol. Chem. **276:** 488-494.

CHEN, H. R., S. P. JAN, T. Y. TSAO, Y. J. SHEU, J. BANROQUES et al., 1998 Snt309p, a component of the Prp19p-associated complex that interacts with Prp19p and associates with the spliceosome simultaneously with or immediately after dissociation of U4 in the same manner as Prp19p. Mol. Cell. Biol. **18:** 2196-2204.

CHEN, J. Y., L. STANDS, J. P. STALEY, R. R. JACKUPS, JR., L. J. LATUS et al., 2001b Specific alterations of U1-C protein or U1 small nuclear RNA can eliminate the requirement of Prp28p, an essential DEAD box splicing factor. Mol. Cell **7:** 227-232.

COLLINS, C. A., 2001 Genetic and biochemical analysis of interactions involving Prp8 and RNA at the catalytic core of the spliceosome. PhD thesis. Department of Biochemistry and Biophysics, University of California, San Francisco.

COLLINS, C. A., and C. GUTHRIE, 2000 The question remains: is the spliceosome a ribozyme? Nat. Struct. Biol. **7:** 850-854.

COMPANY, M., J. ARENAS and J. ABELSON, 1991 Requirement of the RNA helicase-like protein PRP22 for release of messenger RNA from spliceosomes. Nature **349:** 487-493.

COSTANZO, M. C., J. D. HOGAN, M. E. CUSICK, B. P. DAVIS, A. M. FANCHER et al., 2000 The yeast proteome database (YPD) and Caenorhabditis elegans proteome database (WormPD): comprehensive resources for the organization and comparison of model organism protein information. Nucleic Acids Res. **28:** 73-76.

CZWORKOWSKI, J., J. WANG, T. A. STEITZ and P. B. MOORE, 1994 The crystal structure of elongation factor G complexed with GDP, at 2.7 A resolution. EMBO J. **13:** 3661-3668.

DELANO, W. L., 2002 The PyMOL Molecular Graphics System. on World Wide Web http://www.pymol.org

DIX, I., C. RUSSELL, S. B. YEHUDA, M. KUPIEC and J. D. BEGGS, 1999 The identification and characterization of a novel splicing protein, Isy1p, of Saccharomyces cerevisiae. RNA **5:** 360-368.

DIX, I., C. S. RUSSELL, R. T. O'KEEFE, A. J. NEWMAN and J. D. BEGGS, 1998 Protein-RNA interactions in the U5 snRNP of *Saccharomyces cerevisiae*. RNA **4:** 1239-1250.

DOYE, V., and E. C. HURT, 1995 Genetic approaches to nuclear pore structure and function. Trends Genet. **11:** 235-241.

ELLEDGE, S. J., and R. W. DAVIS, 1988 A family of versatile centromeric vectors designed for use in the sectoring-shuffle mutagenesis assay in Saccharomyces cerevisiae. Gene **70:** 303-312.

FABRIZIO, P., B. LAGGERBAUER, J. LAUBER, W. S. LANE and R. LUHRMANN, 1997 An evolutionarily conserved U5 snRNP-specific protein is a GTP-binding factor closely related to the ribosomal translocase EF-2. EMBO J. **16:** 4092-4106.

GIAEVER, G., A. M. CHU, L. NI, C. CONNELLY, L. RILES et al., 2002 Functional profiling of the Saccharomyces cerevisiae genome. Nature **418:** 387-391.

GOTTSCHALK, A., G. NEUBAUER, J. BANROQUES, M. MANN, R. LUHRMANN et al., 1999 Identification by mass spectrometry and functional analysis of novel proteins of the yeast [U4/U6.U5] tri-snRNP. EMBO J. **18:** 4535-4548.

GRAINGER, R. J., and J. D. BEGGS, 2005 Prp8 protein: At the heart of the spliceosome. RNA In press.

GUARENTE, L., 1993 Synthetic enhancement in gene interaction: a genetic tool come of age. Trends Genet. **9:** 362-366.

HATAKEYAMA, S., M. YADA, M. MATSUMOTO, N. ISHIDA and K. I. NAKAYAMA, 2001 U box proteins as a new family of ubiquitin-protein ligases. J. Biol. Chem. **276:** 33111-33120.

INADA, M., 2004 Genetic, biochemical and genomic analyses of RNP biogenesis in *S. cerevisiae*. PhD thesis. Department of Biochemistry and Biophysics, University of California, San Francisco.

JORGENSEN, R., P. A. ORTIZ, A. CARR-SCHMID, P. NISSEN, T. G. KINZY et al., 2003 Two crystal structures demonstrate large conformational changes in the eukaryotic ribosomal translocase. Nat. Struct. Biol. **10:** 379-385.

JURICA, M. S., and M. J. MOORE, 2003 Pre-mRNA splicing: awash in a sea of proteins. Mol. Cell **12:** 5-14.

KIM, D. H., and J. J. ROSSI, 1999 The first ATPase domain of the yeast 246-kDa protein is required for in vivo unwinding of the U4/U6 duplex. RNA **5:** 959-971.

KIM, S. H., and R. J. LIN, 1996 Spliceosome activation by PRP2 ATPase prior to the first transesterification reaction of pre-mRNA splicing. Mol. Cell. Biol. **16:** 6810-6819.

KISTLER, A. L., and C. GUTHRIE, 2001 Deletion of MUD2, the yeast homolog of U2AF65, can bypass the requirement for sub2, an essential spliceosomal ATPase. Genes Dev. **15:** 42-49.

KUHN, A. N., and D. A. BROW, 2000 Suppressors of a cold-sensitive mutation in yeast U4 RNA define five domains in the splicing factor Prp8 that influence spliceosome activation. Genetics **155:** 1667-1682.

KUHN, A. N., Z. LI and D. A. BROW, 1999 Splicing factor Prp8 governs U4/U6 RNA unwinding during activation of the spliceosome. Mol. Cell **3:** 65-75.

KUHN, A. N., E. M. REICHL and D. A. BROW, 2002 Distinct domains of splicing factor Prp8 mediate different aspects of spliceosome activation. Proc. Natl. Acad. Sci. U S A **99:** 9145-9149.

LAGGERBAUER, B., T. ACHSEL and R. LUHRMANN, 1998 The human U5-200kD DEXH-box protein unwinds U4/U6 RNA duplices in vitro. Proc. Natl. Acad. Sci. U S A **95:** 4188-4192.

LAURBERG, M., O. KRISTENSEN, K. MARTEMYANOV, A. T. GUDKOV, I. NAGAEV et al., 2000 Structure of a mutant EF-G reveals domain III and possibly the fusidic acid binding site. J. Mol. Biol. **303:** 593-603.

LI, Z., and D. A. BROW, 1996 A spontaneous duplication in U6 spliceosomal RNA uncouples the early and late functions of the ACAGA element in vivo. RNA **2:** 879-894.

LIBRI, D., N. GRAZIANI, C. SAGUEZ and J. BOULAY, 2001 Multiple roles for the yeast SUB2/yUAP56 gene in splicing. Genes Dev. **15:** 36-41.

LYGEROU, Z., G. CHRISTOPHIDES and B. SERAPHIN, 1999 A novel genetic screen for snRNP assembly factors in yeast identifies a conserved protein, Sad1p, also required for pre-mRNA splicing. Mol. Cell Biol. **19:** 2008-2020.

MAKAROV, E. M., O. V. MAKAROVA, H. URLAUB, M. GENTZEL, C. L. WILL et al., 2002 Small nuclear ribonucleoprotein remodeling during catalytic activation of the spliceosome. Science **298:** 2205-2208.

MAKAROVA, O. V., E. M. MAKAROV and R. LUHRMANN, 2001 The 65 and 110 kDa SR-related proteins of the U4/U6.U5 tri-snRNP are essential for the assembly of mature spliceosomes. EMBO J. **20:** 2553-2563.

MARTEMYANOV, K. A., and A. T. GUDKOV, 1999 Domain IV of elongation factor G from Thermus thermophilus is strictly required for translocation. FEBS Lett **452:** 155-159.

MARTIN, A., S. SCHNEIDER and B. SCHWER, 2002 Prp43 is an essential RNA-dependent ATPase required for release of lariat-intron from the spliceosome. J Biol. Chem. **277:** 17743-17750.

MAYTAL-KIVITY, V., N. REIS, K. HOFMANN and M. H. GLICKMAN, 2002 MPN+, a putative catalytic motif found in a subset of MPN domain proteins from eukaryotes and prokaryotes, is critical for Rpn11 function. BMC Biochem. **3:** 28.

MOHR, D., W. WINTERMEYER and M. V. RODNINA, 2002 GTPase activation of elongation factors Tu and G on the ribosome. Biochemistry **41:** 12520-12528.

MOORE, M. J., C. C. QUERY and P. A. SHARP, 1993 Splicing of precursors to mRNA by the spliceosome, pp. 303-357 in *The RNA World*, edited by R. F. GESTELAND and J. F. ATKINS. Cold Spring Harbor Laboratory Press, Cold Spring Harbor, NY.

MUHLRAD, D., R. HUNTER and R. PARKER, 1992 A rapid method for localized mutagenesis of yeast genes. Yeast **8:** 79-82.

MURZIN, A. G., 1995 A ribosomal protein module in EF-G and DNA gyrase. Nat. Struct. Biol. **2:** 25-26.

NISSEN, P., M. KJELDGAARD, S. THIRUP, G. POLEKHINA, L. RESHETNIKOVA et al., 1995 Crystal structure of the ternary complex of Phe-tRNAPhe, EF-Tu, and a GTP analog. Science **270:** 1464-1472.

NOBLE, S. M., and C. GUTHRIE, 1996 Transcriptional pulse-chase analysis reveals a role for a novel snRNP-associated protein in the manufacture of spliceosomal snRNPs. EMBO J. **15:** 4368-4379.

OGG, S. C., W. P. BARZ and P. WALTER, 1998 A functional GTPase domain, but not its transmembrane domain, is required for function of the SRP receptor beta-subunit. J. Cell. Biol. **142:** 341-354.

OHI, M. D., C. W. VANDER KOOI, J. A. ROSENBERG, W. J. CHAZIN and K. L. GOULD, 2003 Structural insights into the U-box, a domain associated with multi-ubiquitination. Nat. Struct. Biol. **10:** 250-255.

PENG, J., D. SCHWARTZ, J. E. ELIAS, C. C. THOREEN, D. CHENG et al., 2003 A proteomics approach to understanding protein ubiquitination. Nat. Biotechnol. **21:** 921-926.

RADER, S. D., and C. GUTHRIE, 2002 A conserved Lsm-interaction motif in Prp24 required for efficient U4/U6 di-snRNP formation. RNA **8:** 1378-1392.

RAGHUNATHAN, P. L., and C. GUTHRIE, 1998a RNA unwinding in U4/U6 snRNPs requires ATP hydrolysis and the DEIH-box splicing factor Brr2. Curr. Biol. **8:** 847-855.

RAGHUNATHAN, P. L., and C. GUTHRIE, 1998b A spliceosomal recycling factor that reanneals U4 and U6 small nuclear ribonucleoprotein particles. Science **279:** 857-860.

RODNINA, M. V., K. B. GROMADSKI, U. KOTHE and H. J. WIEDEN, 2005 Recognition and selection of tRNA in translation. FEBS Lett. **579:** 938-942.

RODNINA, M. V., A. SAVELSBERGH, V. I. KATUNIN and W. WINTERMEYER, 1997 Hydrolysis of GTP by elongation factor G drives tRNA movement on the ribosome. Nature **385:** 37-41.

RODNINA, M. V., H. STARK, A. SAVELSBERGH, H. J. WIEDEN, D. MOHR et al., 2000 GTPases mechanisms and functions of translation factors on the ribosome. Biol. Chem. **381:** 377-387.

RUBY, S. W., T. H. CHANG and J. ABELSON, 1993 Four yeast spliceosomal proteins (PRP5, PRP9, PRP11, and PRP21) interact to promote U2 snRNP binding to pre-mRNA. Genes Dev. **7:** 1909-1925.

SALI, A., and T. L. BLUNDELL, 1993 Comparative protein modelling by satisfaction of spatial restraints. J. Mol. Biol. **234:** 779-815.

SAVELSBERGH, A., N. B. MATASSOVA, M. V. RODNINA and W. WINTERMEYER, 2000 Role of domains 4 and 5 in elongation factor G functions on the ribosome. J. Mol. Biol. **300:** 951-961.

SCHMITT, M. E., T. A. BROWN and B. L. TRUMPOWER, 1990 A rapid and simple method for preparation of RNA from Saccharomyces cerevisiae. Nucleic Acids Res. **18:** 3091-3092.

SCHWER, B., and C. GUTHRIE, 1991 PRP16 is an RNA-dependent ATPase that interacts transiently with the spliceosome. Nature **349:** 494-499.

SCHWER, B., and T. MESZAROS, 2000 RNA helicase dynamics in pre-mRNA splicing. EMBO J. **19:** 6582-6591.

SIGAL, I. S., J. B. GIBBS, J. S. D'ALONZO, G. L. TEMELES, B. S. WOLANSKI et al., 1986 Mutant ras-encoded proteins with altered nucleotide binding exert dominant biological effects. Proc. Natl. Acad. Sci. U S A **83:** 952-956.

SIKORSKI, R. S., and P. HIETER, 1989 A system of shuttle vectors and yeast host strains designed for efficient manipulation of DNA in Saccharomyces cerevisiae. Genetics **122:** 19-27.

SPRANG, S. R., 1997 G protein mechanisms: insights from structural analysis. Annu. Rev. Biochem. **66:** 639-678.

STALEY, J. P., and C. GUTHRIE, 1998 Mechanical devices of the spliceosome: motors, clocks, springs, and things. Cell **92:** 315-326.

STALEY, J. P., and C. GUTHRIE, 1999 An RNA switch at the 5' splice site requires ATP and the DEAD box protein Prp28p. Mol. Cell. **3:** 55-64.

STARK, H., M. V. RODNINA, H. J. WIEDEN, M. VAN HEEL and W. WINTERMEYER, 2000 Large-scale movement of elongation factor G and extensive conformational change of the ribosome during translocation. Cell **100:** 301-309.

STEVENS, S. W., I. BARTA, H. Y. GE, R. E. MOORE, M. K. YOUNG et al., 2001 Biochemical and genetic analyses of the U5, U6, and U4/U6 x U5 small nuclear ribonucleoproteins from Saccharomyces cerevisiae. RNA **7:** 1543-1553.

STEVENS, S. W., D. E. RYAN, H. Y. GE, R. E. MOORE, M. K. YOUNG et al., 2002 Composition and functional characterization of the yeast spliceosomal penta-snRNP. Mol. Cell **9:** 31-44.

STRAUSS, E. J., and C. GUTHRIE, 1991 A cold-sensitive mRNA splicing mutant is a member of the RNA helicase gene family. Genes Dev. **5:** 629-641.

TARN, W. Y., K. R. LEE and S. C. CHENG, 1993 Yeast precursor mRNA processing protein PRP19 associates with the spliceosome concomitant with or just after dissociation of U4 small nuclear RNA. Proc. Natl. Acad. Sci. U S A **90:** 10821-10825.

THOMPSON, J. D., D. G. HIGGINS and T. J. GIBSON, 1994 CLUSTAL W: improving the sensitivity of progressive multiple sequence alignment through sequence weighting, position-specific gap penalties and weight matrix choice. Nucleic Acids Res. **22:** 4673-4680.

UMEN, J. G., and C. GUTHRIE, 1995 A novel role for a U5 snRNP protein in 3' splice site selection. Genes Dev. **9:** 855-868.

UMEN, J. G., and C. GUTHRIE, 1996 Mutagenesis of the yeast gene PRP8 reveals domains governing the specificity and fidelity of 3' splice site selection. Genetics **143:** 723-739.

VAN NUES, R. W., and J. D. BEGGS, 2001 Functional contacts with a range of splicing proteins suggest a central role for Brr2p in the dynamic control of the order of events in spliceosomes of Saccharomyces cerevisiae. Genetics **157:** 1451-1467.

VARANI, G., and K. NAGAI, 1998 RNA recognition by RNP proteins during RNA processing. Annu. Rev. Biophys. Biomol. Struct. **27:** 407-445.

VERMA, R., L. ARAVIND, R. OANIA, W. H. MCDONALD, J. R. YATES, 3RD et al., 2002 Role of Rpn11 metalloprotease in deubiquitination and degradation by the 26S proteasome. Science **298:** 611-615.

VIDAVER, R. M., D. M. FORTNER, L. S. LOOS-AUSTIN and D. A. BROW, 1999 Multiple functions of Saccharomyces cerevisiae splicing protein Prp24 in U6 RNA structural rearrangements. Genetics **153:** 1205-1218.

VIJAYRAGHAVAN, U., M. COMPANY and J. ABELSON, 1989 Isolation and characterization of pre-mRNA splicing mutants of Saccharomyces cerevisiae. Genes Dev. **3:** 1206-1216.

WANG, Y., and C. GUTHRIE, 1998 PRP16, a DEAH-box RNA helicase, is recruited to the spliceosome primarily via its nonconserved N-terminal domain. RNA **4:** 1216-1229.

ZEIDLER, W., C. EGLE, S. RIBEIRO, A. WAGNER, V. KATUNIN et al., 1995 Site-directed mutagenesis of Thermus thermophilus elongation factor Tu. Replacement of His85, Asp81 and Arg300. Eur. J. Biochem. **229:** 596-604.

ZHANG, M., and M. R. GREEN, 2001 Identification and characterization of yUAP/Sub2p, a yeast homolog of the essential human pre-mRNA splicing factor hUAP56. Genes Dev. **15:** 30-35.

Table 1. Yeast strains used in this study.

Strain	Genotype
yTB2	*MAT* **a** *trp1-Δ1 his3-Δ ura3-52 lys2-801 ade2-101 snu114::HIS3* pTB1
yTB13	*MAT* **a** *lys2Δ trp1Δ snu114::KanMX* pTB1
yTB23	*MAT* **a** *lys2Δ snu114::KanMX* pTB1
yTB100	*MAT* **a** *lys2Δ snu66::KanMX*
yTB102	*MAT* **a** *lys2Δ snu66::KanMX snu114::KAN* pTB1
yTB103	*MAT* **a** *lys2Δ brr2::KanMX snu114::KAN* pTB1 pPR151
yTB105	*MAT* **a** *lys2Δ brr2::KanMX snu114::KAN* pTB1 pTB150
yTB106	*MAT* α *lys2Δ met15Δ prp28::KanMX snu114::KanMX* pTB1 pPR9
yTB107	*MAT* α *lys2Δ met15Δ prp28::KanMX snu114::KanMX* pTB1 pPR8
yTB108	*MAT* **a** *lys2Δ trp1Δ prp8::LYS2 snu114::KanMX* pTB1 ySN25
yTB111	*MAT* α *lys2Δ trp1Δ snu114::KanMX isy1::KanMX* pTB1
yTB117	*MAT* α *HIS3 prp5-1 snu114::KanMX* pTB1
yTB118	*MAT* α *HIS3 snu114::KanMX* pTB1
yTB128	*MAT* α *met15Δ*
yTB133	*MAT* α *lys2Δ brr1::KanMX snu114::KanMX* pTB1
yTB134	*MAT* **a** *trp1Δ prp22::KanMX snu114::KanMX* pTB1 pTB122
yTB135	*MAT* **a** *trp1Δ lys2Δ prp43::KanMX snu114::KanMX* pTB1 pTB123
yTB136	*MAT* **a** *lys2Δ met15Δ prp24::KanMX snu114::KanMX* pTB1 pPR097
yTB139	*MAT* **a** *lys2Δ snt309::KanMX snu114::KanMX* pTB1
yTB142	*MAT* α *met15Δ sad1-1 snu114::KanMX* pTB1
yTB143	*MAT* α *met15Δ snu114::KanMX* pTB1
yTB144	*MAT* α *lys2Δ prp19-1 snu114::KanMX* pTB1
yTB145	*MAT* α *lys2Δ snu114::KanMX* pTB1
yTB146	*MAT* α *lys2Δ prp2-1 snu114::KanMX* pTB1
yTB148	*MAT* **a** *lys2Δ met15Δ sub2::KanMX snu114::KanMX* pTB1 pCG466
yTB163	*MAT* α *met15Δ snu114-40*
yTB165	*MAT* α *met15Δ snu114-60*
yTB171	*MAT* α *met15Δ snu114-12*
yTV161	*MAT* **a** *trp1 lys2 prp16::LYS snu114::KanMX* pSB2 pTB1

All strains are *his3Δ leu2Δ ura3Δ* unless otherwise noted.

Table 2. Plasmids used in this study.

Name	Genotype	Source/reference
pPR8	pSE362/*PRP28*	P. Raghunathan
pPR9	pSE362/*prp28-1*	P. Raghunathan
pPR150	pSE362/*BRR2-pya*	RAGHUNATHAN and GUTHRIE (1998)
pPR151	pSE362/*brr2-1-pya*	RAGHUNATHAN and GUTHRIE (1998)
pSN25	YCp50/*PRP8*	S. Noble
pJU204	pSE362/*PRP8-HA3*	UMEN and GUTHRIE (1995)
pAK338	pSE362/*prp8-1-HA3*	A. Kutach
pJU206	pSE362/*prp8-101-HA3*	UMEN and GUTHRIE (1995)
pCC18	pSE362/*prp8-brr-HA3*	C. Collins, S. Noble
pCC11	pRS424/*PRP8*	C. Collins
pCC121	pRS424/*prp8-201*	C. Collins, D. Brow
pPR97	pSE360/*PRP24*	RADER and GUTHRIE (2002)
pPR113	pSE362/*PRP24*	RADER and GUTHRIE (2002)
pSR53	pSE362/*prp24-RRM3sub*	RADER and GUTHRIE (2002)
pSR70	pSE362/*prp24-RRM4sub*	RADER and GUTHRIE (2002)
pSR39	pSE362/*prp24Δ10*	RADER and GUTHRIE (2002)
pCG466	pRS316/*SUB2*	KISTLER and GUTHRIE (2001)
pAK354	pRS313/*SUB2*	KISTLER and GUTHRIE (2001)
pAK356	pRS313/*sub2-1*	KISTLER and GUTHRIE (2001)
pAK355	pRS313/*sub2-5*	KISTLER and GUTHRIE (2001)
pSB2	pSE360/*PRP16*	BURGESS and GUTHRIE (1993)
pSB58	pSE358/*PRP16*	BURGESS and GUTHRIE (1993)
BHM108	pSE358/*prp16-101*	H. Madhani
BHM109	pSE358/*prp16-1*	H. Madhani
BHM110	pSE358/*prp16-2*	H. Madhani
BHM115	pSE358/*prp16-302*	H. Madhani
pTB1	pRS316/*SNU114*	FABRIZIO *et al.* (1997)
pTB2	pRS314/*SNU114*	This study
pTB3	pRS316/*SNU114* + *Eco*RI/*Bgl*II sites	This study
pTB4	pRS314/*SNU114* + *Eco*RI/*Bgl*II sites	This study
pTB19	pRS314/myc-*SNU114*	This study
pTB75	pRS314/myc-*snu114-60*	This study
pTB115	pSE358/*PRP22*	SCHWER and MESZAROS (2000)
pTB116	pSE358/*prp22-H606A*	SCHWER and MESZAROS (2000)
pTB117	pSE358/*prp22-R805A*	SCHWER and MESZAROS (2000)
pTB118	pSE358/*PRP43*	MARTIN *et al.* (2002)
pTB119	pSE358/*prp43-H218A*	MARTIN *et al.* (2002)
pTB120	pSE358/*prp43-G429A*	MARTIN *et al.* (2002)
pTB121	pSE358/*prp43(91-732)*	MARTIN *et al.* (2002)
pTB122	pSE360/*PRP22*	SCHWER and MESZAROS (2000)
pTB123	pSE360/*PRP43*	MARTIN *et al.* (2002)

pRS plasmids are described by SIKORSKI and HIETER (1989) and pSE plasmids are described by ELLEDGE and DAVIS (1988).

Table 3. *SNU114* alleles generated by PCR mutagenesis of domains N, I, and II (Fragment 1).

	Name	Alleles used in this study	Growth 37°	Growth 16°	G1 143-149	G3 216-221	Other
	1A-4		+	+++	L149S		N135S, I191S
	1A-6		+	+++	H143R	H218R	
	1A-9		+	+++	S144P		F298L
*	1A-11		-/+	+++			V227D
*	1A-79	*snu114-14*	+	+			L381P
	1C-4		-/+	+++	T147A		Y178C
	1C-5		-/+	+++			L199P, F320L, L435P
	1C-6		-/+	+++			S196P, K325E
	1C-8		-	+++		P216N	S256G, H334Y
	1C-11		+	+++			T321A, F592C
	1C-12		-/+	+++			F19L, N135D, L425P, I488M, D529N, D532N
	1C-13		-/+	+++		H218R	E67V, F265L
	1C-16		-/+	+++			D233G, L589P
	1C-20		-/+	+++		F221S	S339F
	1C-23		-/+	+++	S144L		T107A, D497G
	1C-28		-/+	+++	S148P		T88A, T321A, E365G, L611S

Alleles containing a single mutation are marked by an asterisk (*). Growth at 37° and 16° were scored, as compared to WT (+++). Mutations in the G1 and G3 motifs are listed under the appropriate heading, while remaining mutations are listed as "other."

Table 4. *SNU114* alleles generated by PCR mutagenesis of domains III-V (Fragment 2).

	Name	Alleles used in this study	Growth 37	Growth 16	Domain III 646-664	Domain IVa 842-851	Domain V 909-928	Domain IVb Truncation	Other
*	2A-1		-/+	+++	G648V				
	2A-4		++	+++	D658G		D917G		
*	2A-5	*snu114-30*	-/+	+++	G646R				
*	2A-9		-/+	+++	G646R				
*	2A-11		+	+++	L659P				
	2A-13		-	-/+	S662G	C846R, L851R			
	2A-15		-/+	+++		C846R			N623S
	2A-16	*snu114-50*	-/+	+++			E910G, C928R		
	2A-17		-/+	+++	G646E	L851Q			
	2A-18	*snu114-62*	+	+++				G986fs	V940A
	2A-20		-/+	+++		V848I	S911P		F768S
	2A-24		+	+++	L659R				N743S
*	2B-107	*myc-snu114-60*[a]	-/+	-				K939ns	
	2B-119	*snu114-61*	++	++				G942fs	D585G, N683S
	2C-2		-/+	+++	D653V, A664T				I795T, V876A
	2C-3		-/+	+++	L645P				T753I
	2C-7		-	+++			C928R		N770D, N772D
	2C-9		-	+++		L851P	G913R		
*	2C-11	*snu114-40*	-/+	+++		M842R			
	2C-12		-/+	+++					L607P, L622P, Q721R, I750V
	2C-13		+	+++	L645P				E811K
	2C-14		-/+	+++	Y651C	C846R			
	2C-16		-	+++			I909T		A712P, P812L, K819I

Alleles containing a single mutation are marked by an asterisk (*). Growth at 37° and 16° were scored, as compared to WT (+++). Mutations that were found in small clusters in domain III (aa 646-664), domain IVa (aa 842-851), and domain V (aa 909-928) are listed under the appropriate heading, while remaining mutations are listed as "other." Three alleles with truncations of domain IVb were found; fs = frameshift mutation, ns = nonsense mutation.

[a] *myc-snu114-60* should be compared to *snu114-60* (Table 5).

Table 5. Alleles resulting from site-directed mutagenesis or cloning.

Alleles used in this study	Mutation	Motif	Growth	
			37°	16°
	T147N[a]	G1	-/+	+++
snu114-15	K146I[a]	G1	-	+++
snu114-12	P216N[b]	G3	-/+	+++
	H218R[c]	G3	+	+++
	E910G[d]		+++	+++
	C928R[d]		+++	+++
snu114-60	K939ns[e]		++	++

Growth was scored at 37° and 16°, as compared to WT (+++).
[a] Site-directed mutations based on OGG *et al.* (1998).
[b] Site-directed mutation based on allele 1C-8 (Table 3).
[c] Site-directed mutation based on alleles 1A-6 and 1C-13 (Table 3).
[d] Separation of mutations in *snu114-50* by cloning (Table 4).
[e] Removal of myc tag from *myc-snu114-60* (Table 4).

Table 6. Synthetic interactions between *snu114* alleles and alleles of other splicing factors.

			***snu114* allele**						
Allele	**Activity**	**Particle**	*-12*	*-14*	*-15*	*-30*	*-40*	*-50*	*-60*
prp5-1	ATPase		0	0	0	0	0	0	0
sub2-1	ATPase		1	1	1	1	1	1	0
sub2-5			1	0	3	1	2	2	0
prp24-RRM3sub			0	0	0	0	0	0	3
prp24-RRM4sub			0	0	0	0	0	0	1
prp24-CT10			0	0	0	0	0	0	1
brr1Δ			2	2	2	2	2	2	4
prp8-1		U5/tri-snRNP	3	2	3	3	4	4	5
prp8-brr			3	0	3	0	5	1	5
prp8-201			2	1	2	0	3	2	5
prp8-101			1	1	1	0	0	0	2
sad1-1		tri-snRNP	5	5	5	4	5	4	5
snu66Δ		tri-snRNP	3	3	3	0	0	3	5
prp28-1	ATPase	U5 snRNP	3	3	3	0	0	0	5
brr2-1	ATPase	U5/tri-snRNP	0	1	0	0	2	0	4
prp19-1		NTC	3	3	3	3	1	2	3
isy1Δ		NTC	0	0	0	0	0	0	0
snt309Δ		NTC	0	0	0	0	0	0	0
prp2-1	ATPase		2	2	2	2	2	2	0
prp16-1	ATPase		0	0	0	0	0	0	0
prp16-2			0	0	0	0	0	0	0
prp16-101			0	0	0	0	0	0	0
prp16-302			0	0	0	0	0	0	0
prp22-R805A	ATPase		1	1	1	1	1	1	0
prp22-H606A			0	0	0	0	0	0	0
prp43-H218A	ATPase		0	0	0	0	0	0	0
prp43-G429A			0	0	0	0	0	0	0
prp43(91-732)			0	0	0	0	0	0	0

The strength of synthetic enhancement, based on changes in growth rate at 16°, 25°, 30°, and 37°, was rated on a scale of 0 (no interaction) to 5 (synthetic lethality). Boxes are shaded according to strength of interaction.

Figure 1. Mutagenesis of *SNU114* and mapping mutations to the predicted three-dimensional structure. (A) Linear diagram of the domains of Snu114, as defined by homology to EF2. Domains are labeled in roman numerals. The domain labeled 'N' is not found in EF2. The GTPase motifs G1-G5 are found within domain I and are labeled 1-5. G" is an insertion within domain I unique to EF2 and Snu114. Fragments 1 and 2 represent the portions of the gene that were PCR amplified to screen for conditionally lethal mutations. Each mutation arising from PCR mutagenesis is depicted as a vertical bar below the position of the affected amino acid. The length of the vertical bars represents the number of times an amino acid was identified in our screen (one, two, or three times). Single point mutations that were found to cause a growth phenotype are red. Frameshift and nonsense mutations that result in early truncation of the protein are blue. Clusters of mutations are underlined with a black bar. Arrows indicate the positions of mutations studied in this work. (B) A model of the structure of Snu114, as determined by comparison with the structure of *S. cerevisiae* EF2 using the program MODELLER. Domains are colored as in A. (C) The clusters of mutations underlined in A are shown in color. Of the two clusters identified in Domain I, the G1 motif is the upper purple segment, and the G3 motif is the lower purple segment. The *snu114-14* mutation is colored black. The region of domain IVb that is deleted in *snu114-60* is shown in dark blue. (D) A model of Snu114 based on the structure of EF2 bound to the translocation inhibitor sordarin. Clusters of mutations are colored as in C. (E) ClustalW alignment of domain IVb of Snu114 orthologs, EF2, and EF-G from *S. cerevisiae* (Sc), *S. pombe* (Sp), *A. thaliana* (At), *H. sapiens* (Hs), *C. elegans* (Ce), *D. melanogaster* (Dm), *T. thermophilus* (Tt), and *E. coli* (Ec). Identical residues are shaded yellow and similar residues are shaded blue. The arrow indicates the *snu114-60* truncation.

A

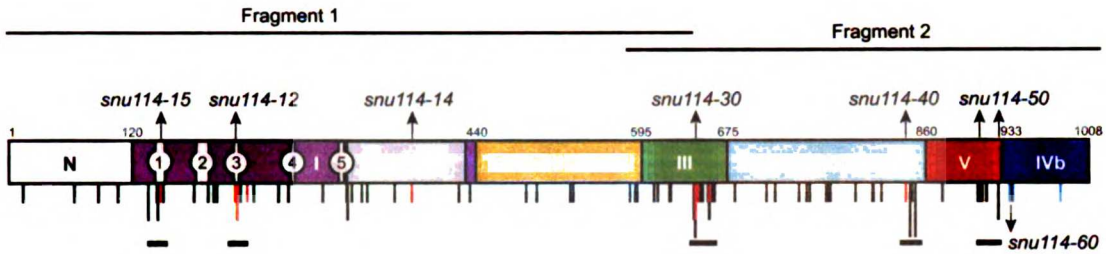
Fragment 1
Fragment 2
snu114-15
snu114-12
snu114-14
snu114-30
snu114-40
snu114-50
1
120
440
595
675
860
933
1008
N
1
2
3
4
I
5
III
V
IVb
snu114-60

B

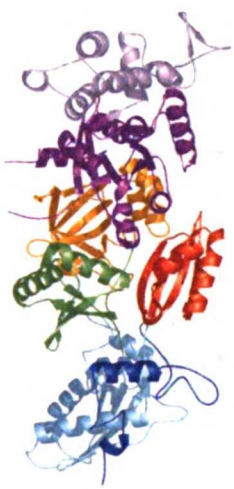

C

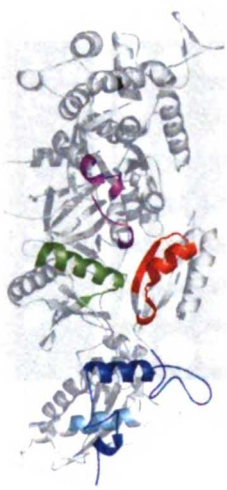

D

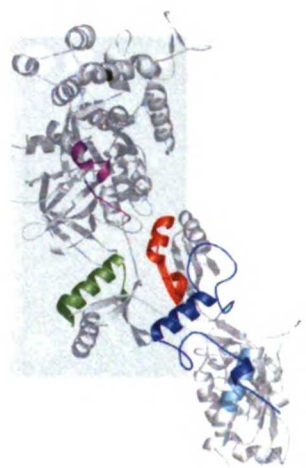

E

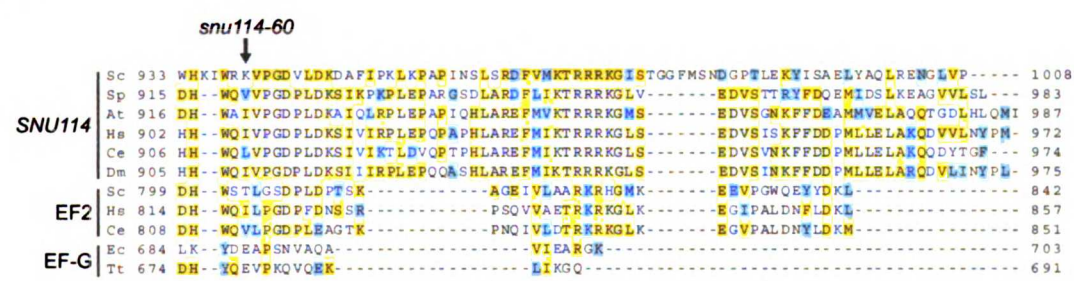
snu114-60
SNU114
EF2
EF-G
Sc 933 WHKIWRKVPGDVLDKDAFIPKLKPAPINSLSRDFVMKTRRRKGISTGGFMSNDGPTLEKYISAELYAQLRENGLVP----- 1008
Sp 915 DH--WQVVPGDPLDKSIKPKPLEPARGSDLARDFLIKTRRRKGLV-------EDVSTTRYFDQEMIDSLKEAGVVLSL--- 983
At 916 DH--WAIVPGDPLDKAIQLRPLEPAPIQHLAREFMVKTRRRKGMS-------EDVSGNKFFDEAMMVELAQQTGDLHLQMI 987
Hs 902 HH--WQIVPGDPLDKSIVIRPLEPQPAPHLAREFMIKTRRRKGLS-------EDVSISKFFDDPMLLELAKQDVVLNYPM- 972
Ce 906 HH--WQLVPGDPLDKSIVIKTLDVQPTPHLAREFMIKTRRRKGLS-------EDVSVNKFFDDPMLLELAKQQDYTGF--- 974
Dm 905 HH--WQIVPGDPLDKSIIIRPLEPQQASHLAREFMIKTRRRKGLS-------EDVSINKFFDDPMLLELARQDVLINYPL- 975
Sc 799 DH--WSTLGSDPLDPTSK----------AGEIVLAARKRHGMK-------EEVPGWQEYYDKL--------------- 842
Hs 814 DH--WQILPGDPFDNSSR----------PSQVVAETRKRKGLK-------EGIPALDNFLDKL--------------- 857
Ce 808 DH--WQVLPGDPLEAGTK----------PNQIVLDTRKRKGLK-------EGVPALDNYLDKM--------------- 851
Ec 684 LK--YDEAPSNVAQA----------VIEARGK---------- 703
Tt 674 DH--YQEVPKQVQEK----------LIKGQ---------- 691

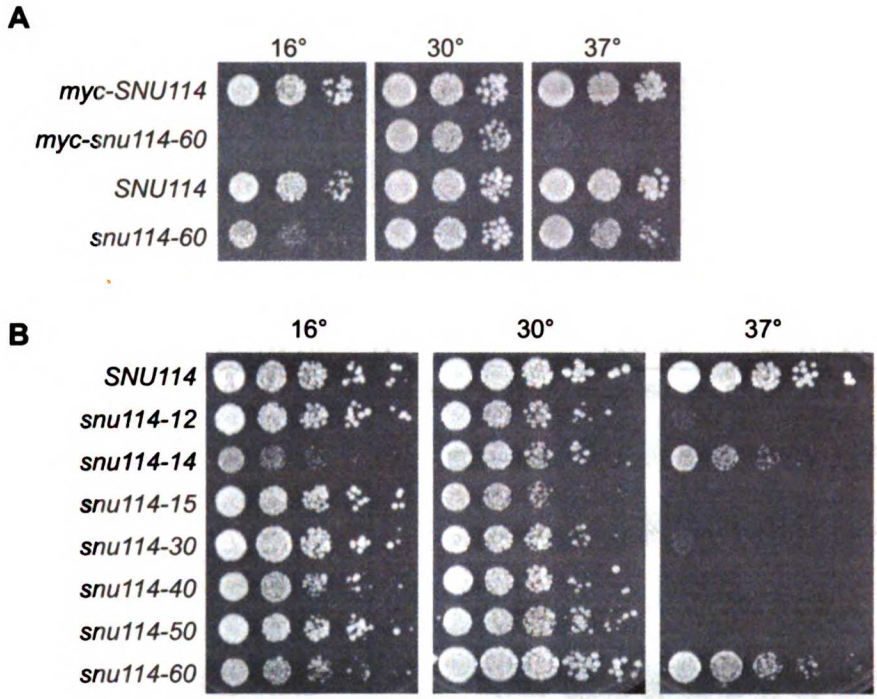

Figure 2. *snu114* alleles exhibit conditional growth defects at 16° and 37°. (A) Growth of serial dilutions of strains carrying *WT SNU114* and *snu114-60*, with and without the myc epitope. (B) Growth of serial dilutions of *snu114* alleles, present as low-copy plasmids with no epitope tag. Cells were spotted onto YPD media and grown at 16° for 8 days, 30° for 2 days, and 37° for 2 days.

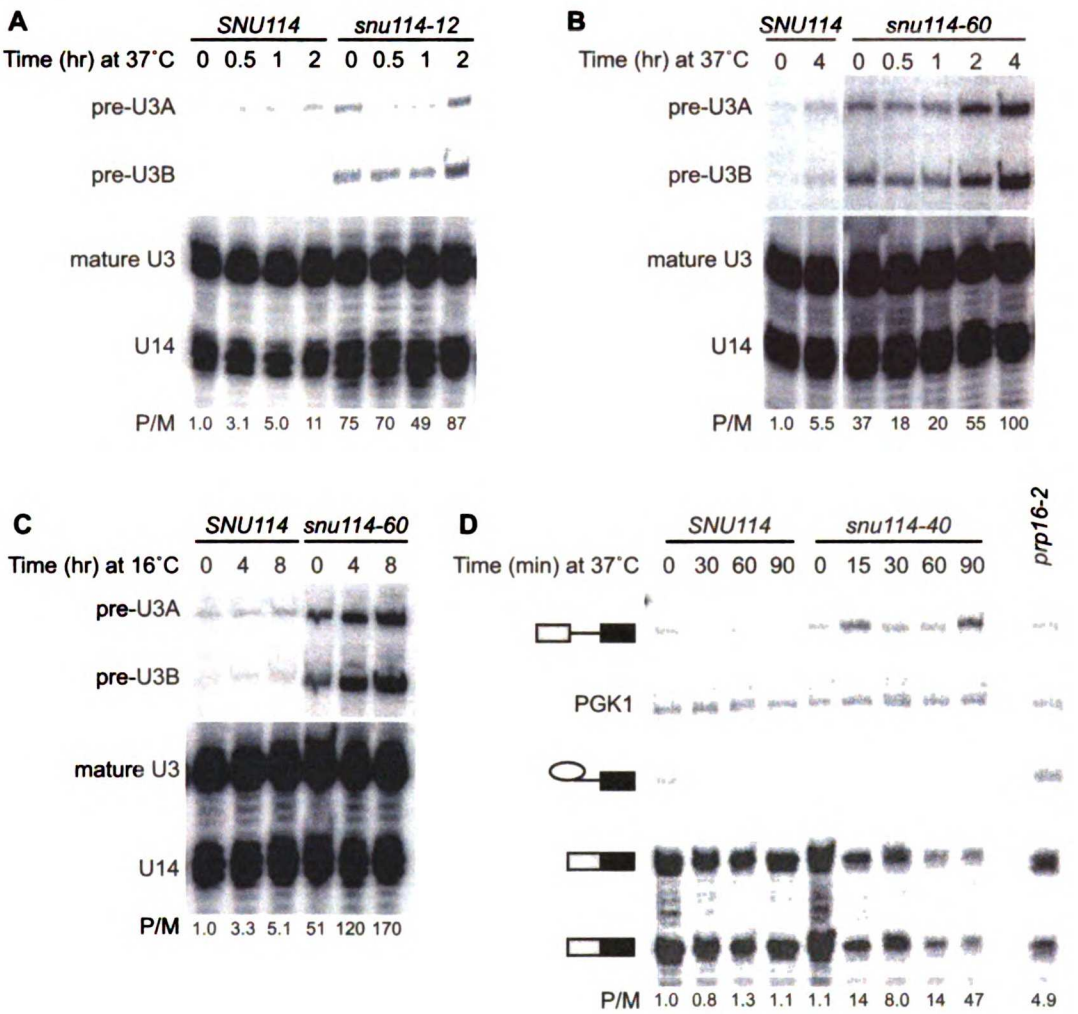

Figure 3. *snu114* mutations block the first step of splicing *in vivo*. (A-C) Primer extensions of U3 RNA from *WT*, *snu114-12* (A), and *snu114-60* (B, C) cells shifted to either 37° (A, B) or 16° (C). The positions of pre-U3A, pre-U3B, and mature U3 are indicated. The snoRNA U14 was used as a loading control. The top portions of the gels are shown at a darker exposure than the bottom portions. (D) Primer extension of *RPS17/RP51* RNA from *WT* and *snu114-40* cells shifted to 37°. RNA from *prp16-2* cells shifted to 37° for 3 hours was included in the right lane as a standard for a second step mutant that causes an increase in the level of lariat intermediate. The two *RPS17* mRNA species arise because the oligo hybridizes to both the *RPS17A* and *RPS17B* transcripts. *PGK1* was used as a loading control. The positions of the unspliced pre-mRNA, lariat intermediate, and spliced mRNA are shown schematically. P/M = ratio of pre-mRNA/mature RNA. In A, B, and C, pre-U3B was used for P. In D, the two mRNA species were summed for M. For each panel, ratios were normalized such that P/M for *WT* at time 0 = 1.0.

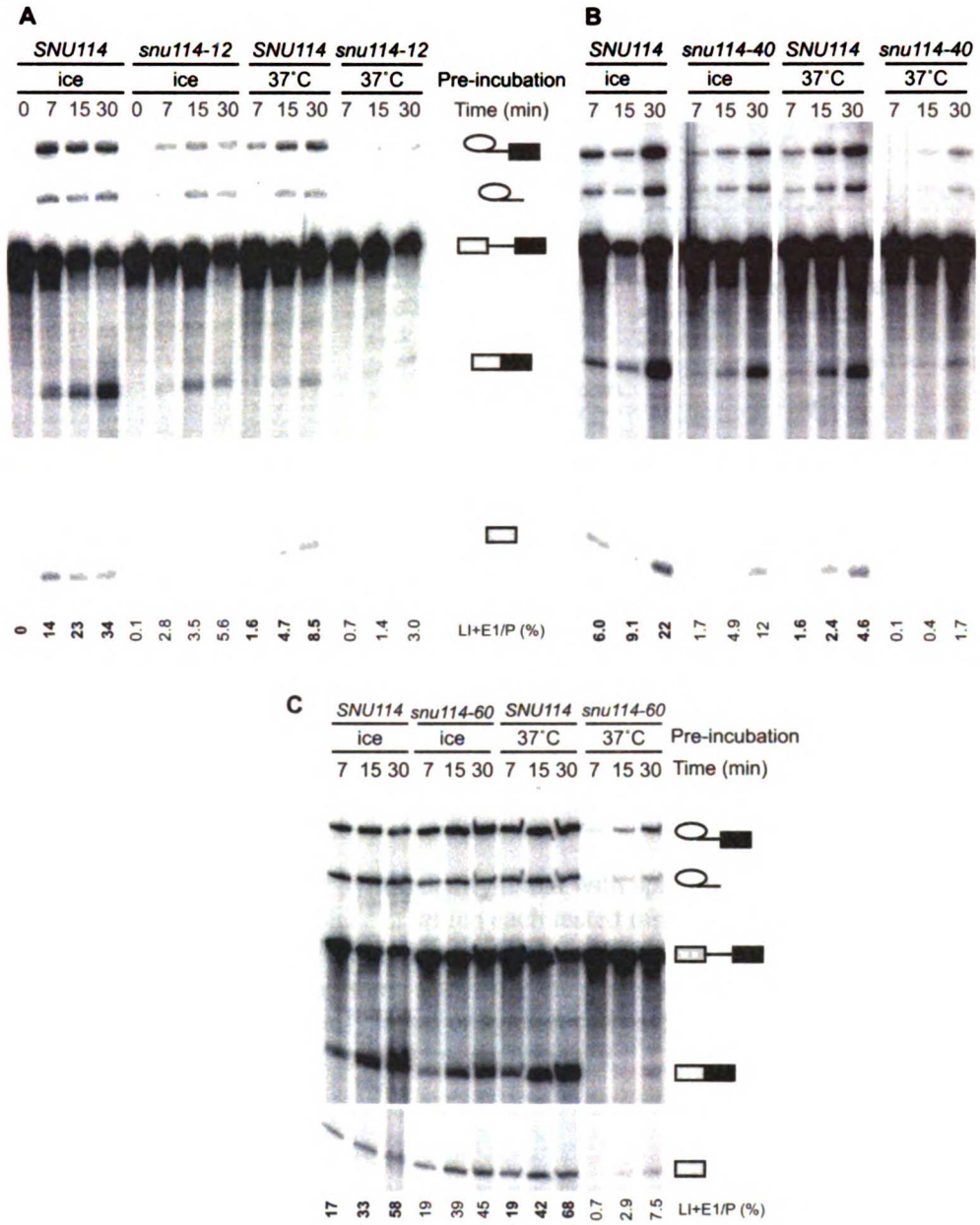

Figure 4. Mutations in *SNU114* inhibit splicing *in vitro*. Extracts from *WT*, *snu114-12* (A), *snu114-40* (B), and *snu114-60* (C) strains were pre-incubated either on ice or at 37° for 20 minutes. Splicing was monitored by adding ATP and ^{32}P labeled actin pre-mRNA and incubating at 25° for the time listed. The positions of the lariat-intermediate, lariat, pre-mRNA, spliced mRNA, and exon 1 are indicated schematically on the right. The products of the first step reaction are expressed as a percentage of the lariat intermediate (LI) + exon 1 (E1) compared to precursor (P).

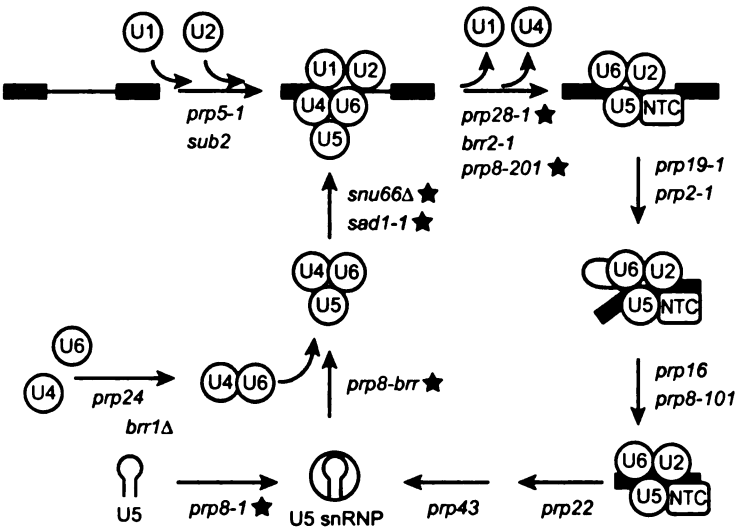

Figure 5. *snu114* alleles are synthetically lethal with splicing factors that act prior to the first step of catalysis. The place at which each tested mutation blocks splicing is depicted on a diagram of the canonical splicing cycle. In cases where multiple alleles of the same gene are thought to affect the same step, only the gene name (and not the allele) is listed. Mutations that are synthetically lethal or synthetically sick with at least one *snu114* allele are symbolized by black and grey stars, respectively.

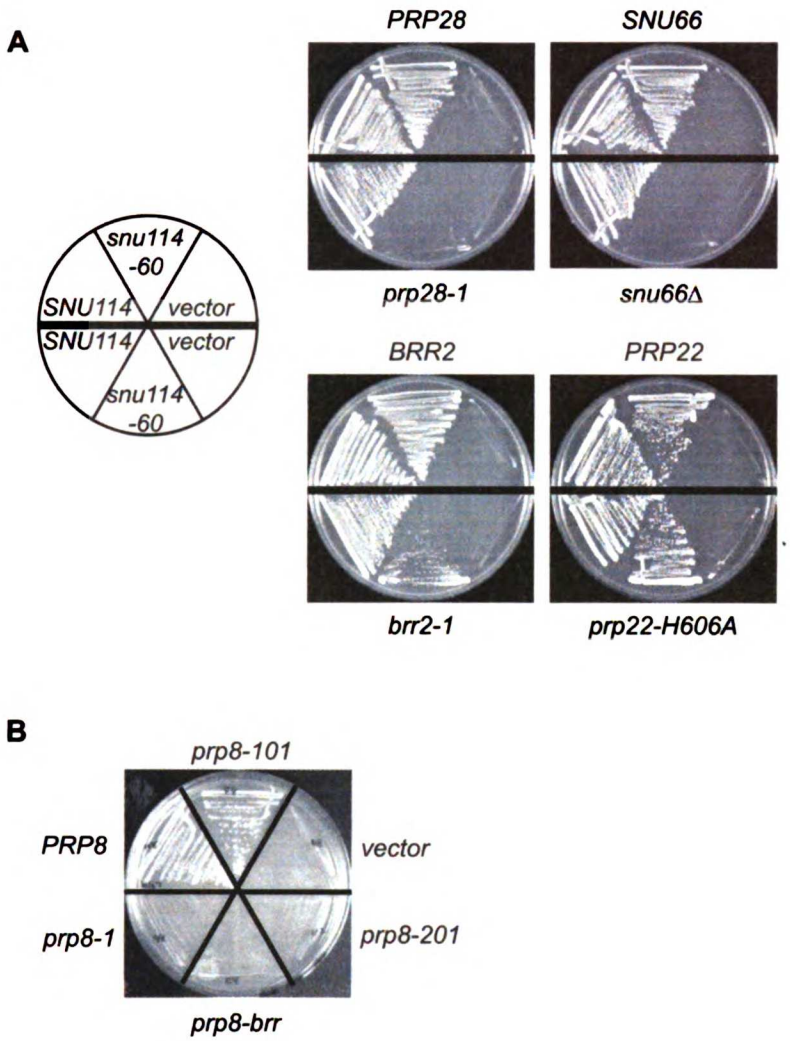

Figure 6. Synthetic lethal interactions of *snu114-60*. The following strains were streaked to 5-FOA media and grown at 25° for three days: (A) *snu114Δ* strains carrying *SNU114* on a *URA3*-marked plasmid, in combination with either a *WT* or mutant copy of the indicated gene, which had been transformed with *SNU114*, *snu114-60,* or an empty *LEU2*-marked vector, and (B) a *Δsnu114Δprp8* strain containing *SNU114* and *PRP8* on URA3-marked plasmids that was transformed with *snu114-60* and the indicated *prp8* allele or empty vector. Some of the sectors in this photo were cropped from different plates.

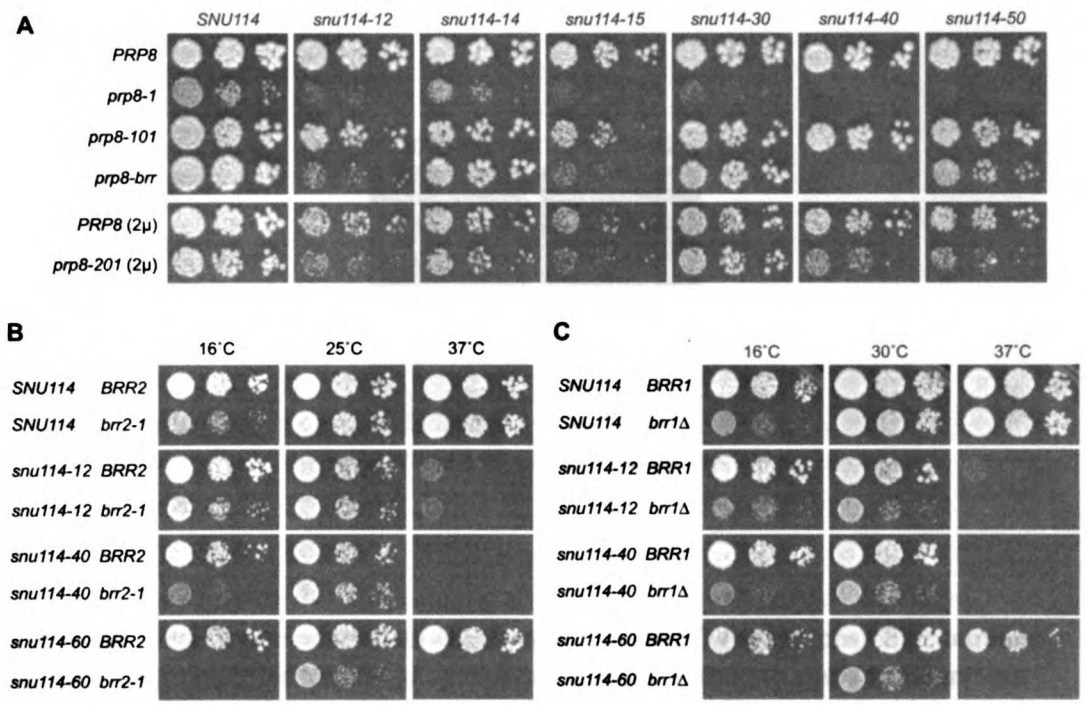

Figure 7. Genetic interactions of *snu114* alleles with *prp8* alleles, *brr2-1,* and *brr1Δ.* (A) Serial dilutions of *snu114Δ prp8Δ* cells carrying the indicated *snu114* and *prp8* alleles were grown at 30° on YPD for 3 days. *prp8-1*, *prp8-101*, and *prp8-brr* were present on low copy (CEN) plasmids; *prp8-201* was present on a high copy (2μ) plasmid. (B) Serial dilutions of *snu114Δ brr2Δ* cells carrying the indicated *snu114* alleles and either *BRR2* or *brr2-1.* (C) Serial dilutions of *snu114Δ brr1Δ* cells and *snu114Δ BRR1* cells carrying the indicated *SNU114* alleles. In B and C, serial dilutions were grown on YPD for 8 days at 16° and 2 days at 25°, 30°, and 37°.

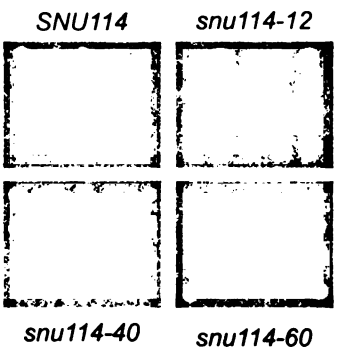

Figure 8. Genetic interactions between *snu66Δ* and *snu114* mutations. Five tetrads dissected from diploids generated by crossing a *snu66Δ* strain to *snu114* mutants are shown, grown on YPD. Tetrads dissected from the cross of *snu114-12* with *snu66Δ* were photographed after 8 days of growth at 25°, while the other tetrads are shown at day 4. *snu114-60 snu66Δ* spores are not viable even after 8 days.

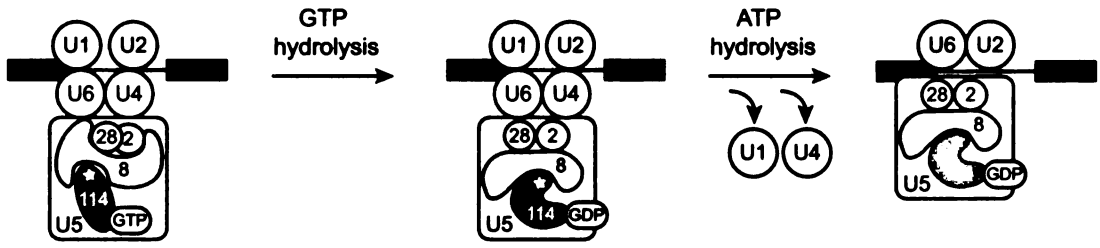

Figure 9. Model for Snu114 activity during spliceosome activation. We propose that Snu114 is bound to GTP when tri-snRNP first interacts with the spliceosome. Proper interaction between tri-snRNP and the spliceosome induces GTP hydrolysis, causing a conformational rearrangement of Snu114. This alters the interaction between domain IV of Snu114 (marked by a star) and Prp8, changing the conformation of Prp8. This triggers the activity of the ATPases Prp28 and Brr2, leading to the release of U1 and U4. Abbreviations: 114: Snu114; 8: Prp8; 2: Brr2; 28: Prp28.

CHAPTER II

Interaction of Snu114 with U5 snRNA requires Prp8 and a functional GTPase domain

Chapter II

Interaction of Snu114 with U5 snRNA requires Prp8 and a functional GTPase domain

ABSTRACT

Snu114 is a U5 snRNP protein essential for pre-mRNA splicing. Based on its homology to the ribosomal translocase EF-G, it is thought that GTP hydrolysis by Snu114 induces conformational rearrangements in the spliceosome. We recently identified allele-specific genetic interactions between *SNU114* and genes encoding three other U5 snRNP components, Prp8 and two RNA-dependent ATPases required for destabilization of U1 and U4 snRNPs prior to catalysis. To shed more light onto the function of Snu114, we have now analyzed snRNP and spliceosome assembly in *SNU114* mutant extracts. The Snu114-60 C-terminal truncation mutant, which is synthetically lethal with the ATPase mutants, assembles spliceosomes but subsequently blocks U4 snRNP release. Conversely, mutants in the GTPase domain fail to assemble U5 snRNPs. These mutations prevent the interaction of Snu114 with Prp8 as well as with U5. Since Prp8 is thought to regulate the activity of the DEAD-box ATPases, this strategy of snRNP assembly could ensure that Prp8 activity is itself regulated by a GTP-dependent mechanism.

INTRODUCTION

The spliceosome, the macromolecular complex that excises introns from pre-mRNA transcripts, is assembled from five snRNPs (small nuclear ribonucleoprotein particles), as well as additional accessory proteins. The U5 snRNP is an integral component of the spliceosome: both the U5 snRNA and the large, conserved U5 snRNP

protein Prp8 can be crosslinked to all sites of chemistry on the pre-mRNA transcript (reviewed in Grainger & Beggs, 2005). Prp8 interacts biochemically and genetically with the GTPase Snu114, which is an essential protein is *S. cerevisiae* (Fabrizio et al., 1997; Achsel et al., 1998; Dix et al., 1998; Grainger & Beggs, 2005). As a homolog of the ribosomal translocase elongation factor G, Snu114 is predicted to mediate rearrangements of the spliceosome (Fabrizio et al., 1997). In order to investigate the function of Snu114, we previously generated conditionally lethal alleles of the gene and tested for synthetic lethal interactions with other spliceosomal factors (Brenner & Guthrie, 2005). We observed genetic interactions with two main classes of proteins: those that are involved in snRNP biogenesis, and those that are involved in spliceosome activation.

While the protein components of U5 snRNP have been identified (Stevens et al., 2001; reviewed in Jurica & Moore, 2003), the process by which the snRNP assembles is poorly understood. During snRNP biogenesis, a heptameric complex of Sm proteins binds to and stabilizes U5 snRNA, as well as most of the other snRNAs (Jones & Guthrie, 1990; Will & Luhrmann, 2001). Snu114 and Prp8 appear to constitute the core of the U5 snRNP, as they both can be crosslinked directly to U5 snRNA (Dix et al., 1998). The strength of interactions among the snRNP protein components has been assessed by treating purified U5 snRNPs from HeLa extract with increasing concentrations of chaotropic salts. At high concentrations, Snu114 (U5-116 kDa in humans) remained bound only to Prp8 (U5-220 kDa) (Achsel et al., 1998). Under less stringent salt conditions, the Prp8/Snu114 dimer interacted with the ATPase Brr2 (U5-200 kDa) and a 40 kDa protein that does not appear to have a yeast ortholog (Achsel

et al., 1998). U5 snRNP can also be found in complexes with other snRNPs; the U5•U4/U6 tri-snRNP includes the base-paired U4/U6 di-snRNP, and the penta-snRNP contains all five snRNPs (Cheng & Abelson, 1987; Stevens et al., 2002).

In vitro studies have shown that during spliceosome assembly, the tri-snRNP binds to the pre-spliceosome, which already contains U1 and U2 snRNP bound to the 5' splice site and branch point sequence, respectively (reviewed in Burge et al., 1998; Staley & Guthrie, 1998). However, isolation of a penta-snRNP suggests that a pre-assembled snRNP complex might bind to the pre-mRNA (Stevens et al., 2002). In either case, a substantial rearrangement of the spliceosome must occur in order for splicing to proceed (Brow, 2002; Turner et al., 2004). During catalytic activation, the interaction between U1 snRNA and the 5' splice site and the extensive base pairings between U4 and U6 snRNAs are destabilized, releasing U1 and U4 snRNPs from tight association with the spliceosome. This allows U6 snRNA to interact with U2 snRNA and the 5' splice site, which is necessary for the chemical steps of splicing. U5 snRNP proteins play an important role during these activation steps (reviewed in Turner et al., 2004). Two DExD/H-box ATPases that are components of U5 snRNP, Prp28 and Brr2, have been implicated in release of U1 and U4, and Prp8 has been posited to play a role in regulating the activity of these ATPases (Laggerbauer et al., 1998; Raghunathan & Guthrie, 1998; Kuhn et al., 1999; Staley & Guthrie, 1999; Kuhn & Brow, 2000; Kuhn et al., 2002). Additionally, several mutations in Snu114 block activation of the spliceosome (Bartels et al., 2002; Bartels et al., 2003).

Here, we analyze our novel set of *snu114* alleles (Brenner & Guthrie, 2005) for *in vitro* defects during snRNP assembly and spliceosome activation. We find that several

alleles, including those with mutations in the GTPase domain, inhibit formation of U5 snRNP. We also analyze the allele *snu114-60*, which truncates the last 70 amino acids; this allele exhibits genetic interactions with factors involved in spliceosome activation, including *prp28-1*, *brr2-1*, and alleles of *prp8* (Brenner & Guthrie, 2005). In this case we find that *snu114-60* blocks spliceosome activation.

RESULTS

Our previous genetic data suggested that *snu114-60*, which causes both thermal-sensitive and cold-sensitive growth defects, inhibits spliceosome activation (Brenner & Guthrie, 2005). We tested this hypothesis by monitoring spliceosome assembly and activation *in vitro*. Heat pre-treatment blocks splicing activity in *snu114-60* extract (Brenner & Guthrie, 2005); we also found that incubating splicing reactions at 30°C instead of 23°C consistently inhibited splicing activity in *snu114-60* extract, but not in wildtype extract (data not shown). In order to affinity purify spliceosomes, mutant and wildtype extracts were incubated with biotinylated pre-mRNA transcript under splicing conditions at 23°C and 30°C. snRNAs that co-purified with the transcript were quantified by real-time PCR. As a control for the specificity of snRNA binding, extracts were incubated with transcript in the absence of ATP. Only U1 snRNA was co-precipitated under these conditions (Figure 1A); ATP is required for the other snRNAs to associate with pre-mRNA (Bindereif & Green, 1987; Legrain et al., 1988; Ruby & Abelson, 1988). While *snu114-60* extract incubated at 23°C behaved similarly to wildtype extract at either temperature, the mutant extract incubated at 30°C showed a different profile of snRNA binding (Figure 1A). Similar amounts of U5 and U6 snRNAs were bound to transcript in all of the extracts, but an increased amount of U4 snRNA was consistently bound in

snu114-60 extract incubated at 30°C. Because U4 and U6 assemble onto the spliceosome together in a based-paired form, and U4 is released during activation while U6 remains bound to transcript throughout splicing, the ratio of transcript-bound U4 to U6 is commonly monitored as a measure of catalytic activation. Over time, the ratio of U4 to U6 bound to transcript was consistently two-fold higher for *snu114-60* (Figure 1B), indicating that *snu114-60* extract is defective for releasing U4 from the spliceosome at elevated temperatures. Although *snu114-60* cells also exhibit a slow-growth phenotype in the cold, incubating *snu114-60* extract at 16° did not block U1 or U4 release (data not shown).

We then used this assay to gain insight into other *snu114* alleles. The thermal-sensitive allele *snu114-12* results from a point mutation within the GTPase domain and has a constitutive splicing defect *in vivo* and *in vitro* (Brenner & Guthrie, 2005). The association of snRNAs with biotinylated transcript in *snu114-12* extract was the same whether the incubation was at 23°C or 30°C; here we show only data from 30°C incubations (Figure 1C). After 20 minutes of incubation, three- to four-fold less U4, U5, and U6 snRNAs bound to transcript in *snu114-12* extract as compared to wildtype. However, the ratio of U4 to U6 snRNAs bound to transcript over time was similar between wildtype and *snu114-12* extracts (Figure 1D). Thus, the main defect in *snu114-12* appears to be spliceosome assembly rather than activation.

In order to determine whether the decreased tri-snRNP binding in *snu114-12* extract resulted from a failure of tri-snRNP to interact with the pre-spliceosome or from decreased tri-snRNP levels, we assayed the snRNP profile of *snu114-12* by native gel analysis (Raghunathan & Guthrie, 1998). We also tested *snu114-60* and five other

conditionally lethal *snu114* alleles that we previously identified (Brenner & Guthrie, 2005). All extracts were made from cells grown at permissive temperature. With the exception of *snu114-60*, all of the mutants showed dramatically lower levels of tri-snRNP (Figure 2). However, these mutants had high levels of U4/U6 di-snRNP and a free U5-species (Figure 2), and the total levels of the snRNAs were not strongly perturbed (Figure 3D and data not shown). Some of the snRNPs from mutant extracts exhibited slightly altered mobility in the native gels, which may reflect an altered conformation or composition. As noted previously, addition of ATP to wildtype extract causes an increase in U4/U6 di-snRNP levels (Figure 2A and 2B, lanes 1 and 2), due to ATP-dependent disassembly of U4/U6•U5 tri-snRNP (Raghunathan & Guthrie, 1998; Stevens et al., 2001). A similar increase in di-snRNP was observed in *snu114-60* extract, the only other extract with abundant tri-snRNP levels (Figure 2A and 2B, lanes 15 and 16). Addition of ATP also led to the appearance of a slow-migrating U5 species in *snu114-60* extract (Figure 2C, lane 16, asterisk) with slightly slower mobility than U4/U6 di-snRNP. The composition of this species is unclear. Overall, the native gel analysis demonstrated that tri-snRNP was abundant in *snu114-60* extract, consistent with ability of tri-snRNP to assemble onto transcript. In contrast, tri-snRNP levels were low in many *snu114* mutants, which could explain the defect of tri-snRNP addition in *snu114-12* extract.

The low levels of tri-snRNP in the *snu114* mutants could arise from a failure of U5 snRNP to interact with U4/U6 di-snRNP, or from a defect in U5 snRNP formation or stability. To differentiate between these possibilities, we tested whether three core U5 snRNP proteins, Snu114, Prp8, and Brr2, were associated with U5 snRNA. We focused this analysis on *snu114-12*, *snu114-60*, and the strong thermal-sensitive allele *snu114-40*.

Extracts were made from cells grown at permissive temperature. Snu114 and Prp8 were immunoprecipitated with polyclonal antibodies, and TAP-tagged Brr2 was precipitated with IgG resin; co-precipitating snRNAs were reversed transcribed and quantified by real-time PCR. In wildtype extract, Snu114 and Brr2 immunoprecipitations pulled down similar amounts of U4, U5, and U6 snRNAs, while the Prp8 antibody pulled down predominantly U5 snRNA (Figure 3A, 3B, and 3C). This difference may suggest that Prp8 that has assembled into tri-snRNP is less accessible to the antibody. As observed previously, Brr2 also immunoprecipitated U2 (Raghunathan & Guthrie, 1998). Consistent with the diminished tri-snRNP levels visualized by native gel, Snu114, Brr2, and Prp8 were each associated with five- to ten-fold less U4 and U6 snRNAs in *snu114-12* and *snu114-40* extracts (Figures 3A, B, and C). Furthermore, these U5 snRNP proteins were bound to similarly low amounts of U5 snRNA in *snu114-12* and *snu114-40* extracts, demonstrating that U5 snRNP itself either fails to form or is unstable in these mutants. In contrast, *snu114-60* exhibited only a modest decrease in association with snRNAs, consistent with the robust tri-snRNP levels visualized by native gel electrophoretic analysis.

To rule out the possibility that decreased association of snRNAs with U5 snRNP proteins resulted from low snRNA levels, we measured the total snRNA levels in the extracts used for the immunoprecipitations. The mutant extracts contained similar amounts of each snRNA as found in wildtype extract (Figure 3D), so this cannot account for the defects in snRNP formation. The stability of the snRNAs also depends on binding of the Sm proteins (Jones & Guthrie, 1990). Therefore, as a further measure of functional snRNAs, we tested the interaction of SmD1 with snRNAs in the *snu114* extracts (Figure

3E). Although SmD1 was associated with slightly lower levels of snRNAs in the mutant extracts, this decrease was never more than two-fold, which contrasts with the much larger changes in association of the other U5 snRNP proteins.

Because of the finding that Snu114, Prp8, and Brr2 associated with lower amounts of snRNAs in *snu114-12* and *snu114-40*, we tested whether these core U5 proteins could interact with each other in the mutants. First, we assayed the total levels of the proteins by Western blot. While the protein levels of Snu114-12 and Snu114-40 were similar to wildtype levels in some cases (Figure 4A), they commonly were two- to three-fold lower (Figure 4B and 4D). Quantitation of Prp8 levels was more challenging, as we found that Prp8 was particularly susceptible to degradation (Figure 4B). In extracts made in the presence of TCA, in which proteolysis of Prp8 was minimal, Prp8 levels were reduced approximately ten- and five-fold in *snu114-12* and *snu114-40* backgrounds, respectively (Figure 4A). In the bead-beat extracts used for immunoprecipitations, where overall degradation of Prp8 occurred, the amount of full-length Prp8 was consistently reduced five-fold in *snu114-12* strains (Figure 4B). When Snu114 was immunoprecipitated with polyclonal antibodies, Prp8 was co-precipitated in wildtype and *snu114-60* extracts (Figure 4C). In contrast, the co-precipitation of Prp8 was diminished to almost background levels in *snu114-12* and *snu114-40* extracts (Figure 4C).

We also monitored the co-purification of Snu114 and Prp8 in Brr2-TAP pull-downs (Figure 4E). Affinity-purified Brr2 from wildtype extract was bound to both Prp8 and Snu114. In *snu114-12* extract, Brr2 levels and Prp8 levels were reduced (Figure 4D), and Brr2 bound to low amounts of both Prp8 and Snu114 (Figure 4E). Brr2 also associated with less Snu114 and Prp8 in *snu114-40* extract (Figure 4C). TAP-tagged Brr2

enhanced the sickness of *snu114-60* (data not shown); perhaps as a result, Brr2 levels were low in this strain (Figures 4D and 4E). Overall, the data show that Prp8 levels are diminished in *snu114-12* and *snu114-40* extracts, and the association of Snu114 with both Prp8 and Brr2 is decreased in these mutants.

DISCUSSION

After the snRNPs have assembled onto the pre-mRNA transcript, dramatic rearrangements of the spliceosome must occur, including the unwinding of several RNA/RNA helices, the formation of new RNA helices, and a corresponding remodeling of protein interactions. The C-terminal truncation allele *snu114-60* is synthetically lethal with mutations in *PRP28* and *BRR2* (Brenner & Guthrie, 2005), ATPases that are believed to unwind and release U1 and U4 snRNAs during spliceosome activation (Laggerbauer et al., 1998; Raghunathan & Guthrie, 1998; Staley & Guthrie, 1999). Here we show that *snu114-60* inhibits activation: release of U4 from spliceosomes was blocked when extract was incubated at elevated temperature. Although the unwinding of U1 is generally believed to be highly coupled with that of U4 (Kuhn et al., 1999; Staley & Guthrie, 1999; Kuhn et al., 2002), U1 and U4 unwinding are separable in some *in vitro* assays (Xie et al., 1998). While the *snu114-60* allele predominantly affects the release of U4, likely through the activity of Brr2, genetic interactions suggest that the activities of Prp28, Brr2, and Snu114 *in vivo* are highly interrelated.

Previous studies have implicated additional regions of Snu114 in spliceosome activation. Truncation of the N-terminal 120 amino acids of Snu114, which corresponds to a domain that is not found in EF-G, inhibits release of U4, as does the allele D271N, which converts the protein from a GTPase to an XTPase (Bartels et al., 2002; Bartels et

al., 2003). GTP hydrolysis was directly implicated, since addition of XTP, but not non-hydrolysable analogs, could relieve the block in D271N (Bartels et al., 2003). Altogether, this suggests that catalytic activation requires GTP hydrolysis by Snu114, and that both the N- and C- terminal domains are required to transmit a resulting rearrangement of the protein. A reasonable hypothesis is that upon GTP hydrolysis, Snu114 alters its interactions with Prp8 (Brenner & Guthrie, 2005). This would relieve the inhibition by Prp8 on the ATPases Prp28 and Brr2, leading to U1 and U4 unwinding (Kuhn et al., 1999; Kuhn & Brow, 2000; Kuhn et al., 2002).

It has long been known that Prp8 is essential for the formation of U5 snRNP and tri-snRNP, as illustrated by genetic depletion of Prp8 or heat inactivation of the *prp8-1* allele (Brown & Beggs, 1992). We previously found that *prp8-1* is synthetically sick or lethal with many *snu114* alleles, suggesting that these *snu114* alleles may also affect snRNP formation (Brenner & Guthrie, 2005). Here we demonstrate that the mutations *snu114-12* and *snu114-40* cause a defect in the assembly of U5 snRNP. These alleles disrupt the interaction between Snu114 and Prp8, cause lower Prp8 protein levels, and lead to low levels of U5 snRNP. Our data indicate that the stability of Prp8 depends its ability to interact with Snu114. Additionally, the binding of Prp8 and Snu114 to U5 snRNA is decreased five- to ten-fold in *snu114-12* and *snu114-40* extracts. Because the levels of mutant Snu114 protein are similar to the wildtype protein and because the interaction of mutant Snu114 with Prp8 is reduced, we conclude that Snu114 does not bind to U5 snRNA without Prp8. It is unclear if Prp8 is unable to bind U5 alone, or if the decreased association of Prp8 with U5 in the *snu114* mutants results from instability of Prp8.

We also found that a decreased interaction between Snu114 and Prp8 correlates with diminished co-purification of Snu114 with Brr2. This corroborates yeast-two-hybrid and far-western analyses indicating Prp8 interacts directly with Brr2 and Snu114, while Brr2 and Snu114 do not directly interact (Achsel et al., 1998; Dix et al., 1998; van Nues & Beggs, 2001; Grainger & Beggs, 2005). Furthermore, our finding that the interaction of Brr2 with U5 snRNA is reduced when the interaction between Snu114 and Prp8 is low suggests that Brr2 does not bind to the snRNA alone.

U5 snRNA is relatively stable in the *snu114* mutants, despite the decrease in binding of U5 snRNP proteins. Previously, the stability of various U5 deletion mutants, many of which do not support yeast viability, was assayed in the presence of wildtype U5 snRNA (Frank et al., 1994). Deletion of Internal loop 1 (IL2 in human), a domain that can be crosslinked to Snu114 and Prp8 (Dix et al., 1998), abolishes binding of both proteins to the RNA in yeast and mammalian systems (Hinz et al., 1996; Dix et al., 1998; Segault et al., 1999). However, this deletion did not affect U5 RNA stability (Frank et al., 1994). Only mutations that affect the binding of the Sm proteins caused degradation of the RNA (Frank et al., 1994). Thus, the binding of the Sm proteins in the *snu114* alleles assayed here appears to maintain the stability of the snRNAs, despite decreased Prp8 and Snu114 binding. While Brown and Beggs (1992) found that depletion of Prp8 caused a drop in U4, U5, and U6 snRNA levels, it is likely that the degree of Prp8 depletion was much greater under their conditions than in the *snu114* mutants, thus giving rise to a more severe phenotype than we observed.

Reduced levels of U5- and tri-snRNP have been observed in two other *snu114* mutants: R487E, which disrupts a predicted inter-domain salt bridge, and the XTPase

allele D271N (Bartels et al., 2003). Unlike the *snu114* alleles characterized here, the snRNP defects caused by these mutations may be attributable to decreased amounts of Snu114 protein. Although the level of Snu114-R487E protein was not assayed, it is likely that disruption of an inter-domain salt bridge would destabilize the protein. When the *snu114-D271N* allele was grown at 30°C instead of 25°C, both the total level of mutant protein and the amounts of Snu114 and Prp8 interacting with U4, U5, and U6 snRNAs were reduced to 40% of wildtype. This phenotype of *snu114-D271N* may arise from defects in nucleotide binding, due to low cellular levels of XTP (Bartels et al., 2003).

Many of the *snu114* alleles that we characterized here may affect a conformational rearrangement of the protein that arises from changes in nucleotide binding. Based on homology with EF-G, it is likely that GTP hydrolysis causes the C-terminal domains (domains III-V) of the protein to undergo a large movement with respect to the GTPase domain. We observed decreases in tri-snRNP levels, which we suspect correspond with decreases in U5 snRNP levels, in six *snu114* alleles containing single point mutations in domains outside of the extreme N- and C- termini. Two of these mutations are within conserved motifs in the GTPase domain. The mutation in *snu114-12*, P216N, falls within the G3 motif of the GTPase domain. Several mutations within the G3 motif in other GTPases have been shown to decrease GTP hydrolysis; however, some mutations in this motif also affect nucleotide binding (Anborgh et al., 1989; Krengel et al., 1990; Cool & Parmeggiani, 1991; Zeidler et al., 1995; Diaz et al., 2000). To our knowledge, the specific mutation found in *snu114-12* has not been characterized in other GTPases. Mutations in the conserved lysine of the GKT motif,

which is mutated to isoleucine in *snu114-15*, decease nucleotide binding in Ras (Sigal et al., 1986). While the mutations *snu114-30*, *snu114-40*, and *snu114-50* are outside of the GTPase domain, they may affect transmission of a signal from the GTPase domain, which is caused by a change in nucleotide binding, to the C-terminal domains of Snu114 and to factors that interact with the protein (Brenner & Guthrie, 2005). Overall, each of these mutations may stabilize a protein conformation that is unfavorable for binding to Prp8. It is possible that Snu114 must hydrolyze GTP in order to stabilize the interaction with Prp8. However, since GTP hydrolysis is likely needed at the time of spliceosome activation, we favor the model that GTP *binding* is required for stable interaction with Prp8. Formation of the Prp8/Snu114 heterodimer would allow productive association with U5 snRNA and subsequent formation of tri-snRNP. This mechanism would ensure that U5 snRNP cannot join the spliceosome without the presence of GTP-bound Snu114. Following addition of tri-snRNP to the spliceosome, GTP hydrolysis by Snu114 would be stimulated, allowing spliceosome activation to occur.

MATERIALS AND METHODS

Strains

Strains and plasmids were described in Brenner and Guthrie (2005), except as noted. For affinity purification of spliceosomes, strains derived from yTB23 by replacing pTB1 with pTB106 (*SNU114*), pTB107 (*snu114-12*), or pTB113 (*snu114-60*) were grown at 30°C. The strains for the native gel analysis were derived from yTB13 by replacing pTB1 with plasmids pTB92 through pTB102; cells were grown at 30°C, with the exception of *snu114-15*, which was grown at 25°C.

For immunoprecipitations, the following *MATa* and *MATα* strains were used: *SNU114* (yTB127 and yTB128), *snu114-12* (yTB175 and yTB171), *snu114-40* (yTB162 and yTB163), and *snu114-60* (yTB164 and yTB165). The *MATa* strains were constructed from yTB127 (*MATa his3Δ leu2Δ ura3Δ met15Δ*) in an identical manner to the *MATα* strains, as described in Brenner and Guthrie (2005). The TAP-tagged Brr2 strain (*MATa his3Δ leu2Δ ura3Δ met15Δ BRR2-TAP::HIS3*), a gift from the O'Shea lab (Ghaemmaghami et al., 2003), was crossed to yTB171 (*snu114-12*), yTB163 (*snu114-40*), and yTB165 (*snu114-60*) and sporulated to obtain yTB176, yTB177, and yTB178, respectively, which contain both *BRR2-TAP::HIS3* and chromosomal *snu114* mutations. Because the integrated *snu114* alleles exhibited a more severe thermal-sensitive growth phenotype than strains carrying the mutant alleles on plasmids, cells were grown at 25°C. At 25°C, the doubling time of *snu114-12* was 1.3 times slower than wildtype, *snu114-40* was 1.1 times slower, and *snu114-60* grew similarly to wildtype.

Affinity purification of spliceosomes

Splicing extracts were prepared as described (Umen & Guthrie, 1995). The following protocol was adapted from Staley and Guthrie (1999). Actin pre-mRNA was transcribed in the presence of 5% biotin-11-UTP (Sigma). Standard splicing reactions (Lin et al., 1985) included 4 nM biotinylated actin and were performed at 23°C or 30°C. At 1.5, 5, 12, 20, and 30 minutes, 20 μL aliquots were removed into siliconized tubes containing 60 μL ice-cold splicing buffer/buffer D (40%/60%) with 20 mM EDTA and 25 μL streptavidin sepharose beads (Amersham), prepared according to Staley and Guthrie (1999). As a control, ATP was depleted from extracts by incubating splicing reactions in the presence of 2 mM glucose for 20 minutes at room temperature prior to adding pre-

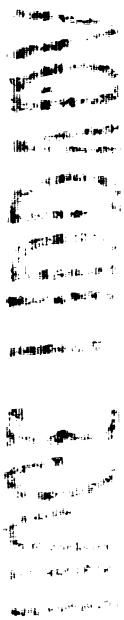

mRNA. Following addition of biotinylated transcript, glucose-treated reactions were incubated for 12 minutes at 23°C or 30°C and quenched as above. Spliceosomes and beads were incubated with rotation for 90 minutes at 4°C. Beads were washed four times with 1 mL of Net2-50 (50 mM Tris pH 8.0, 50 mM NaCl, 0.5 mM DTT, 0.05% NP40). To elute the RNA, 100 μL Buffer G (0.3 M NaOAc, 10 mM EDTA, 1% SDS) with 0.0125 mg/mL proteinase K were added and tubes were incubated at 37° for 20 minutes. RNA was phenol extracted and ethanol precipitated in the presence of glycogen. The five snRNAs and the actin transcript were reverse transcribed and quantified by real-time PCR. The levels of co-purifying snRNAs were normalized to the amount of precipitated actin in each reaction.

Oligos

U2, U4, U5, and U6 oligos were described by Inada and Guthrie (2004). Oligos for U1 were oTB148 (5'-TGACTACTTTTCTCTAGCGTGCC-3') and oTB149 (5'-CATAACGGGAACGAGCAAAGTTG-3'). Actin was amplified using oTB141 (5'-CGGTTCTGGTATGTGTAAAGC-3') and oTB142 (5'-CAGGTCGACTCTAGAGGATC-3'). When *in vitro* transcribed snRNAs were used as a standard, the original U2 oligos could not be used, as they amplify a region of the fungal domain that is not included in the *in vitro* transcript. Instead, oTB166 (5'-GGCTTAGATCAAGTGTAGTATCTGT-3') and oTB167 (5'-TTTTATTATTTTGGGTGCCAAAAAA-3') were used.

Quantitation of RNAs

In order to reverse transcribe the RNAs, a mix of the primers used for reverse PCR amplification (250 nM final concentration) was incubated with RT buffer (50 mM

Hepes pH 8.3, 75 mM KCl) and RNA at 65°C for five minutes and then on ice for 5 minutes. Reverse transcription reactions, containing 3 mM $MgCl_2$, 10 mM DTT, 500 μM each dNTP, 50 mM Hepes pH 8.3, 75 mM KCl, and MMLV reverse transcriptase, were then incubated at 42°C for two hours. Quantitative real-time PCR was performed as described (Inada & Guthrie, 2004). PCR conditions were as follows: 95°C for 3 min; 32 cycles of 95°C for 15 seconds, 57°C for 30 seconds, 72°C for 60 seconds, followed by measuring; 72°C for 5 min; and determination of melting curves.

In vitro transcribed actin was reverse transcribed and used for normalization of affinity purified biotinylated actin. Standard curves of each snRNA were initially generated from cDNA of reverse transcribed total RNA isolated from wildtype splicing extract. We then decided to compare absolute amounts of snRNAs, as opposed to proportions of total levels in extract. Therefore, the five snRNAs were *in vitro* transcribed using T7 polymerase using previously described constructs (Fabrizio et al., 1989; McPheeters et al., 1989; Ghetti et al., 1995). The concentrations of gel-purified RNAs were determined by A260. To validate our quantitations, we *in vitro* transcribed the snRNAs in the presence of γ^{32}P GTP, which labels only the 5' end of each snRNA. Gel purified snRNAs were quantified both by A260 and by scintillation counting; there was virtually a 1:1 correspondence between the measurements. Equal molar amounts of each snRNA were then reverse transcribed and used for standard curves. According to this method, the relative levels of snRNAs in splicing extract are approximately as follows: U2 and U6 are at similar levels, U4 and U5 are approximately three-fold less abundant, and U1 is three-fold less abundant yet. In a standard splicing extract, the concentrations of U2 and U6 are approximately 2 nM.

snRNAs affinity purified by binding to biotinylated pre-mRNA in *SNU114* versus *snu114-60* extract were normalized based on total WT RNA. In all other experiments, the *in vitro* transcribed snRNAs were used for normalization. Because we found that U4 was three-fold less abundant than U6 in total RNA, the initial values for the ratios of U4 to U6 in *snu114-60* extracts were divided by three to obtain the values shown in Figure 1B. In Figure 3A, 3B, and 3C, snRNA levels reflect absolute amounts; in all other cases, levels were normalized to 1.0 for wildtype. One "arbitrary unit" in Figure 3A, 3B, and 3C corresponds to the precipitation of 0.24 fmol of RNA in the IP.

Native gels

Native gel analysis was performed as described by Raghunathan and Guthrie (1998), with the following changes. Reactions were incubated with or without 2mM ATP for 30 minutes at 25°C. Spermidine was not included in the reactions. Gels were transferred to Hybond-N membrane in 0.5X TAE. Northern blots were sequentially reprobed after being stripped with 0.1% SDS in boiling water.

Immunoprecipitations

Between 50 and 200 mL of culture were grown at 25°C to OD 0.8 to 1.0. Pellets were resuspended in 1 mL IPP150 (10 mM Tris pH 8.0, 150 mM NaCl, 0.1% NP40) in the presence of 1 mM PMSF, 1 mM benzamidine, 1 μg/mL leupeptin, 1 μg/mL aprotinin, and 0.5 μg/mL pepstatin A. Cells were disrupted in the presence of 0.5 mm zirconia/silica beads (Biospec Products, Inc.) by four 1.5 minute pulses in a Mini-beadbeater (Biospec Products, Inc.). Extracts were normalized to the same concentration by Bradford assay (BioRad). For each immunoprecipitation, 10 μL Protein A sepharose (Amersham) were pre-incubated for 2 hours at 23°C with 2 μL Snu114 antisera, 5 μL

Prp8 antisera, 2 μL SmD1 antisera, or 2 μL non-immune sera in the presence of IPP150. Resin was washed three times with IPP150; 500 μg extract plus IPP150 were added to a total volume of 300 μL. For TAP purifications, 10 μL bed volume IgG sepharose (Amersham) were used. Reactions were incubated at 4°C for two hours and washed four times with 1 mL IPP150. Proteins were eluted by adding 80 μL elution buffer (50 mM Tris pH 8.0, 150 mM NaCl, 10 mM EDTA, 1% SDS) and rotating at room temperature for five minutes. Half of the supernatant was removed into 6X SDS-PAGE loading dye. Proteinase K was added to the remaining liquid and resin, and tubes were incubated at 37°C for 20 minutes. RNA was phenol extracted and ethanol precipitated. In parallel, RNA was also isolated from 20 μL of total extract to determine total snRNA levels.

Antibodies and western blot analysis

Polyclonal Snu114, Prp8, and SmD1 antibodies were gifts from P. Fabrizio, J. Beggs, and S.-C. Cheng, respectively. The Prp8.4 antibody was used for immunoprecipitations, while the Prp8.1 antibody was used for western blotting (Lossky et al., 1987; Jackson et al., 1988). Monoclonal Rpl3 was a gift from J. Warner (Vilardell & Warner, 1997). As a negative control, we used antisera from rabbits that failed to interact with any of the snRNAs above the level of background of Protein A Sepharose alone; the antisera was a gift from A. Kutach.

TCA extracts of proteins were prepared as described (Preker et al., 2002). Extracts were separated by electrophoresis on 7.5% SDS-polyacrylamide gels (with the exception of Prp8 in Figure 4B, which used a 10% gel) and blotted to nitrocellulose membrane. Membranes were cut and separate portions were probed with antibodies against Prp8 (1:1000 dilution), Snu114 (1:5000 dilution), and Rpl3 (1:5000 dilution).

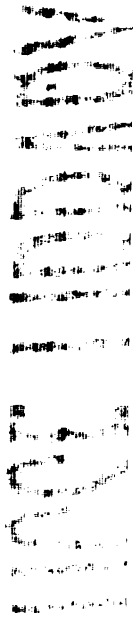

Protein A within the TAP-tag of Brr2-TAP was detected with Prp8 antibodies. Proteins were detected with enhanced chemiluminescence (Amersham) using goat anti-rabbit or goat anti-mouse antibodies conjugated to horseradish peroxidase (BioRad) at a dilution of 1:3000. Alternatively, proteins were detected and quantified using the Odyssey System (Li-Cor Biosciences) with fluorescent Alexa Fluor 680 goat anti-rabbit (Molecular Probes) and IR dye 800 donkey anti-mouse (Rockland) antibodies at a dilution of 1:20,000.

ACKNOWLEDGEMENTS

We thank Jean Beggs, Soo-Chen Cheng, Patrizia Fabrizio, and John Warner for gifts of antibodies, and Jon Staley for sharing protocols. Thank you to John Abelson, Hiten Madhani, Mike Springer, and members of the Guthrie lab for discussions and comments on the manuscript. T.J.B. was a Howard Hughes Medical Institute predoctoral fellow. C.G. is an American Cancer Society Research Professor of Molecular Genetics. This work was supported by National Institutes of Health Grant GM21119.

REFERENCES

Achsel T, Ahrens K, Brahms H, Teigelkamp S, Luhrmann R. 1998. The human U5-220kD protein (hPrp8) forms a stable RNA-free complex with several U5-specific proteins, including an RNA unwindase, a homologue of ribosomal elongation factor EF-2, and a novel WD-40 protein. *Mol Cell Biol 18*:6756-6766.

Anborgh PH, Cool RH, Jacquet M, Parlato G, Parmeggiani A. 1989. Structure-function relationships of the GTP-binding domain of Elongation Factor Tu. In: Bosch L, Kraal B, Parmeggiani A, eds. *The guanine-nucleotide binding proteins: common structural and functional properties*. New York: Plenum Press. pp 67-75.

Bartels C, Klatt C, Luhrmann R, Fabrizio P. 2002. The ribosomal translocase homologue Snu114p is involved in unwinding U4/U6 RNA during activation of the spliceosome. *EMBO Rep 3*:875-880.

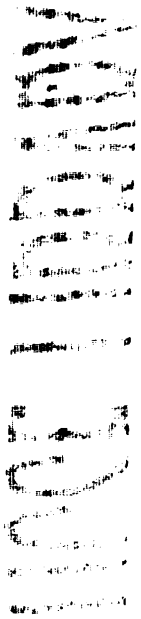

Bartels C, Urlaub H, Luhrmann R, Fabrizio P. 2003. Mutagenesis suggests several roles of Snu114p in pre-mRNA splicing. *J Biol Chem 278*:28324-28334.

Bindereif A, Green MR. 1987. An ordered pathway of snRNP binding during mammalian pre-mRNA splicing complex assembly. *EMBO J 6*:2415-2424.

Brenner TJ, Guthrie C. 2005. Genetic analysis reveals a role for the C terminus of the Saccharomyces cerevisiae GTPase Snu114 during spliceosome activation. *Genetics 170*:1063-1080.

Brow DA. 2002. Allosteric cascade of spliceosome activation. *Annu Rev Genet 36*:333-360.

Brown JD, Beggs JD. 1992. Roles of PRP8 protein in the assembly of splicing complexes. *EMBO J 11*:3721-3729.

Burge CB, Tuschl TH, Sharp PA. 1998. Splicing of precursors to mRNAs by the spliceosomes. In: Gesteland RF, Cech TR, Atkins JF, eds. *RNA World II*. Cold Spring Harbor, NY: Cold Spring Harbor Laboratory Press. pp 525-560.

Cheng SC, Abelson J. 1987. Spliceosome assembly in yeast. *Genes Dev 1*:1014-1027.

Cool RH, Parmeggiani A. 1991. Substitution of histidine-84 and the GTPase mechanism of elongation factor Tu. *Biochemistry 30*:362-366.

Diaz JF, Escalona MM, Kuppens S, Engelborghs Y. 2000. Role of the switch II region in the conformational transition of activation of Ha-ras-p21. *Protein Sci 9*:361-368.

Dix I, Russell CS, O'Keefe RT, Newman AJ, Beggs JD. 1998. Protein-RNA interactions in the U5 snRNP of *Saccharomyces cerevisiae*. *RNA 4*:1239-1250.

Fabrizio P, Laggerbauer B, Lauber J, Lane WS, Luhrmann R. 1997. An evolutionarily conserved U5 snRNP-specific protein is a GTP-binding factor closely related to the ribosomal translocase EF-2. *EMBO J 16*:4092-4106.

Fabrizio P, McPheeters DS, Abelson J. 1989. In vitro assembly of yeast U6 snRNP: a functional assay. *Genes Dev 3*:2137-2150.

Frank DN, Roiha H, Guthrie C. 1994. Architecture of the U5 small nuclear RNA. *Mol Cell Biol 14*:2180-2190.

Ghaemmaghami S, Huh WK, Bower K, Howson RW, Belle A, Dephoure N, O'Shea EK, Weissman JS. 2003. Global analysis of protein expression in yeast. *Nature 425*:737-741.

Ghetti A, Company M, Abelson J. 1995. Specificity of Prp24 binding to RNA: a role for Prp24 in the dynamic interaction of U4 and U6 snRNAs. *RNA 1*:132-145.

Grainger RJ, Beggs JD. 2005. Prp8 protein: at the heart of the spliceosome. *Rna 11*:533-557.

Hinz M, Moore MJ, Bindereif A. 1996. Domain analysis of human U5 RNA. Cap trimethylation, protein binding, and spliceosome assembly. *J Biol Chem 271*:19001-19007.

Inada M, Guthrie C. 2004. Identification of Lhp1p-associated RNAs by microarray analysis in Saccharomyces cerevisiae reveals association with coding and noncoding RNAs. *Proc Natl Acad Sci U S A 101*:434-439.

Jackson SP, Lossky M, Beggs JD. 1988. Cloning of the RNA8 gene of Saccharomyces cerevisiae, detection of the RNA8 protein, and demonstration that it is essential for nuclear pre-mRNA splicing. *Mol Cell Biol 8*:1067-1075.

Jones MH, Guthrie C. 1990. Unexpected flexibility in an evolutionarily conserved protein-RNA interaction: genetic analysis of the Sm binding site. *EMBO J 9*:2555-2561.

Jurica MS, Moore MJ. 2003. Pre-mRNA splicing: awash in a sea of proteins. *Mol Cell 12*:5-14.

Krengel U, Schlichting L, Scherer A, Schumann R, Frech M, John J, Kabsch W, Pai EF, Wittinghofer A. 1990. Three-dimensional structures of H-ras p21 mutants: molecular basis for their inability to function as signal switch molecules. *Cell 62*:539-548.

Kuhn AN, Brow DA. 2000. Suppressors of a cold-sensitive mutation in yeast U4 RNA define five domains in the splicing factor Prp8 that influence spliceosome activation. *Genetics 155*:1667-1682.

Kuhn AN, Li Z, Brow DA. 1999. Splicing factor Prp8 governs U4/U6 RNA unwinding during activation of the spliceosome. *Mol Cell 3*:65-75.

Kuhn AN, Reichl EM, Brow DA. 2002. Distinct domains of splicing factor Prp8 mediate different aspects of spliceosome activation. *Proc Natl Acad Sci U S A 99*:9145-9149.

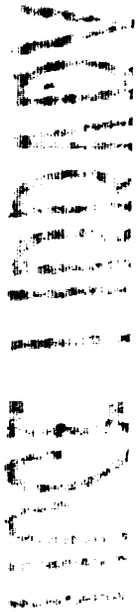

Laggerbauer B, Achsel T, Luhrmann R. 1998. The human U5-200kD DEXH-box protein unwinds U4/U6 RNA duplices in vitro. *Proc Natl Acad Sci U S A 95*:4188-4192.

Legrain P, Seraphin B, Rosbash M. 1988. Early commitment of yeast pre-mRNA to the spliceosome pathway. *Mol Cell Biol 8*:3755-3760.

Lin RJ, Newman AJ, Cheng SC, Abelson J. 1985. Yeast mRNA splicing in vitro. *J Biol Chem 260*:14780-14792.

Lossky M, Anderson GJ, Jackson SP, Beggs J. 1987. Identification of a yeast snRNP protein and detection of snRNP-snRNP interactions. *Cell 51*:1019-1026.

McPheeters DS, Fabrizio P, Abelson J. 1989. In vitro reconstitution of functional yeast U2 snRNPs. *Genes Dev 3*:2124-2136.

Preker PJ, Kim KS, Guthrie C. 2002. Expression of the essential mRNA export factor Yra1p is autoregulated by a splicing-dependent mechanism. *RNA 8*:969-980.

Raghunathan PL, Guthrie C. 1998. RNA unwinding in U4/U6 snRNPs requires ATP hydrolysis and the DEIH-box splicing factor Brr2. *Curr Biol 8*:847-855.

Ruby SW, Abelson J. 1988. An early hierarchic role of U1 small nuclear ribonucleoprotein in spliceosome assembly. *Science 242*:1028-1035.

Segault V, Will CL, Polycarpou-Schwarz M, Mattaj IW, Branlant C, Luhrmann R. 1999. Conserved loop I of U5 small nuclear RNA is dispensable for both catalytic steps of pre-mRNA splicing in HeLa nuclear extracts. *Mol Cell Biol 19*:2782-2790.

Sigal IS, Gibbs JB, D'Alonzo JS, Temeles GL, Wolanski BS, Socher SH, Scolnick EM. 1986. Mutant ras-encoded proteins with altered nucleotide binding exert dominant biological effects. *Proc Natl Acad Sci U S A 83*:952-956.

Staley JP, Guthrie C. 1998. Mechanical devices of the spliceosome: motors, clocks, springs, and things. *Cell 92*:315-326.

Staley JP, Guthrie C. 1999. An RNA switch at the 5' splice site requires ATP and the DEAD box protein Prp28p. *Mol Cell 3*:55-64.

Stevens SW, Barta I, Ge HY, Moore RE, Young MK, Lee TD, Abelson J. 2001. Biochemical and genetic analyses of the U5, U6, and U4/U6 x U5 small nuclear ribonucleoproteins from Saccharomyces cerevisiae. *RNA 7*:1543-1553.

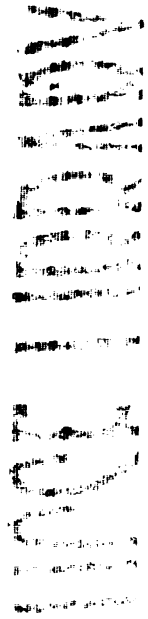

Stevens SW, Ryan DE, Ge HY, Moore RE, Young MK, Lee TD, Abelson J. 2002. Composition and functional characterization of the yeast spliceosomal penta-snRNP. *Mol Cell 9*:31-44.

Turner IA, Norman CM, Churcher MJ, Newman AJ. 2004. Roles of the U5 snRNP in spliceosome dynamics and catalysis. *Biochem Soc Trans 32*:928-931.

Umen JG, Guthrie C. 1995. A novel role for a U5 snRNP protein in 3' splice site selection. *Genes Dev 9*:855-868.

van Nues RW, Beggs JD. 2001. Functional contacts with a range of splicing proteins suggest a central role for Brr2p in the dynamic control of the order of events in spliceosomes of Saccharomyces cerevisiae. *Genetics 157*:1451-1467.

Vilardell J, Warner JR. 1997. Ribosomal protein L32 of Saccharomyces cerevisiae influences both the splicing of its own transcript and the processing of rRNA. *Mol Cell Biol 17*:1959-1965.

Will CL, Luhrmann R. 2001. Spliceosomal UsnRNP biogenesis, structure and function. *Curr Opin Cell Biol 13*:290-301.

Xie J, Beickman K, Otte E, Rymond BC. 1998. Progression through the spliceosome cycle requires Prp38p function for U4/U6 snRNA dissociation. *EMBO J 17*:2938-2946.

Zeidler W, Egle C, Ribeiro S, Wagner A, Katunin V, Kreutzer R, Rodnina M, Wintermeyer W, Sprinzl M. 1995. Site-directed mutagenesis of Thermus thermophilus elongation factor Tu. Replacement of His85, Asp81 and Arg300. *Eur J Biochem 229*:596-604.

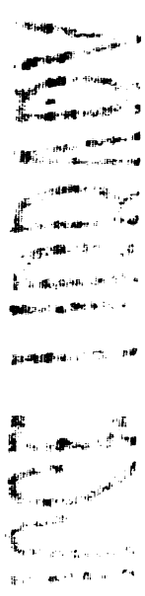

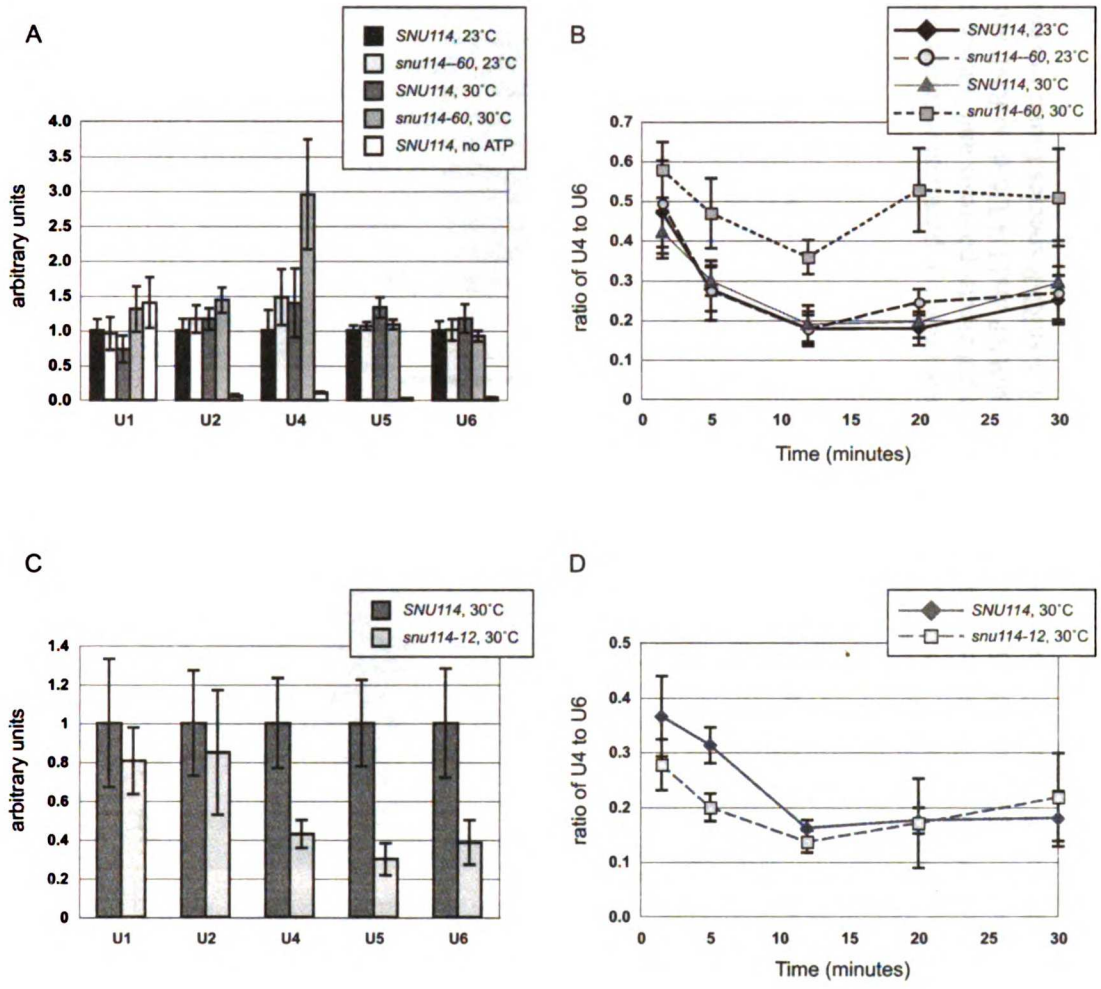

Figure 1. Spliceosome assembly and activation in *snu114-60* and *snu114-12* extracts. **A:** *SNU114* and *snu114-60* extracts were incubated at 23°C and 30°C with biotinylated pre-mRNA and spliceosomes were affinity purified. Levels of snRNAs associated with transcript after 20 minutes of incubation under splicing conditions are shown, as quantified by real-time PCR. Each co-precipitating snRNA was normalized to 1.0 for *SNU114* at 23°C. As a control, *SNU114* extract was incubated at 23°C with pre-mRNA in the absence of ATP. **B:** Ratio of transcript-bound U4 snRNA versus U6 snRNA over time for *SNU114* and *snu114-60* extracts. **C:** snRNAs bound to biotinylated transcript after 20 minutes of incubation under splicing conditions in *SNU114* and *snu114-12* extract at 30°C. Each snRNA was normalized to 1.0 for *SNU114*. **D:** Ratio of transcript-bound U4 snRNA versus U6 snRNA over time for *SNU114* and *snu114-12* extracts. Data represent the average of at least five experiments; in A and B, n = 7 for the 30°C data, n = 5 for the 25°C data, and in C and D, n = 5. Error bars indicate standard error.

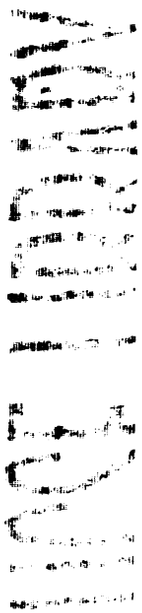

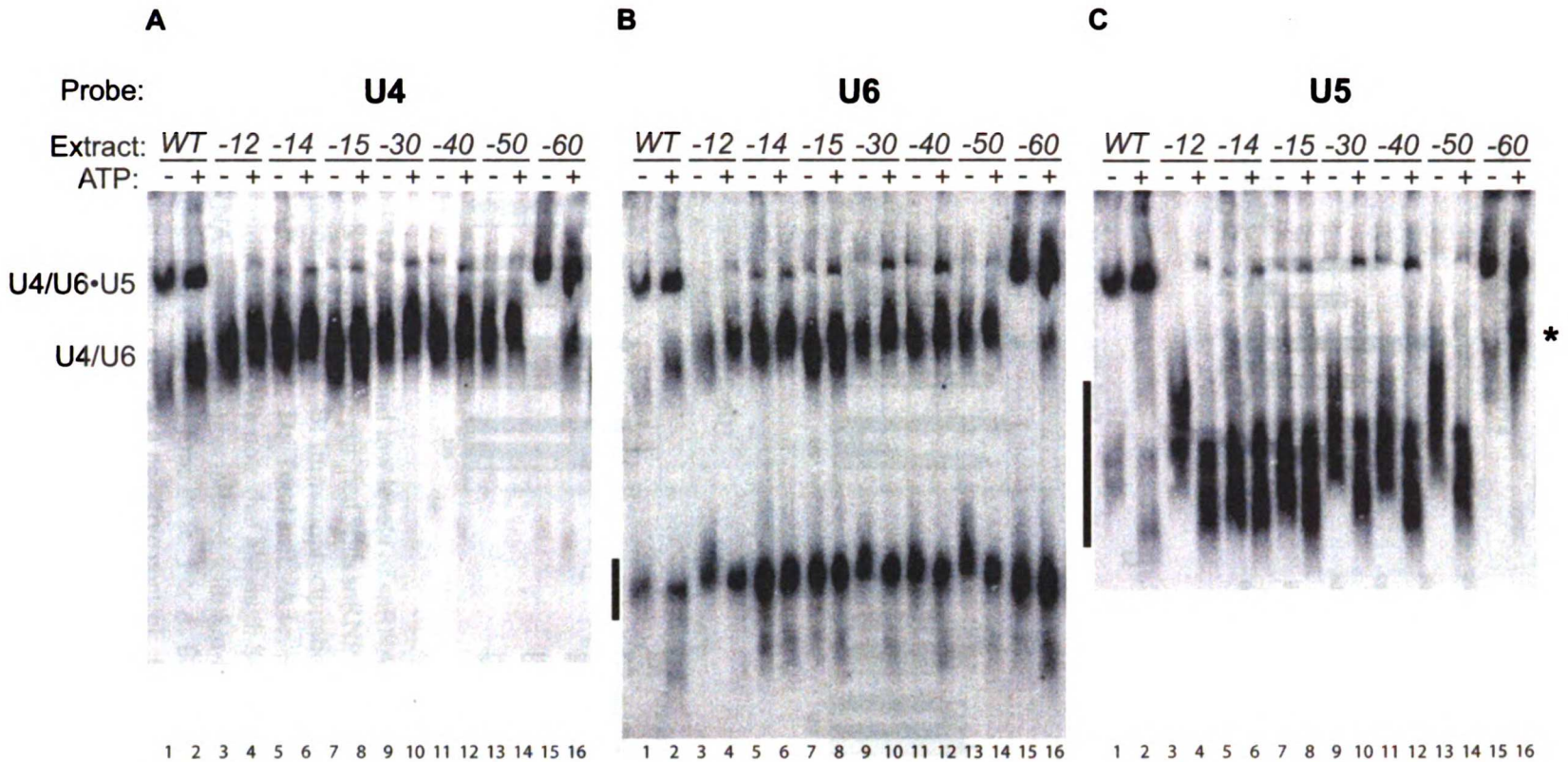

Figure 2. *snu114* mutants have low levels of tri-snRNP. Extracts from *snu114* mutant strains grown at permissive temperature were incubated under splicing conditions, with or without ATP. snRNPs were resolved by native gel electrophoresis and transferred to nitrocellulose. Northern blots were probed for U4 (**A**), U6 (**B**), and U5 (**C**). U4/U6•U5 tri-snRNP and U4/U6 di-snRNP are labeled; free snRNPs are indicated by black bars to the left of each panel. The asterisk indicates the U5-snRNP species found in *snu114-60*.

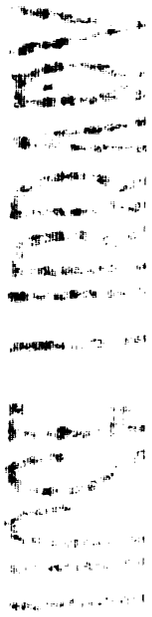

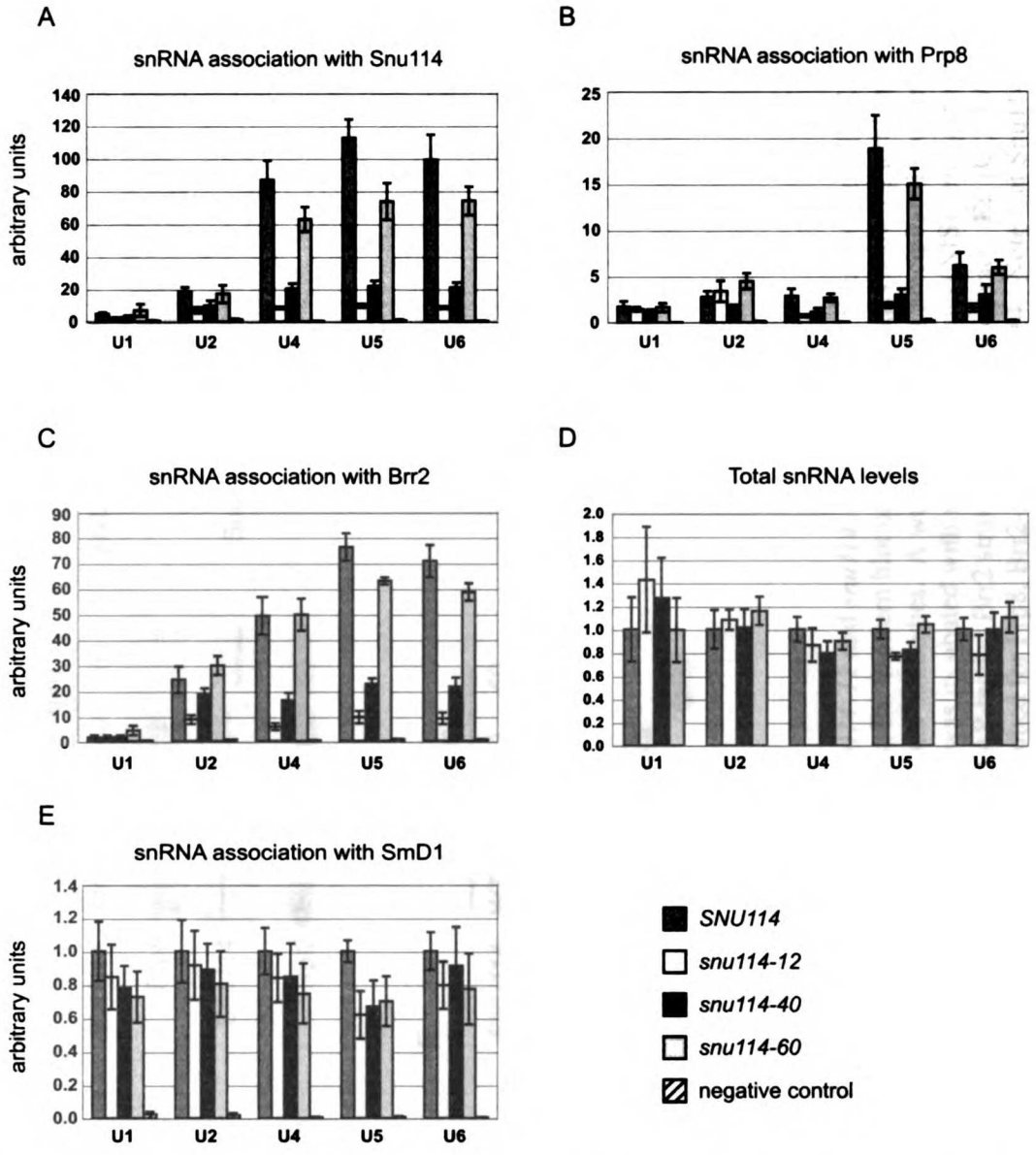

Figure 3. U5 snRNP proteins bind low levels of snRNAs in *snu114-12* and *snu114-40*. Bars indicate levels of snRNAs co-purified with snRNP proteins. **A:** Immunoprecipitation of Snu114. **B:** Immunoprecipitation of Prp8. **C:** Affinity purification of TAP-tagged Brr2. **D:** Total snRNA levels in the untagged extracts. **E:** Immunoprecipitation of SmD1. We note that although SmD1 does not bind directly to U6 snRNA, U6 snRNA was likely co-precipitated with Sm-bound U4 snRNA. Co-purifying snRNAs were quantified using real-time PCR. For A, B, and E, *SNU114* extract was incubated with non-immune sera as a negative control. For C, untagged *SNU114* extract was used as negative control. In A, B, and C, quantitation represents equal molar amounts of snRNAs (see Materials and Methods). In D and E, snRNA levels were normalized to 1.0 for SNU114. Data represent the average of at least three experiments. In A, n=6; B, n = 5; C, n = 3; D, n = 5; E, n = 5. Error bars indicate standard error.

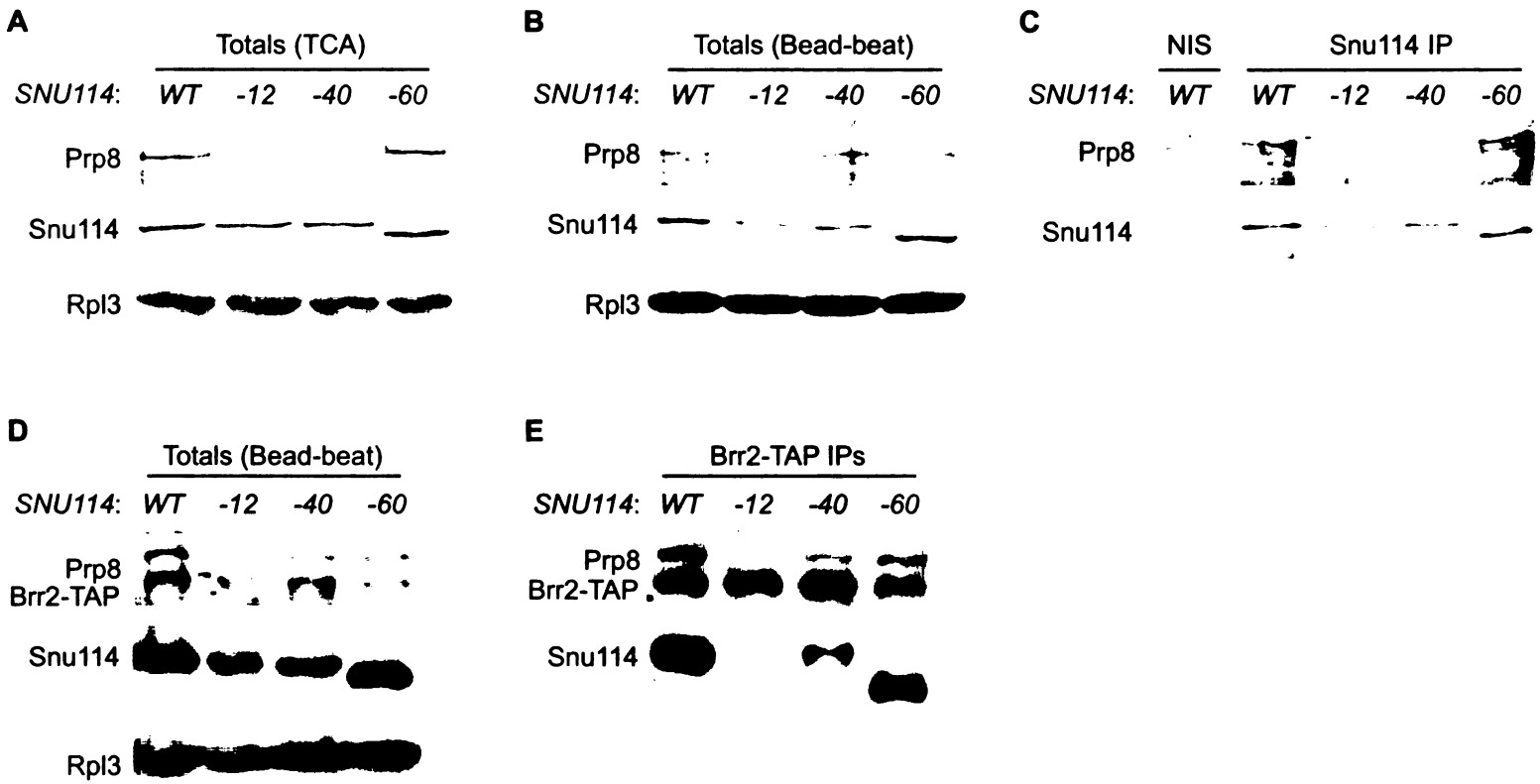

Figure 4. Decreased association of Snu114 with Prp8 and Brr2 in *snu114-12* and *snu114-40* extracts. **A:** Western blot of TCA extracts showing the levels of Prp8 and Snu114 in the indicated strains. **B:** Western blot of bead-beat extracts showing total levels of Prp8 and Snu114. **C:** Snu114 was immunoprecipitated using polyclonal antibodies. A western blot of the precipitated proteins was probed for Snu114 and Prp8. As a control for the IP, *SNU114* extract was incubated with non-immune serum (NIS) conjugated to Protein A sepharose. **D:** Levels of Prp8, Brr2-TAP, a nd Snu114 in TAP-tagged Brr2 strains in bead-beat extract. **E:** Brr2-TAP was affinity purified, and a western blot of the precipitated proteins was probed for Prp8, Brr2-TAP, and Snu114. Note that Snu114-60 migrates faster than Snu114 because the protein contains 70 fewer amino acids. In A, B, and D, Rpl3 was used as a loading control.

EPILOGUE

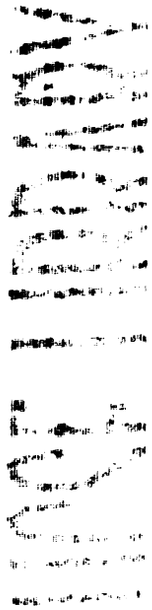

EPILOGUE

Splicing is a remarkably dynamic process, requiring multiple rearrangements of the spliceosomal RNA and protein components before, during, and after the two chemical reactions (reviewed by Staley and Guthrie 1998). Due to its homology to EF-G (Fabrizio et al. 1997), we hypothesized that Snu114 would be involved in mediating conformational rearrangements in the spliceosome. When I started this project, I could only conjecture when and where Snu114 would be operating. During the past five years, my work and the work of others have demonstrated that Snu114 plays important roles during U5 snRNP formation, spliceosome activation, and spliceosome disassembly. Intriguingly, GTP binding and hydrolysis by Snu114 have been implicated at distinct stages of splicing, potentially contributing to proper ordering of spliceosomal steps.

I began my investigation into the function of Snu114 by creating conditionally lethal alleles via random mutagenesis (Chapter 1). I identified a large number of mutations within conserved motifs in the GTPase domain, confirming the importance of the protein's enzymatic activity. A cluster of temperature-sensitive mutations was located in each of domains III and V. Mapping these mutations onto a model of Snu114 based on the crystal structure of EF2 showed that they are adjacent to the G2 and G3 (Switch I and Switch II) motifs that change conformation upon GTP hydrolysis. It is likely that these mutations impair domain movements resulting from changes in the bound nucleotide. Lastly, I found two types of mutations in domain IV. EF-G—the homolog of Snu114—structurally structurally resembles EF-Tu bound to tRNA (Nissen et al. 1995); in this analogy, domain IV is similar to the anticodon loop domain. Notably, this domain of EF-G appears to move considerably upon GTP hydrolysis (Stark et al. 2000). Domain IV

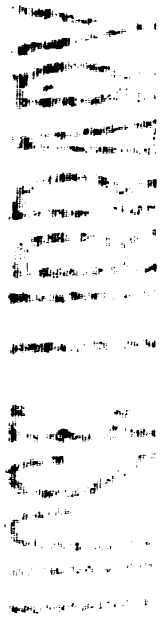

is interrupted in primary sequence by domain V; thus I termed the two portions Domain IVa and IVb. A cluster of mutations in domain IVa causes temperature-sensitive growth, and deletion of most of domain IVb (*snu114-60*) leads to modest growth defects at both low and high temperatures. Genetic and biochemical analyses of these *snu114* alleles implicate Snu114 in the assembly of U5 snRNP and spliceosome activation.

In Chapter 2, I showed that Snu114 is essential for the formation of U5 snRNP. My work suggests that neither Snu114 nor Prp8 can interact with U5 snRNA alone, indicating that Snu114 and Prp8 must form a heterodimer prior to interacting with U5 snRNA. Additionally, Snu114 mutants show a decreased association with Prp8 and cause a drop in the level of Prp8 protein, suggesting that the stability of Prp8 depends on its ability to interact with Snu114. GTP binding or hydrolysis is likely to be important for the formation of a Snu114/Prp8 heterodimer, as several of the mutations that disrupt this interaction are within conserved GTPase motifs. Since several mutations outside of the G domain cause a similar phenotype, these may affect regions that are the effectors of the change in nucleotide status. I proposed that GTP-bound Snu114 binds to Prp8, and that this heterodimer is then able to bind to U5 snRNA (Figure 1).

A common theme among members of the GTPase superfamily is that they productively interact with other molecules when bound to GTP, but not GDP (Bourne et al. 1990; Bourne et al. 1991). Thus, the idea that an interaction between Snu114 and Prp8 could depend on GTP is not without precedent. While the initial interaction between Snu114 and Prp8 may depend on the bound nucleotide, it seems unlikely that a sustained interaction requires GTP, since Snu114 probably hydrolyzes GTP at least once during the splicing cycle. A model can be envisioned whereby GTP-bound Snu114 is

[redacted]

required for initial interaction with Prp8; GTP hydrolysis at the time that U5 snRNP interacts with the spliceosome could allow this particle to rearrange to a conformation that would have been unstable before spliceosomal interaction. Additional interactions, either between the two proteins or with other proteins and/or RNA, could then support the Snu114-Prp8 interaction regardless of the nucleotide status. Lastly, it cannot be excluded that the initial interaction between Snu114 and Prp8 does not actually depend upon GTP binding or hydrolysis. Although we do not favor this model, it is possible that the Snu114 mutants alter the conformation of the protein in a manner not specifically related to its ability to bind or hydrolyze GTP.

The formation of a Snu114/Prp8 heterodimer, and perhaps its association with the U5 snRNA, appears to be a prerequisite for addition of other U5 snRNP proteins. A U5 snRNP particle containing Snu114, Prp8, U5 snRNA, and Aar2 can be purified from yeast (Gottschalk et al. 2001); we think it is likely that this complex represents an early stage in snRNP formation (Figure 1). Aar2 interacts directly with Prp8, and *in vitro* this interaction is mutually exclusive with the interaction of Prp8 with Brr2 (A. Kutach, unpublished). Work by Alan Kutach suggests that Snu114 functions during a transition from the Aar2-containing particle to a Brr2-containing U5 snRNP, which could then be assembled into tri-snRNP and the spliceosome. Overexpression of Aar2, which is expected to affect a potential equilibrium between the two particles, is synthetically lethal with *snu114-60,* a truncation of 70 amino acids of the C-terminus. Additionally, I found that overexpression of Aar2 in a *snu114-60* strain decreases the association of Brr2 with U5 snRNA (T.J.B. unpublished data). In this experiment, the association of Aar2 with

U5 snRNA was not correspondingly increased, as we had predicted; however, this may be an artifact of immunoprecipitating a highly overexpressed protein.

We do not currently know whether the Aar2 particle is a necessary intermediate in the assembly pathway of U5 snRNP, or if it represents an alternative, and potentially regulatory, pathway. This could be tested by inducing the transcription of a modified U5 snRNA containing a tag, which allows incorporation of the newly transcribed U5 snRNA into snRNPs to be monitored. Are snRNP complexes that contain Aar2 present prior to Brr2-containing complexes? It would also be useful to generate conditional alleles of Aar2 and determine how U5 snRNP formation is affected. Based on the finding that Aar2 overexpression decreases the levels of the Brr2-snRNP in the background of mutations in *SNU114*, *PRP8*, and *BRR2* (T.J.B. and A.K.K., unpublished data), we currently support the model that the Aar2 complex is a precursor to the Brr2 complex. It seems unlikely that ATP hydrolysis by Brr2 is required for the transition between the two particles, since the mutation *brr2-1*, which impairs hydrolysis, is not sensitive to Aar2 overexpression. Could changes in the nucleotide-binding status of Snu114 regulate this transition? Such a change could alter the interaction between the C-terminus of Snu114 and Prp8 and either lead to the displacement of Aar2 or create a binding site for Brr2. This model would explain why Aar2 overexpression is synthetically lethal with *snu114-60*. While we do not currently have any evidence for nucleotide hydrolysis or exchange during this transition, it is an interesting question to pursue.

A number of distinct mutations in Snu114 block spliceosome activation. In Chapter 1, I found that *snu114-60* is synthetically lethal with mutations in factors involved in spliceosome activation, including *PRP28*, *BRR2*, and *PRP8*. Moreover, in

Chapter 2 I showed that *in vitro*, *snu114-60* blocks release of U4 from assembled spliceosomes. Truncation of the N-terminus of the Snu114, a domain that is not found in the homologue EF-G, causes a similar phenotype as *snu114-60*, both biochemically (Bartels et al. 2002) and genetically (T.J.B. unpublished data). Additionally, the allele *snu114-D271N*, which converts the nucleotide specificity from GTP to XTP, blocks release of U4 when extracts are incubated at non-permissive temperature (Bartels et al. 2003). Release of U4 from the stalled spliceosomes could be achieved by lowering the temperature and adding both ATP and hydrolysable XTP (Bartels et al. 2003). Together, the data show that Snu114 functions during spliceosome activation, and that GTP hydrolysis is required at this time. Based on homology with EF-G, I suggested that truncation of the C-terminus of Snu114 could phenocopy a mutation affecting GTP hydrolysis because the C-terminus is necessary to transmit a conformational rearrangement of the protein resulting from hydrolysis. A good candidate for a factor that interacts with domain IV of Snu114 is Prp8; it is known that the two proteins physically interact (Achsel et al. 1998; Dix et al. 1998), and I observed particularly strong genetic interactions between mutations in *SNU114* domain IV and *PRP8* (Chapter 1). Our work on Snu114 was complemented by results from Kuhn and Brow suggesting that Prp8 negatively regulates the activities of the ATPases Prp28 and Brr2 (Kuhn et al. 1999; Kuhn and Brow 2000; Kuhn et al. 2002). I therefore proposed that GTP hydrolysis by Snu114 would cause Prp8 to relieve the inhibition of Prp28 and Brr2, leading to the release of U1 and U4.

Before I began this project, Snu114 had been implicated in the second step of splicing. Antibodies against U5-116 kDa (the human ortholog of Snu114) inhibit the

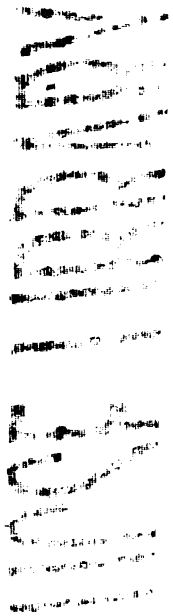

second step when added to HeLa extract (Fabrizio et al. 1997). Furthermore, U5-116 kDa crosslinks to the intron upstream of the 3' splice site between the two chemical steps (Liu et al. 1997). Because of these two lines of evidence, I initially proposed that Snu114 would function during the second step of splicing, but genetic and biochemical analyses in yeast have not supported this hypothesis. All of the *snu114* alleles that I tested inhibit the first step of splicing. While it is possible an allele that blocks the first step of splicing would mask a block in the second step, none of the alleles showed genetic interactions with second step factors, either. The inconsistency between the human and yeast results could be due to divergent functions of the protein between humans and yeast or an artifact of the methods. The antibody inhibition method is an imperfect assay. If U5-116 kDa were already assembled into snRNPs at the time of antibody addition, the epitopes for the antibody may not be accessible. If spliceosomal rearrangements made the epitopes accessible after the first step, adding a large mass to U5 snRNP potentially could affect the activities or binding of other proteins. Furthermore, while U5-116 kDa crosslinks to intron between the steps of splicing, the presence of the protein at this location does not necessarily indicate an active role. Alternatively, it remains a possibility that Snu114 functions at the second step, but the appropriate second-step alleles have not yet been identified.

Recently, work by Eliza Small in Jon Staley's lab has demonstrated a role for Snu114 during spliceosome disassembly (personal communication). As a model for the post-catalytic spliceosome and spliceosome disassembly, they affinity purify Prp43, which co-precipitates U2, U5, and U6 snRNAs. Addition of ATP causes release of all three snRNAs into the supernatant, presumably due to the activity of the ATPase Prp43.

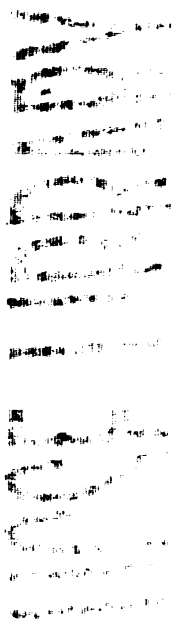

Addition of CTP, UTP, or GTP does not support release of the snRNAs. The presence of GDP along with ATP inhibits release, but including GTP rescues this inhibition. Non-hydrolysable GTP analogs also rescue the inhibition, showing that GTP *binding* is sufficient for this activity. Small and Staley then used the XTPase allele of Snu114 (*snu114-D271N*) to show that Snu114 is responsible for the inhibition by GDP on snRNA release. That is, when they repeat the affinity purification of Prp43 using *snu114-D271N* extract, addition of XDP prevents the ATP-dependent release of snRNAs, and XTP rescues this inhibition. Neither GDP nor GTP has an effect in this case. Together, the data show that Snu114 must be in the GTP-bound conformation in order for Prp43 to hydrolyze ATP and disassemble the spliceosome.

While snRNA release from an immunopurified Prp43 complex can serve as a model for spliceosome disassembly, spliceosome activation can be modeled by monitoring the release of U4 and U6 snRNAs from a Brr2 purification (Raghunathan and Guthrie 1998a). The Staley lab has preliminary evidence that release of U4 and U6 snRNAs from a Brr2 pull-down similarly can be inhibited by GDP and rescued by GTP (personal communication). The identity of the GTPase responsible for this behavior has not been confirmed, but Snu114 is obviously the best candidate. This would agree with my genetic and biochemical data that Snu114 is important for spliceosome activation, and with my model that the nucleotide-status of Snu114 changes at the time of spliceosome activation. The Staley data suggest that Snu114 must exchange GDP for GTP in order to activate Brr2, while the data of Bartels *et al.* (2003) indicate that GTP hydrolysis by Snu114 occurs at the time of Brr2 activity. My own data provide little insight into this issue. Bartels' conclusion that Snu114 requires GTP hydrolysis relied on

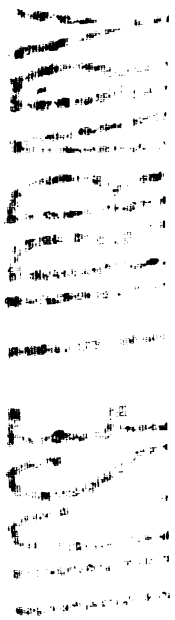

the finding that XTP led to the dissociation of U4 from stalled spliceosomes, but XMPPNP did not (Bartels et al. 2003). However, they did not test the ability of XMPPNP to compete with XTP for binding to Snu114. If XMPPNP bound to Snu114-D271N more poorly than XTP, then their data could be reinterpreted to mean that GTP binding—and not necessarily hydrolysis—is required for U4 release. Alternatively, both nucleotide exchange and GTP hydrolysis could be required for U4 release.

In Figure 2A, I present a simple model for the nucleotide-dependent activities of Snu114 during the splicing cycle. When tri-snRNP joins the spliceosome, Snu114 is bound to GTP. Proper interaction with the spliceosome, perhaps dependent on contacts with U1 snRNP, activates GTP hydrolysis. This modifies the conformation of Prp8, leading to ATP hydrolysis by Prp28 and Brr2 and unwinding of U1 and U4 snRNAs. Following the two chemical steps of splicing, and perhaps also release of the mRNA, release of GDP from Snu114 is triggered. Exchange of GDP for GTP activates Prp43, leading to spliceosome disassembly.

Staley's Brr2 data, however, leads to an alternative model, shown in Figure 2B. In this scenario, exchange of GDP for GTP occurs not only at the Prp43-dependent step, but also at the Brr2-dependent step. This implies that the splicing cycle must include at least two rounds of GTP hydrolysis and exchange by Snu114. It is unclear in this model at precisely which steps GTP hydrolysis would occur. One potential place of regulation between spliceosome disassembly and spliceosome activation at which GTP hydrolysis could be stimulated is the formation of tri-snRNP from U4/U6 di-snRNP and the GTP-bound U5 snRNP. Between spliceosome activation and disassembly, GTP hydrolysis could occur concomitant with Brr2 activity or during the catalytic steps.

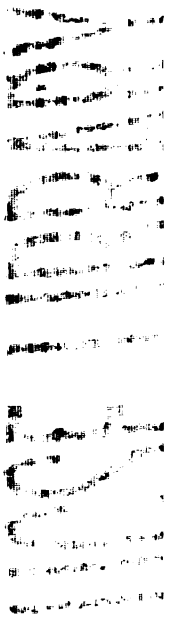

Overall, the data suggest that Snu114 plays a regulatory role in activating spliceosome activation and disassembly. It seems likely that GTP hydrolysis and nucleotide exchange by Snu114 are triggered only when the spliceosome has achieved a particular conformation. In this way, Snu114 functions as checkpoint to ensure that the spliceosome is ready to advance to the next step. Several of the translational GTPases similarly regulate fidelity. A "correct" conformation of interacting factors triggers GTP hydrolysis, and because GTP hydrolysis commits the process to progression to the next step, this ensures accuracy. For example, the GTPase activity of EF-Tu, which causes its associated tRNA to be deposited in the ribosome, is strongly stimulated by cognate codon-codon interactions (Pape et al. 1998; Gromadski and Rodnina 2004; Rodnina et al. 2005). In a second example, GTP-bound eIF2 escorts met-tRNA to the ribosome. Only when the tRNA reaches a start codon is Pi from hydrolyzed GTP released, leading to eIF2 release and committing the ribosome to using that start codon (Algire et al. 2005).

Further investigations into GTP binding and hydrolysis

In order to better assess the role of GTP hydrolysis and nucleotide exchange by Snu114 during splicing, the biochemical properties of our *snu114* alleles need to be determined. Wildtype and mutant Snu114 should be expressed and purified, and the ability of the proteins to bind and hydrolyze GTP should be assayed. If the existing alleles do not specifically affect hydrolysis or nucleotide binding, then new alleles should be created. A residue that is likely to be involved in hydrolysis is H218 in the G3 motif (Sprinzl et al. 2000). Although I did try to create the mutation H218L, I did not realize until much later that a duplication had occurred during the PCR mutagenesis; likely for this reason, the mutant was inviable. It would also be useful to test whether mutation of

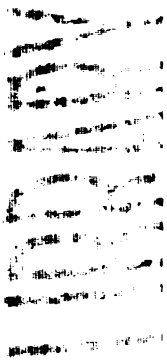

any of the arginine residues within the G domain affect hydrolysis, since GTPases universally seem to require an arginine supplied either in *–cis* or in *–trans* (Bourne 1995; Scheffzek et al. 1998). Mutation of R29 in *E. coli* EF-G decreases GTP hydrolysis (Mohr et al. 2000); however, this residue is not conserved in Snu114. Once we have identified particular alleles of Snu114 affect GTP binding or hydrolysis, we will be able to more definitively correlate these phenotypes with effects on splicing.

In Chapter 2, I proposed that Snu114 must bind GTP in order to interact with Prp8. The nucleotide-binding requirements of Snu114 during U5 snRNP formation could be tested with an *in vitro* system involving Snu114, Prp8, and U5 snRNA. U5 snRNA can be transcribed *in vitro*, and Snu114 could be prepared either recombinantly or via overexpression from yeast. Although full-length Prp8 has been difficult to express bacterially, the Beggs lab has used yeast two-hybrid analyses to identify a minimal region of 50 amino acids of Prp8 that interacts with Snu114 *in vivo* (Grainger and Beggs 2005). This small region of the N-terminus of Prp8 could potentially be expressed recombinantly. Additionally, it is possible that co-expression of Snu114 with full length Prp8 from bacteria would improve the stability of Prp8. The ability of each of the three molecules to interact with the others could then be tested, alone and in combination. Are these interactions stabilized or destabilized by the presence of different guanine nucleotides and analogs? Do any of the interactions stimulate GTP hydrolysis? This *in vitro* system could also be used to determine what domains of Snu114 are required for interaction with Prp8 and/or U5 snRNA. Smaller portions of Snu114, such as the G domain, domains III-V, and domain IV, could be expressed and tested for binding. In

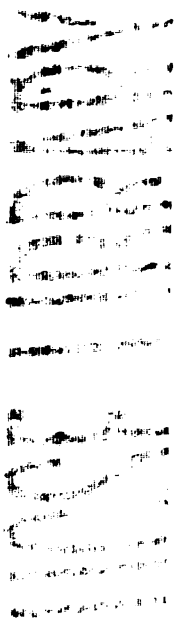

this purified system, are the mutants Snu114-12 and Snu114-40 defective in binding Prp8, as suggested by my immunoprecipitations in Chapter 2?

An undated, unfinished manuscript from Lothar Krinke and John Abelson, which has been handed down through the generations, suggests that GDP stimulates the formation of U5 snRNP in an *in vitro* reconstitution system. GTP, hydrolysable or not, did not provide any advantage over GDP. This is an intriguing observation. More recent reconstitution systems do not involve the addition of GDP (O'Keefe et al. 1996), although it is not clear if the nucleotide requirements have been systematically tested.

The study of GTP hydrolysis by Snu114 on the spliceosome is intrinsically complicated. Unlike the ribosome, a purified system for studying the spliceosome does not exist due its extremely dynamic nature. Consequently, splicing is currently assayed in extract, which likely contains a myriad of other GTPases. It is not possible to monitor the activity of Snu114 by simply adding γ^{32}P GTP to a splicing reaction, as GTP hydrolysis occurs immediately upon addition to the extract (T.J.B. unpublished data). Furthermore, several of the spliceosomal ATPase are able to hydrolyze GTP (Kim et al. 1992; Schwer and Guthrie 1992). As shown by Bartels *et al.* (2003) and Small and Staley (personal communication), use of the Snu114-XTPase allele can prove to be a powerful tool in studying this GTPase within a sea of other GTPases. Since extract from the Snu114-XTPase allele supports splicing at the permissive temperature (Bartels et al. 2003), one should be able to monitor the hydrolysis of γ^{32}P XTP in a splicing reaction to determine the timing of Snu114 activity in relationship to particular blocks in splicing. Progress can be made by use of simplified systems, as shown by Jon Staley in monitoring the nucleotide-dependence of snRNA release from Brr2 and Prp43 pull-downs. One

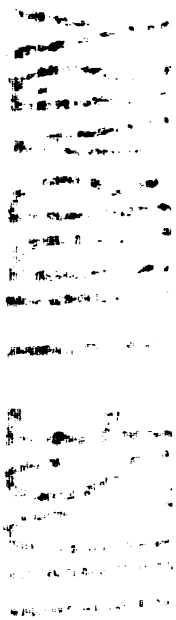

could also study GTP hydrolysis in the context of purified spliceosomes that have been stalled on biotinylated transcript. Although much development remains, Scott Stevens' purification of a penta-snRNP under low salt conditions suggests that in the future, it may be possible to splice within a more purified complex (Stevens et al. 2002).

Because the functions of most GTPases are regulated by GAPs and GEFs (Bourne et al. 1991; Vetter and Wittinghofer 2001), it will be most informative to determine what factors induce the activities of Snu114. Although it is not trivial to determine what constitutes a GAP in cases where a particular conformation of a macromolecular complex is required, some success can be achieved in the context of a simpler system. For example, while the GTPase activity of EF-G is stimulated maximally by the ribosome, the L7/L12 proteins alone can substantially induce GTP hydrolysis: the intrinsic rate of GTP hydrolysis by EF-G is $<10^{-5}$ s^{-1}, the rate with L7/L12 is 0.3 s^{-1}, while the ribosome stimulates the rate to 170 s^{-1} (Savelsbergh et al. 2000). Similarly, the GAP eIF5 can increase the GTPase activity of eIF2 by 800-fold, although the additional presence of the 40S-mRNA complex induces the rate by 10^6 fold (Algire et al. 2005). Thus, it is plausible that one could determine individual factors that induce GTP hydrolysis by Snu114, even if this induction is not as great as what occurs within the spliceosome. The GTPase activity of purified Snu114 could be monitored when additional splicing factors, such as Prp8, Brr2, and U5 snRNA are included, or when Snu114 is purified from yeast within various snRNP subcomplexes. It is useful to note that both GTP hydrolysis and release of P_i should be monitored, as the two activities often are not simultaneous (Algire et al. 2005; Savelsbergh et al. 2005).

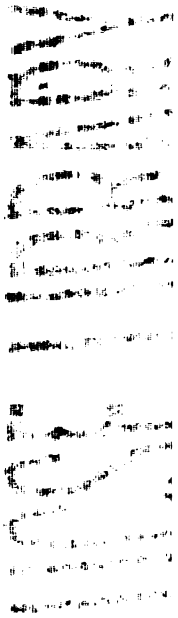

The commonly held view that EF-G does not require a GEF has recently be questioned (Zavialov et al. 2005). Thirty years ago, it was reported that EF-G binds to GTP with ten-fold lower affinity than GDP (Baca et al. 1976); however, Zavialov *et al.* (2005) found that it binds GDP 60-fold more tightly than GTP To determine whether Snu114 requires a GEF, the affinities of the protein for GTP and GDP should be determined. In the case of translation, the ribosome itself has been shown to function as a GEF, as well as a GAP, for RF3 (Zavialov et al. 2001),and it has also been proposed that the ribosome serves as the GEF for EF-G (Zavialov et al. 2005). The spliceosome may induce nucleotide exchange by Snu114 following the catalytic steps of splicing, given the Staley lab's data indicating that a switch from GDP to GTP is required for spliceosome disassembly.

Genetic strategies could be pursued to identify the GAP and GEF for Snu114. This strategy would require first identifying mutations within Snu114 that affect the protein's intrinsic GTPase activity and its ability to bind nucleotides, and secondly screening for mutations that exacerbate or suppress the resulting growth defects. Mutations that decrease GTP hydrolysis might be synthetically lethal with mutations in the GAP. One could conceivably identify mutations in Snu114 that either increase or decrease its binding affinity for GDP. Growth defects caused by these different types of mutations could be suppressed or enhanced, respectively, by mutations in the GEF that decrease nucleotide release by Snu114.

Musings on Mimicry

I was initially excited about the idea that Snu114 could mimic an RNA, based on the resemblance between the crystal structure of EF-G and that of EF-Tu bound to tRNA

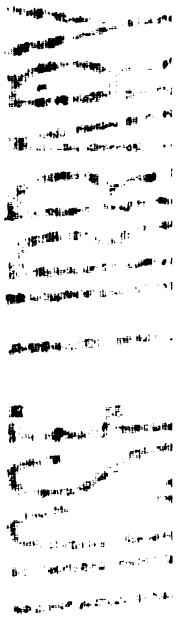

(Nissen et al. 1995). As other translation factors were crystallized, the idea of mimicry began to emerge as a unifying principle (Nissen et al. 2000; Nakamura 2001). However, recent studies have shown that RRF (ribosome recycling factor) and RF2 (release factor 2) do not bind to the ribosome in the same place as EF-Tu/tRNA, questioning the mimicry hypothesis for some of the translation factors (Lancaster et al. 2002; Brodersen and Ramakrishnan 2003; Klaholz et al. 2003; Rawat et al. 2003). Additionally, domain IV—the putative anticodon arm mimic—in eukaryotic EF2 is much larger than in bacterial EF-G, decreasing its resemblance to tRNA (Figure 3) (Jorgensen et al. 2003). Domain IV of Snu114 is required for the protein's function, since cells are not viable when this domain is deleted (Bartels et al. 2003; T.J.B. unpublished data). However, this requirement for domain IV likely arises from its role as the lever arm of the GTPase motor.

Since the similar dimensions of the many translation factors may result from constraints imposed by binding to the ribosome, is there a deeper significance to the resemblance between EF-G and tRNA? The structural similarity allows the two molecules to interact with the ribosome in a similar location (Stark et al. 1997; Agrawal et al. 1998). If domain IV of Snu114 does mimic an RNA, what would this mean? For the sake of argument, let us assume that this domain resembles the conserved loop of U5 snRNA (Staley and Guthrie 1998). Does domain IV of Snu114 bind to the spliceosome in the same place as the U5 conserved loop, perhaps replacing it? Although the experiments are not trivial, one could test whether domain IV specifically crosslinks to the exon/intron boundaries, as U5 does. However, it is difficult to know *a priori* which RNA Snu114 might resemble, and thus what the functional consequences might be.

Regardless of the significance of the potential mimicry domain, the homology between Snu114 and EF-G is intriguing. The ribosomal GTPases (the translation factors and the SRP receptors) were likely the original GTPases, as these are the only members of the GTPase superfamily found in prokaryotes, archae, and eukaryotes (Caldon et al. 2001). Given that life is thought to have begun in an RNA world, it is not surprising that the first GTPases were associated with RNA. The spliceosome resembles the ribosome in that both are large, RNA-based macromolecular complexes. How is it that a spliceosomal GTPase evolved from a ribosomal GTPase?

Beyond genetics

While genetics is a powerful tool, it also raises many new questions. For example, *brr1Δ* is synthetically lethal with *sad1-1* and *snu66Δ* (Inada 2004), and I found strong genetic interactions between *snu114* mutations and *brr1Δ, sad1-1, and snu66Δ* (Chapter 1). Unfortunately, not enough is known about each these factors to ascertain the importance of these interactions. While Brr1 and Sad1 have been implicated in snRNP biogenesis in yeast (Noble and Guthrie 1996; Lygerou et al. 1999), analysis of the human homologues suggests that Snu66 and Sad1 are required for addition of tri-snRNP to the spliceosome (Makarova et al. 2001). A more detailed analysis of the phenotypes of *snu66Δ* and *sad1-1* in yeast would be helpful. One could also construct strains containing two mutations, such as *snu66Δ* and *snu114-60*, in which a wildtype copy of one of the genes was provided under control of an inducible promoter. Depletion of the wildtype copy could be used to ascertain the stage of splicing that is inhibited and hence why the two mutations are synthetically lethal.

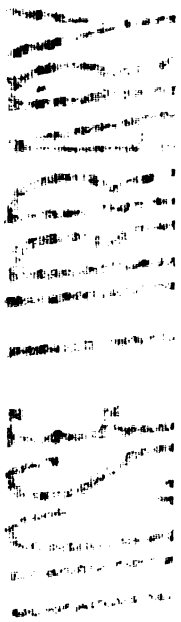

The enigmatic C-terminus

Strikingly, *snu114-60* shows only a modest growth defect and yet is synthetically lethal in combination with mutations in a large number of other splicing factors (Chapter 1, appendix). A second EF-G homolog has been found in yeast. Ria1/Efl1 plays a role in ribosome biogenesis, and short truncations of the C-terminus of this protein also cause lethality (Becam et al. 2001; Senger et al. 2001). To my knowledge, truncations of the C-terminal domains of EF-G and EF2—which are smaller than in Snu114—have not been studied. Clearly, the C-terminus of Snu114 has an essential function, but what?

Why does *snu114-60* exhibit such strong genetic interactions? This domain could be important for relaying information about the bound nucleotide to other factors. *snu114-60* might then be synthetically lethal with mutations in other factors (such as *PRP28* and *BRR2*) that are involved with inducing transitions in the nucleotide status or in relaying signals that result from changes in the bound nucleotide. Perhaps the C-terminus is an important interaction domain within U5 and tri-snRNP. This could explain the synthetically lethality with *snu66Δ* and mutations in *PRP8*, since it is likely that these factors also contribute to the stability of the snRNPs. Proteins that interact specifically with domain IVb could be determined via a yeast-two-hybrid assay, using full-length Snu114, a fragment containing just domain IVb alone, and the truncation Snu114-60.

Making progress

In the past five years, great strides have been made in proteomic and structural analyses of the spliceosome. Proteomic studies have identified both Snu114 and Prp8 as components of all active splicing complexes and U5-containing particles (reviewed by Jurica and Moore 2003). Mass spectroscopy also has the potential to inform us about

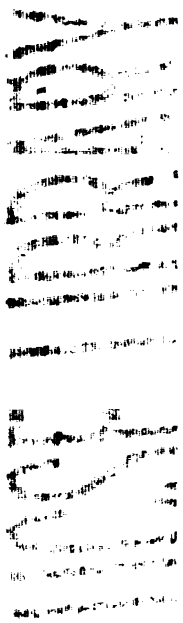

post-translational modifications of Snu114 and other splicing proteins, adding another layer to our understanding of the regulation to splicing.

Excitingly, structural studies of the spliceosome are beginning to emerge (Boehringer et al. 2004; Jurica et al. 2004). As techniques for identifying particular proteins within larger complexes improve, it will be informative to locate Snu114 in relationship to other proteins and RNAs. Structures of smaller complexes, such as the U5 snRNP or even just the Prp8/Snu114 dimer, could help resolve questions about the interactions between Snu114 and Prp8. An intriguing question is whether the interactions between Snu114 and Prp8—and perhaps other molecules as well—are altered when Snu114 is bound to GTP versus GDP. Lastly, it will be interesting to determine the relative positions of the N- and C-terminal domains of Snu114, since both domains appear to be involved in similar processes (Bartels et al. 2002; Chapters 1 and 2).

Much has been learnt about Snu114 since I began this project, but many questions remain. In particular, the exact timing of GTP hydrolysis and exchange is still unknown. A better grasp on these activities is essential for understanding how this protein might regulate—and be regulated by—spliceosomal transitions. I am excited that Corina Maeder will pursue these questions, and so we will continue to gain insight into the spliceosome's only GTPase.

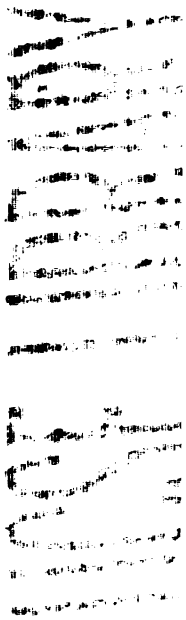

Figure 1. A model for U5-snRNP formation. GTP-bound Snu114 and Prp8 form a heterodimer and then bind to Sm-bound U5 snRNA. Addition of Aar2 forms the 16S U5 snRNP; exchange of Aar2 for Brr2 allows addition of other U5- and tri-snRNP factors. Potentially, an equilibrium may exist between the Aar2-containing and Brr2-containing U5 snRNPs. It is also possible that formation of the Aar2-snRNP is not a prerequisite for Brr2 assembly. Additional U5 snRNP and the U4/U6 di-snRNP can interact with the Brr2 particle, but not with the Aar2 particle.

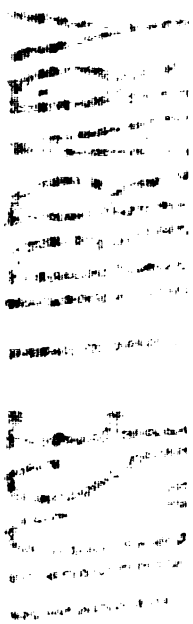

114
GTP
+
8
8
114
GTP
8
U5
114
GTP
8
U5
114
GTP
Aar2
?
?
Brr2
8
U5
114
GTP
Brr2
8
U5
114
GTP
U5-snRNP
U4
U6
Brr2
8
U5
114
GTP
tri-snRNP

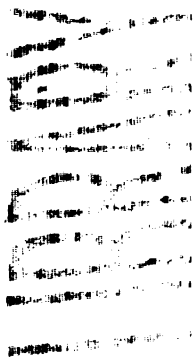

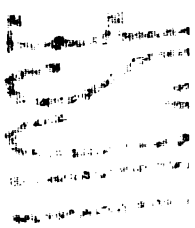

Figure 2. Models for the activity of Snu114. **A:** In the simplest model, GTP is hydrolyzed during spliceosome activation, and exchange of GDP for GTP occurs during spliceosome disassembly. **B:** An alternative model of the activity of Snu114. See text for details.

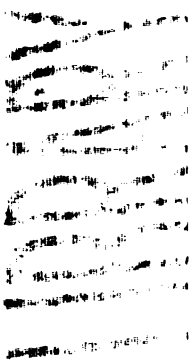

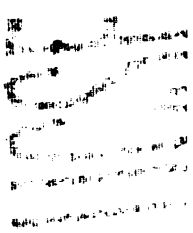

A

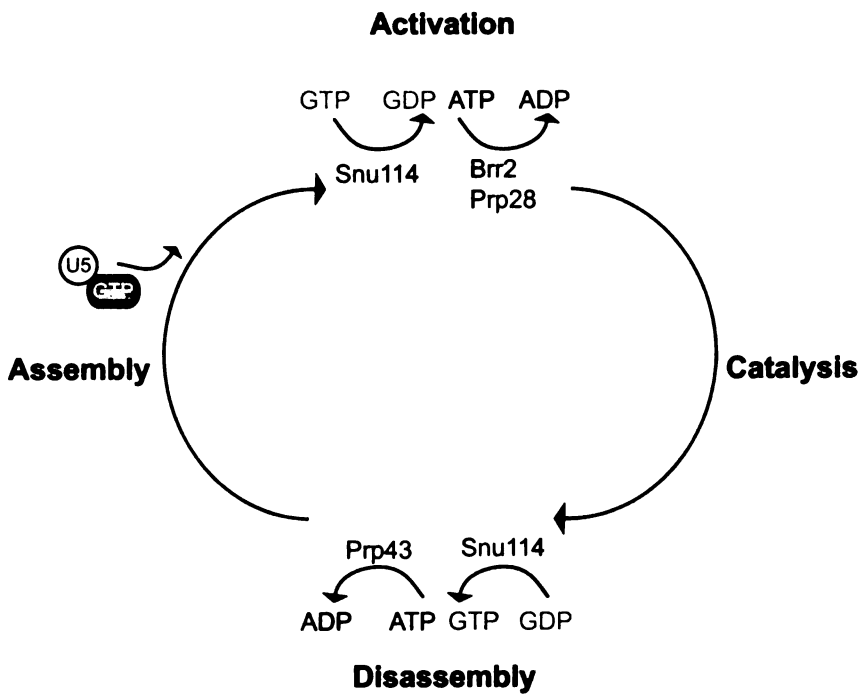
Activation
GTP GDP ATP ADP
Snu114
Brr2
Prp28
U5
GTP
Assembly
Catalysis
Prp43
Snu114
ADP ATP GTP GDP
Disassembly

B

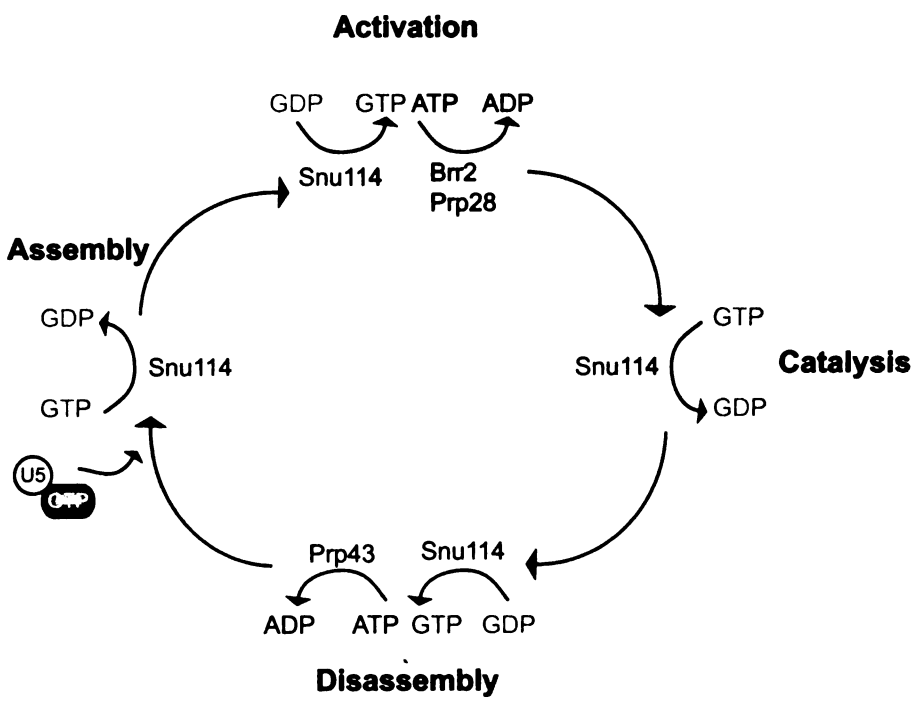
Activation
GDP GTP ATP ADP
Snu114
Brr2
Prp28
Assembly
GDP
Snu114
GTP
GTP
Snu114
GDP
Catalysis
U5
GTP
Prp43
Snu114
ADP ATP GTP GDP
Disassembly

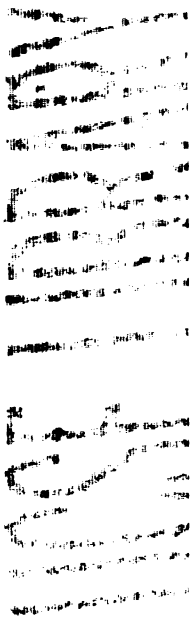

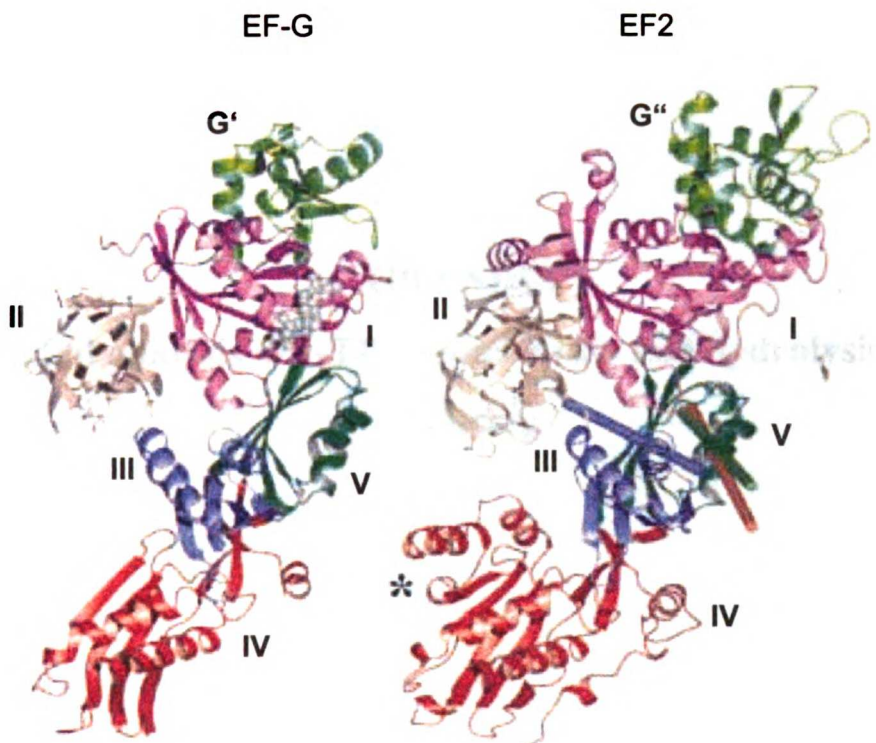

Figure 3. The structures of prokaryotic and eukaryotic EF-G/EF2. EF-G from *T. thermophilus* is shown on the left, and EF2 from *S. cerevisiae* on the right. The asterisk indicates insertions within domain IV that are specific to eukaryotic EF2. Reproduced from Jorgensen *et al.* (2003).

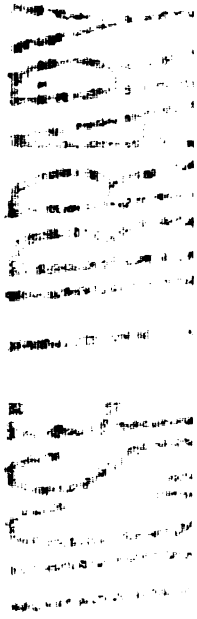

APPENDIX I

An initial analysis of GTP requirements and hydrolysis during splicing

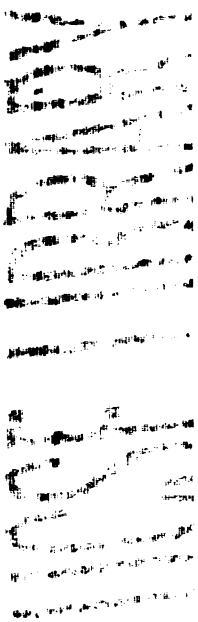

APPENDIX I

An initial analysis of GTP requirements and hydrolysis during splicing

INTRODUCTION

One of the most salient features of Snu114 is that it contains a GTPase domain, as defined by homology to other members of the GTPase superfamily (Bourne et al. 1990; Bourne et al. 1991; Fabrizio et al. 1997). When I started this project in 2000, key questions regarding Snu114 as a GTPase had not been answered. Is Snu114 a *bona fide* GTPase? Under what conditions does the protein hydrolyze GTP, and under what conditions is GDP exchanged for GTP? Is GTP required for splicing?

In this appendix, I begin to address the following questions:

1. Does Snu114 hydrolyze GTP *in vitro*, and if so, under what conditions? Fabrizio *et al* (1997) showed that U5-116K from purified HeLa U5 snRNP could be cross-linked specifically to GTP. Later, Bartels et al (2003) overexpressed His-tagged Snu114 in yeast and purified the protein by nickel-agarose chromatography followed by size-exclusion chromatography. This purified Snu114 also could be cross-linked to GTP. They report that the protein also hydrolyzed some GTP, but they could preclude the possibility that this activity resulted from co-purifying proteins (Bartels et al. 2003).
2. Does addition of GTP enhance *in vitro* splicing reactions? When an *in vitro* splicing system was initially established in yeast, the nucleotide requirements were tested (Lin et al. 1985). While ATP at a concentration of 1 mM supported robust splicing, minimal splicing was observed with 0.5 mM CTP, GTP, or UTP. I was curious whether additional GTP could provide an advantage.

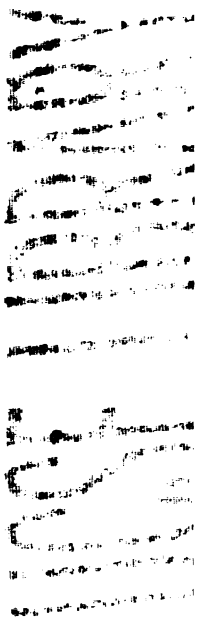

3. Do non-hydrolysable GTP analogs inhibit splicing *in vitro*? Fabrizio *et al* (1997) reported that concentrations of GTPγS or GMPPNP greater than 4 mM could inhibit splicing *in vitro* from HeLa extracts. I wanted to determine whether this was reproducible in yeast extract.
4. When during splicing does GTP hydrolysis occur?

RESULTS AND DISCUSSION

GTPase activity

I was first interested in determining whether Snu114 is capable of hydrolyzing GTP *in vitro*. As an initial method for investigating this question, I obtained purified U5- and tri-snRNP from Scott Stevens (Stevens et al. 2001). The snRNPs were purified from a Brr2-polyoma tagged strain by polyoma-agarose chromatography; U5 snRNP and tri-snRNP were then separated by glycerol gradient centrifugation. Testing GTP hydrolysis in the context of the snRNPs was expedient, in that it did not require me to purify Snu114 immediately. It also had the potential benefit that if the GAP for Snu114 were a protein associated with U5 or tri-snRNP, stimulatory activity would already be present.

snRNPs were incubated in the presence of γ^{32}P GTP, and GTP hydrolysis was monitored by thin-layer chromatography (TLC). As a positive control for the assay conditions, the bacterial SRP receptor Ffh, which is a GTPase, was also incubated with γ-^{32}P GTP (Figure 1A, 1B). I found that U5 snRNP hydrolyzed γ^{32}P GTP (Figure 1A). The amount of hydrolysis by Ffh and U5 snRNP was reduced by the presence of excess cold GTP (Figure 1A). In contrast, GTP was not hydrolyzed in the presence of tri-snRNP (Figure 1B). Unfortunately, the lab's supply of U5- and tri-snRNP quickly disappeared, and further purifications and experiments were not pursued.

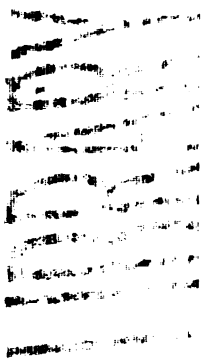

A number of reasons could explain the difference between the ability of U5 and tri-snRNP to hydrolyze GTP. It is possible that GTPase activity was lost during tri-snRNP purification, due to denaturation, degradation, or other deleterious events. However, this seems unlikely, since the U5- and tri-snRNP purification protocols are so similar. Differences in protein composition between U5 and tri-snRNP could lead to the observed result. For example, Prp28 is found specifically in purified U5 snRNP and not in tri-snRNP (Gottschalk et al. 1999; Stevens and Abelson 1999; Stevens et al. 2001). The nucleotide specificity by Prp28 has not been examined, so it is possible that it is capable of hydrolyzing GTP, like Prp2 and Prp16 (Kim et al. 1992; Schwer and Guthrie 1992). The ATPase Brr2, which is found in both snRNPs, exhibits a strong preference for ATP over GTP (Laggerbauer et al. 1998). To test whether Prp28 or Snu114 was responsible for the GTPase activity of U5 snRNP, the complex could be purified from extracts containing mutations in the ATPase domain of Prp28. Although mutations in the GTPase domain of Snu114 prevent U5 snRNP formation, U5 snRNP could be purified from the XTPase-allele grown at permissive temperature; if XTP were hydrolyzed, this would definitively show that Snu114 is responsible for the activity. Assuming that Snu114 was responsible for the observed GTP hydrolysis, it is possible that the GTPase activity of Snu114 is stimulated by a co-factor found specifically in U5 snRNP or repressed by a protein found specifically in tri-snRNP. Other than Prp28, one of only proteins found specifically in U5 snRNP and not in tri-snRNP is Snu40/Lin1; however, this protein is a substoichiometric component of the complex and thus not a good candidate for an activator (Stevens et al. 2001; TJB unpublished data). Tri-snRNP contains many proteins not found in U5-snRNP that could potentially repress Snu114

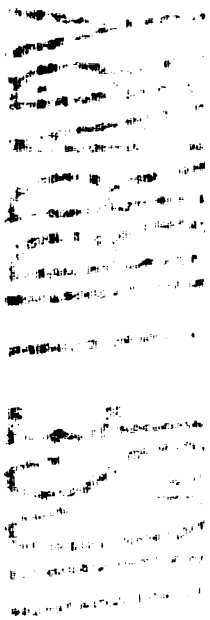

activity, including Snu66; interestingly, *snu66Δ* is synthetically with *SNU114* alleles. Given the model that GTP hydrolysis leads to Prp28 and Brr2 activity (Chapters 1 and 2), repression of Snu114's GTPase activity within tri-snRNP could prevent premature unwinding of the U4/U6 duplex. Theoretically, this repression would be relieved after tri-snRNP interacts with transcript, when the activity of Snu114 is presumably needed for catalytic activation.

Lastly, it would be interesting to determine whether GTP hydrolysis occurs within the 16S U5 snRNP that contains only Prp8, Snu114, Aar2, the Sm proteins, and U5 snRNA (Gottschalk et al. 2001). Since the presence of Aar2 and Brr2 seem to be mutually exclusive (Gottschalk et al. 2001; A. Kutach and C. Guthrie, personal communication), and since the snRNPs analyzed here were purified through a tag on Brr2, it is unlikely that Aar2 was present in the complexes that I assayed. Comparing the differences in GTPase activity between the Aar2 U5-snRNP and the Brr2 U5-snRNP could provide insight into what proteins repress or stimulate this activity.

Effect of nucleotides on *in vitro* splicing

In order to test whether GTP could support or enhance *in vitro* splicing, splicing extracts were incubated with different nucleotides. Splicing reactions usually include ATP at a concentration of 2 mM, although it has been shown that concentrations as low as 0.2 mM are sufficient (Tarn et al. 1993). When low concentrations (1 or 2 mM) of a single nucleotide were included in splicing reactions, the efficiency of splicing was much better with ATP than with GTP (Figure 2A, compare lanes 1 and 2; 3 and 4). Including 1 mM GTP with 1 mM ATP did not improve splicing as compared to ATP alone (Figure 2A, compare lane 6 with lanes 2 and 3). At increasing concentrations (up to 5 mM was

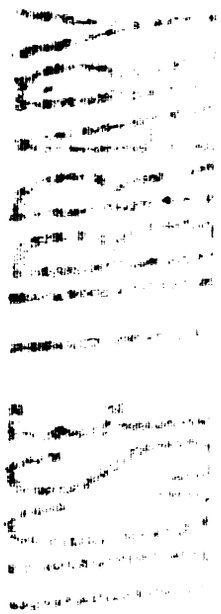

tested), addition of GTP alone supported splicing (Figure 2B, lane 9). ATP is known to be required for splicing; at high concentrations, GTP may support splicing either by phosphate transfer from GTP to endogenous ADP, because the nucleotide was contaminated with ATP, or because the spliceosomal ATPases have some lower ability to hydrolyze GTP.

I next asked whether non-hydrolysable analogs of GTP would inhibit splicing in extracts from *S. cerevisiae*. As a control, I also tested non-hydrolysable ATP analogs. Addition of 2 mM ATPγS alone to extracts allowed a low level of splicing (Figure 2B, lane 3). Although ATPγS is poorly hydrolysable, it appears that the degree and rate of hydrolysis are sufficient to support splicing *in vitro*. In contrast, AMPPNP, GMPPNP, and GTPγS individually did not support splicing (Figure 2B, lanes 4 and 5; and data not shown). Increasing concentrations of AMPPNP or GMPPNP were incubated with extracts prior to addition of ATP and radiolabeled pre-mRNA. While 5 mM AMPPNP inhibited splicing (Figure 2B, lane 11), GMPPNP did not inhibit splicing at concentrations up to 5 mM (Figure 2B, lanes 15-19). It is possible that GMPPNP does not prevent splicing *in vitro*, or that higher concentrations of the nucleotide analog are required.

Adding GMPPNP to extract would not reveal a requirement for hydrolysable GTP if GTP hydrolysis occurs between rounds of splicing. Alternatively, it is plausible that Snu114 (as do most GTPases) binds nucleotides tightly, and that simply adding GMPPNP to the extract is not sufficient to induce nucleotide exchange. To address both of these possibilities, I performed a recycling assay (Raghunathan and Guthrie 1998b) in the presence of GMPPNP. In this assay, extracts are incubated with increasing amounts

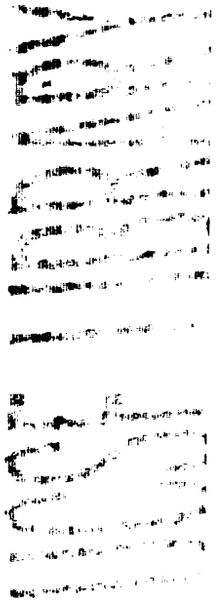

of cold pre-mRNA prior to addition of radiolabeled pre-mRNA. In contrast to wildtype spliceosomes, spliceosomes that are defective for recycling are not expected to be able to undergo multiple rounds of splicing and consequently will exhibit enhanced defects in splicing the radiolabeled transcript. I also reasoned that nucleotide exchange by Snu114 must occur at some point during the splicing cycle, and that adding GMPPNP during the incubation with cold pre-mRNA would allow maximum probability of the GTPase binding to the nucleotide analog. However, I found that regardless of GMPPNP addition, all of the extracts were similarly affected by pre-incubation with cold transcript (Figure 3). Unlike the previous assay (Figure 2), less mRNA was observed in extracts incubated with 5 mM GMPPNP (Figure 3, compare lanes 1, 6, and 11). Since the levels of the splicing intermediates were not decreased, it is unclear whether GMPPNP inhibited splicing or perhaps was correlated with an increase in degradation of the mRNA. It would be worth testing the effects of GMPPNP on splicing again, even without the recycling assay.

Because GTPases bind to nucleotides very tightly (Sprang 1997), I incubated extract in the presence of 10 mM EDTA to chelate magnesium, which should cause NTPases to release bound nucleotide. Extracts were then run through size exclusion columns to remove the EDTA and free nucleotides (Figure 4A). I first asked whether ATP alone is sufficient for splicing if all nucleotides have been removed, and whether GMPPNP could now inhibit splicing. Strikingly, addition of 2 mM ATP alone did not support splicing (Figure 4B, lane 2), but 2 mM of each NTP together led to splicing (Figure 4B, lane 3). Even more intriguingly, addition of GMPPNP now abolished splicing (Figure 4B, lane 5). Extracts incubated with EDTA looked similar to those

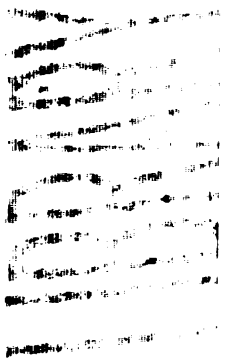

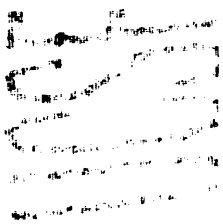

simply run through the sizing column, except the overall splicing efficiency was much reduced (Figure 4B, lanes 7-12). Therefore, future experiments did not include EDTA.

When I repeated the experiment with additional controls, however, I found that higher concentrations of nucleotides and magnesium were required for splicing after extract had been run through a sizing column. While 2 mM ATP and 2.5 mM Mg were not sufficient to support splicing (Figure 4C, lane 3), increasing the Mg concentration and the total amount of nucleotides improved splicing (Figure 4C, lanes 6-11). Using different combinations of nucleotides did not reveal much specificity for any particular nucleotide, although the combination of GTP, CTP, and UTP without ATP may have spliced worse than other combinations that included ATP (Figure 4C, lane 8; note that less transcript overall was recovered from this sample). Thus, it does not appear that addition of GTP enhances splicing *in vitro*. Unfortunately, the inhibition by GMPPNP did not repeat (Figure 4C, lanes 12-17). The GMPPNP experiment in 4C included an excess of Mg^{2+} compared to the experiment in 4B; it is possible that the Mg^{2+} in 4B was limiting for splicing.

Effects of GTP on snRNPs

To test the effects of GTP on snRNP profile, extracts were incubated with GTP prior to native gel analysis (Raghunathan and Guthrie 1998a). As a control, extracts were also incubated with ATP or ATP and actin pre-mRNA. The presence of actin did not greatly alter the phenotypes. Incubation with ATP caused a slight increase in di-snRNP levels in wildtype extract, and a more dramatic increase in *snu114-60* (Figure 5). However, addition of GTP did not increase the abundance of di-snRNP in either extract. This is consistent with Stevens' (2001) report that ATP but not GTP causes dissociation of

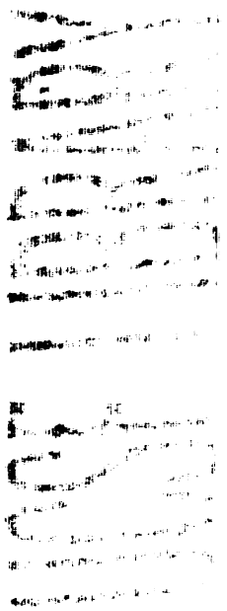

purified tri-snRNP. When either ATP or GTP was added to WT extract, U5 snRNP shifted to a lower mobility (Figure 5). Addition of GTP, similarly to ATP, induced an increase in the intensity of U5 snRNP in *snu114-60* (see Appendix III). These results suggest that both ATP and GTP can induce rearrangements of U5 snRNP. Either Prp28 or Brr2 could hydrolyze ATP to cause rearrangements, while Snu114 is probably the enzyme that hydrolyzes GTP.

Monitoring the nucleotide status of Snu114

Lastly, I started to devise a strategy to determine when during splicing Snu114 is bound to GTP versus GDP. Splicing reactions—which could be blocked at different stages—would be incubated with α^{32}P GTP. Snu114 or other associated proteins would be immunoprecipitated, and bound nucleotides would be eluted and separated by TLC. I tested the method by immunoprecipitating either Prp8 or Snu114 from splicing extract. Although I did not observe a reproducible signal from α^{32}P GTP (data not shown), I realized later that both of the antibodies that I was using have poor IP efficiency. I also tried the experiment by purifying spliceosomes bound to biotinylated pre-mRNA. While I did observe a radiolabeled signal that co-purified with the transcript, it was unclear whether the signal was reproducible (data not shown). In the future, this experiment could be optimized using either TAP-tagged proteins, such as Brr2-TAP, or the improved Snu114 antibody (Bartels et al. 2003).

CONCLUSION

My initial studies showed that GTP is hydrolyzed by U5 snRNP. Further analysis of complexes containing Snu114 will lead to insight about what conditions permit and activate GTPase activity. Although I did not find evidence that GTP is necessary for or

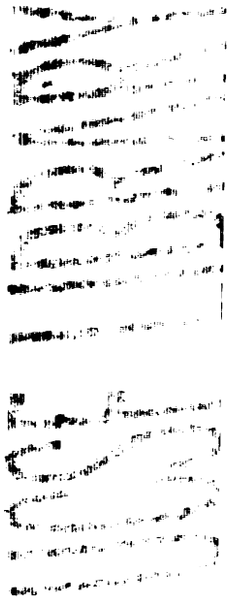

enhances splicing *in vitro*, I obtained contradictory results regarding the ability of GMPPNP to inhibit splicing. This is an experiment worth repeating. Finally, development of an assay to determine the nucleotide-bound status of Snu114 during splicing will help clarify when GTP hydrolysis and exchange occur within the context of the spliceosome.

MATERIALS AND METHODS

GTPase assays

U5- and tri-snRNP were gifts from Scott Stevens (Stevens et al. 2001), and the bacterial SRP protein Ffh was a gift from the Walter lab. Proteins were incubated in the presence of 50 mM Hepes pH 7.9, 150 mM potassium acetate, 2.5 mM magnesium acetate, and 2 mM DTT in a total volume of 20 μL. For the reactions with snRNPs, polyU was added to a final concentration of 0.1 mg/mL. The final concentration of Ffh was 100 nM. 2 ul of U5 snRNP or tri-snRNP were used, for final concentrations of approximately 2 to 8 nM. In Figure 1A, 2 μL of γ^{32}P GTP (30 Ci/mmol, 2 mCi/mL; Amersham) were used, and in Figure 1B, 0.5 μL of fresh γ^{32}P GTP were used. Cold GTP was included at a concentration of 20 μM, which is approximately a three-fold excess over the hot GTP. After zero or 60 minutes of incubation at 30°C, 5 μL aliquots were removed to 95 μL of 0.35 M KP pH 7.5. 1 μl of each reaction was run on a TLC plate, using 0.35 M KP pH 7.5 as running buffer.

In vitro splicing reactions

Splicing extract (Umen and Guthrie 1995)was prepared from *SNU114* cultures, and splicing reactions were performed as described (Lin et al. 1985), with the following changes. Extract was incubated at 25°C for ten minutes under splicing conditions (2.5

mM $MgCl_2$, 3% PEG, 60 mM KP) with 2 mM glucose to deplete ATP. In Figure 2A, ATP or GTP (or H20) were added at the indicated concentrations, along with radiolabeled actin pre-mRNA, and reactions were incubated at 25°C for 20 minutes. In Figure 2B, AMPPNP or GMPPNP (ranging from 0.002 mM to 5 mM) were added to reactions 10-19, and reactions were incubated for 10 minutes at 25°C. Radiolabeled pre-mRNA plus 2 mM ATP or the indicated nucleotides were then added, and reactions were incubated for an additional 15 minutes at 25°C. To compensate for higher amounts of nucleotide, additional $MgCl_2$ was added to the glucose-depletion reactions in Figure 2B. The final concentration of $MgCl_2$ was 8 mM for reactions 6, 7, 8, 9, 10, and 15 was 8 mM; 4.5 mM for reactions 11 and 16, and 2.5 mM for all others.

For the recycling assay (Raghunathan and Guthrie 1998b), extract was first incubated with 2 mM glucose. The concentration of $MgCl_2$ was 2.5 mM for reactions 1-5, 4.5 mM for reactions 6-10, and 8 mM for reactions 11-15. 2 mM ATP, unlabeled actin pre-mRNA (0, 0.6 nM, 1.5 nM, 3 nM, and 7.5 nM), and GMPPNP (0, 2, or 5 mM) were added to the extracts, and reactions were incubated for 15 minutes at 25°C. Hot actin was added at 0.3 nM, followed by another 15 minute incubation at 25°C.

G25 spin columns (Amersham) were washed with six column volumes (300 μL each) of splicing buffer (20 mM KCl, 60 mM KP pH 7.0, 8 mM Hepes pH 7.9, 3% PEG, 80 uM EDTA, 8% glycerol, 0.2 mM DTT) by spinning at 3000 rpm for 1 minute. For Figure 4B, 30 μL wildtype splicing extract was incubated with or without 10 mM EDTA for 10 minutes at room temperature followed by 15 minutes on ice. These extracts were added to the G25 columns, which were spun for 1 minute at 3000 rpm. An additional 30 μL splicing buffer was added to the columns and eluted. The 60 μL of eluate were split

into two 30 μL aliquots. One aliquot was incubated with 2.5 mM $MgCl_2$, and the other with 5 mM GMPPNP and 7.5 mM $MgCl_2$for 15 minutes at 25°C. In parallel, these reactions were then split into 10 μL aliquots, to which were added 0.3 nM radiolabeled actin and either splicing buffer, 2 mM ATP, or 2 mM each NTP plus 8 mM $MgCl_2$ (final concentrations). Reactions were incubated for 20 minutes at 25°C.

For Figure 4C, extract was not treated with EDTA prior to the spin column. For the GMPPNP reactions, 17 ul extract was incubated for 15 minutes at 25°C with 5 mM, 2 mM, or 0.2 mM GMPPNP and 5, 2.5, or 1.25 mM $MgCl_2$, respectively. Extracts were then divided such that 10 μL reactions contained the indicated nucleotides (2 mM each), adjusted amounts of $MgCl_2$, and 0.3 nM radiolabeled actin. Reactions were incubated for 30 minutes at 25°C. Total $MgCl_2$ concentrations were as follows: lanes 1,2, 10, and 11: 10 mM; lanes 3 and 4: 2.5 mM; lane 5: 2.5 mM; lanes 6-9: 8 mM; lanes 12 and 13: 15 mM; lanes 14 and 15: 12.5 mM; lanes 17 and 18: 11.25 mM.

I also determined conditions for using NAP-10 sizing columns (Amersham), which allows larger volumes of extract to be used. Columns were washed three times with 5 mL splicing buffer. 200 μL extract (incubated with or without EDTA at 4° for one hour) were added to each column. 1.1 mL splicing buffer were added to the column, and the first 1.3 mL eluate were discarded. Another 500 μL splicing buffer were added, and this eluate, which contained most of the protein, was saved. Because dilute extracts spliced more poorly, extracts were then concentrated to 400 μL in a Centricon 3 kDa column by spinning at 14K for 30 minutes at 4°C. I found that 4 mM excess $MgCl_2$ was required for optimal splicing with either 1 or 2 mM ATP. If all four NTPs were included

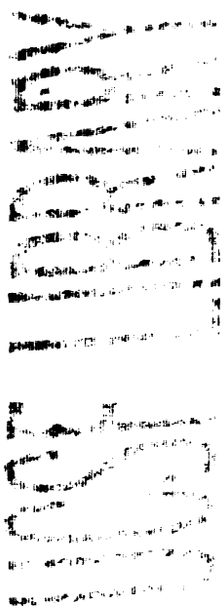

at 1 or 2 mM each, an excess of 0.5 or 1 mM $MgCl_2$ allowed optimal splicing. Unfortunately, I never conducted any productive assays using this technique.

snRNP gels

Native gel analysis was performed as described (Raghunathan and Guthrie 1998a). *SNU114* and *snu114-60* extracts were incubated either with buffer, 2 mM ATP, 2 mM GTP, or 2 mM ATP and 4 nM actin pre-mRNA.

Figure 1. GTP is hydrolyzed by U5 snRNP. **A:** The bacterial GTPase Ffh and U5 snRNP were incubated with γ^{32}P GTP for zero or 60 minutes. As a control for the specificity of the reaction, a three-fold excess of cold GTP was included in parallel reactions. **B:** The bacterial GTPase Ffh and tri-snRNP were incubated with γ^{32}P GTP for zero or 60 minutes. γ^{32}P GTP was separated from the product of the reaction, P_i, by thin layer chromatography.

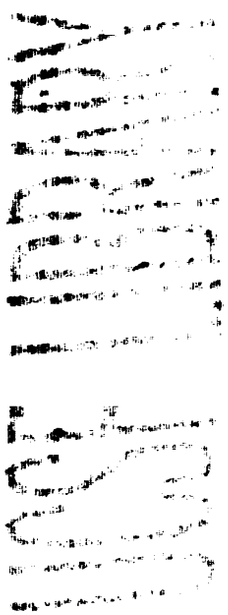

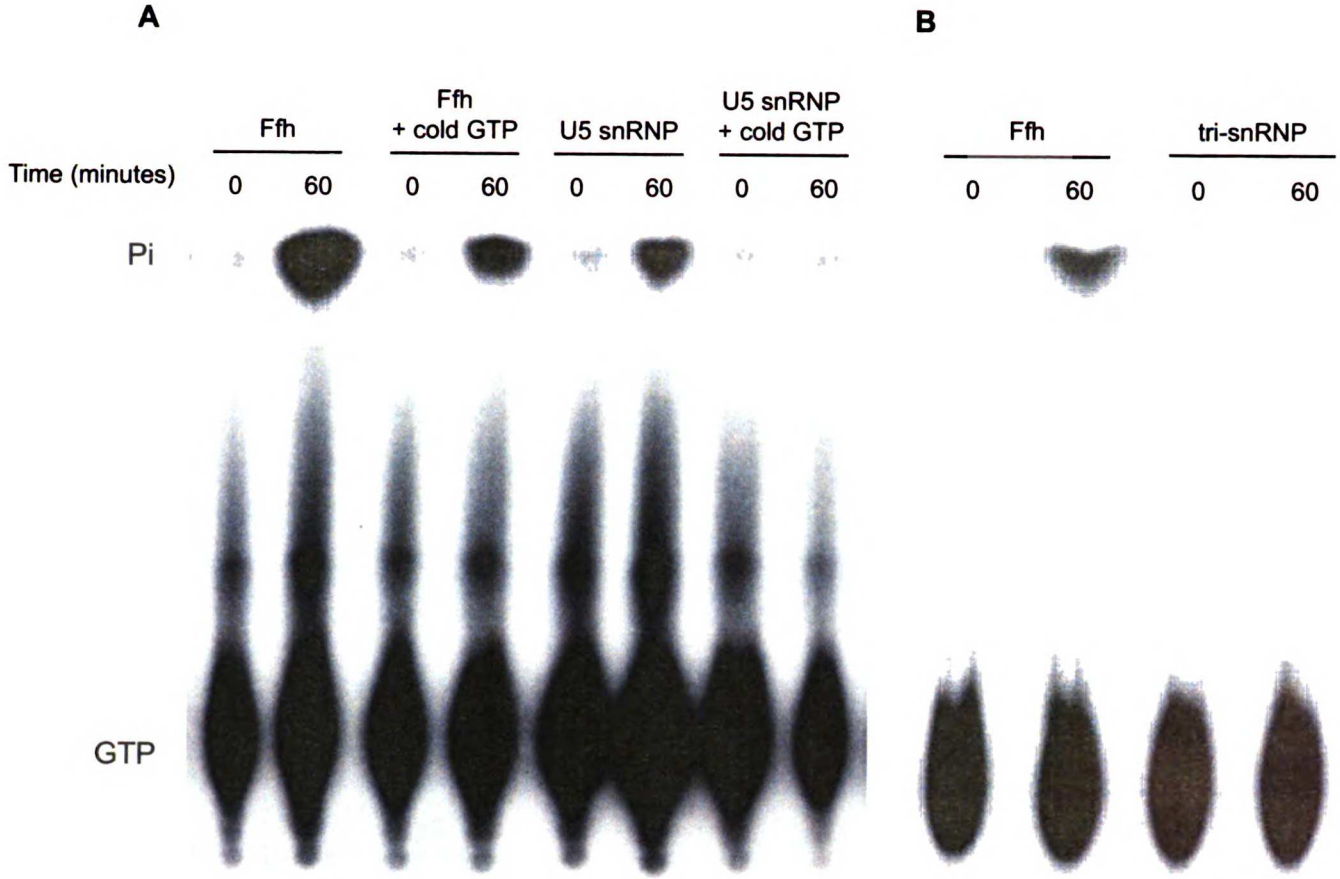
A
B
Ffh
Ffh
+ cold GTP
U5 snRNP
U5 snRNP
+ cold GTP
Ffh
tri-snRNP
Time (minutes)
0
60
0
60
0
60
0
60
0
60
0
60
Pi
GTP

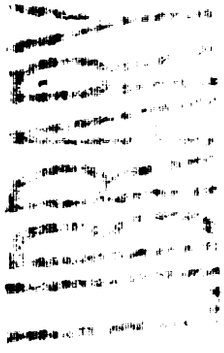

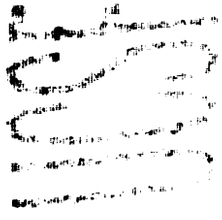

Figure 2. Assaying nucleotide requirements for *in vitro* splicing. **A:** ATP or GTP, as indicated, and radiolabeled actin pre-mRNA were incubated with wildtype splicing extract that had been depleted of ATP. **B:** Wildtype extracts were depleted of ATP. Reactions 10-19 were incubated with AMPPNP or GMPPNP, and radiolabeled actin pre-mRNA and the indicated nucleotides were then added. For reactions 10-14 and 15-19, the concentrations of AMPPNP and GMPPNP were 5 mM, 2 mM, 0.2 mM, 0.02 mM, and 0.002 mM.

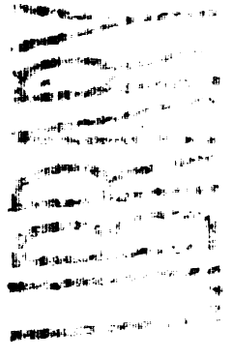

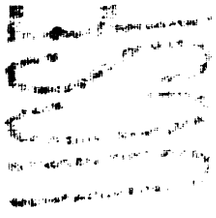

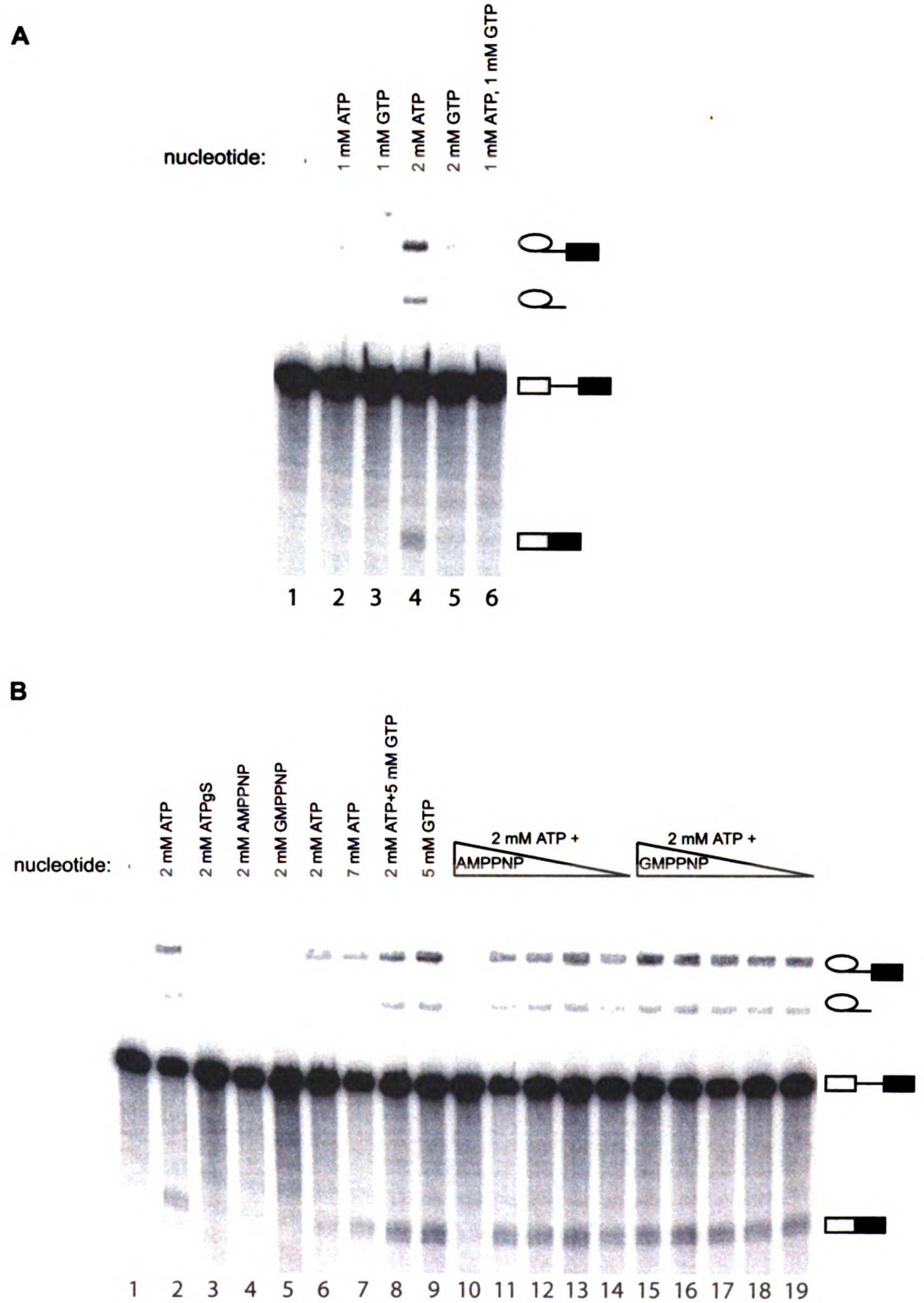
A
nucleotide:
-
1 mM ATP
1 mM GTP
2 mM ATP
2 mM GTP
1 mM ATP, 1 mM GTP
1 2 3 4 5 6
B
nucleotide:
-
2 mM ATP
2 mM ATPgS
2 mM AMPPNP
2 mM GMPPNP
2 mM ATP
7 mM ATP
2 mM ATP+5 mM GTP
5 mM GTP
2 mM ATP +
AMPPNP
2 mM ATP +
GMPPNP
1 2 3 4 5 6 7 8 9 10 11 12 13 14 15 16 17 18 19

Figure 3. Recycling assay in the presence of GMPPNP. Extracts were incubated under splicing conditions for 15 minutes at 25°C with increasing concentrations of cold actin pre-mRNA and 0, 2, or 5 mM GMPPNP. Radiolabeled pre-mRNA was added, and reactions continued for an additional 15 minutes at 25°C.

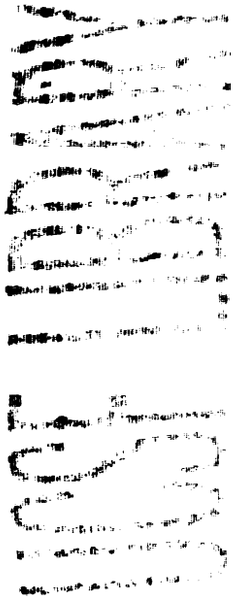

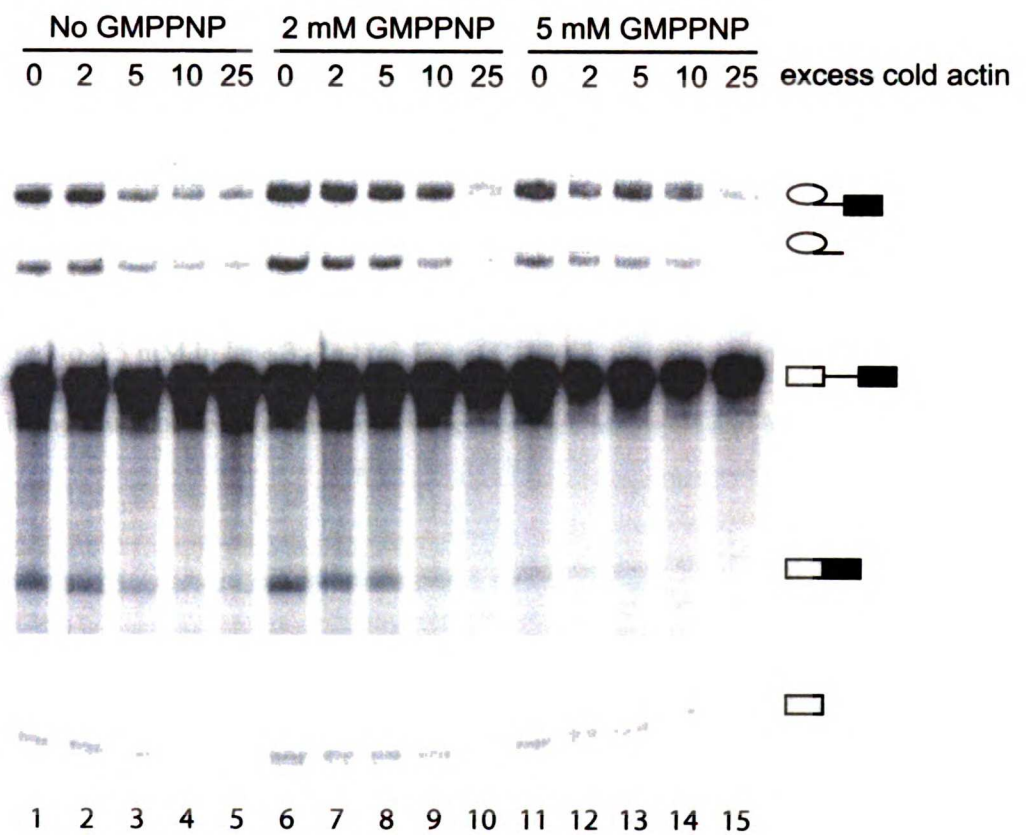
No GMPPNP
2 mM GMPPNP
5 mM GMPPNP
0 2 5 10 25 0 2 5 10 25 0 2 5 10 25
excess cold actin
1 2 3 4 5 6 7 8 9 10 11 12 13 14 15

[redacted]

[redacted]

Figure 4. Assaying nucleotide requirements following removal of endogenous nucleotides by EDTA addition and size exclusion chromatography. **A:** Schematic of experiment. **B:** Wildtype extracts were incubated with (lanes 7-12) or without (lanes 1-6) EDTA and passed over a size exclusion column. Extracts were then incubated with buffer or 5 mM GMPPNP, followed by addition of no nucleotide, 2 mM ATP, or 2 mM of each NTP as well as radiolabeled actin pre-mRNA. **C:** The experiment was performed as in B, except that extracts were not treated with EDTA, and the added nucleotides were varied. Each nucleotide was included at 2 mM, with the exception of 10 mM ATP in lane 10. In lane 11, the $MgCl_2$ concentration was increased to 10 mM, as compared to 2.5 mM in lane 3. In both B and C, $MgCl_2$ concentrations were increased when higher nucleotide concentrations were used (see Materials and Methods).

A

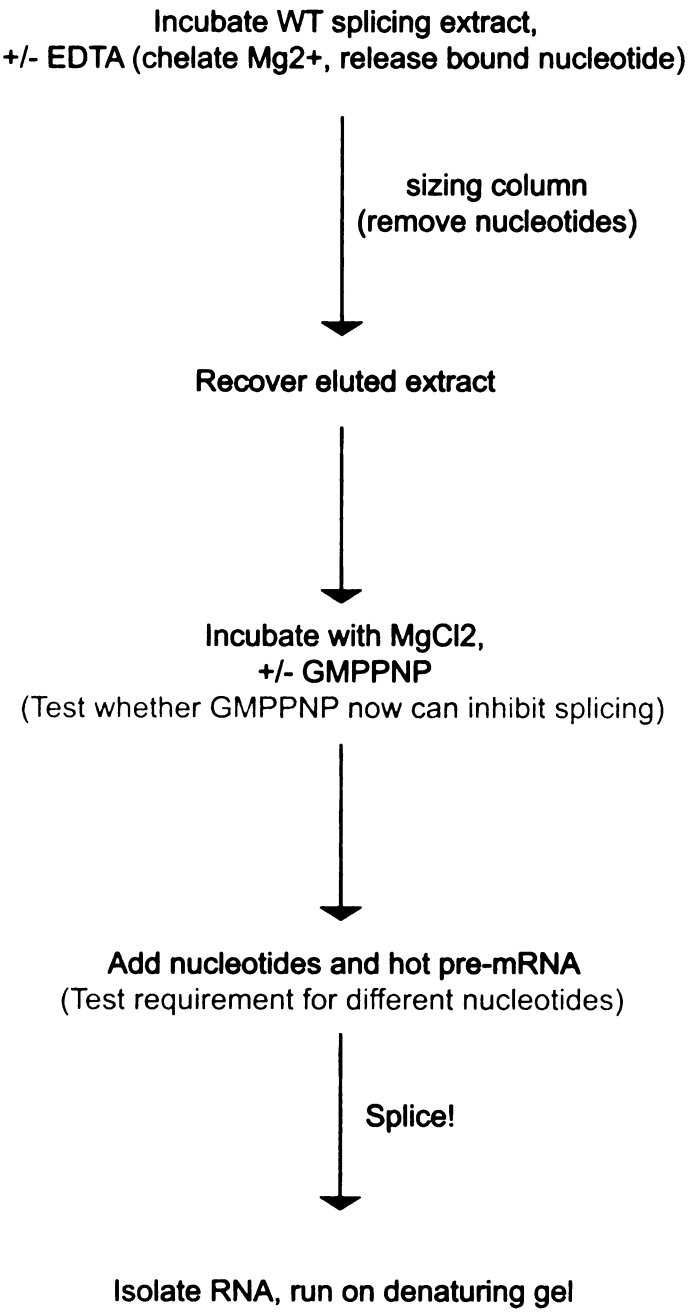
Incubate WT splicing extract,
+/- EDTA (chelate Mg2+, release bound nucleotide)
sizing column
(remove nucleotides)
Recover eluted extract
Incubate with MgCl2,
+/- GMPPNP
(Test whether GMPPNP now can inhibit splicing)
Add nucleotides and hot pre-mRNA
(Test requirement for different nucleotides)
Splice!
Isolate RNA, run on denaturing gel

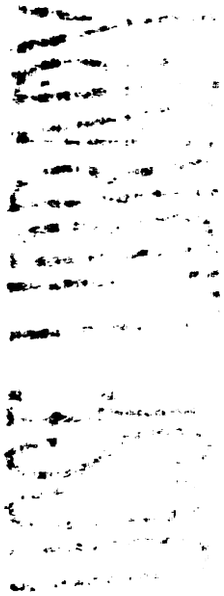

B

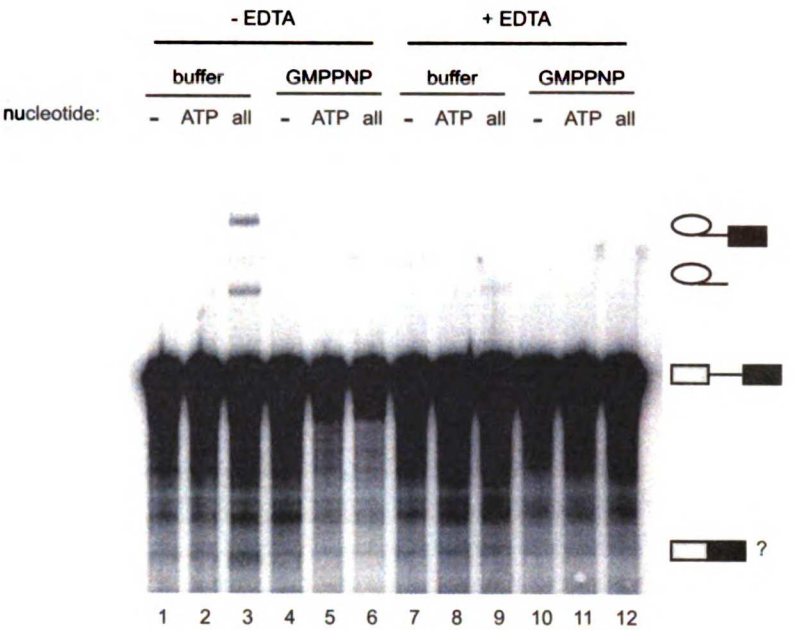
- EDTA
+ EDTA
buffer
GMPPNP
buffer
GMPPNP
nucleotide:
- ATP all - ATP all - ATP all - ATP all
?
1 2 3 4 5 6 7 8 9 10 11 12

C

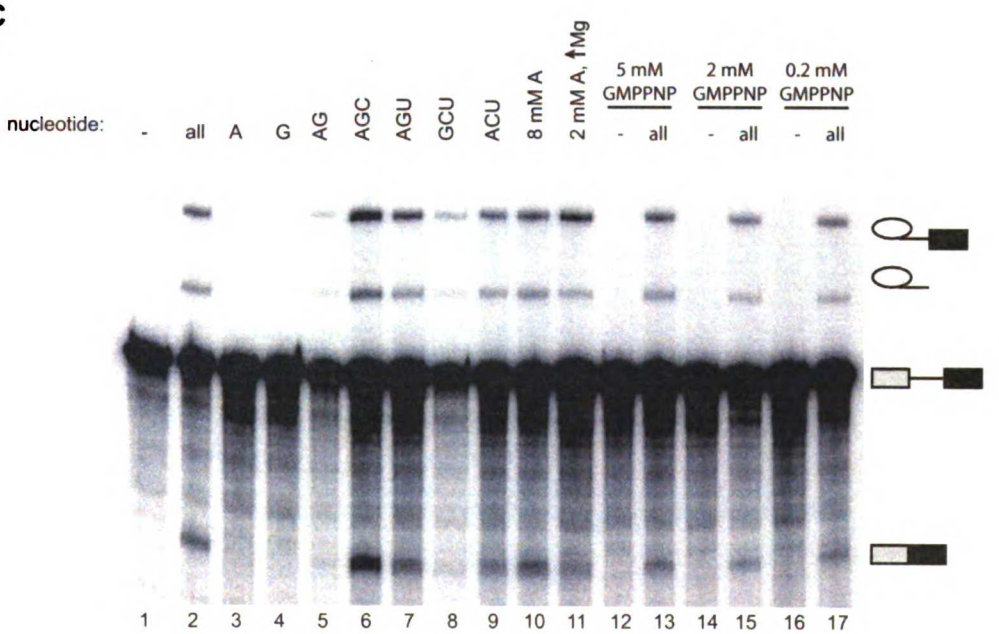
nucleotide:
- all A G AG AGC AGU GCU ACU 8 mM A 2 mM A, ↑Mg
5 mM GMPPNP
2 mM GMPPNP
0.2 mM GMPPNP
- all - all - all
1 2 3 4 5 6 7 8 9 10 11 12 13 14 15 16 17

Figure 5. Effects of ATP and GTP on snRNPs. *SNU114* and *snu114-60* splicing extracts was incubated with buffer (-), 2 mM ATP (A), 2 mM GTP (G), or 2 mM ATP plus 4 nM actin pre-mRNA (Tx) and were resolved by native gel electrophoresis. Gels were transferred to N-Hybond, and Northern blots were probed for U4, U6, and U5 snRNAs. Bars to the left of the blots indicate free U6 and U5 snRNPs; the asterisk indicates free U5 snRNP in *snu114-60* extract.

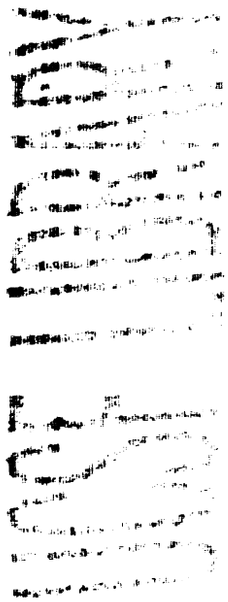

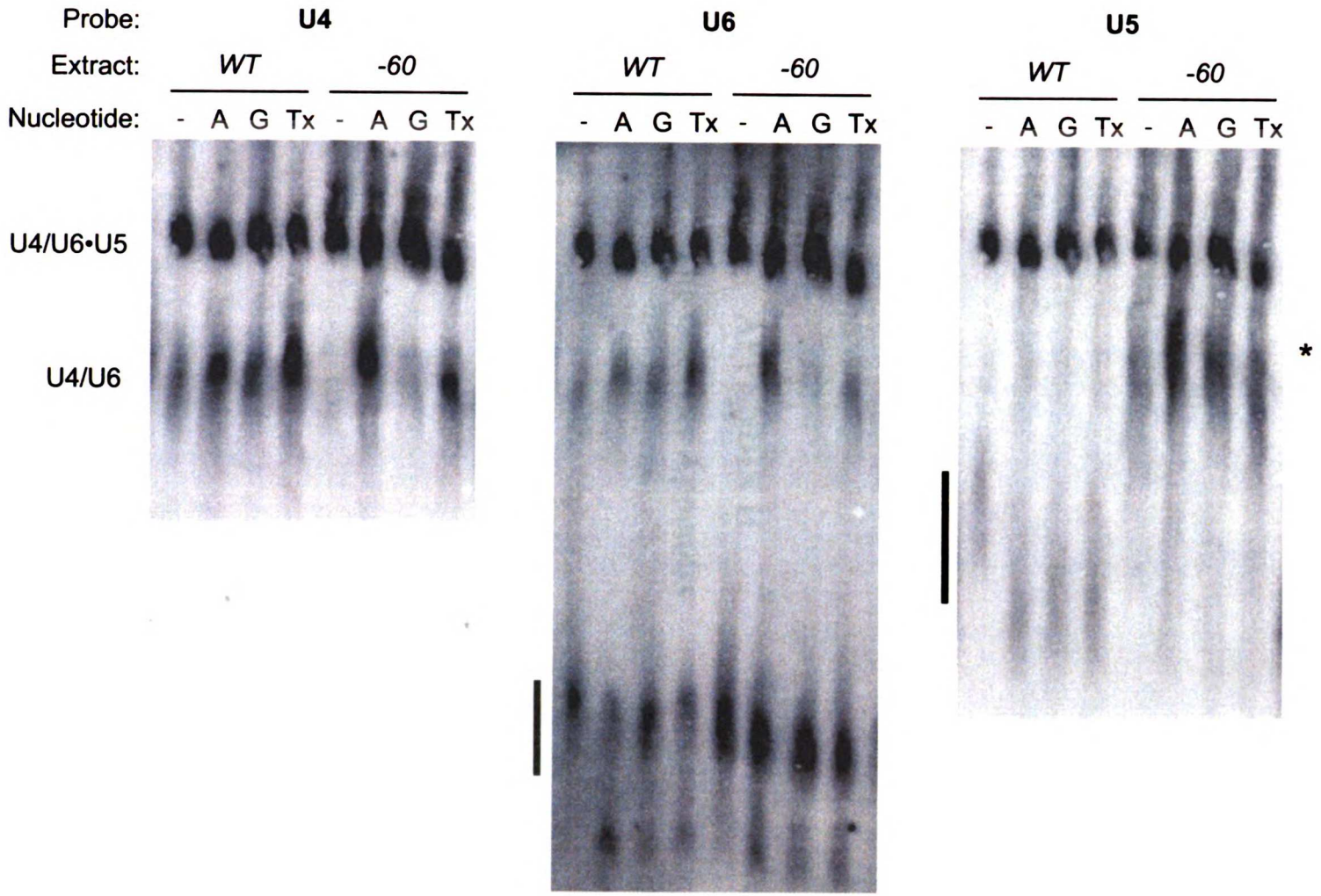
Probe:
U4
U6
U5
Extract:
WT
-60
WT
-60
WT
-60
Nucleotide:
- A G Tx - A G Tx
- A G Tx - A G Tx
- A G Tx - A G Tx
U4/U6•U5
U4/U6
*

APPENDIX II

The Genetics Appendix

APPENDIX II

The Genetics Appendix

INTRODUCTION

In Chapter 1, I analyzed genetic interactions between seven mutations in *SNU114* and mutations in 16 other splicing factors. Synthetic growth defects were summarized in Table 6 of Chapter 1. Here I have included photos showing growth of the double mutants at 16°C, 25°C, 30°C, and 37°C (Figure 1). Following the publication of Chapter 1, I tested additional genetic interactions that are presented here.

Prp43

Prp43 is an ATPase that has been implicated in spliceosome disassembly (Arenas and Abelson 1997; Martin et al. 2002). The *prp43* alleles that I initially tested did not exhibit a growth defect in the consortium strain (Chapter 1). Jon Staley's lab subsequently created two cold-sensitive alleles of *prp43*, which cause a build-up of lariat intermediate *in vivo* and *in vitro* (Eliza Small and Jon Staley, personal communication). In a model for spliceosome disassembly, Small and Staley found that ATP could cause the release of U2, U5, and U6 snRNAs from a complex affinity purified using TAP-tagged Prp43. Addition of GDP inhibits this release, while GTP rescues the inhibition. This GTP-dependent behavior was attributed to Snu114 though analysis of the *snu114-XTPase* allele. Because the Staley data shows that the nucleotide status of Snu114 affects spliceosome disassembly, I predicted that mutations in Snu114, especially those in the G domain, would be synthetically lethal with mutations in Prp43.

Spliceosome activation: U1 and U4 snRNAs

snu114-60 is synthetically lethal with *prp28-1* and sick with *brr2-1*, suggesting an effect on spliceosome activation (Chapter 1). To further test the hypothesis that *snu114-*

60 impairs release of U1 and U4 from the spliceosome, I tested mutations in the U1 and U4 snRNAs. First, I tested the allele U1-2A, 10A, which causes increased base pairing with the 5' splice site. This mutation exacerbates the cold-sensitive growth defect of *prp28-1*, which, along with other biochemical data, led to the idea that Prp28 is directly involved in U1 unwinding (Staley and Guthrie 1999). Second, I tested the cold-sensitive allele U4-cs1, which increases the base pairing between U4 and U6 and obscures the region of U6 that base pairs with the 5' splice site (Li and Brow 1996; Kuhn et al. 1999). U4-cs1 stalls the spliceosome prior to release of both U1 and U4, and is synthetically lethal with *prp28-1* and *brr2-1* (Kuhn et al. 1999; Kuhn and Brow 2000; Kuhn et al. 2002). I predicted that *snu114-60* would be synthetically lethal with these mutations in U1 and U4 snRNAs.

Brr2 and Prp8

Because of the strong, allele-specific interactions that I found between mutations in *SNU114* and *PRP8* (Chapter 1), I was interested in further analyzing the relationship between the two proteins by testing additional alleles of *PRP8*. Although Prp8 has long been thought to be devoid of functional motifs, a region in the C-terminus of the protein was recently identified as homologous to the ubiquitin hydrolysis Jab/MPN domain (Maytal-Kivity et al. 2002; Verma et al. 2002; Bellare et al. 2005; Grainger and Beggs 2005). Bellare et al (2005) showed that ubiquitin can bind to a fragment of Prp8 containing this domain, and the ts allele *prp8-602*, which contains four mutations in conserved residues (Figure 5A), disrupts this binding. In contrast, the ts allele *prp8-28*, which also lies within the Jab/MPN domain (Figure 5A), does not affect ubiquitin binding. The C-terminus of Prp8 is of interest for a second reason: a cluster of mutations

[redacted]

in residues at the extreme C-terminus have been linked to the human disease retinitis pigmentosa (RP). Alan Kutach has generated the analogous mutations in *S. cerevisiae PRP8* (Figure 5A) and observed varying effects on growth (A.K.K. personal communication).

The C-terminus of Prp8 interacts with Brr2 *in vivo* and *in vitro* (van Nues and Beggs 2001). Alan found that this region of Prp8 also interacts with a 42 kDa protein named Aar2, and this interaction *in vitro* is mutually exclusive with Brr2 binding (A.K.K. and C.G. personal communication). Aar2 is found in a 16S U5 snRNP that contains only Prp8, Snu114, and the Sm proteins, but it is not found in any larger snRNP complexes (Gottschalk et al. 1999; Stevens and Abelson 1999; Gottschalk et al. 2001; Stevens et al. 2001). Brr2, in contrast, is found in an 18S U5 snRNP, in tri-snRNP, and most splicing complexes (Gottschalk et al. 1999; Stevens and Abelson 1999; Stevens et al. 2001; Jurica and Moore 2003). Due to the composition of these different particles, we have proposed that during snRNP biogenesis Aar2 initially assembles with Snu114 and Prp8 into a 16S U5 snRNP. A switch from Aar2 to Brr2 binding to Prp8 would lead to the formation of the splicing-competent Brr2-containing 18S U5 snRNP. Alan hypothesized that mutations that disrupt the interaction between Prp8 and Brr2 would decrease the formation of the Brr2-containing 18S U5 snRNP. If one imagines an equilibrium between the Aar2- and Brr2-particles, then overexpression of Aar2 would be predicted to cause lethality in the context of mutations that decrease the formation of the Brr2-particle.

Alan has found that Aar2 overexpression is synthetically lethal with a specific subset of mutations in three genes: *PRP8*, *BRR2*, and *SNU114*. First, the RP mutations

in Prp8 are sensitive to Aar2 overexpression, but mutations in the Jab/MPN domain are not. Second, a subset of conditionally lethal alleles of *BRR2* that were created by random mutagenesis are sensitive to Aar2 overexpression. Interestingly, all of these alleles contain a mutation within a putative α helix, residues 1075-1091, located within a domain that contains homology to the protein Sec63 (Figure 5A). (Sec63 is involved in the formation of a channel that allows transport of proteins into the ER.). Third, Aar2 overexpression is synthetically lethal with *snu114-60* but not *snu114-12* or *snu114-40*. This implicates the C-terminus of Snu114 in the transition between the 16S and 18S U5 snRNPs.

I then tested genetic interactions between *SNU114* alleles and C-terminal mutations of *PRP8* and a range of *BRR2* alleles. I predicted that *snu114-60*, but not *snu114-12* and *snu114-40*, would be synthetically lethal with the mutations in *PRP8* and *BRR2* that are sensitive to Aar2 overexpression, with the idea that each of these mutations affects the transition from the Aar2 snRNP to the Brr2 snRNP.

RESULTS AND DISCUSSION

Prp43

The *prp43* alleles Q423E and Q423N cause a cold-sensitive growth defect in the consortium strain. However, neither of these alleles enhanced the growth defects of any snu114 alleles (Figure 1I). While the *prp43* mutations lead to an accumulation of lariat intermediate, it is likely that they primarily affect rRNA processing (J. Staley, personal communication). Thus, the failure to detect a genetic interaction does not preclude the possibility that Snu114 is involved in spliceosome disassembly.

Spliceosome activation: U1 and U4 snRNAs

The mutations U1-2A, 10A increase base pairing with the 5' splice site. Although this allele does not affect growth of a cell when a wild-type copy of U1 snRNA is also present, it does exacerbate the cold-sensitivity of *prp28-1* (Figure 2B) (Staley and Guthrie 1999). The growth defect of *snu114-60* was also exacerbated by U1-2A, 10A at 16°C and 22°C, and modestly affected at 37°C (Figure 2A). The cs allele *snu114-14* was slightly sicker at 16°C with the U1 mutant (Figure 2A), while the other *snu114* alleles were not affected (data not shown). I also tested copper reporters containing mutations at the 5' splice site that increase base pairing with U1; growth on copper was not affected by any *snu114* mutations (data not shown).

SNU114 mutations were strongly affected by U4-cs1. Consistent with an effect of *snu114-60* on the release of U4 snRNA from assembled spliceosomes (Chapter 2), U4-cs1 and *snu114-60* were synthetically lethal (Figure 3A). Additionally, *snu114-12* and *snu114-40* were synthetically lethal and sick, respectively, with U4-cs1 (Figure 3A and 3B). This could implicate *snu114-12* and *snu114-40* in spliceosome activation. However, my biochemical analysis suggests that *snu114-12* and *snu114-40* cause defects in U5 snRNP and tri-snRNP formation but not in spliceosome activation (Chapter 2). It is possible that spliceosome activation is affected by events during snRNP formation and recycling. In support of this model, U4-cs1 is also synthetically lethal with mutations in the U4/U6 annealing factor *PRP24* (Kuhn and Brow 2000).

Overall, the genetic interactions between *snu114-60* and U1-2A,10A and U4-cs1 support the model that the C-terminus of Snu114 plays an essential role during spliceosome activation. Additionally, synthetic interactions between U4-cs1 and *snu114-*

12 and *snu114-40* suggest that these mutations also could affect spliceosome activation *in vivo*, although they do not seem to affect this process *in vitro*.

Brr2 and Prp8

Genetic interactions of *snu114* alleles with *prp8* and *brr2* alleles are summarized in Table 1, and Figures 4A and 5A depict the locations of the of the *prp8* and *brr2* mutations that I tested. Here, I tested five alleles of *prp8* that contain C-terminal mutations: *prp8-28*, *prp8-602*, and three RP (retinitis pigmentosa) alleles (Figure 4A, 4D, and 4E). Unlike the *prp8* alleles that were previously tested (Figure 4B and 4C), these alleles did not exhibit genetic interactions with any *snu114* alleles other than *snu114-60* (Figure 4D). The *prp8* alleles that are sensitive to Aar2 overexpression—88G, 88K, and 92L—also exacerbated the growth defects of *snu114-60* (Figure 4E). The mutations within the Jab/MPN domain, *prp8-28* and *prp8-602*, are not sensitive to Aar2 overexpression. Correspondingly, *prp8-28* was not synthetically lethal with *snu114-60*. In contrast, *prp8-602* was moderately sick with *snu114-60*, although it should be noted that this *prp8* allele contained an epitope tag at the C-terminus, which enhances sickness with *snu114-60*. Nonetheless, this genetic interaction could implicate a role for ubiquitin in Prp8-Snu114 interactions, since the *prp8-602* mutation diminishes the ability of Prp8 to bind ubiquitin (Bellare et al. 2005).

Each of the Aar2-sensitive *brr2* alleles was synthetically lethal with all three *snu114* alleles that I tested (Figure 5C and 5D). Thus, *snu114-60* is synthetically lethal with the mutations that are sensitive to Aar2 overexpression: mutations in the RP region of *PRP8* and in the Sec63 homology domain of *BRR2*. It is likely that each of these mutations impedes the transition from the 16S Aar2-containing U5 snRNP to the 18S

Brr2-containing U5 snRNP. Alternatively, the effect of *snu114-60* on spliceosome activation might explain the genetic interactions with *brr2* and *prp8*. For example, GTP hydrolysis at the time of spliceosome activation could cause Snu114 to alter the interaction of the C-terminus of Prp8 with Sec63 homology domain of Brr2, leading to U4/U6 unwinding; these interactions might be compromised by the *brr2*, *prp8*, and *snu114-60* mutations. Nonetheless, the synthetic lethality of *snu114-60* with Aar2 overexpression strongly implicates the C-terminus of Snu114 in snRNP formation.

The Aar2-sensitive alleles of *BRR2* and *PRP8* did not phenocopy each other, in that the *PRP8* alleles did not interact genetically with *snu114-12* and *snu114-40*, while the *BRR2* alleles were synthetically lethal with the mutations in *SNU114*. It seems unlikely that *snu114-12* and *snu114-40* affect the transition between the 16S and 18S U5 snRNPs, since these alleles are not synthetically lethal with Aar2 overexpression. However, they inhibit overall U5 snRNP formation by decreasing the interaction with Prp8. If the mutations in BRR2 affect its interaction with Prp8, this combination might cause synthetic lethality.

I observed a wide range of genetic interactions between *brr2* alleles and *snu114* alleles (Figure 5). Until the *brr2* mutations within each allele are separated and the phenotypes caused by these mutations better characterized, the significance of these interactions will be difficult to interpret. Two of the *brr2* alleles—*brr2-11* and *brr2-39*—are cs, and both are either synthetically lethal or sick with all *snu14* mutations that were tested (Figure 5C and 5E). *brr2-39* contains four mutations, one of which affects the amino acid adjacent to the mutation in *brr2-1* and one of which is within the Sec63-homology domain, adjacent to Aar2-sensitive mutations (Figure 5A); either of

[redacted]

[redacted]

these mutations would be expected to enhance growth defects of *snu114* mutations. *brr2-11* contains two mutations, both of which are outside of the ATPase domain; it will be intriguing to further characterize this allele. Specifically, does this mutation affect U5 snRNP formation, spliceosome activation, or ATPase activity? Does it affect the GTPase activity of Snu114?

Notably, *snu114-40* exhibited stronger genetic interactions than *snu114-12* with many of the *brr2* and *prp8* alleles (Table 1 and Figures 4 and 5), suggesting that domain IV of Snu114 is important for interactions with U5 snRNP proteins. Despite the genetic interactions between *brr2* and *snu114*, the two proteins are not believed to physically interact. It is likely that Prp8 mediates interactions between domain IV of Snu114 and Brr2.

Interactions with TAP-tagged proteins

When crossing TAP-tagged strains to *snu114* strains, I found that strains containing *snu114-60* and either TAP-tagged Prp8 or Prp4 were extremely sick (Figure 6A and 6B). Some mutations that cause retinitis pigmentosa lead to an extension of the C-terminus of Prp8; thus, an epitope tag at the C-terminus may function similarly to the RP alleles, which also were synthetically sick with *snu114-60*. Notably, even the smaller 3HA tag at the C-terminus of Prp8 exacerbated the growth defect of *snu114-60* (Figure 4C).

Synthetic lethality between Prp4-TAP and *snu114-60* could arise either from defects during tri-snRNP formation or during spliceosome activation. Interestingly, the U4/U6 snRNP protein Prp4 has been implicated in spliceosome activation (Ayadi et al. 1997). Mutations within the second of five WD-repeats, which are found near the C-

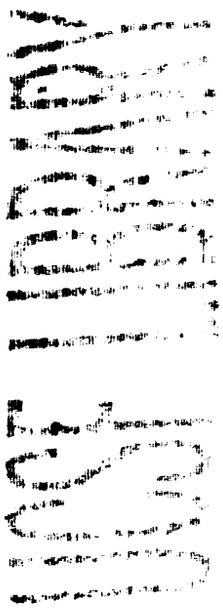

terminus of the protein, inhibit release of U4 from spliceosomes, phenocopying *snu114-60*. In contrast to Prp8 and Prp4, TAP-tagged Brr2 and Aar2 did not visibly affect growth of *snu114-60* on plates (Figure 6C), although the *snu114-60 BRR2-TAP* strain did grow slowly in liquid culture.

Prp8 overexpression

Due to the finding that Prp8 levels were low in *snu114-12* and *snu114-40* strains, I tested whether overexpression of Prp8 could rescue the growth defects of these strains. High expression of Prp8 was induced by the Galactose promoter; however, this did not affect the growth of the *snu114* strains (Figure 7). One should confirm by Western blots that Prp8 was overexpressed in these strains. If Snu114 and Prp8 interact poorly, excess Prp8 may still not allow sufficient production of U5 snRNP. Alternatively, the results indicate that low levels of Prp8 were not the growth-limiting factor in these strains.

CONCLUSION

The genetic interactions that I observed here reinforce the idea that *snu114-60* affects spliceosome activation, since this allele is synthetically lethal with U4-cs1 and U1-2A,10A. The genetics provide support for interrelated functions of Snu114, Prp8, and Brr2, as I found *snu114* alleles to be synthetically lethal with a wide array of mutations in *PRP8* and *BRR2*. In particular, *snu114-60* is synthetically lethal with mutations in *PRP8* and *BRR2* that cause sensitivity to Aar2 overexpression, implicating particular domains in each of these proteins in the transition from an Aar2-containing U5 snRNP to a Brr2-containing U5 snRNP. I also found that the mutation *snu114-12*, within the GTPase domain of Snu114, and the mutation *snu114-40* are synthetically lethal with many *brr2* alleles. This suggests that the GTPase activity of Snu114 could affect the

activity of the ATPase Brr2, in agreement with data from Small and Staley (personal communication) and Bartels *et al.* (Bartels et al. 2003).

MATERIALS AND METHODS

Yeast strains are listed in Table 2. Genetic methods were described in Chapter 1. Wildtype U1 and U1-2A, 10A (Siliciano and Guthrie 1988; Staley and Guthrie 1999) were transformed into yTB13, in which the *URA3/SNU114* plasmid had been replaced with the *snu114* alleles pTB106-113. pRS313-based plasmids containing U4 or U4-cs1 (gifts from Jon Staley) were transformed into yTB204-yTB207. *PRP8* and *BRR2* plasmids (pRS313) were gifts from Alan Kutach. TAP-tagged strains were obtained from E.K. O'Shea (Ghaemmaghami et al. 2003). Prp8 under the control of the Galactose promoter (a gift of Alan Kutach) was transformed into yTB127, yTB175, yTB162, and yTB164.

Table 1. Genetic interactions between *snu114-12, snu114-40, snu114-60* and alleles of *BRR2* and *PRP8*.

	Growth defect	Sensitive to Aar2 o/x?	*snu114-12*	*snu114-40*	*snu114-60*
brr2-A	ts	yes	4	4.5	5
brr2-B	ts	yes	4	5	5
brr2-BF	ts	yes	4	5	5
brr2-M	ts	no	0	1	3
brr2-C	ts	no	0	3	2
brr2-39	cs	no	4	3	3
brr2-11	cs	no	5	5	5
brr2-1	cs	no	0	2	4
rss1-1	ts (weak)	no	0	0	0
slt22-1	ts (weak)	no	0	0	0
prp8-28	ts	no	0	0	1
prp8-602	ts	no	0	0	4
prp8-88G	-	yes	0	0	4
prp8-88K	-	yes	ND	ND	4.5
prp8-92L	-	moderate	ND	ND	3
prp8-1	ts	yes	3	4	5
prp8-brr	cs	ND	3	5	5
prp8-201	ts	ND	2	3	5
prp8-101	ts, cs	ND	1	0	2

Synthetic enhancement was rated on a scale of 0 (no interaction) to 5 (synthetic lethality). Boxes are shaded according to strength of interaction. Thermosensitive (ts) and cold-sensitive (cs) alleles are listed, and synthetic lethality with Aar2 overexpression is noted. ND= not determined.

[redacted]

[redacted]

Table 2. Yeast strains used in this appendix.

Strain	Genotype
YTB13	*MATa lys2Δ trp1Δ snu114::KAN pRS316/SNU114*
YTB108	*MATa lys2Δ trp1Δ prp8::LYS snu114::KAN pRS316/SNU114 yCP50/PRP8*
YTB127	*MATa*
YTB128	*MATα*
YTB162	*MATa snu114-40*
YTB163	*MATα snu114-40*
YTB164	*MATa snu114-60*
YTB165	*MATα snu114-60*
YTB171	*MATα snu114-12*
YTB175	*MATa snu114-12*
YTB176	*MATa BRR2-TAP-HIS snu114-12*
YTB177	*MATa BRR2-TAP-HIS snu114-40*
YTB178	*MATa BRR2-TAP-HIS snu114-60*
yTB183	*MATa AAR2-TAP-HIS*
yTB184	*MATa AAR2-TAP-HIS snu114-12*
yTB185	*MATa AAR2-TAP-HIS snu114-40*
yTB186	*MATa AAR2-TAP-HIS snu114-60*
yTB187	*MATa BRR2-TAP-HIS*
yTB188	*MATa PRP8-TAP-HIS*
yTB190	*MATα BRR2::KAN*
yTB191	*MATα BRR2::KAN snu114-12*
yTB192	*MATα BRR2::KAN snu114-40*
yTB193	*MATa BRR2::KAN snu114-60*
yTB194	*MATa PRP8-TAP-HIS snu114-12*
yTB195	*MATa PRP8-TAP-HIS snu114-40*
yTB196	*MATa PRP8-TAP-HIS snu114-60*
yTB197	*MATa PRP4-TAP-HIS*
yTB198	*MATa PRP4-TAP-HIS snu114-12*
yTB199	*MATa PRP4-TAP-HIS snu114-40*
yTB200	*MATα PRP4-TAP-HIS snu114-60*
yTB204	*MATα snr14::LYS2 pSE360/U4*
yTB205	*MATα snr14::LYS2 snu114-12 pSE360/U4*
yTB206	*MATα snr14::LYS2 snu114-40 pSE360/U4*
yTB207	*MATα snr14::LYS2 snu114-60 pSE360/U4*

All strains are *his3Δ leu2Δ ura3Δ met15Δ*, with the exception of yTB13 and yTB108, which are *MET15*.

Figure 1. Growth of strains containing a *snu114* allele and a mutation in an additional splicing factor. Data from these photos were summarized in Chapter 1, Table 6. Serial dilutions of cells were spotted onto YPD and grown for the number of indicated days. **A:** *brr1Δ*. **B:** *prp2-1*. **C:** *prp16 alleles*. **D:** *prp19-1*. **E:** *prp22 alleles*. **F:** *prp24 alleles*. **G:** *prp28-1*. Note that strains containing *prp28-1* and *snu114-12*, *snu114-14*, or *snu114-15* were difficult to recover from 5-FOA plates. **H:** *prp43 alleles*. **I:** *prp43-Q423E* and *prp43-Q423N*. **J:** *snu114Δ sad1-1* strains, carrying a *URA3*-marked *SNU114* plasmid and a *LEU2*-marked plasmid with a *snu114* allele, were streaked to 5-FOA media and grown at 25°C. **K:** *sad1-1* strains grown on YPD. **L:** *snu66Δ*. Note that strains containing both *snu66Δ* and *snu114-12*, *snu114-14*, *snu114-15*, or *snu114-50* were difficult to recover from 5-FOA plates. **M:** *sub2 alleles*.

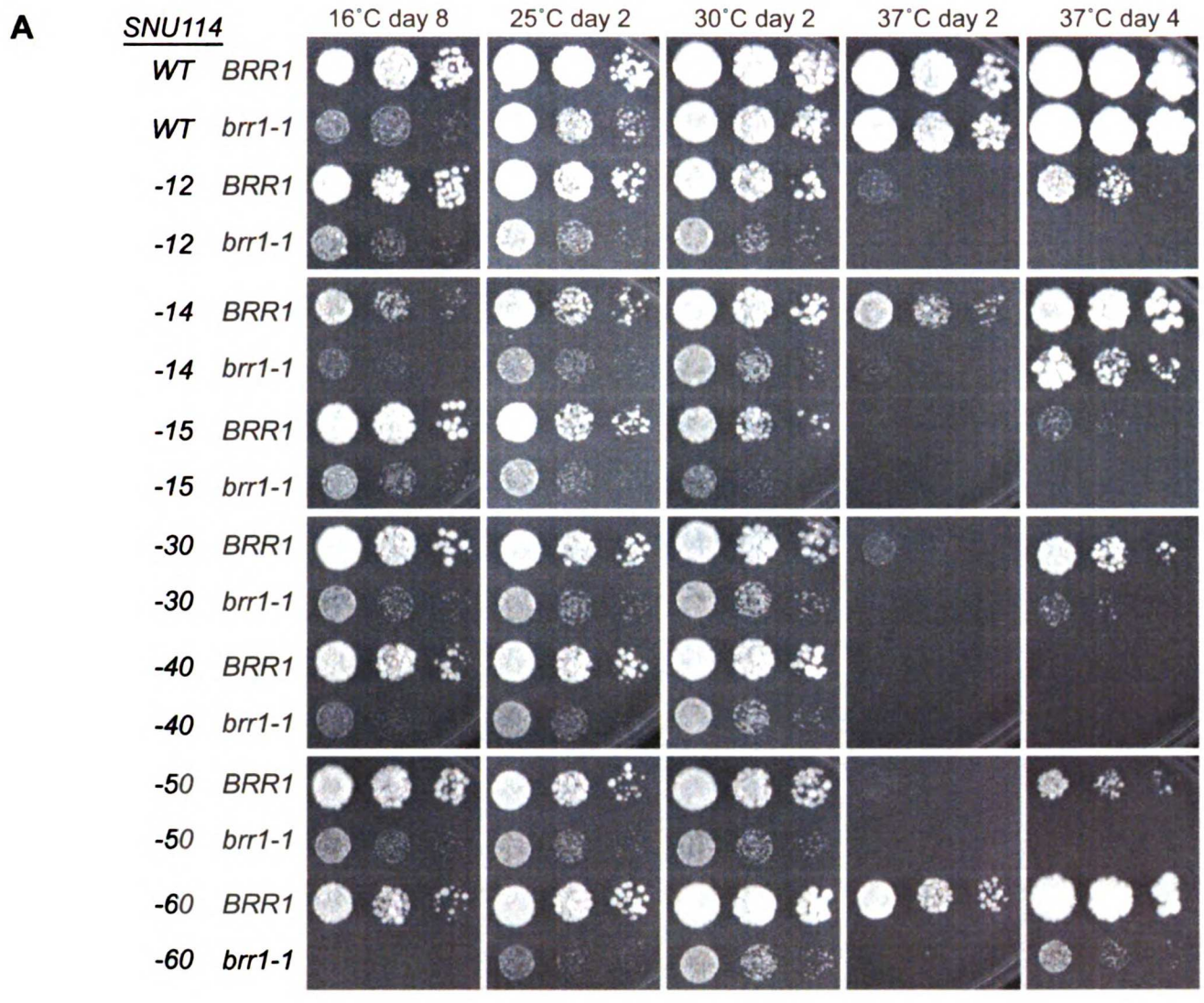
A
SNU114
16˚C day 8
25˚C day 2
30˚C day 2
37˚C day 2
37˚C day 4
WT BRR1
WT brr1-1
-12 BRR1
-12 brr1-1
-14 BRR1
-14 brr1-1
-15 BRR1
-15 brr1-1
-30 BRR1
-30 brr1-1
-40 BRR1
-40 brr1-1
-50 BRR1
-50 brr1-1
-60 BRR1
-60 brr1-1

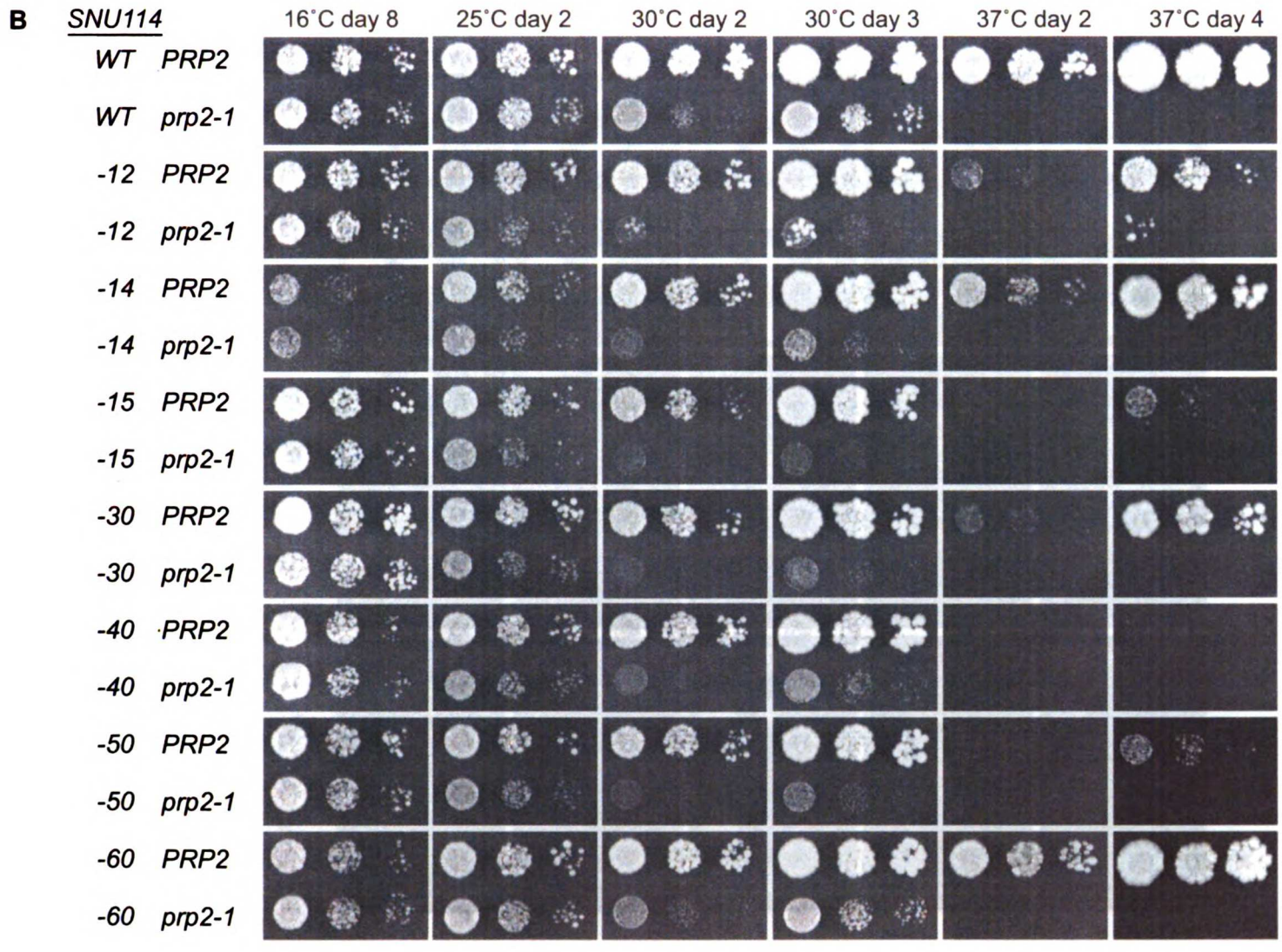
B
SNU114
16˚C day 8
25˚C day 2
30˚C day 2
30˚C day 3
37˚C day 2
37˚C day 4
WT PRP2
WT prp2-1
-12 PRP2
-12 prp2-1
-14 PRP2
-14 prp2-1
-15 PRP2
-15 prp2-1
-30 PRP2
-30 prp2-1
-40 PRP2
-40 prp2-1
-50 PRP2
-50 prp2-1
-60 PRP2
-60 prp2-1

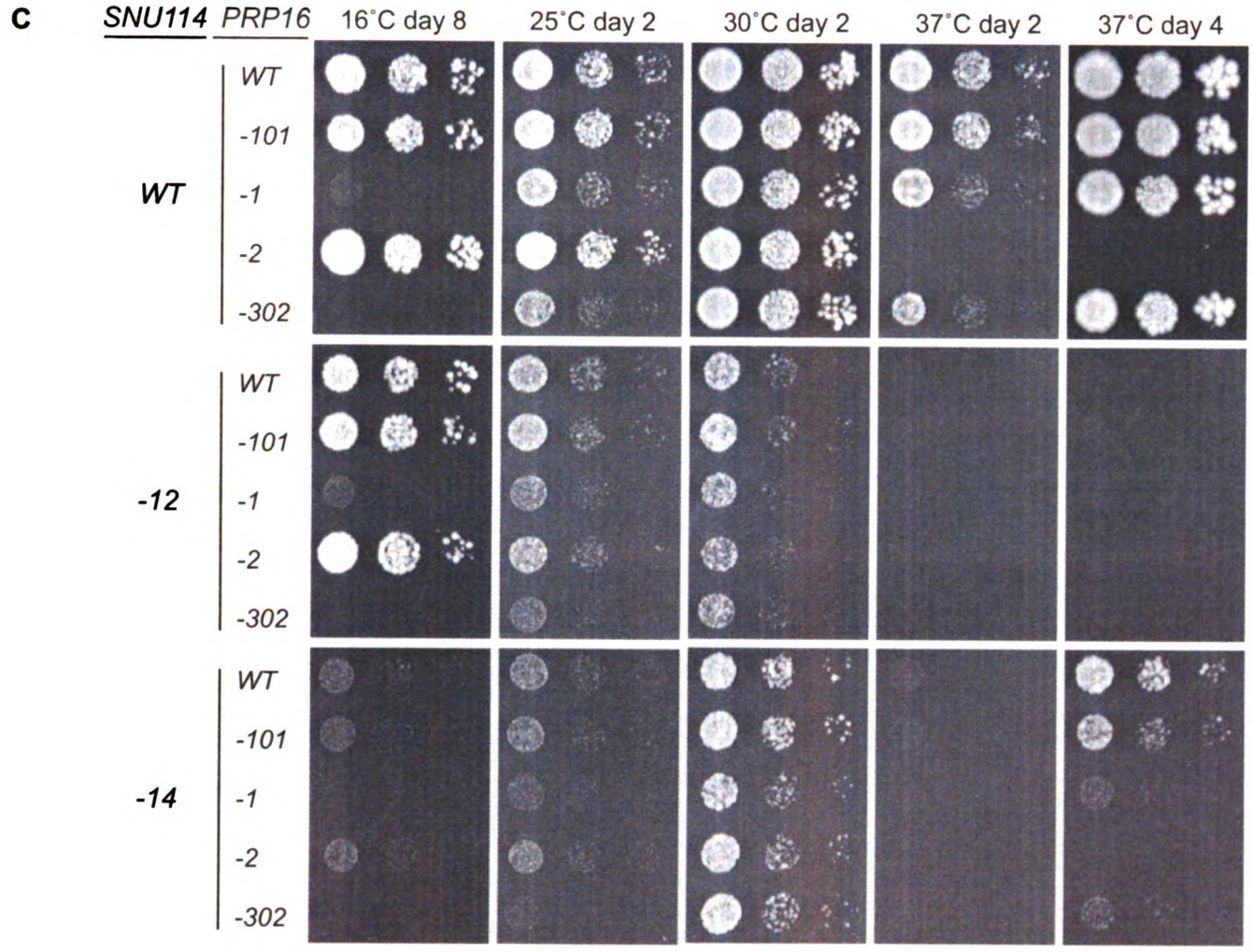
C
SNU114
PRP16
16˚C day 8
25˚C day 2
30˚C day 2
37˚C day 2
37˚C day 4
WT
-101
-1
-2
-302
WT
-12
-14

C, continued

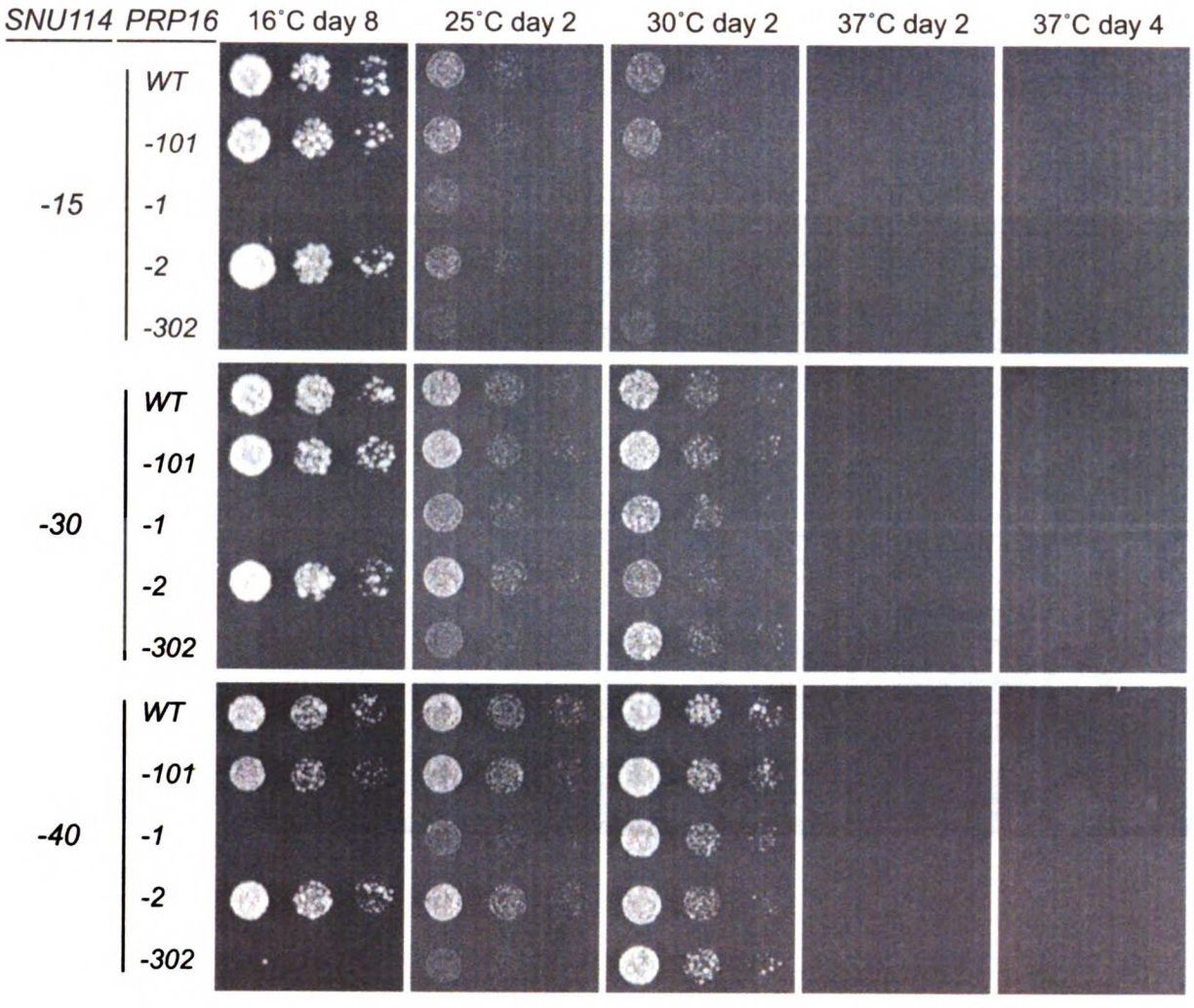
SNU114
PRP16
16˚C day 8
25˚C day 2
30˚C day 2
37˚C day 2
37˚C day 4
-15
WT
-101
-1
-2
-302
-30
WT
-101
-1
-2
-302
-40
WT
-101
-1
-2
-302

C, continued

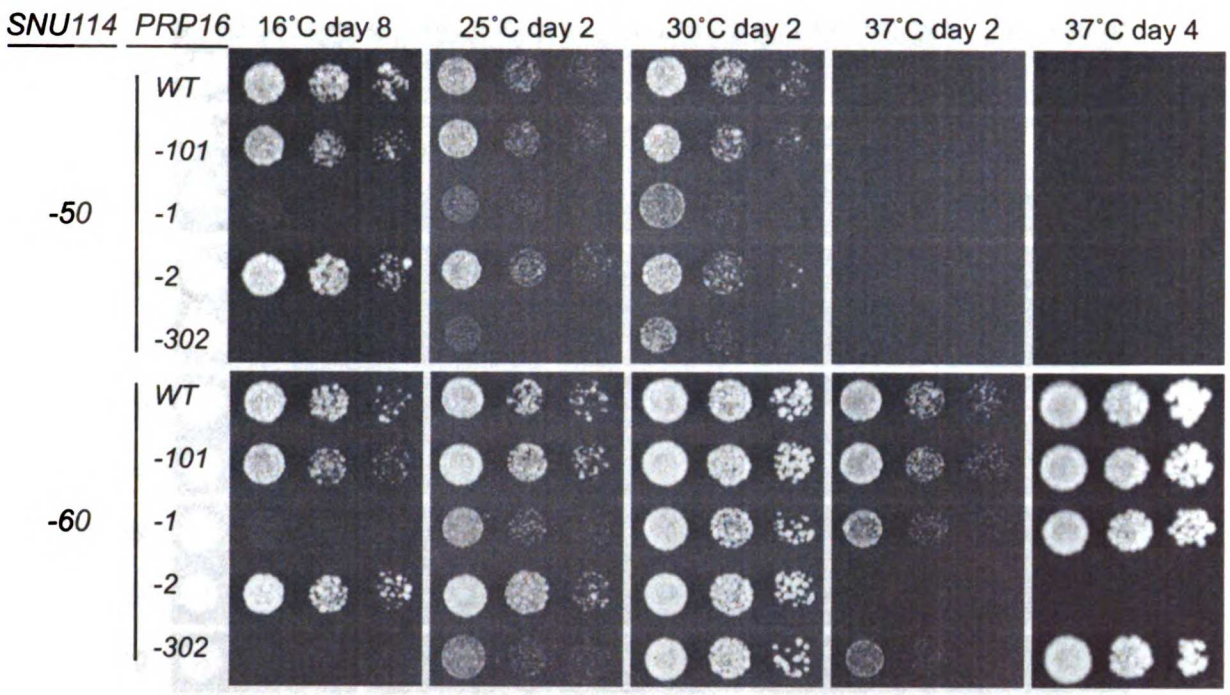
SNU114
PRP16
16°C day 8
25°C day 2
30°C day 2
37°C day 2
37°C day 4
-50
WT
-101
-1
-2
-302
-60
WT
-101
-1
-2
-302

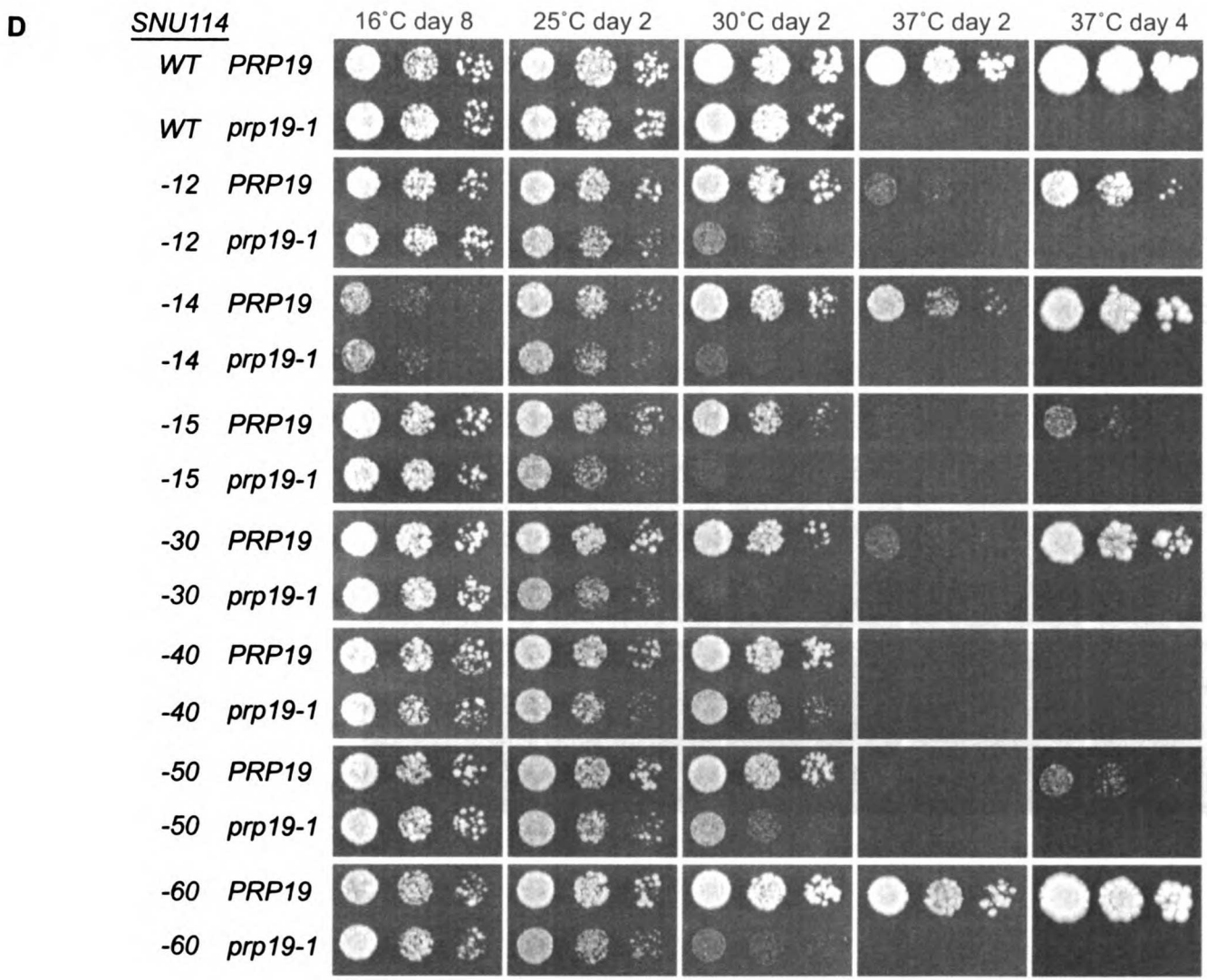
D
SNU114
16˚C day 8
25˚C day 2
30˚C day 2
37˚C day 2
37˚C day 4
WT PRP19
WT prp19-1
-12 PRP19
-12 prp19-1
-14 PRP19
-14 prp19-1
-15 PRP19
-15 prp19-1
-30 PRP19
-30 prp19-1
-40 PRP19
-40 prp19-1
-50 PRP19
-50 prp19-1
-60 PRP19
-60 prp19-1

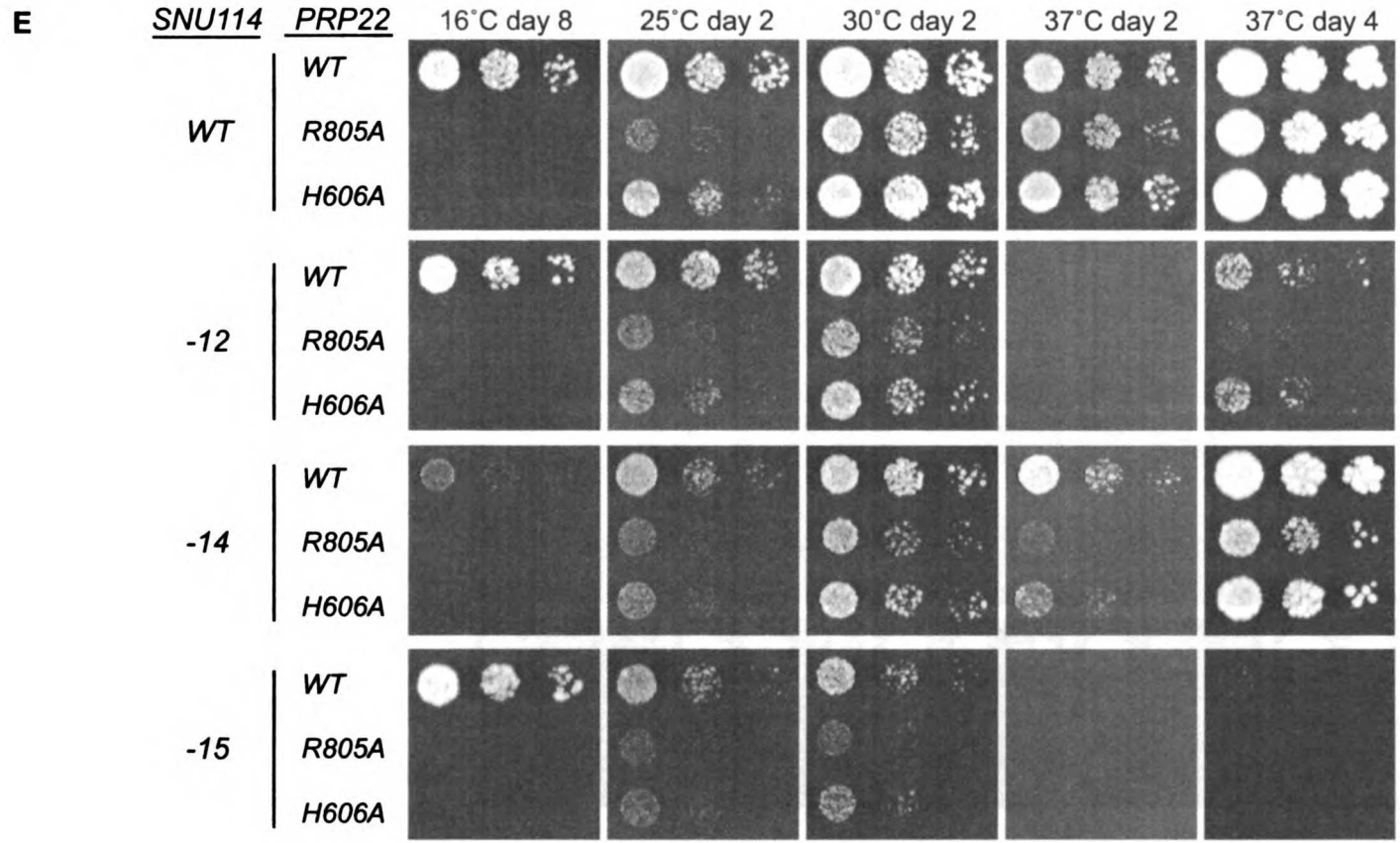
E
SNU114
PRP22
16˚C day 8
25˚C day 2
30˚C day 2
37˚C day 2
37˚C day 4
WT
WT
R805A
H606A
-12
WT
R805A
H606A
-14
WT
R805A
H606A
-15
WT
R805A
H606A

E, continued

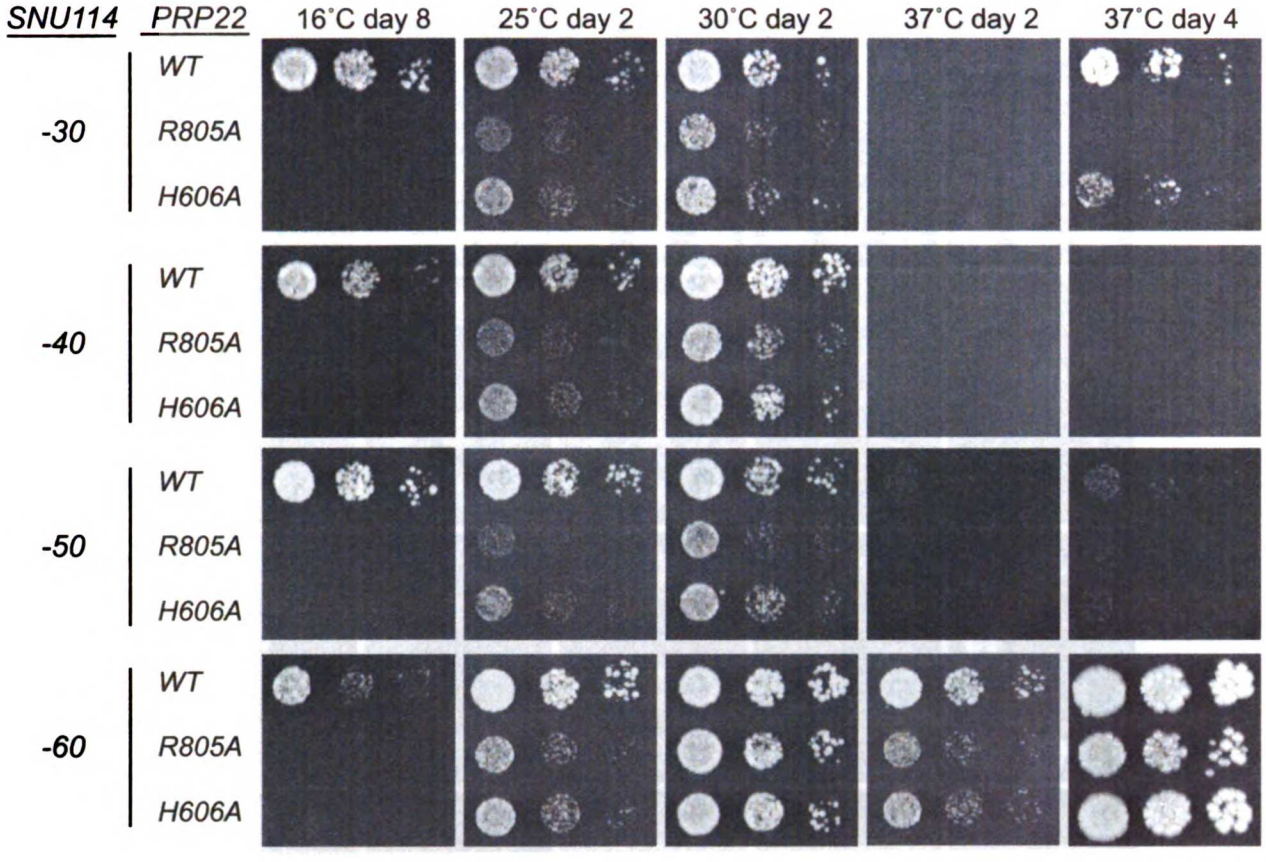
SNU114
PRP22
16˚C day 8
25˚C day 2
30˚C day 2
37˚C day 2
37˚C day 4
-30
WT
R805A
H606A
-40
WT
R805A
H606A
-50
WT
R805A
H606A
-60
WT
R805A
H606A

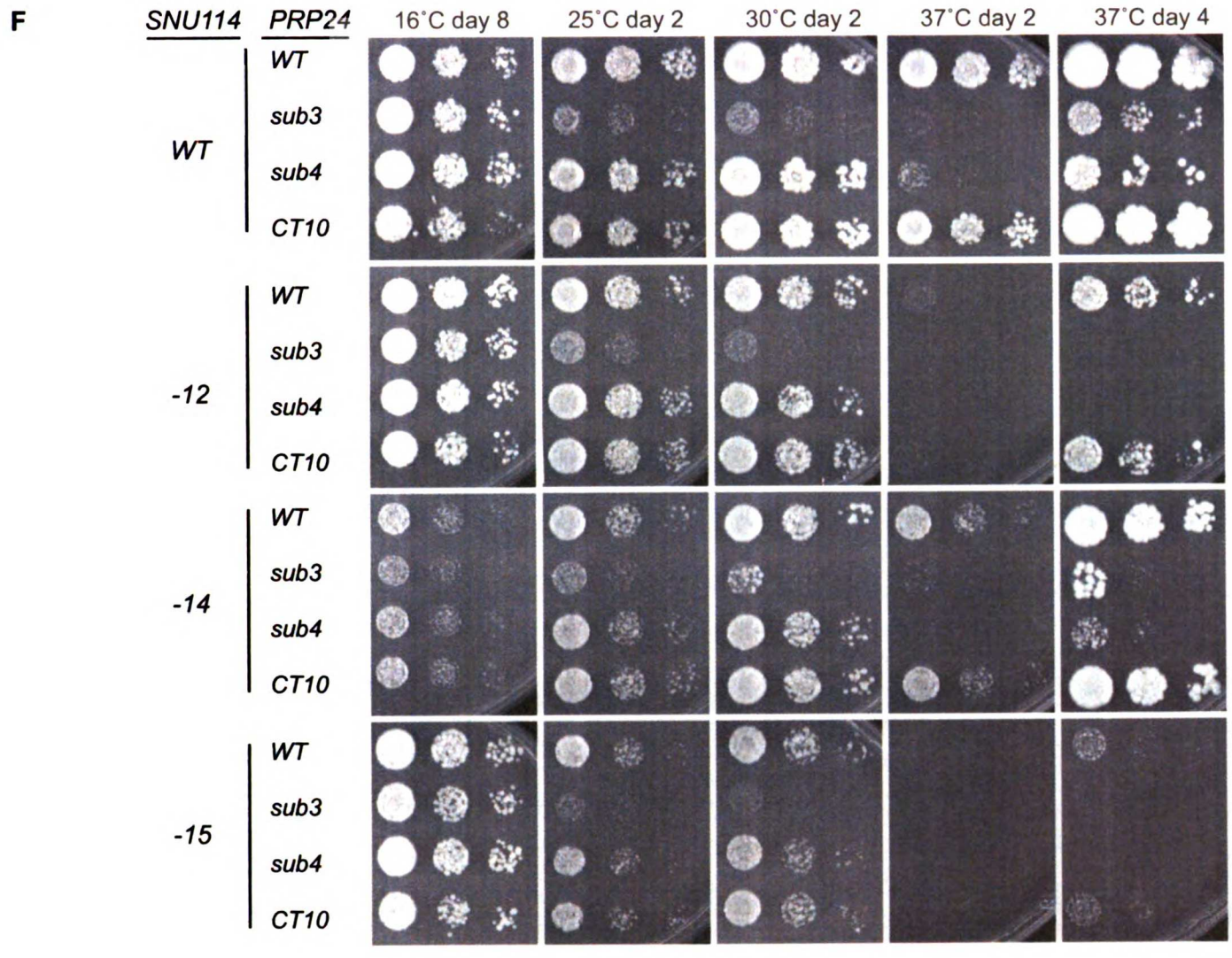
F
SNU114
PRP24
16°C day 8
25°C day 2
30°C day 2
37°C day 2
37°C day 4
WT
WT
sub3
sub4
CT10
-12
WT
sub3
sub4
CT10
-14
WT
sub3
sub4
CT10
-15
WT
sub3
sub4
CT10

[redacted]

F, continued

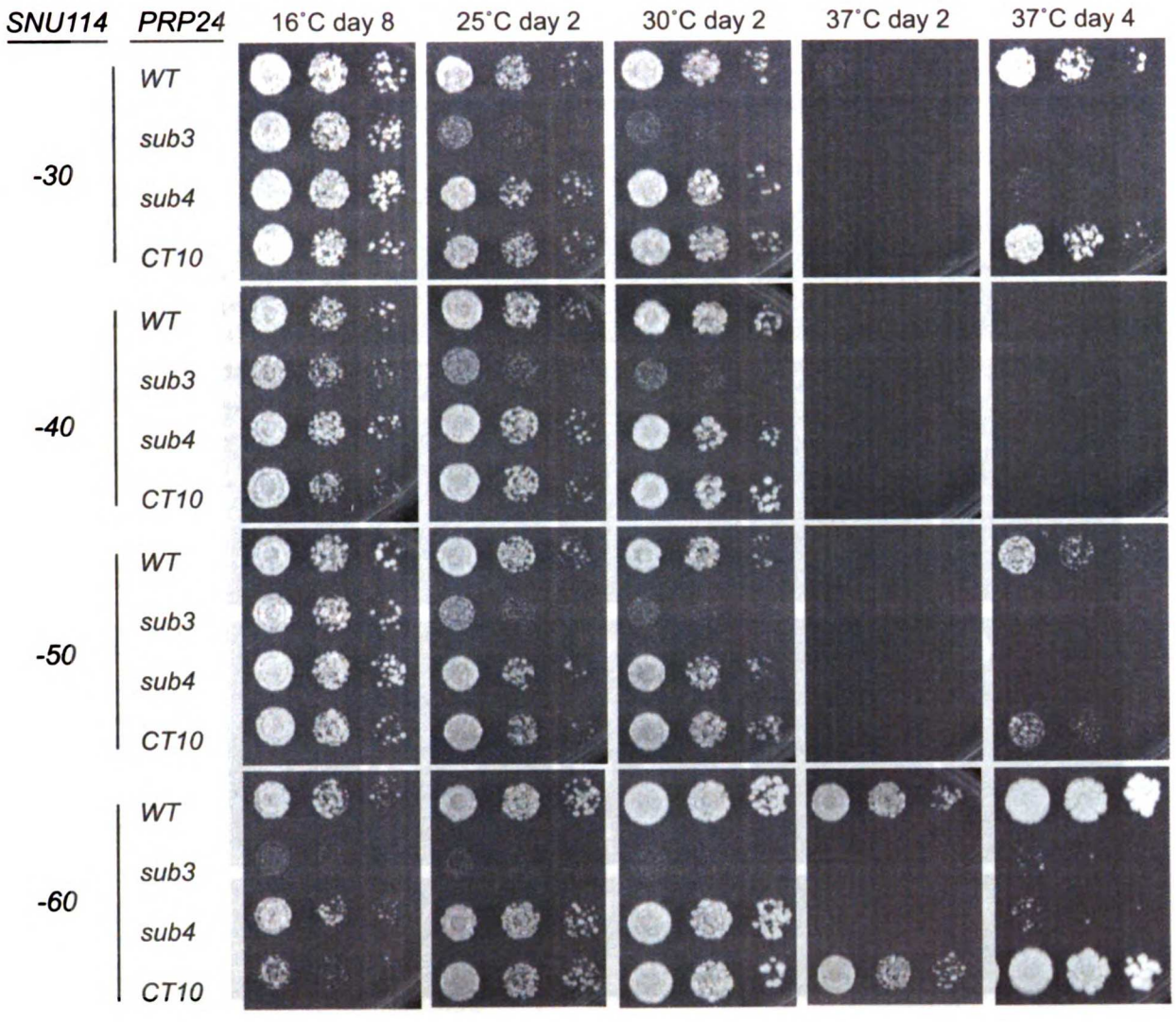
SNU114
PRP24
16˚C day 8
25˚C day 2
30˚C day 2
37˚C day 2
37˚C day 4
-30
-40
-50
-60
WT
sub3
sub4
CT10

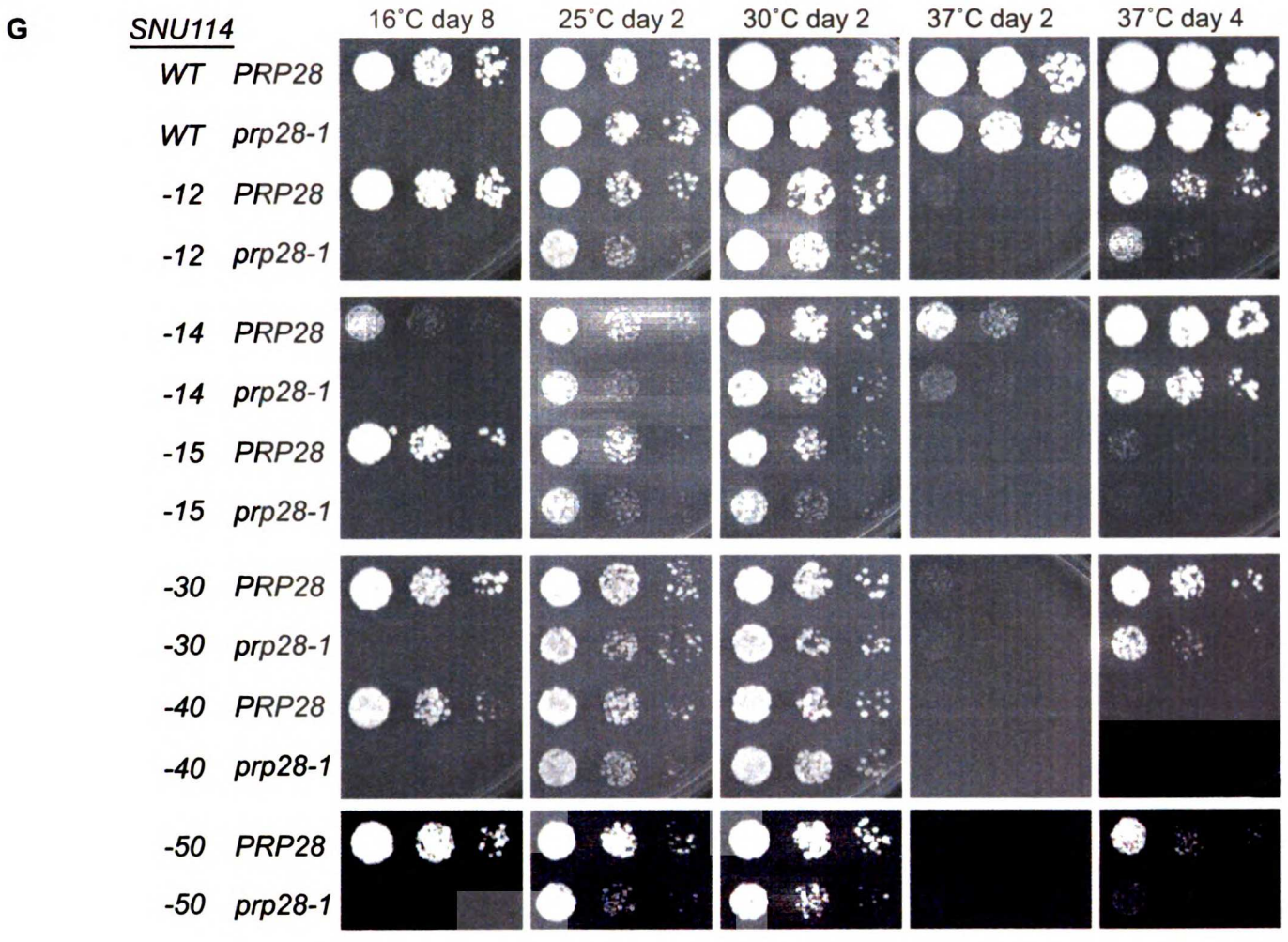
G
SNU114
16˚C day 8
25˚C day 2
30˚C day 2
37˚C day 2
37˚C day 4
WT PRP28
WT prp28-1
-12 PRP28
-12 prp28-1
-14 PRP28
-14 prp28-1
-15 PRP28
-15 prp28-1
-30 PRP28
-30 prp28-1
-40 PRP28
-40 prp28-1
-50 PRP28
-50 prp28-1

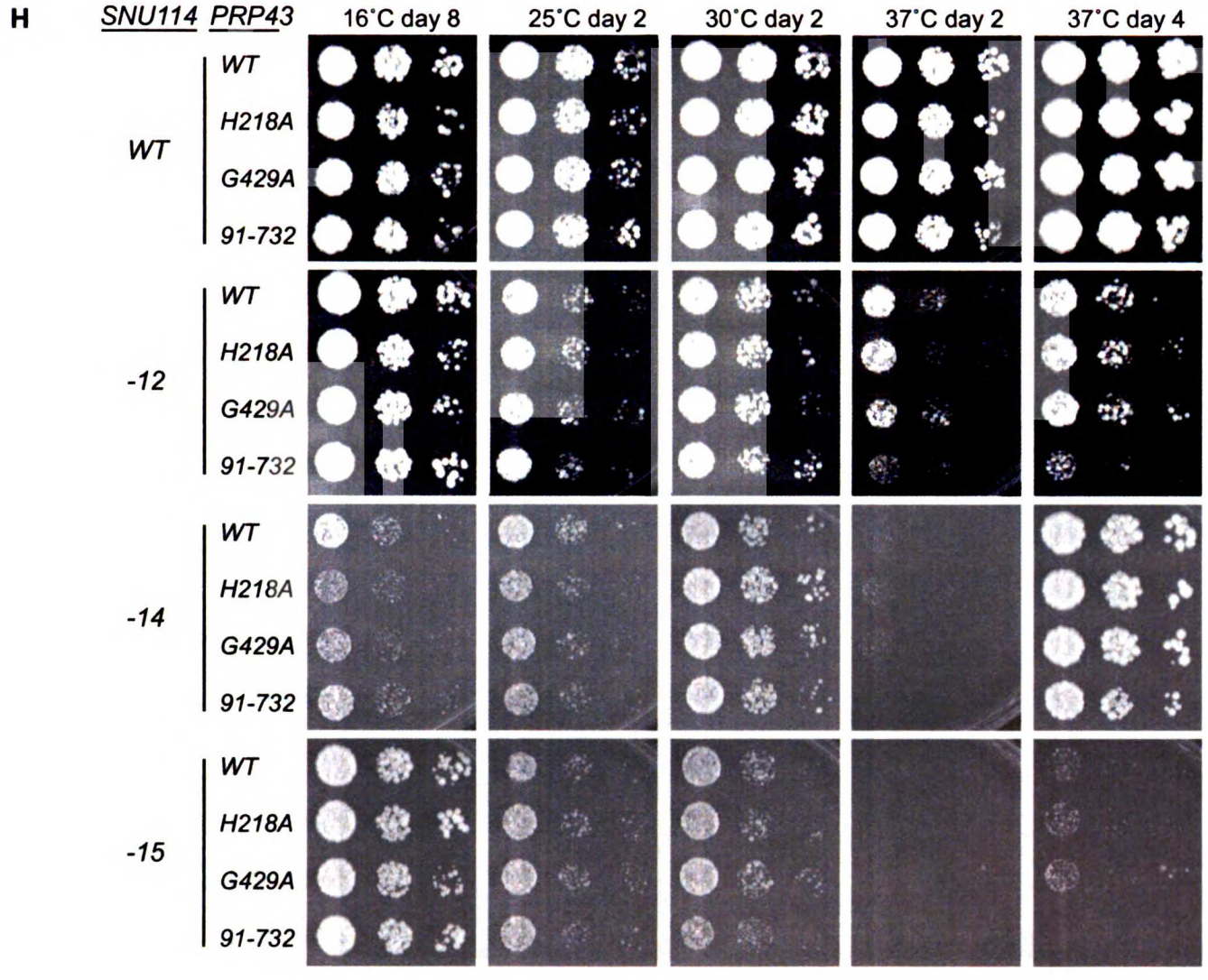
H
SNU114
PRP43
16°C day 8
25°C day 2
30°C day 2
37°C day 2
37°C day 4
WT
WT
H218A
G429A
91-732
-12
WT
H218A
G429A
91-732
-14
WT
H218A
G429A
91-732
-15
WT
H218A
G429A
91-732

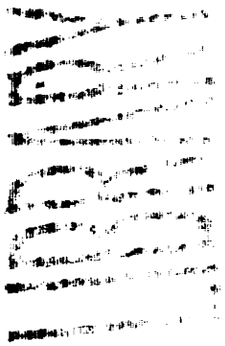

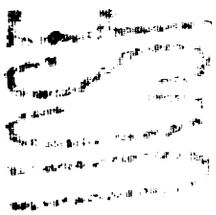

H, continued

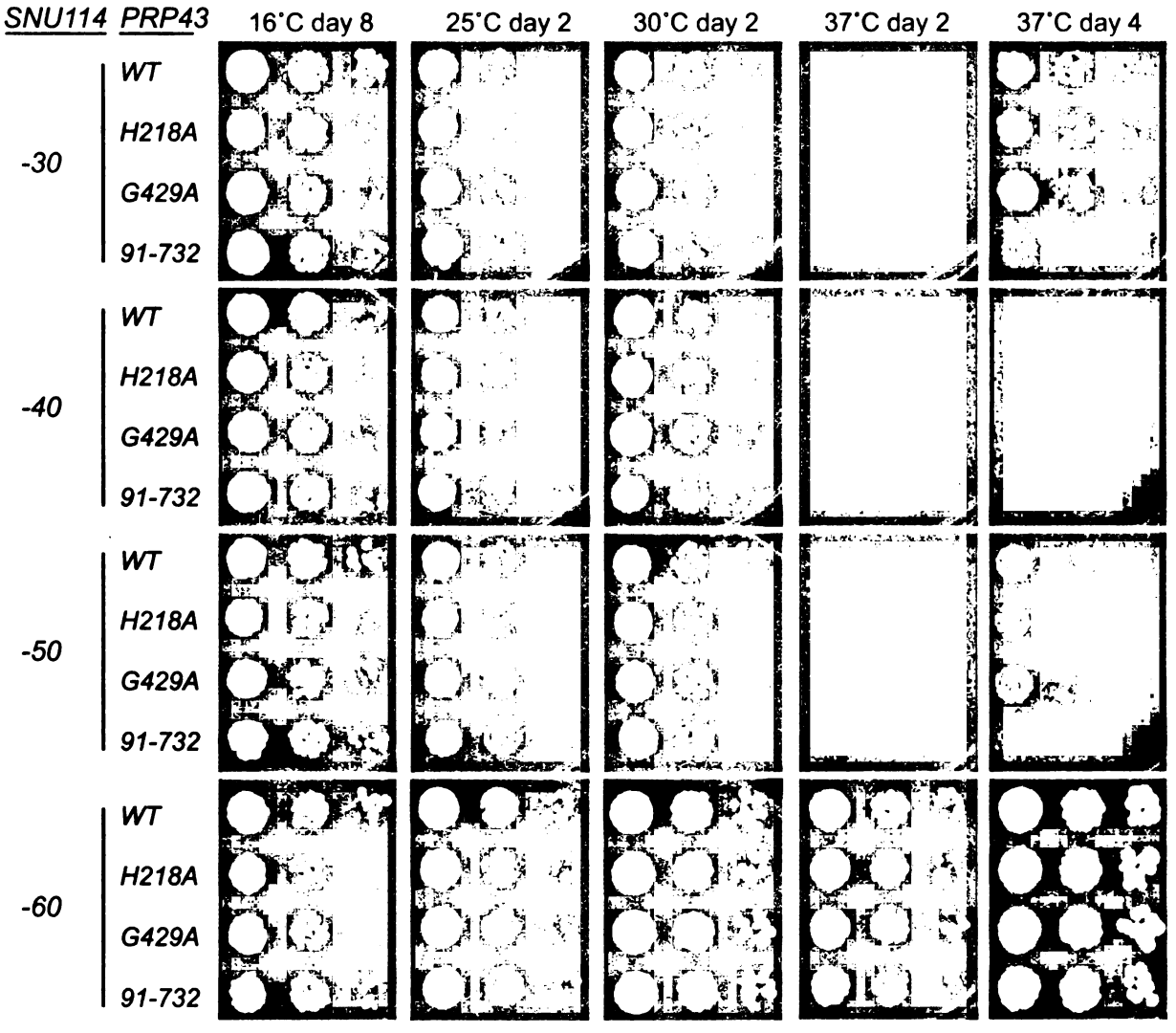
SNU114
PRP43
16°C day 8
25°C day 2
30°C day 2
37°C day 2
37°C day 4
-30
-40
-50
-60
WT
H218A
G429A
91-732

I

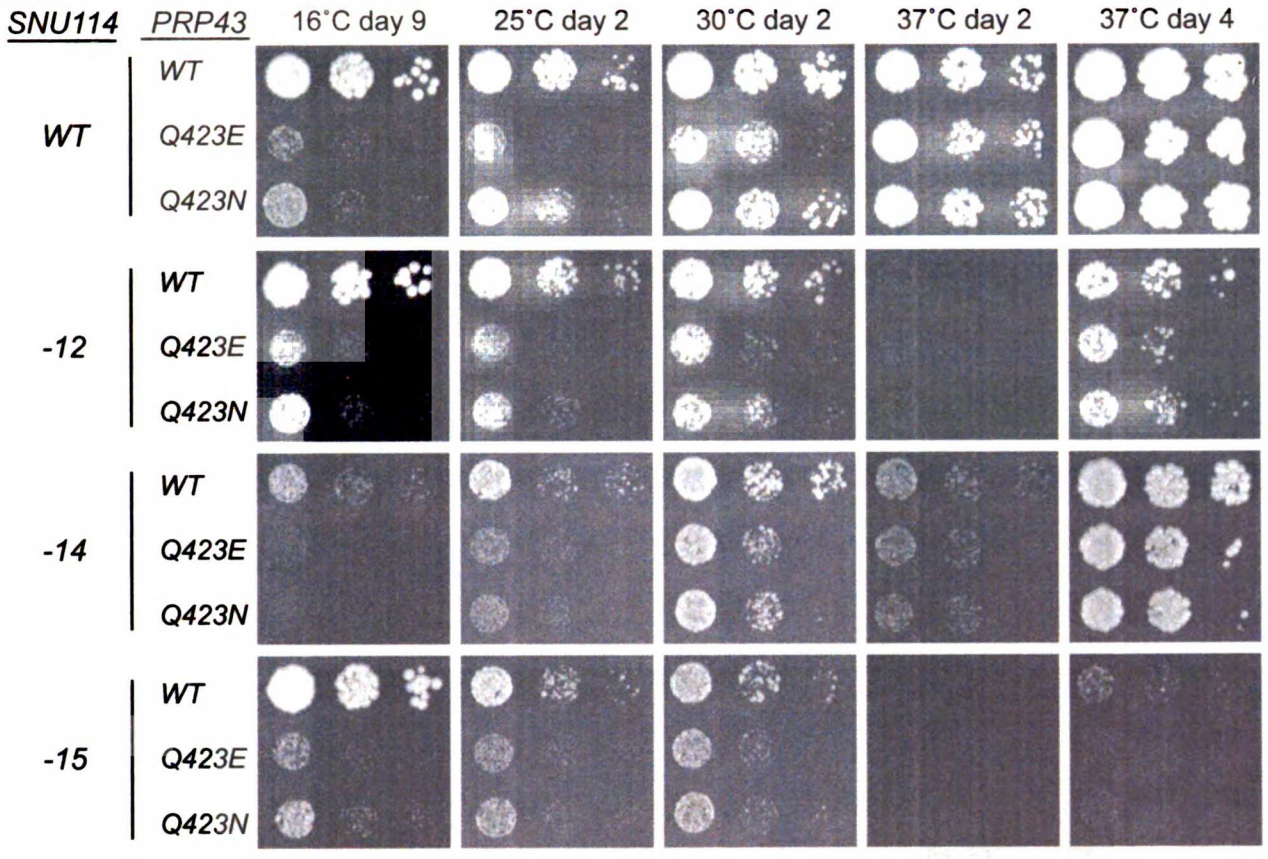
SNU114
PRP43
16°C day 9
25°C day 2
30°C day 2
37°C day 2
37°C day 4
WT
WT
Q423E
Q423N
-12
WT
Q423E
Q423N
-14
WT
Q423E
Q423N
-15
WT
Q423E
Q423N

I, continued

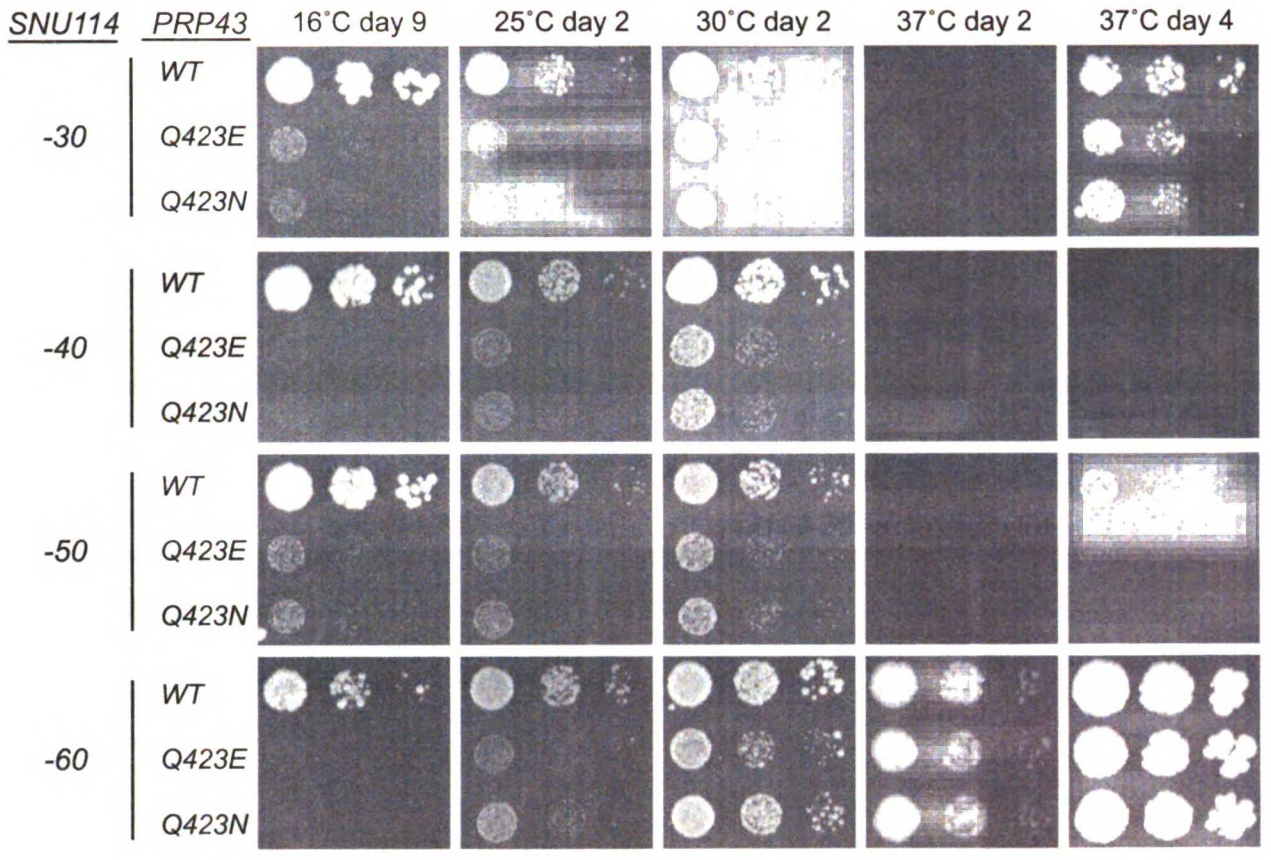
SNU114
PRP43
16˚C day 9
25˚C day 2
30˚C day 2
37˚C day 2
37˚C day 4
-30
-40
-50
-60
WT
Q423E
Q423N

[redacted]

J

5-FOA plates

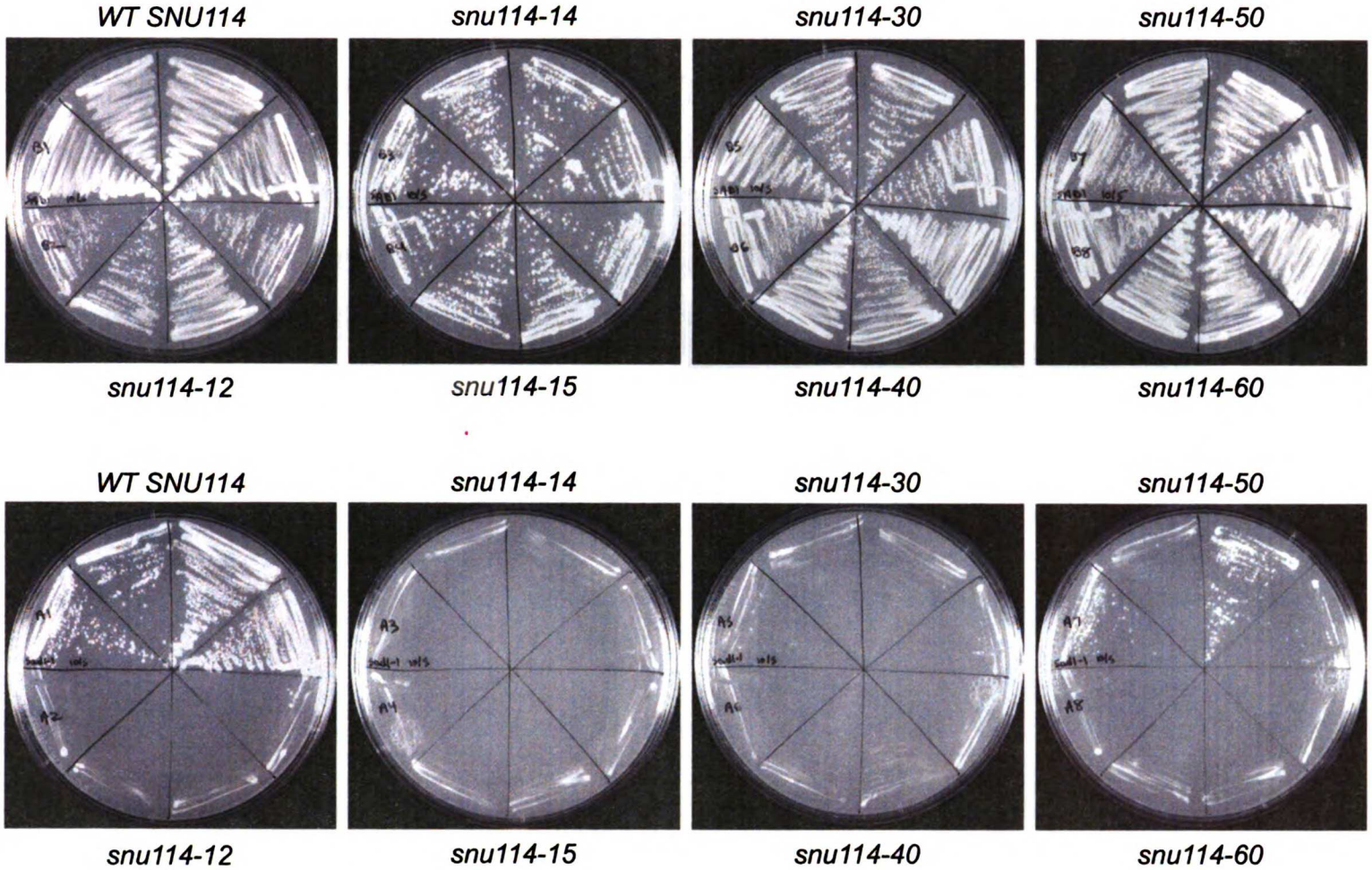

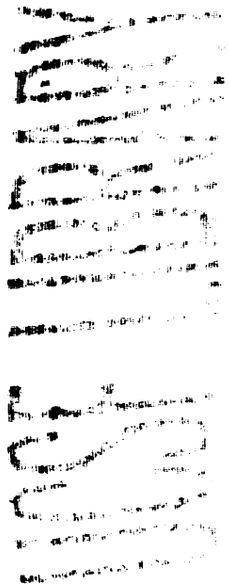

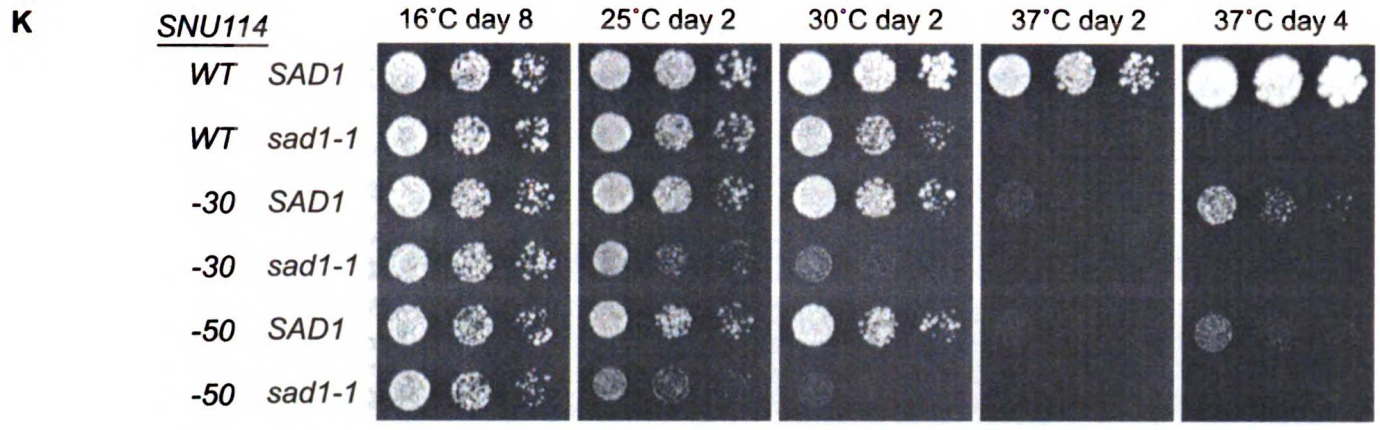
K
SNU114
16°C day 8
25°C day 2
30°C day 2
37°C day 2
37°C day 4
WT SAD1
WT sad1-1
-30 SAD1
-30 sad1-1
-50 SAD1
-50 sad1-1

L

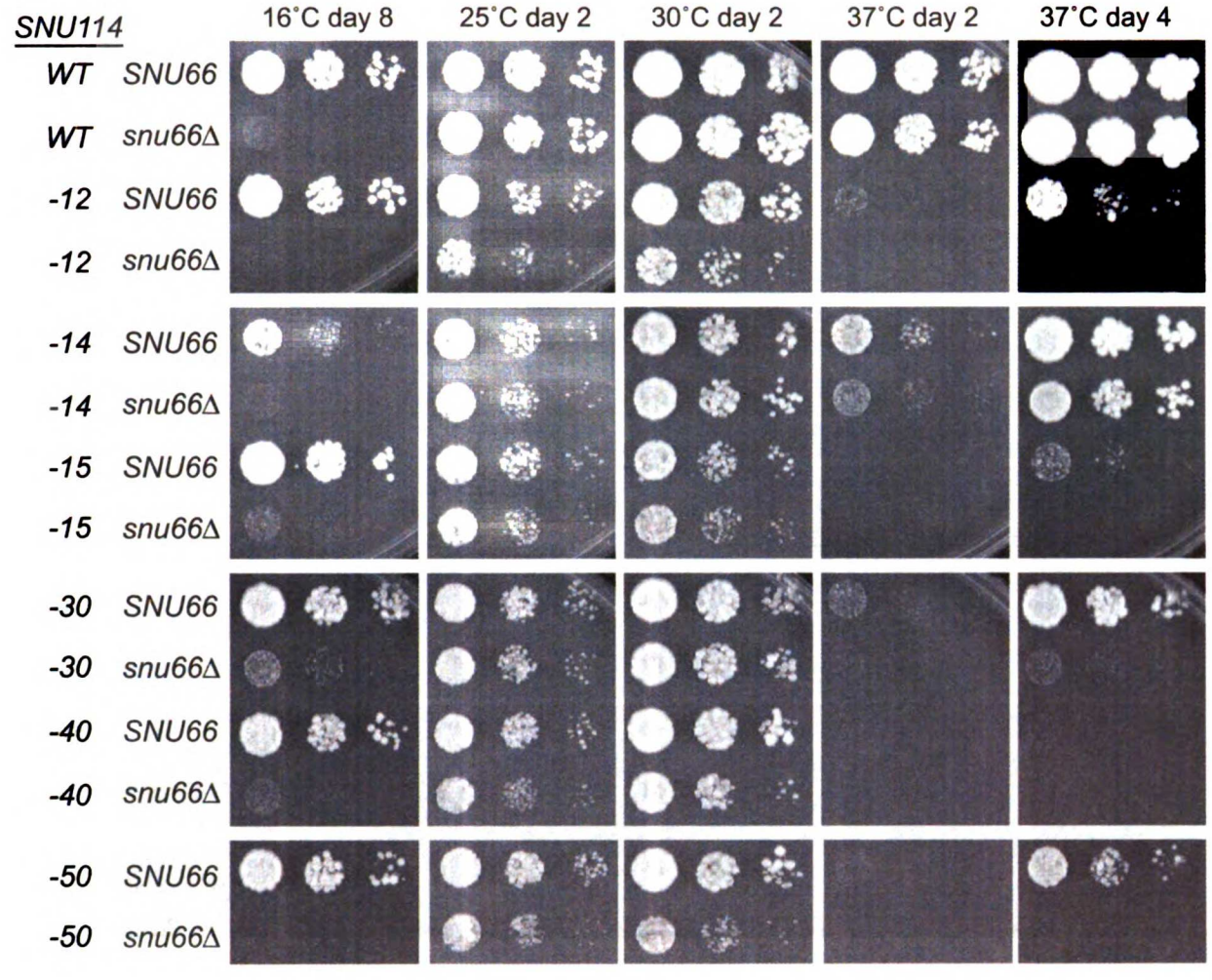
SNU114
16°C day 8
25°C day 2
30°C day 2
37°C day 2
37°C day 4
WT SNU66
WT snu66Δ
-12 SNU66
-12 snu66Δ
-14 SNU66
-14 snu66Δ
-15 SNU66
-15 snu66Δ
-30 SNU66
-30 snu66Δ
-40 SNU66
-40 snu66Δ
-50 SNU66
-50 snu66Δ

[redacted]

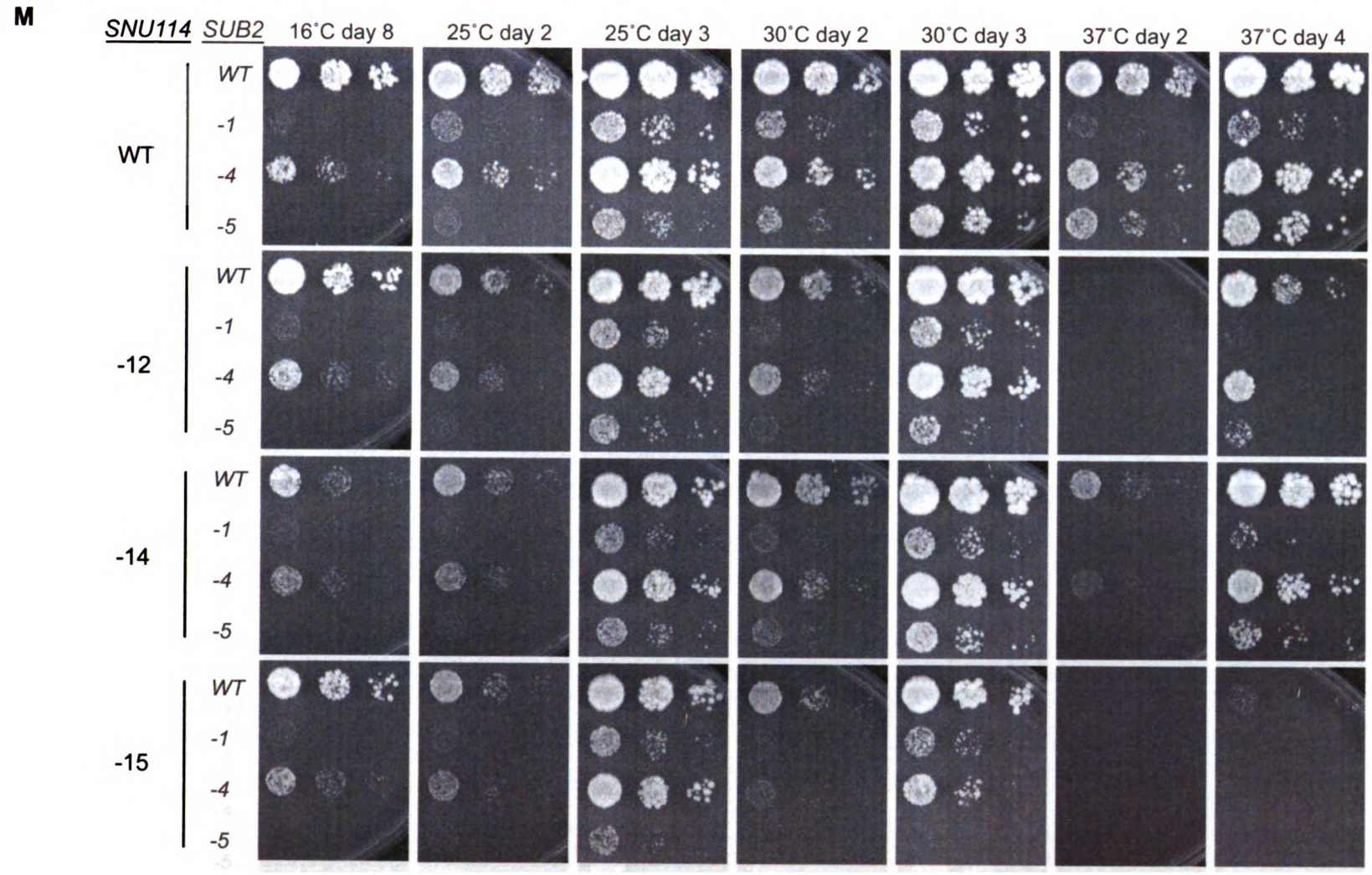
M
SNU114
SUB2
16°C day 8
25°C day 2
25°C day 3
30°C day 2
30°C day 3
37°C day 2
37°C day 4
WT
-12
-14
-15
WT
-1
-4
-5

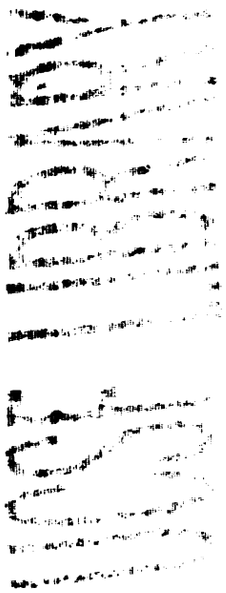

M, continued

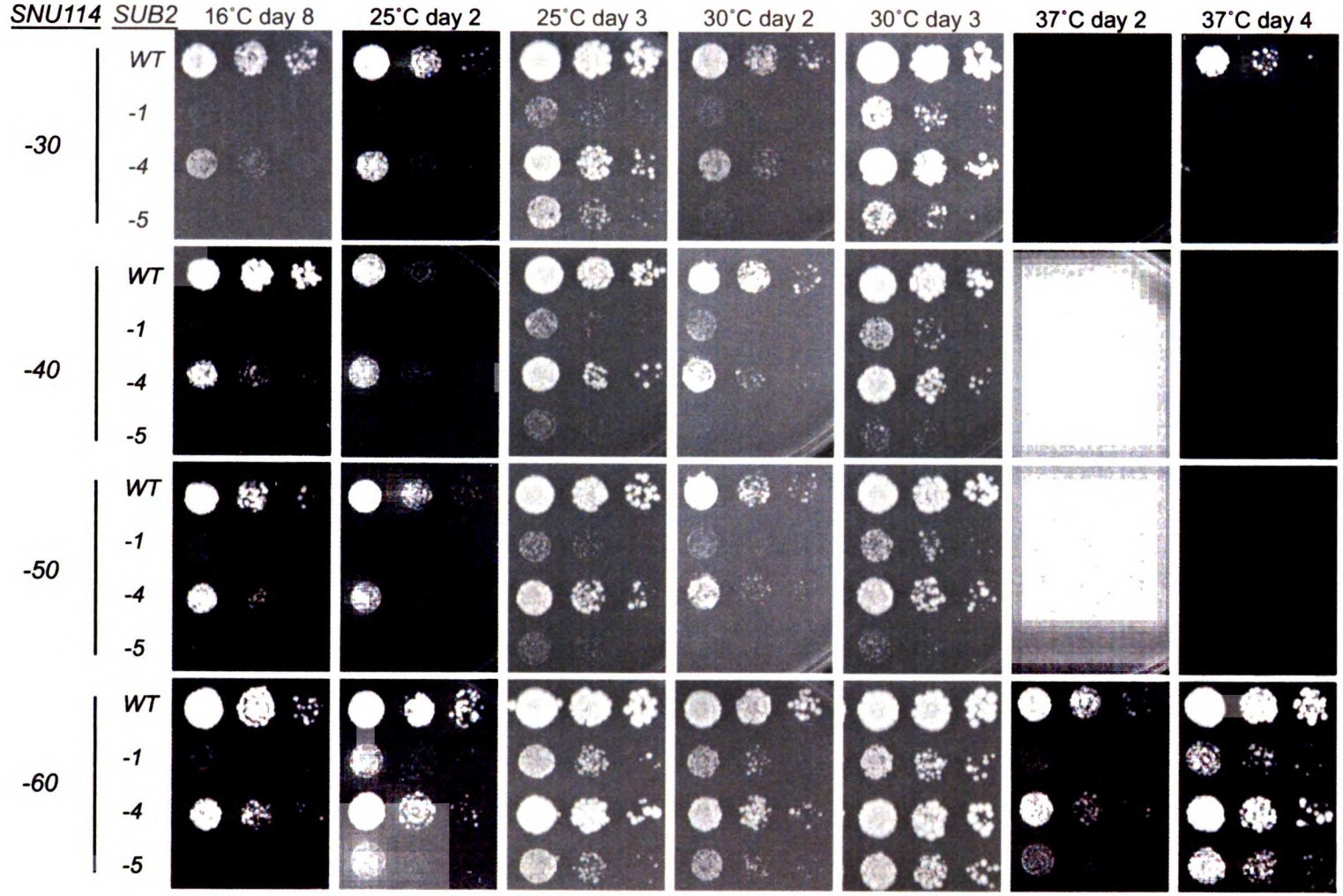
SNU114
SUB2
16°C day 8
25°C day 2
25°C day 3
30°C day 2
30°C day 3
37°C day 2
37°C day 4
-30
-40
-50
-60
WT
-1
-4
-5

Figure 2. Increasing the base pairing between U1 and the 5' splice site exacerbates the growth defect of snu114-60. **A:** Growth of *SNU114*, *snu114-60*, and *snu114-40* with a plasmid bearing WT U1; U1-2A, 10A; or an empty vector. Cells were spotted onto -TRP media to select for the plasmid. **B:** Growth of *PRP28* or *prp28-1* with a plasmid bearing WT U1 or U1-2A, 10A.

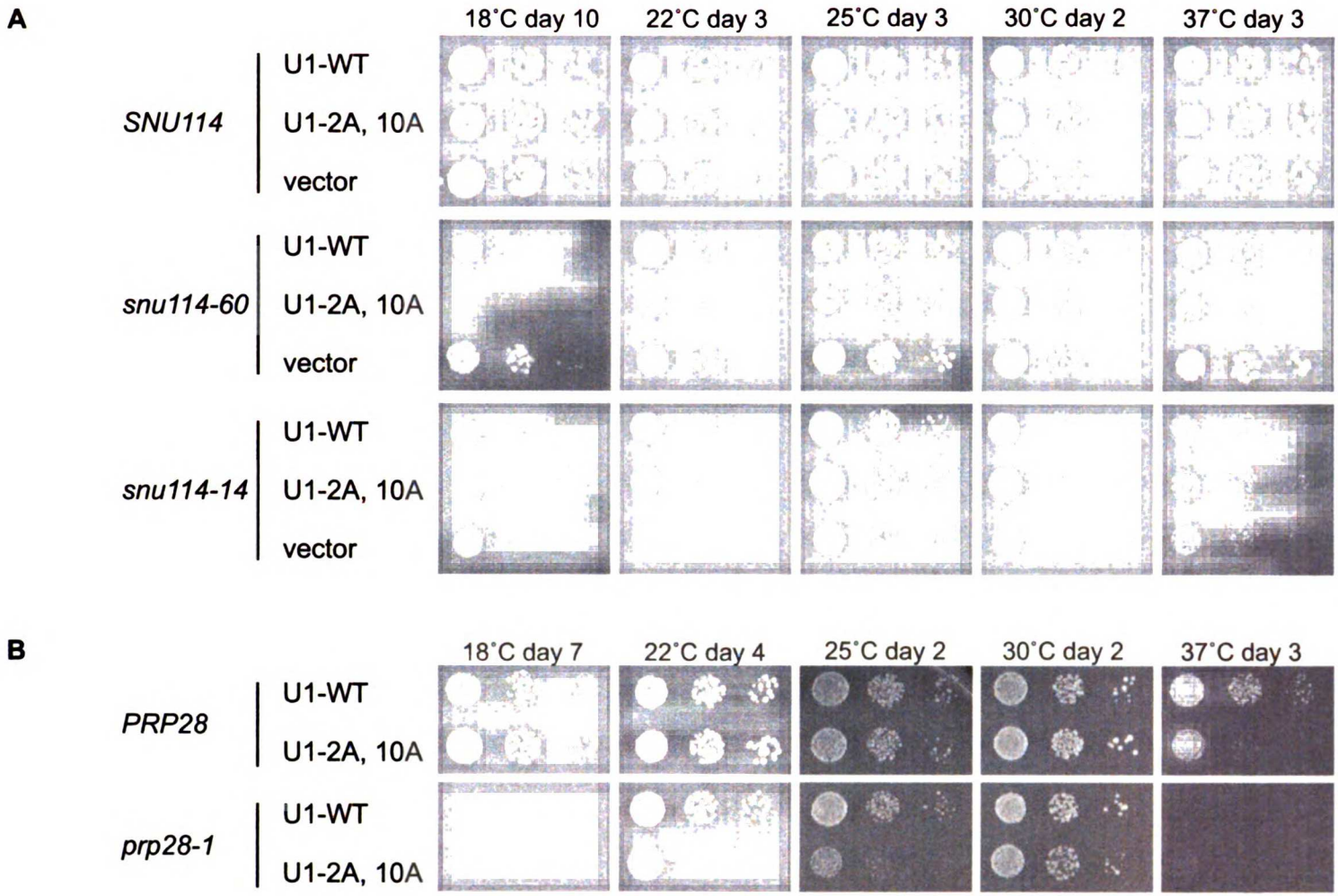
A
18°C day 10
22°C day 3
25°C day 3
30°C day 2
37°C day 3
SNU114
U1-WT
U1-2A, 10A
vector
snu114-60
U1-WT
U1-2A, 10A
vector
snu114-14
U1-WT
U1-2A, 10A
vector
B
18°C day 7
22°C day 4
25°C day 2
30°C day 2
37°C day 3
PRP28
U1-WT
U1-2A, 10A
prp28-1
U1-WT
U1-2A, 10A

Figure 3. U4-cs1 is synthetically lethal with *snu114* mutations. **A:** *U4Δ* strains with a chromosomal *snu114* mutation, carrying U4 on a *URA3*-marked plasmid and U4-cs1 on a *HIS3* plasmid, were streaked onto 5-FOA media and grown for five days at 30°C. **B.** *SNU114* and *snu114-40* cells recovered from the 5-FOA plates in A were spotted on YPD and grown at 16°C, 25°C, 30°C, and 37°C for the indicated number of days.

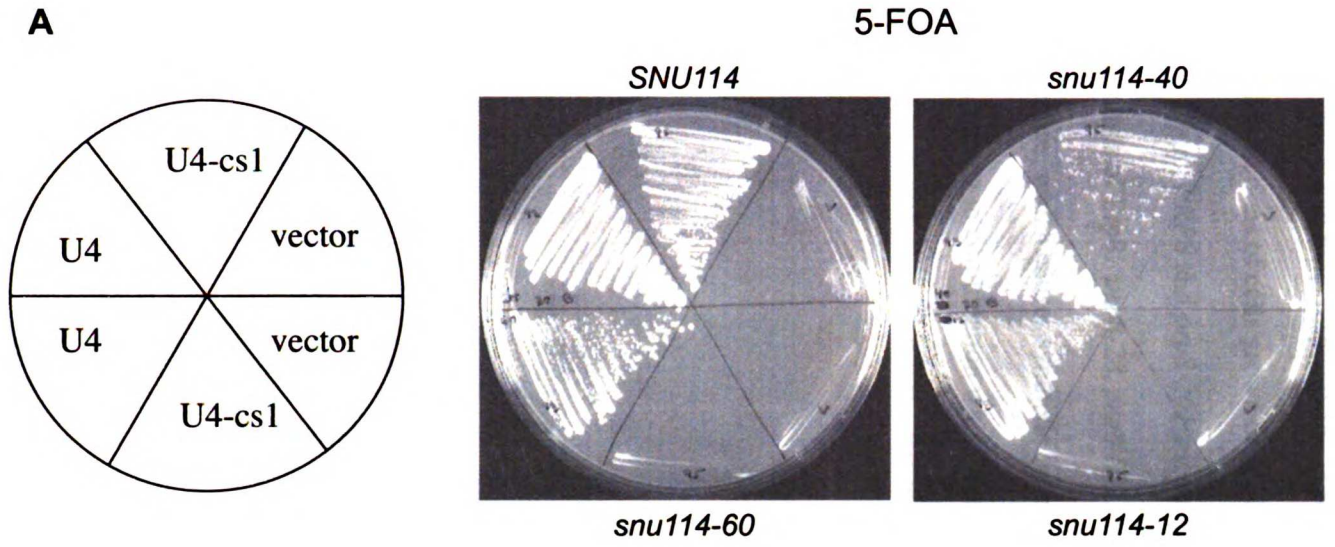
A
5-FOA
SNU114
snu114-40
U4-cs1
vector
U4
U4
vector
U4-cs1
snu114-60
snu114-12

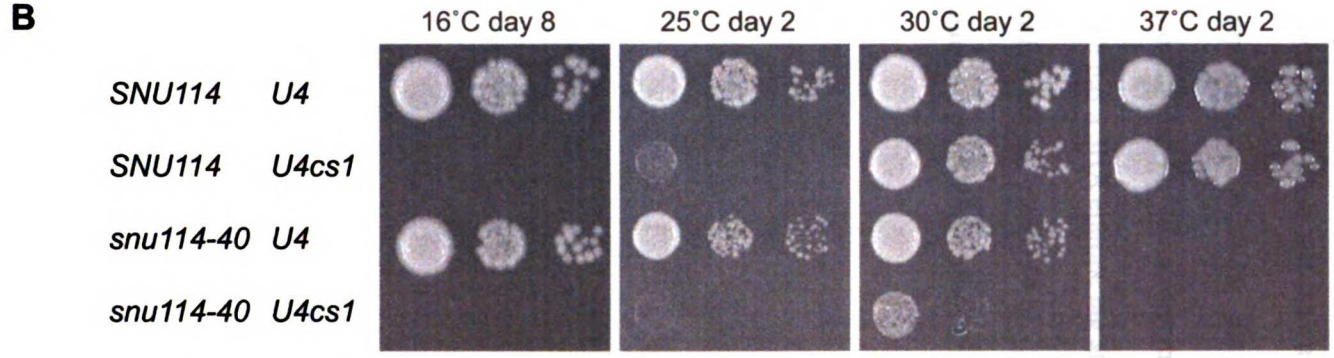
B
16˚C day 8
25˚C day 2
30˚C day 2
37˚C day 2
SNU114 U4
SNU114 U4cs1
snu114-40 U4
snu114-40 U4cs1

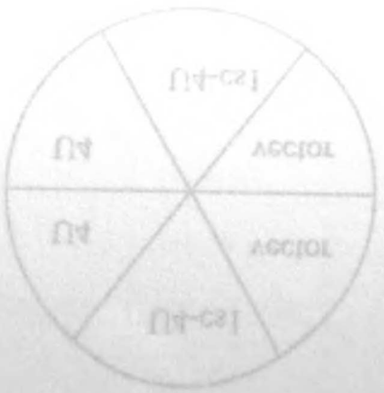

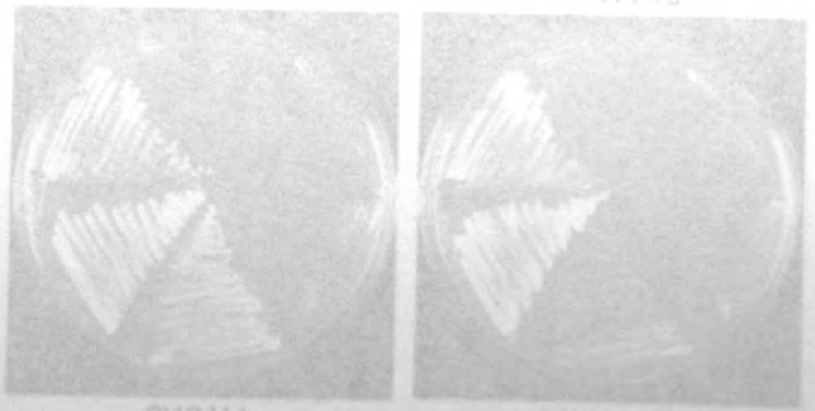

Figure 4. Genetic interactions between *snu114* and *prp8* alleles. **A:** Diagram of the location of the *prp8* mutations that were tested. The Jab/MPN and RP domains are shown in yellow and blue, respectively. The *prp8-brr* mutation, G1563R, is not shown. **B-E:** Serial dilutions of cells grown on YPD. **B:** *prp8-1*, *prp8-101*, and *prp8-brr*. **C:** *prp8-201*. Here, *PRP8* and *prp8-201* are on 2μ (high copy) plasmids. **D:** Mutations in the C-terminus of Prp8: *prp8-28*, *prp8-602*, *prp8-88G*. *PRP8* has a 3HA epitope tag at the C-terminus, which causes synthetic interactions with *snu114-60*. **E:** *SNU114* or *snu114-60* strains in combination with C-terminal Prp8 mutations: *prp8-28*, *prp8-602*, *prp8-88G*, *prp8-88K*, and *prp8-92L*. *PRP8* is untagged.

[redacted]

[redacted]

A

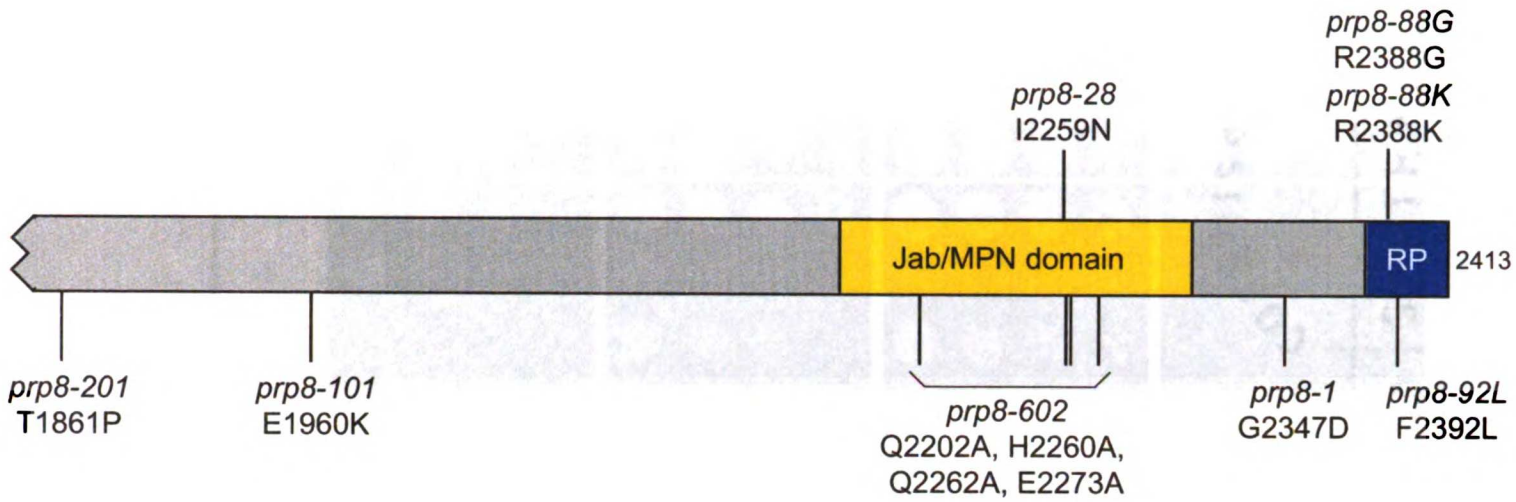
prp8-88G
R2388G
prp8-88K
R2388K
prp8-28
I2259N
Jab/MPN domain
RP
2413
prp8-201
T1861P
prp8-101
E1960K
prp8-602
Q2202A, H2260A,
Q2262A, E2273A
prp8-1
G2347D
prp8-92L
F2392L

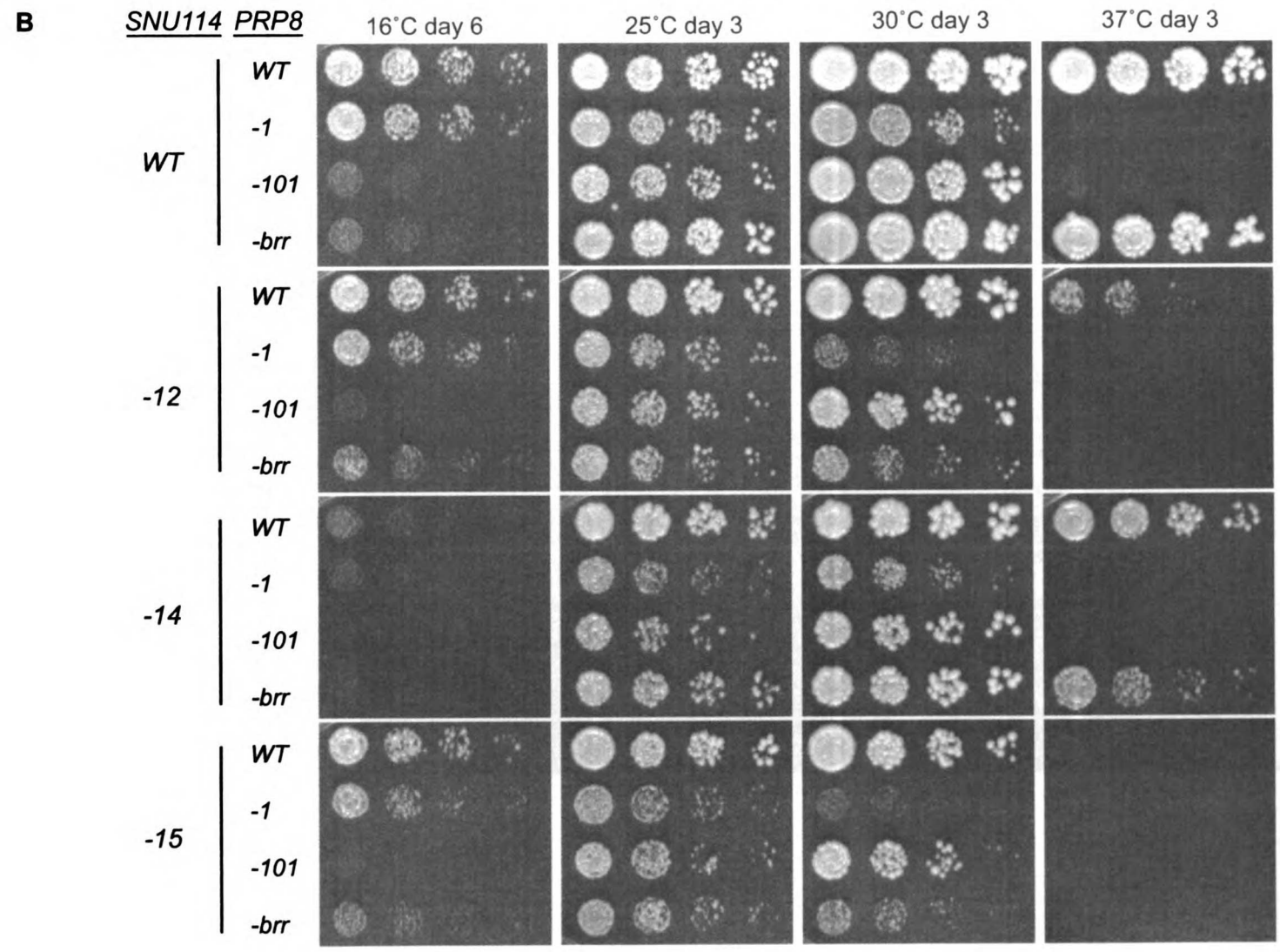
B
SNU114
PRP8
16˚C day 6
25˚C day 3
30˚C day 3
37˚C day 3
WT
-1
-101
-brr
-12
-14
-15

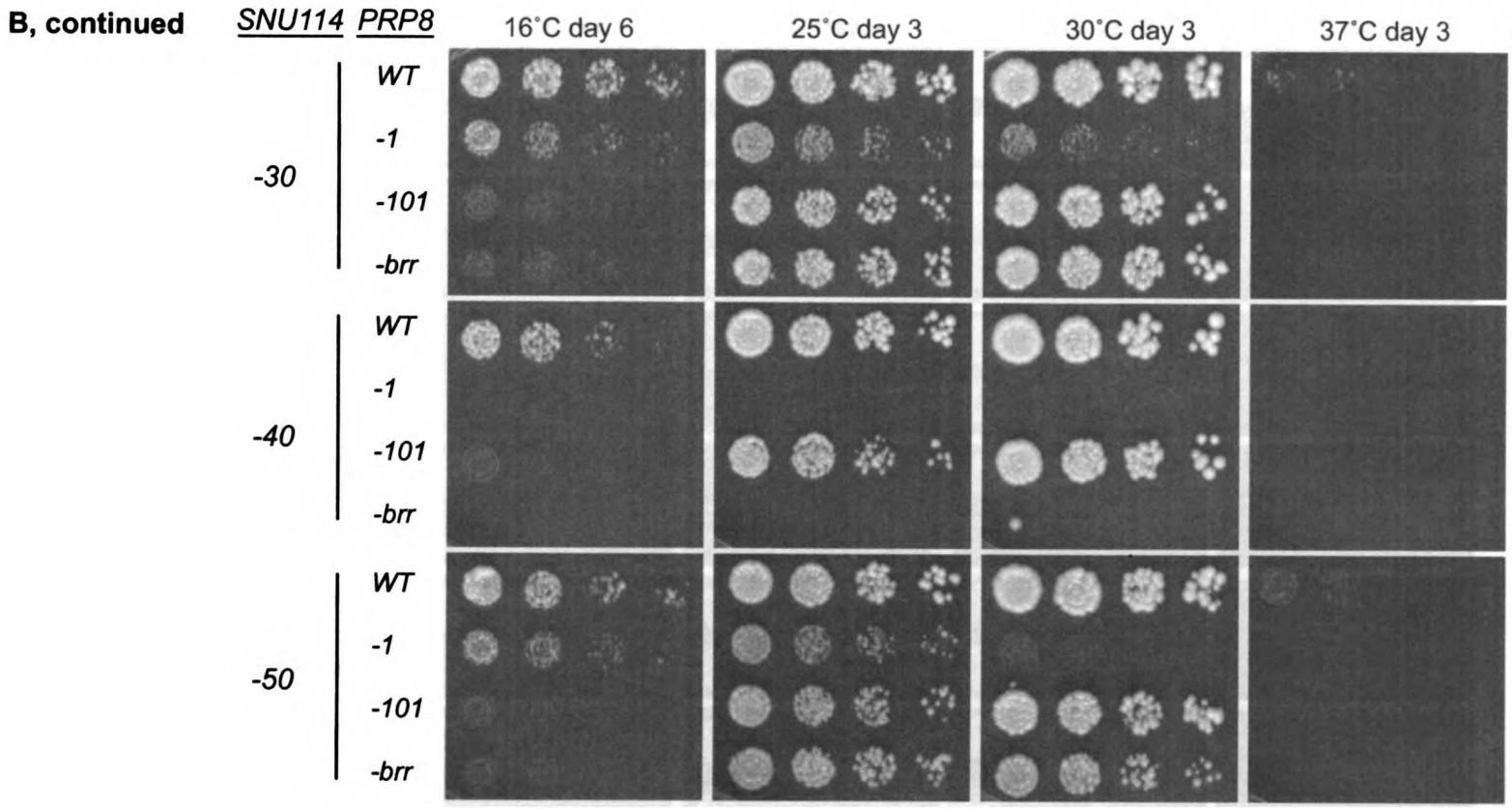
B, continued
SNU114
PRP8
16˚C day 6
25˚C day 3
30˚C day 3
37˚C day 3
-30
WT
-1
-101
-brr
-40
WT
-1
-101
-brr
-50
WT
-1
-101
-brr

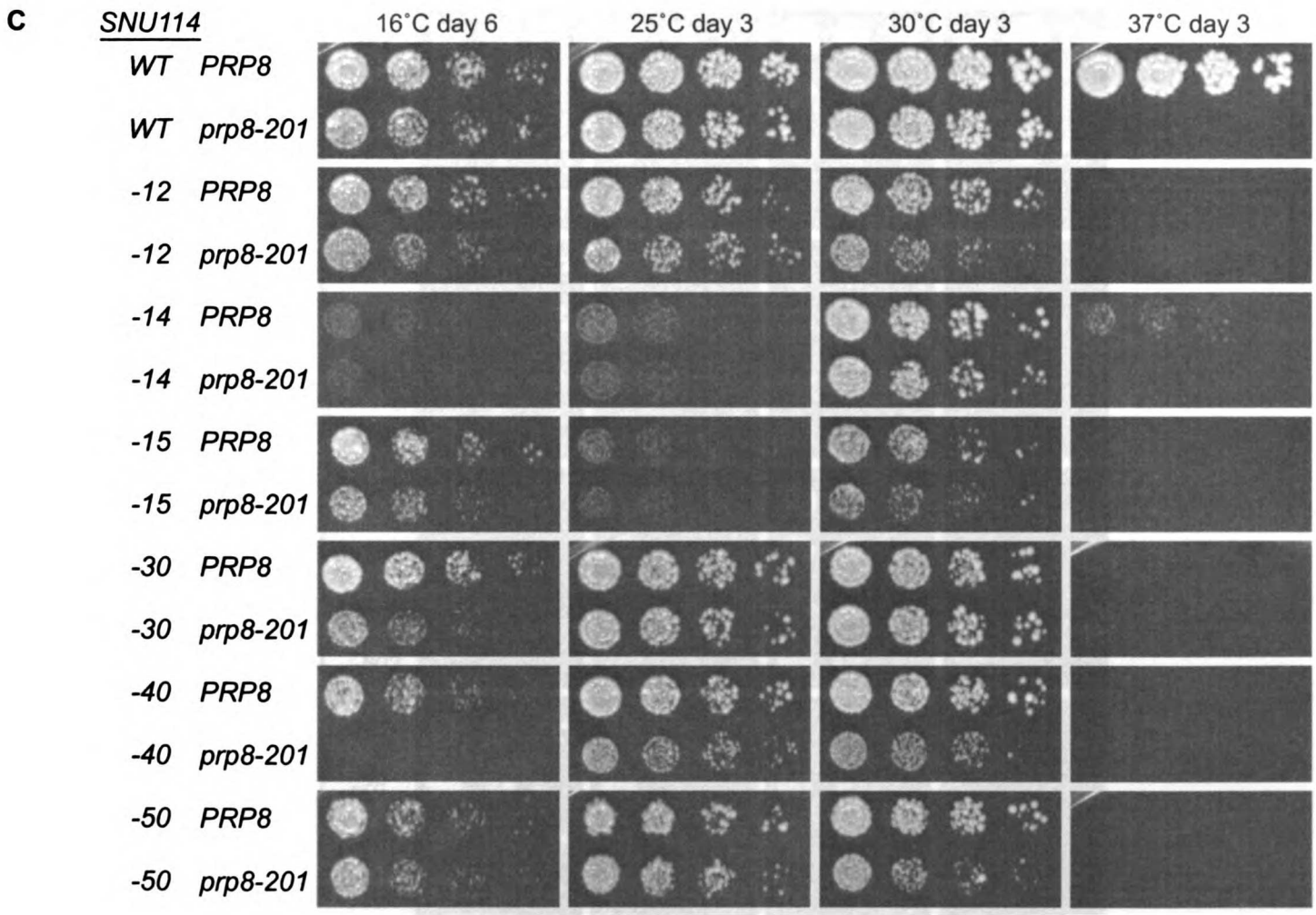
C
SNU114
16°C day 6
25°C day 3
30°C day 3
37°C day 3
WT PRP8
WT prp8-201
-12 PRP8
-12 prp8-201
-14 PRP8
-14 prp8-201
-15 PRP8
-15 prp8-201
-30 PRP8
-30 prp8-201
-40 PRP8
-40 prp8-201
-50 PRP8
-50 prp8-201

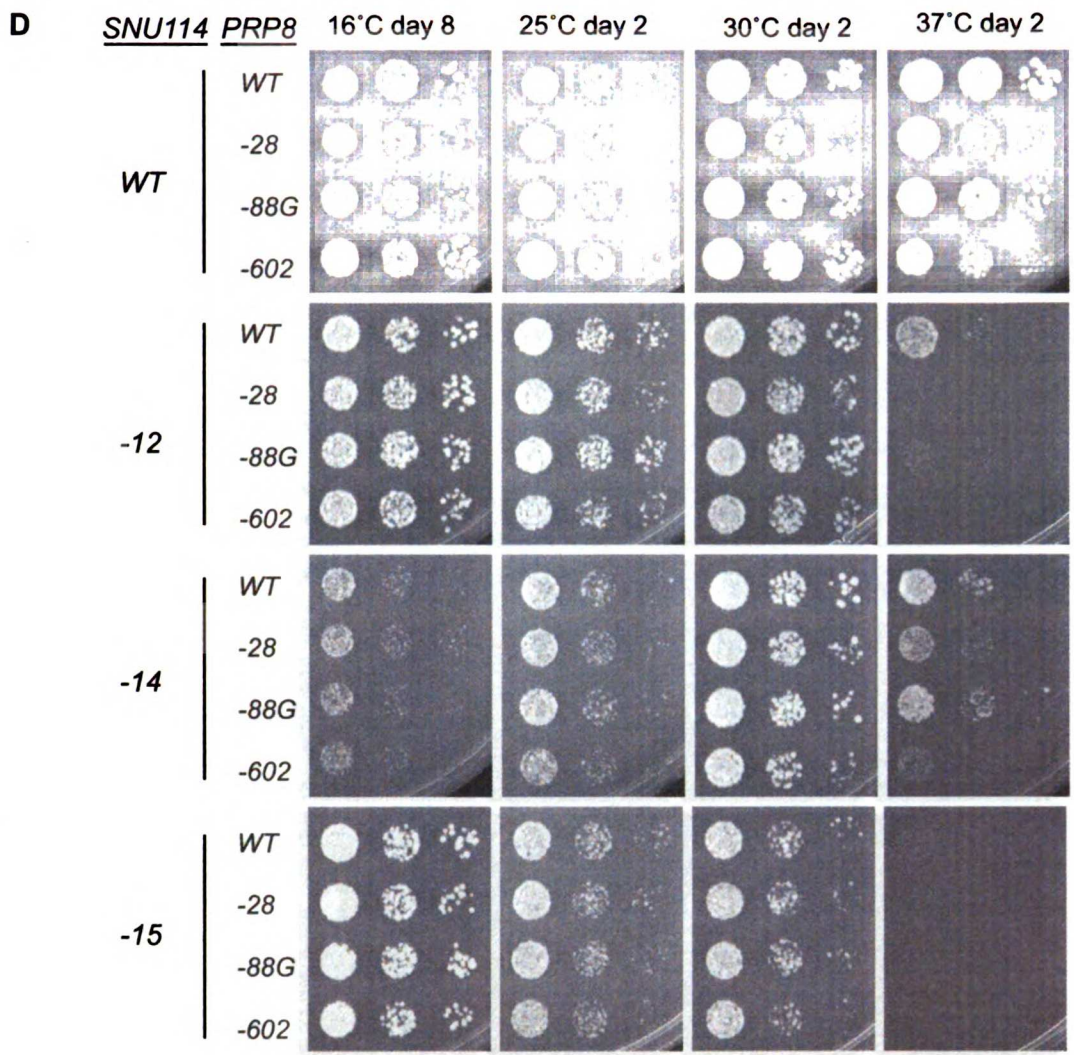
D
SNU114
PRP8
16°C day 8
25°C day 2
30°C day 2
37°C day 2
WT
-28
-88G
-602
-12
-14
-15

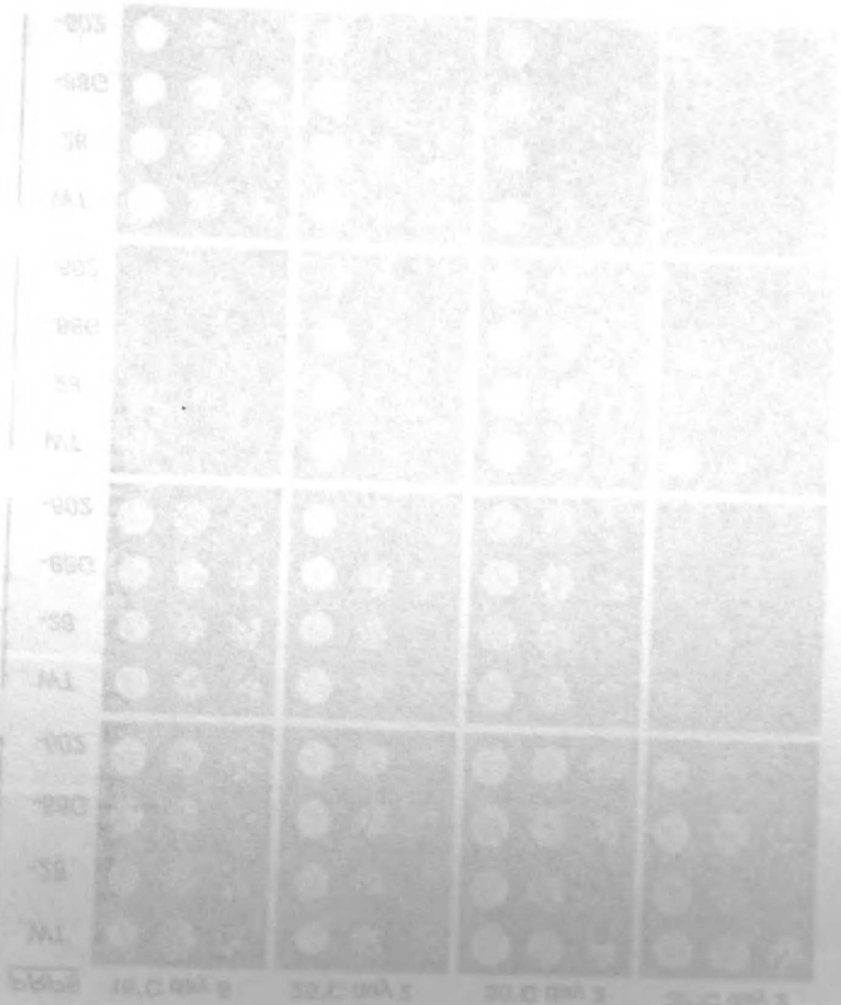

D, continued

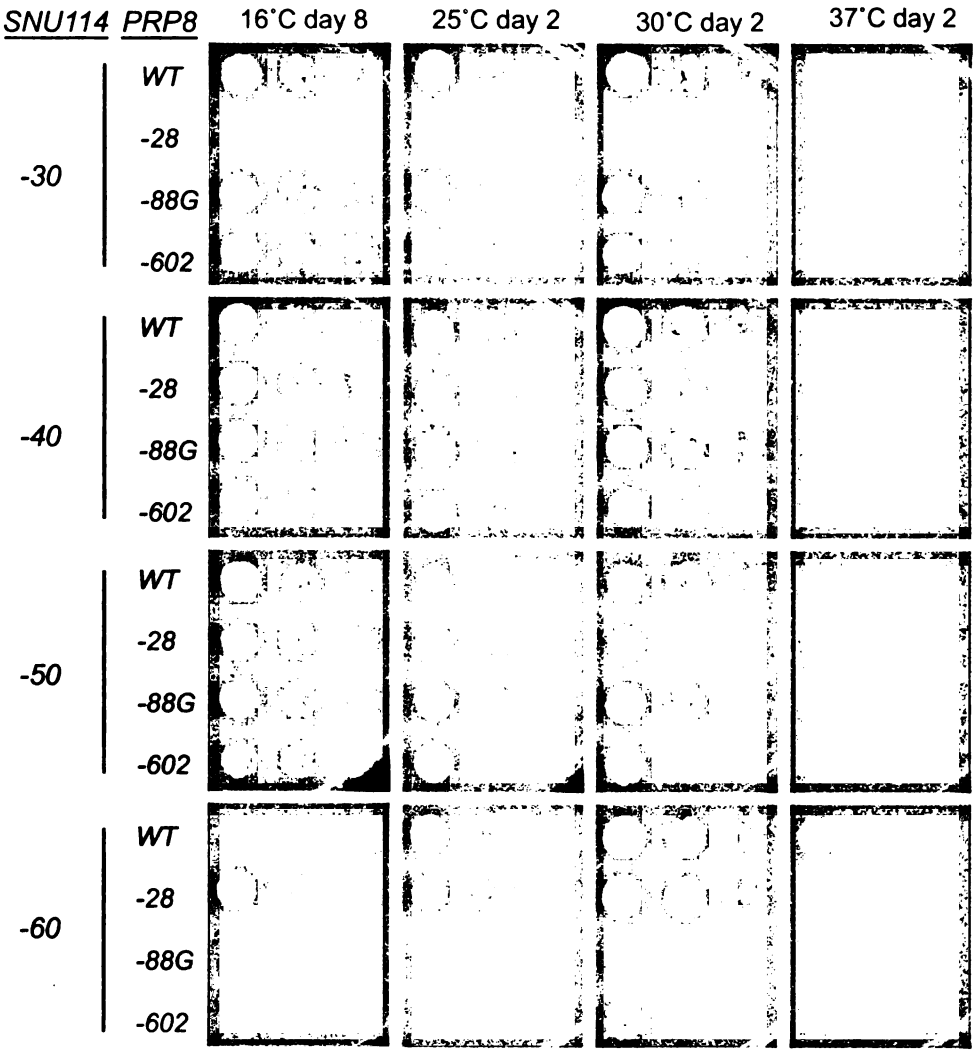
SNU114
PRP8
16°C day 8
25°C day 2
30°C day 2
37°C day 2
-30
WT
-28
-88G
-602
-40
WT
-28
-88G
-602
-50
WT
-28
-88G
-602
-60
WT
-28
-88G
-602

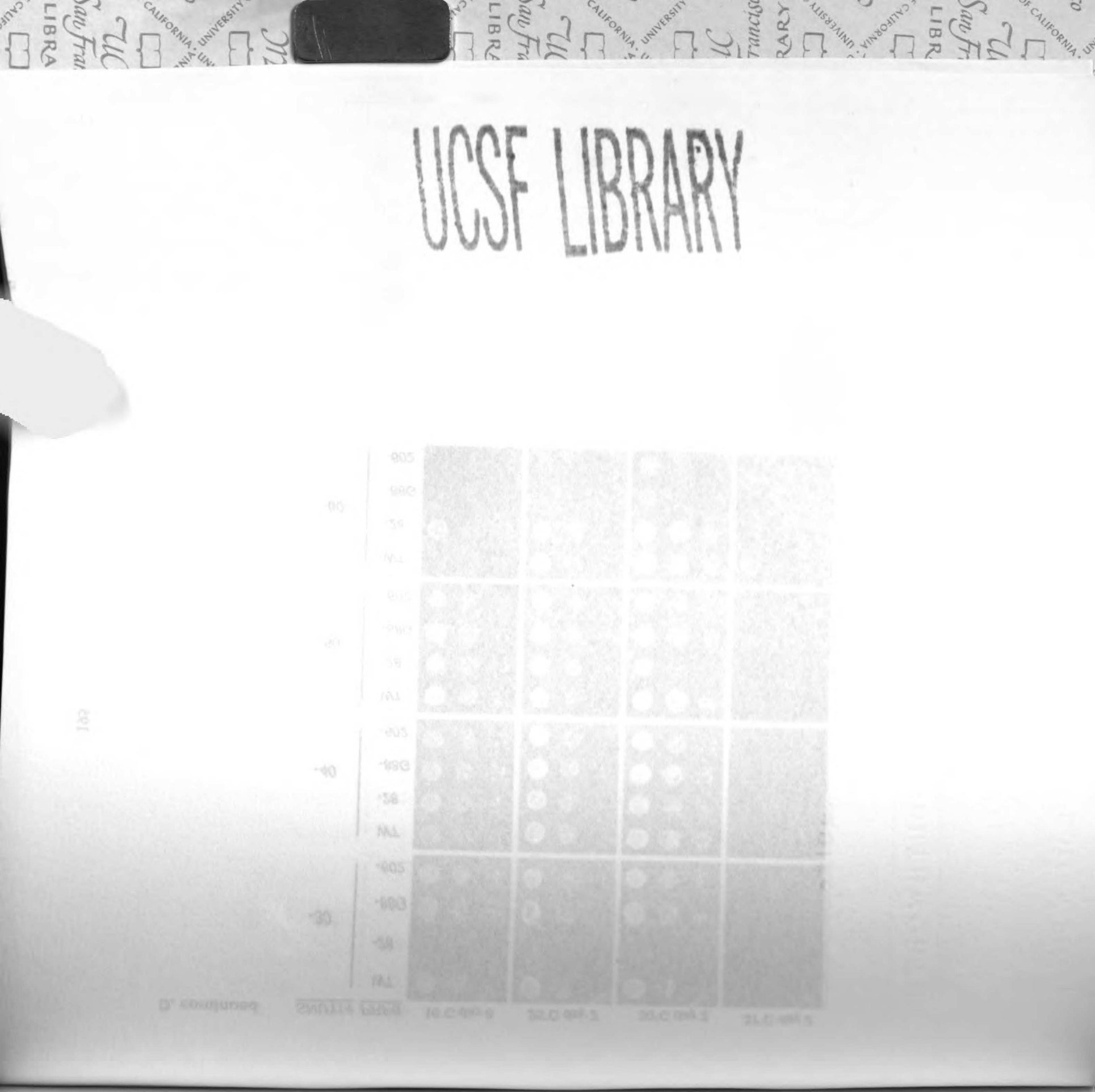

E

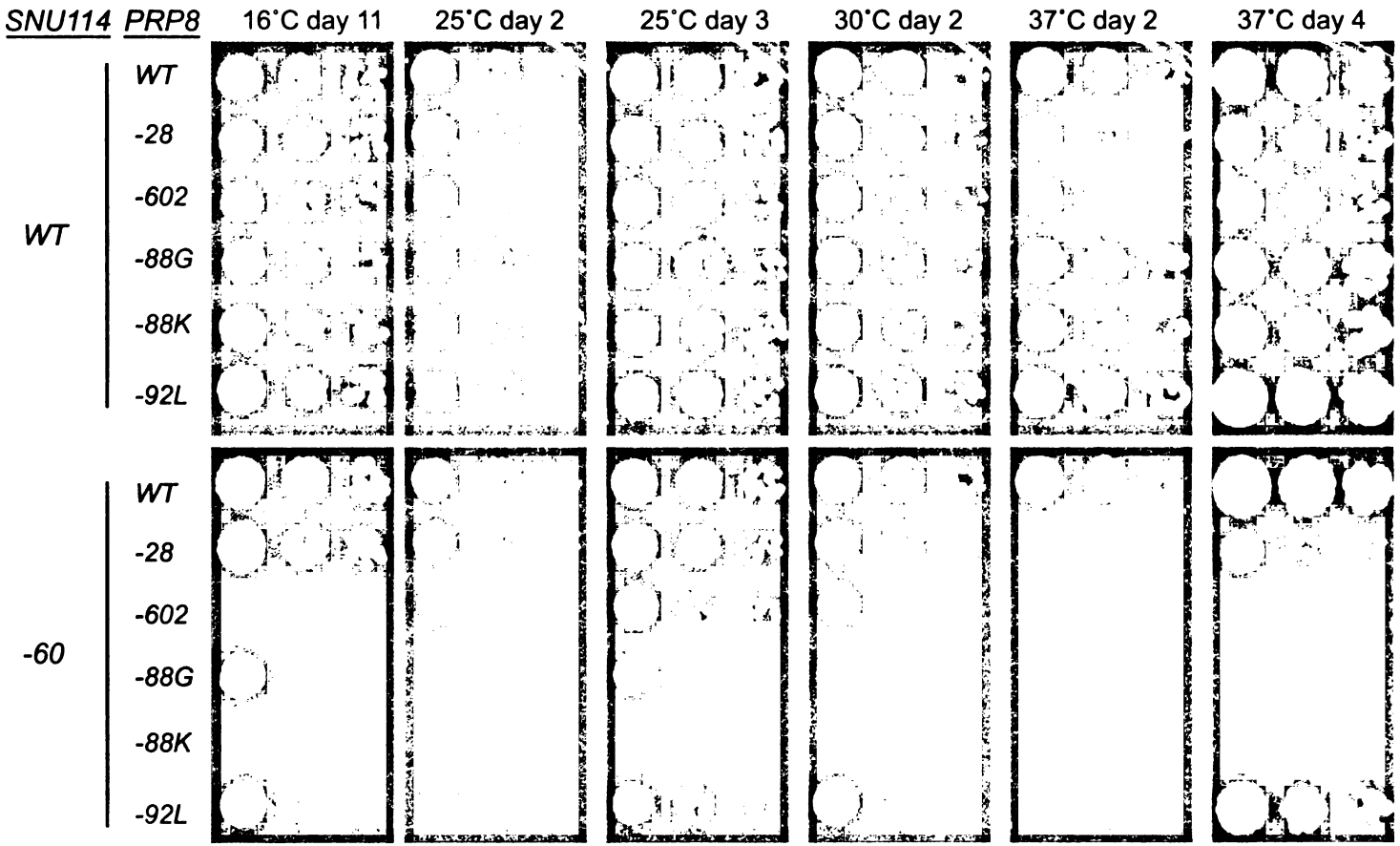
SNU114
PRP8
16°C day 11
25°C day 2
25°C day 3
30°C day 2
37°C day 2
37°C day 4
WT
WT
-28
-602
-88G
-88K
-92L
-60
WT
-28
-602
-88G
-88K
-92L

[redacted]

[redacted]

Figure 5. Genetic interactions between *snu114* and *brr2* alleles. **A:** Diagram of location of *brr2* mutations that were tested. Most of the alleles contain multiple mutations, which are represented by vertical bars. **B:** Serial dilutions of *snu114* alleles in combination with *brr2-1* were grown on YPD . **C:** *brr2Δ* strains with a chromosomal *snu114* mutation, carrying *BRR2* on a *URA3*-marked plasmid and the indicated *brr2* allele on a *HIS3* plasmid, were streaked onto 5-FOA media and grown for five days at 25°C. **D:** Growth of *snu114* alleles with *brr2-A*, *brr2-B*, and *brr2-BF* on YPD. *WT BRR2* is shown in panel E. **E:** Growth of *snu114* alleles with *brr2-M*, *brr2-C*, and *brr2-39* on YPD.

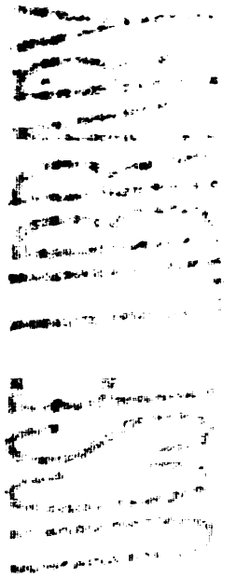

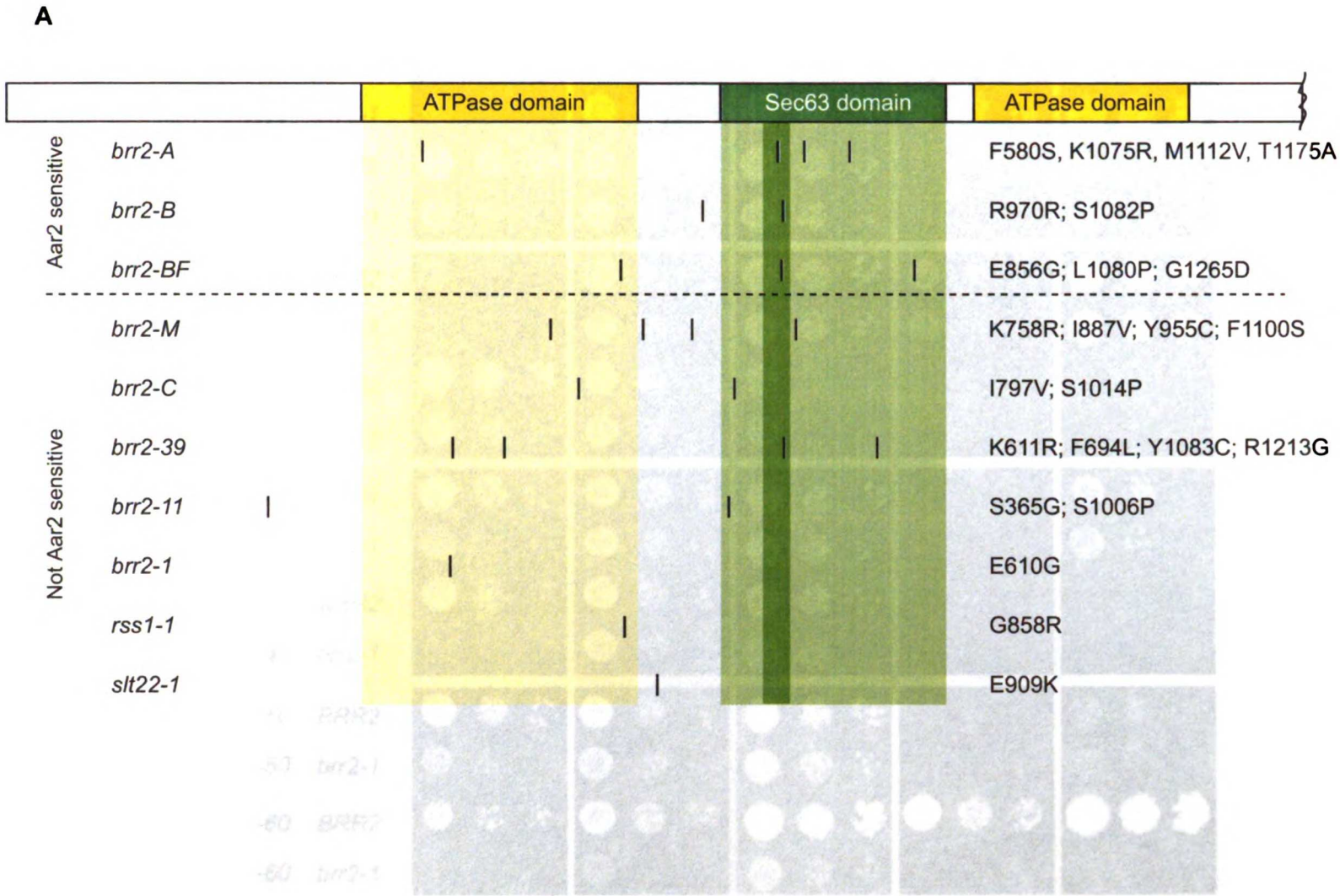
A
ATPase domain
Sec63 domain
ATPase domain
Aar2 sensitive
brr2-A
F580S, K1075R, M1112V, T1175A
brr2-B
R970R; S1082P
brr2-BF
E856G; L1080P; G1265D
brr2-M
K758R; I887V; Y955C; F1100S
brr2-C
I797V; S1014P
Not Aar2 sensitive
brr2-39
K611R; F694L; Y1083C; R1213G
brr2-11
S365G; S1006P
brr2-1
E610G
rss1-1
G858R
slt22-1
E909K

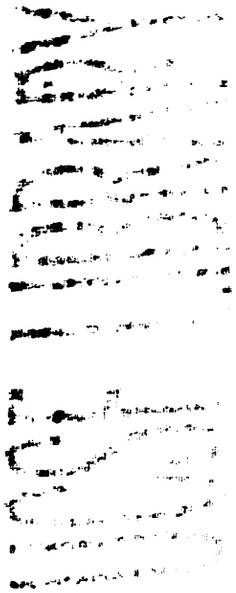

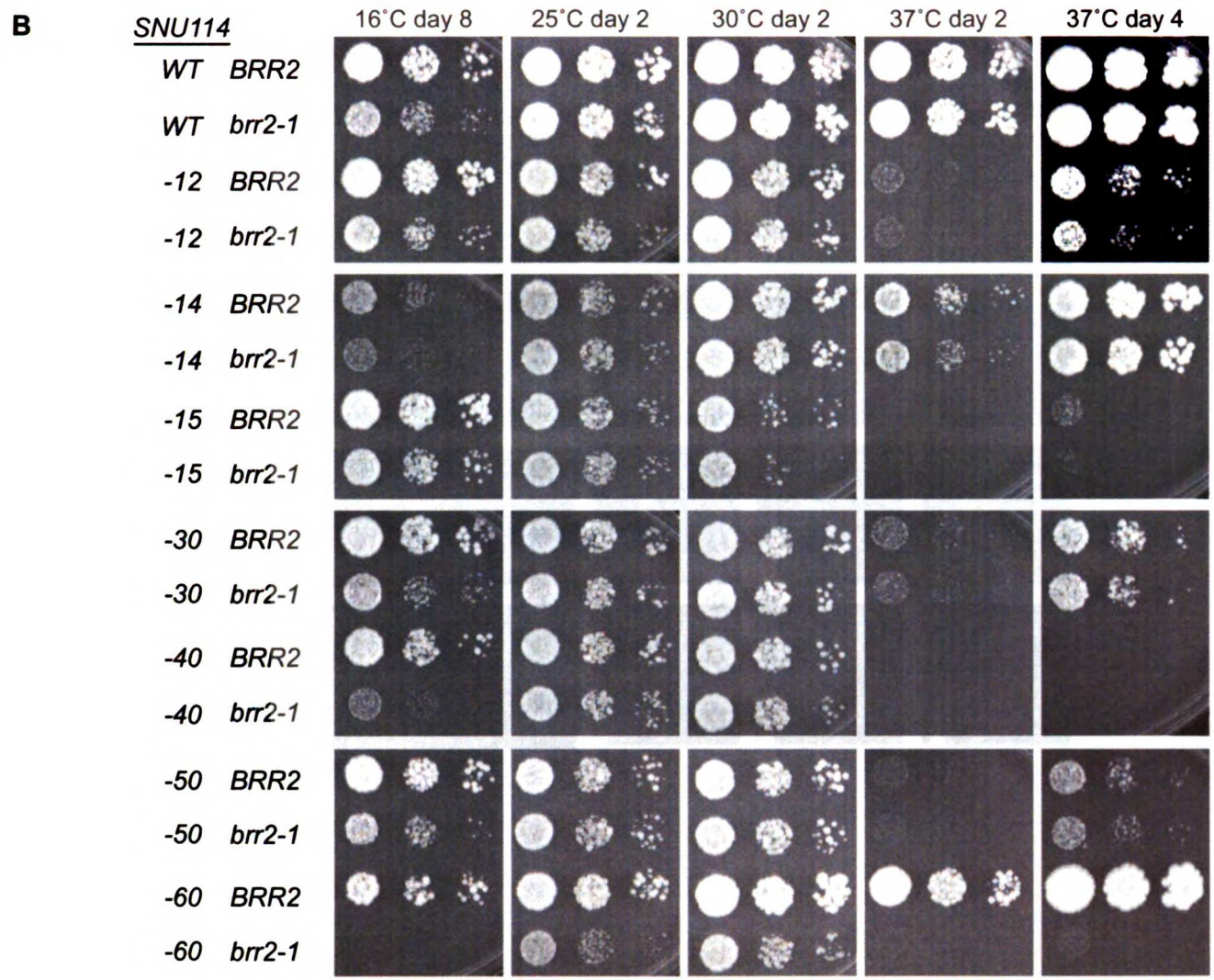
B
SNU114
16˚C day 8
25˚C day 2
30˚C day 2
37˚C day 2
37˚C day 4
WT BRR2
WT brr2-1
-12 BRR2
-12 brr2-1
-14 BRR2
-14 brr2-1
-15 BRR2
-15 brr2-1
-30 BRR2
-30 brr2-1
-40 BRR2
-40 brr2-1
-50 BRR2
-50 brr2-1
-60 BRR2
-60 brr2-1

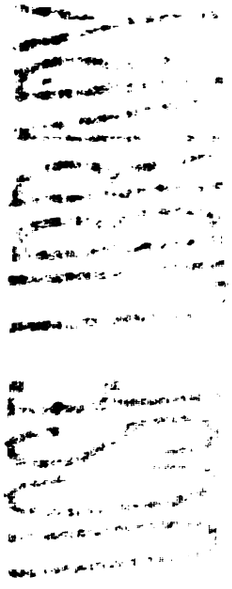

C

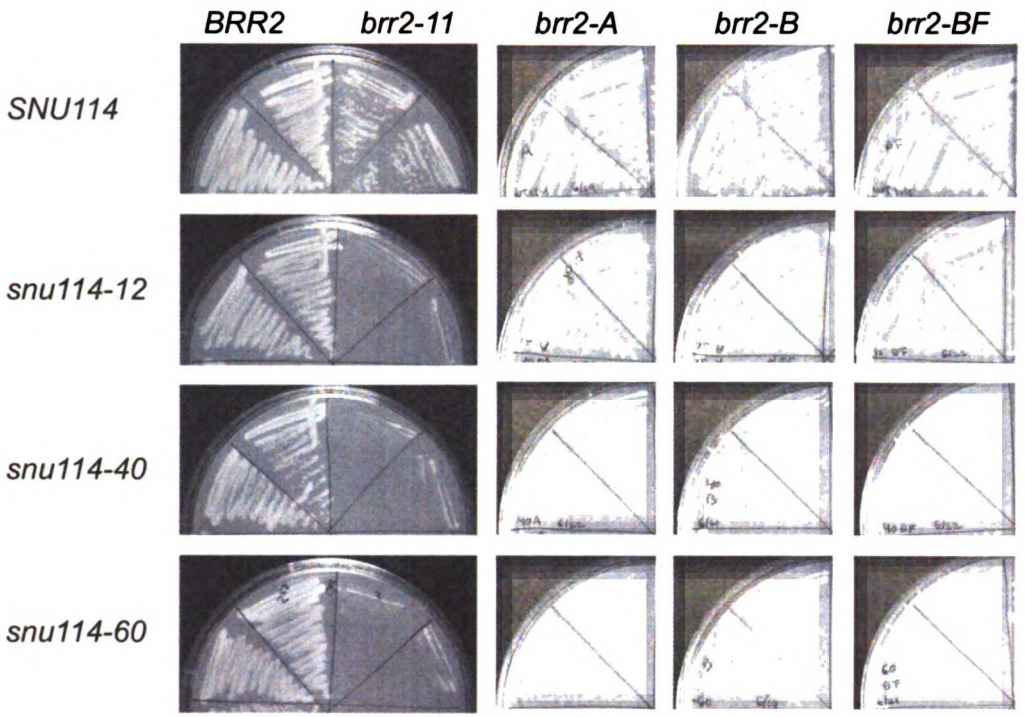
BRR2
brr2-11
brr2-A
brr2-B
brr2-BF
SNU114
snu114-12
snu114-40
snu114-60

D

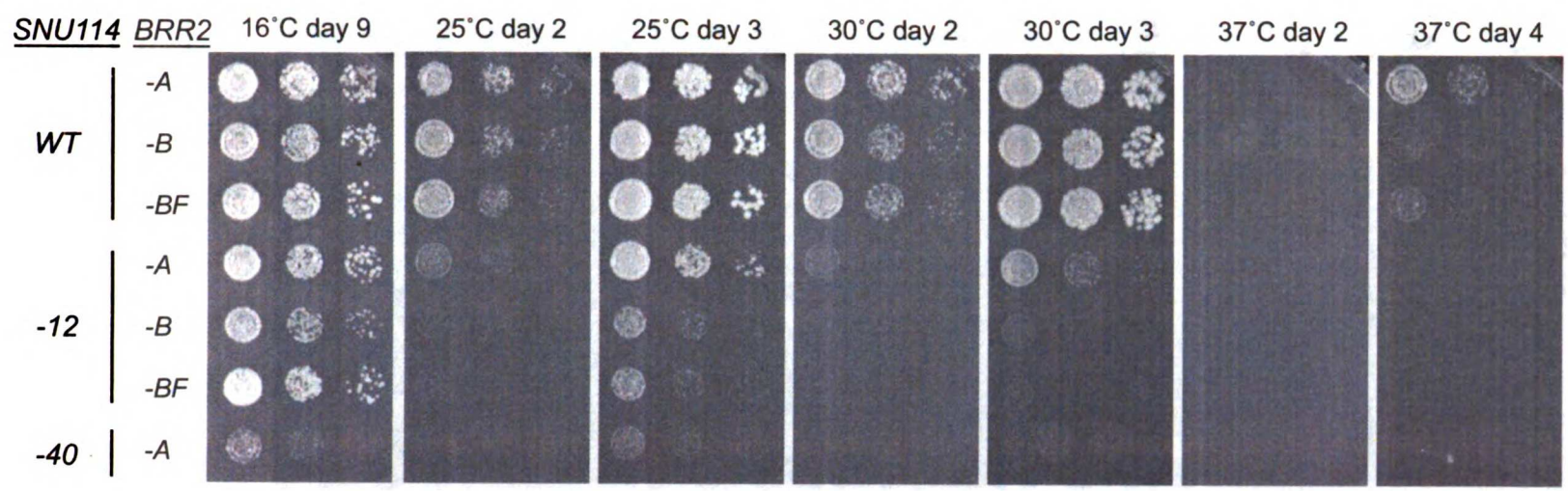
SNU114
BRR2
16˚C day 9
25˚C day 2
25˚C day 3
30˚C day 2
30˚C day 3
37˚C day 2
37˚C day 4
WT
-A
-B
-BF
-12
-A
-B
-BF
-40
-A

E

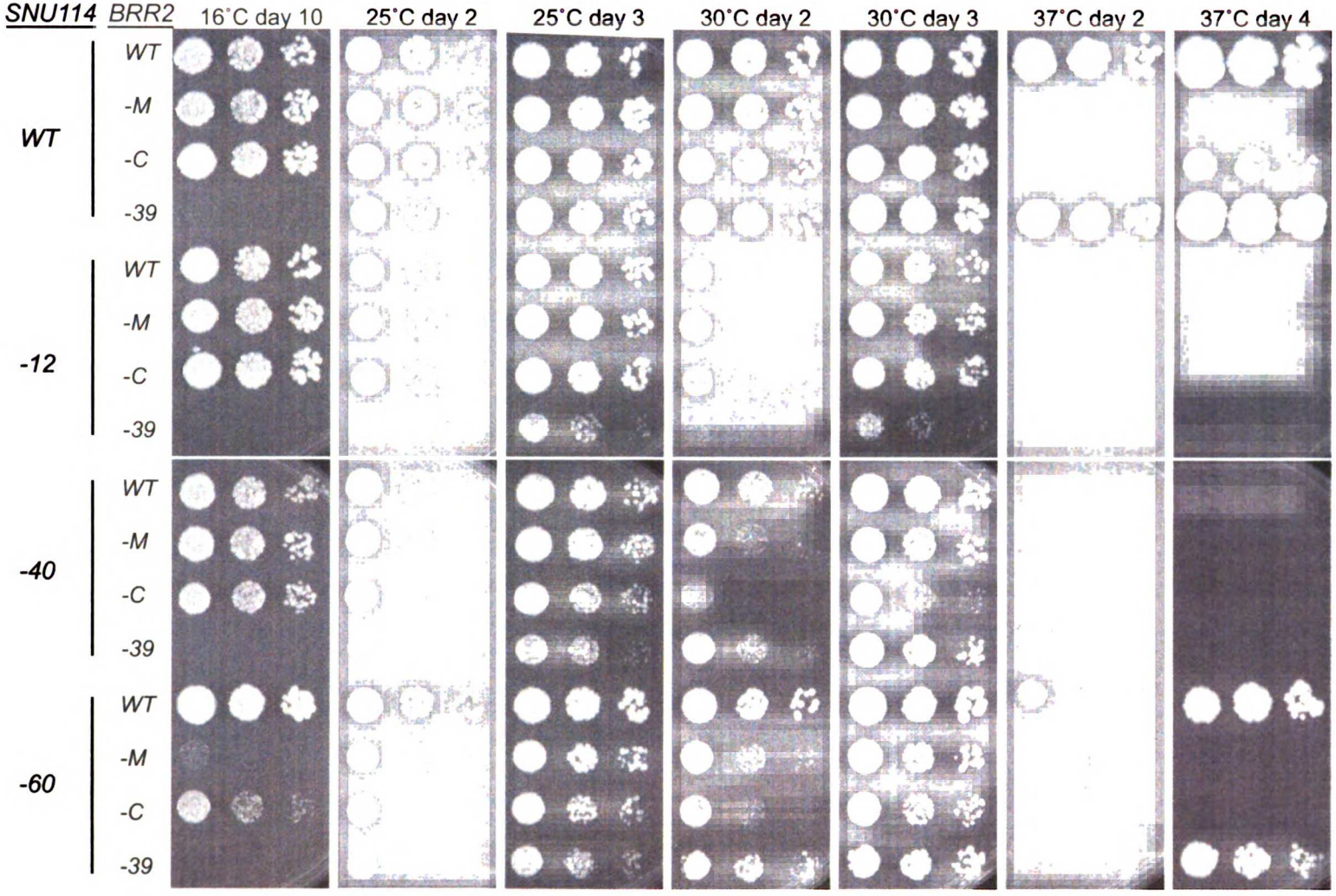
SNU114
BRR2
16°C day 10
25°C day 2
25°C day 3
30°C day 2
30°C day 3
37°C day 2
37°C day 4
WT
-M
-C
-39
WT
-12
-40
-60

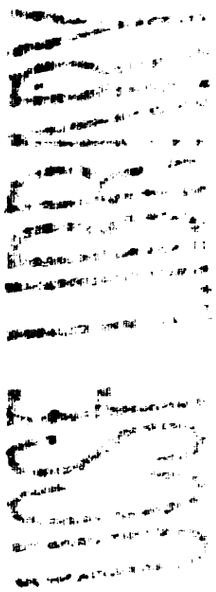

Figure 6. TAP-tagged Prp4 and Prp8 are synthetically sick with *snu114-60*. **A:** *SNU114*, *PRP4-TAP*, *snu114-60*, and *snu114-60 PRP4-TAP* strains were streaked to YPD and grown at 16°C, 25°C, and 37°C. **B:** *SNU114*, *PRP8-TAP*, *snu114-60*, and *snu114-60 PRP8-TAP* strains were streaked to YPD and grown at 16°C, 25°C, and 37°C. **C:** The effects of Aar2-TAP and Brr2-TAP on *snu114-60* on YPD at 16°C, 30°C, and 37°C.

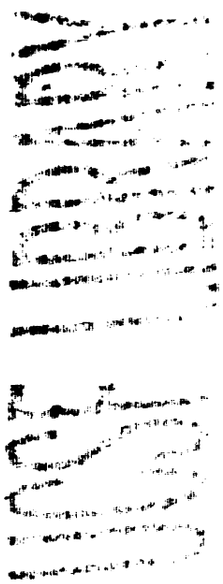

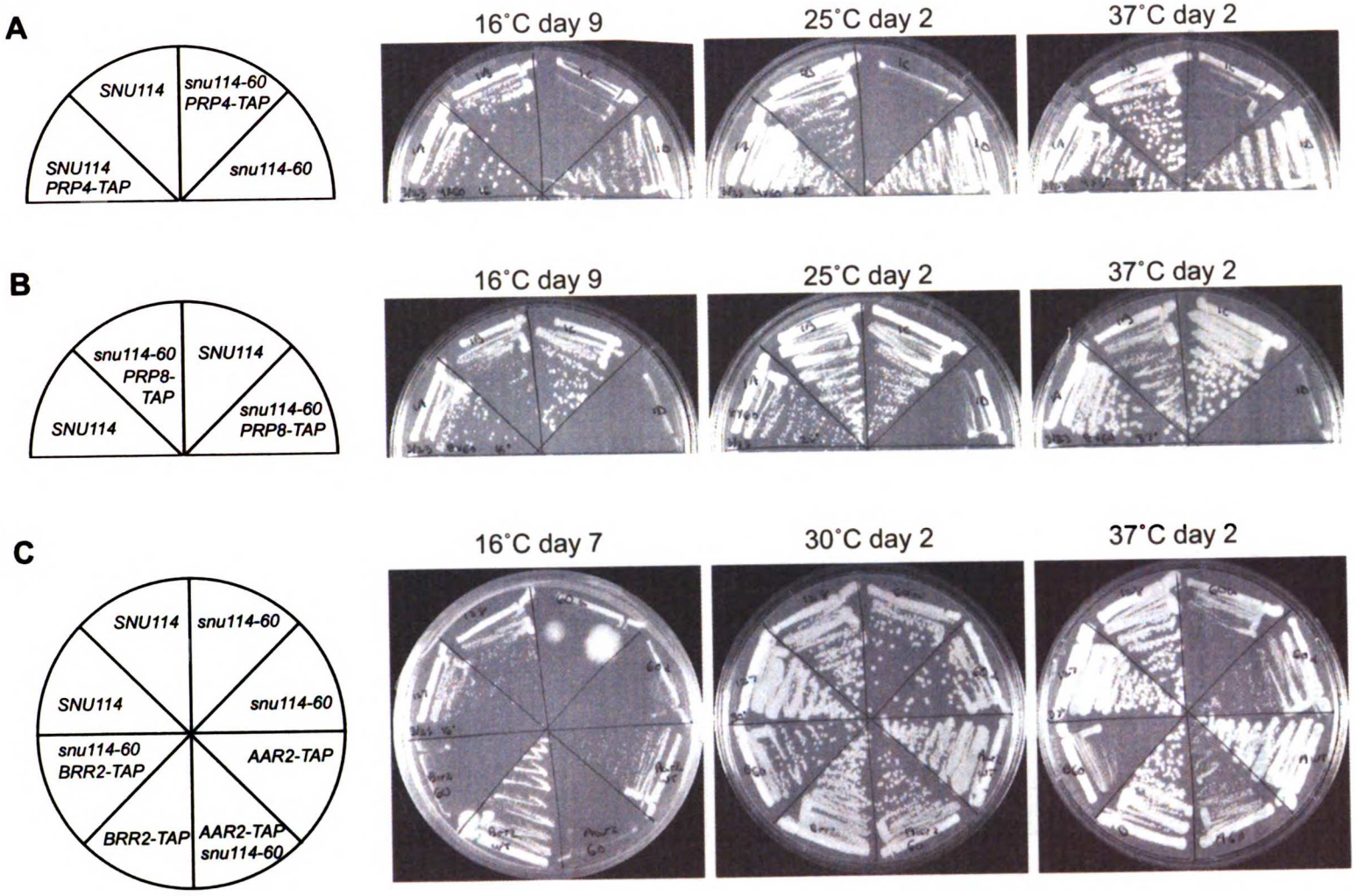
A
SNU114
snu114-60
PRP4-TAP
SNU114
PRP4-TAP
snu114-60
16°C day 9
25°C day 2
37°C day 2
B
snu114-60
PRP8-
TAP
SNU114
SNU114
snu114-60
PRP8-TAP
16°C day 9
25°C day 2
37°C day 2
C
SNU114
snu114-60
SNU114
snu114-60
snu114-60
BRR2-TAP
AAR2-TAP
BRR2-TAP
AAR2-TAP
snu114-60
16°C day 7
30°C day 2
37°C day 2

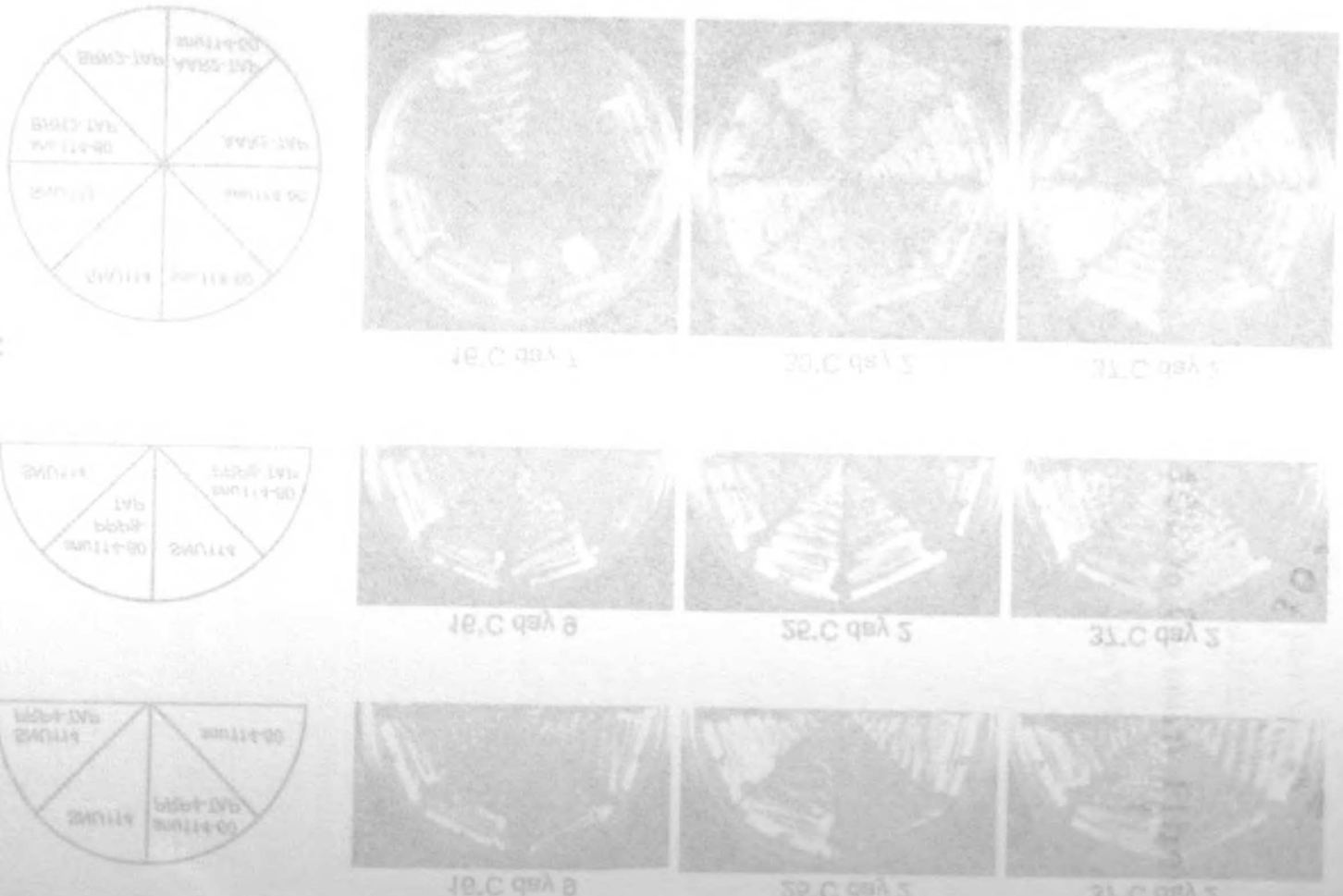

Figure 7. Overexpression of Prp8 does not suppress the growth defects of *snu114* alleles. Strains with integrated *snu114* alleles were transformed with either a *HIS3* plasmid or a *HIS3* plasmid with Prp8 under control of the *GAL* promoter. Transformants were grown on selective media containing either glucose to suppress the *GAL* promoter (top) or galactose to induce Prp8 expression (bottom).

Glucose, -His
Galactose, -His
16˚C day 15
25˚C day 3
30˚C day 3
37˚C day 3
Gal
SNU114 PRP8
SNU114 vector
snu114-12 PRP8
snu114-12 vector
snu114-40 PRP8
snu114-40 vector
snu114-60 PRP8
snu114-60 vector
SNU114 PRP8
SNU114 vector
snu114-12 PRP8
snu114-12 vector
snu114-40 PRP8
snu114-40 vector
snu114-60 PRP8
snu114-60 vector

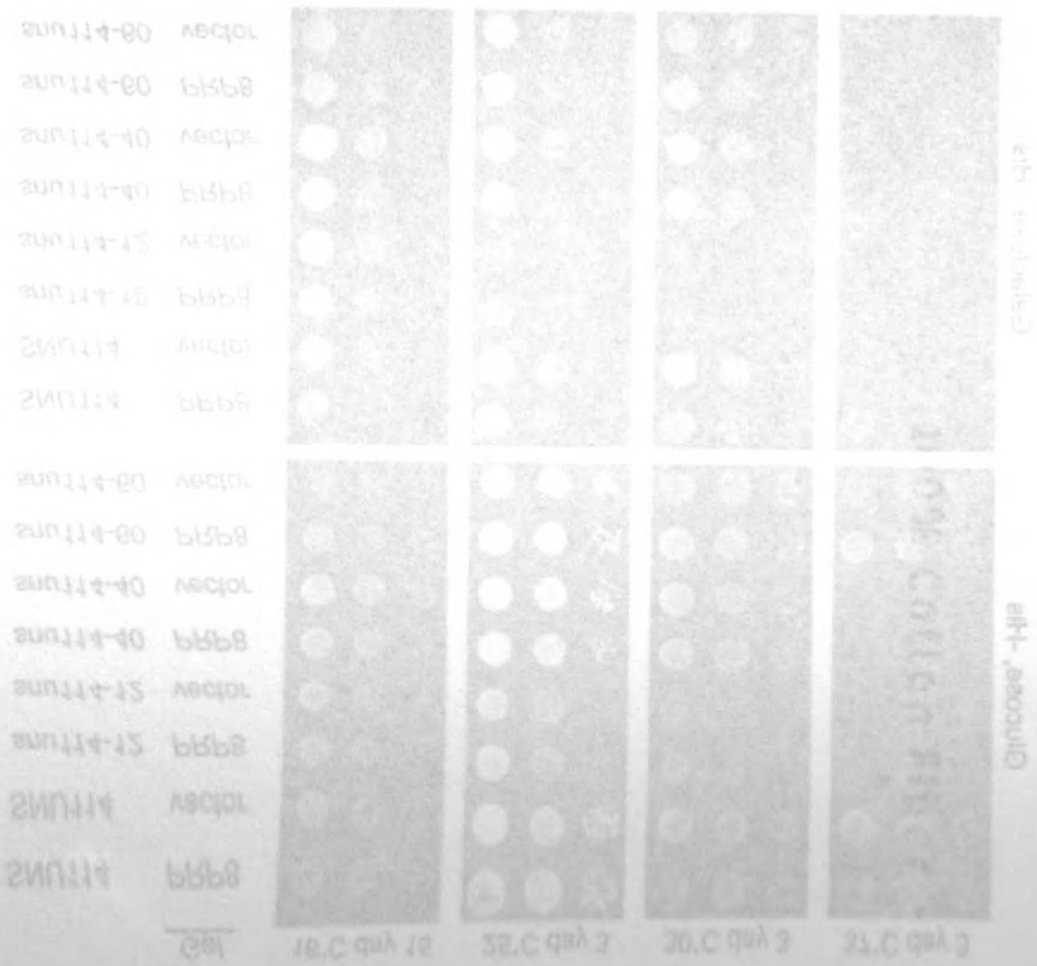

APPENDIX III

Characterization of U5 snRNP in *snu114-60*

APPENDIX III

Characterization of U5 snRNP in *snu114-60*

In Chapter 2, I analyzed the snRNP profiles of *snu114* alleles in order to determine whether defects in splicing could be attributable to defects in snRNP formation. By native gel analysis (Raghunathan and Guthrie 1998a), *SNU114* and *snu114-60* exhibited different snRNP profiles (Figure 1A). As seen in Northern blots, the majority of U5 snRNA in *SNU114* extract was found within tri-snRNP (Figure 1A, lanes 9 and 10). In contrast, *snu114-60* extract contained a larger abundance of free U5 snRNP, and the abundance of this species increased when the extract was incubated with ATP (Figure 1A, lanes 11 and 12). This U5 snRNP migrated much slower than the free U5 snRNP found in *SNU114* extract. Although the U4/U6 di-snRNP migrated at a similar position to the U5 snRNP and also increased in abundance upon ATP incubation, closer inspection shows that di-snRNP migrated slightly faster than the U5 snRNP in *snu114-60* (Figure 1A, compare lanes 4, 8, and 12).

In order to disrupt weaker protein-RNA interactions, extracts were treated with heparin prior to electrophoresis. A strong effect of heparin was that snRNP complexes were no longer retained in the wells of the gel. In the presence of heparin, addition of ATP caused tri-snRNP dissociation and an increase in U4/U6 snRNP levels in both *SNU114* and *snu114-60* extracts (Figure 1B, lanes 1-8). A fast-migrating free U5 snRNP was abundant in both extracts following heparin treatment (Figure 1B, lanes 9-12). This suggests that the slow mobility of U5 snRNP in snu114-60 extract, shown in Figure 1A, was caused by extra protein components that dissociated in the presence of heparin.

Glycerol gradients also indicated that free U5 snRNP was smaller in *SNU114* than *snu114-60* extract (Figure 2A). Unlike the native gels, addition of ATP to the extracts did not affect snRNP profiles in the glycerol gradients. The amount of U5 snRNA in each fraction was quantitated by phosphorimager analysis (Figure 2B). In *SNU114* extract, U5 snRNP peaked in fractions 13-15 and tri-snRNP peaked in fractions 21-25. In *snu114-60* extract, U5 snRNA within tri-snRNP was also found in fractions 21-25. However, the peak of free U5 snRNA was shifted to fraction 15, and the abundance of free U5 snRNP was much lower than in the corresponding wildtype fractions.

It remains a formal possibility that my *SNU114* extracts behaved aberrantly. Raghunathan and Guthrie (1998a) found that U5 snRNP from wildtype extracts migrated in a large smear just below tri-snRNP, which is much slower than my wildtype U5 snRNP. Nonetheless, my *SNU114* and *snu114-60* strains were isogenic, both carrying a chromosomal deletion of *SNU114* and a plasmid with the gene, and I repeatedly observed differences between multiple extract preparations from each strain.

It certainly can be argued that the very concept of individual snRNPs arises from artificial *in vitro* conditions that are more stringent than what is encountered within the cell (Stevens et al. 2001; Stevens et al. 2002). Nonetheless, analysis of individual snRNPs provides information about interactions that likely occur within a larger particle. That the abundance of the large U5 snRNP in *snu114-60* increases upon ATP addition suggests that particle dissociates from a larger complex. The aberrant mobility of U5 snRNP in *snu114-60* may indicate a difference in the composition of the particle, which could in turn lead to the defects that I observed during spliceosome activation. Another possibility is that the large U5 snRNP represents a post-catalytic complex. In HeLa

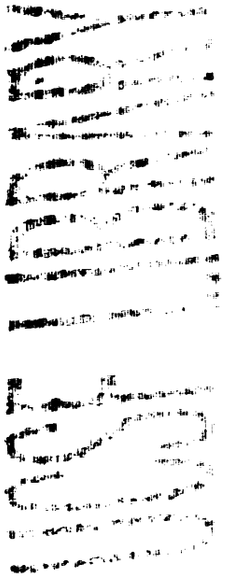

extract, U5 snRNP has been found in a complex with the NTC (Prp NineTeen Complex) following splicing (Makarov et al. 2002). Although a similar complex has not yet been observed in yeast, most of the mechanisms of splicing have been conserved between the two species. The large U5 snRNP in *snu114-60* could represent the NTC bound to U5 snRNP.

To test whether the NTC is bound to an increased amount of U5 snRNA in *snu114-60*, I immunoprecipitated the NTC component Ntc85 from *SNU114* and mutant extracts (Tsai et al. 1999). The first time I performed this experiment (in duplicate), Ntc85 was bound to two-fold more U2, U5, and U6 in *snu114-60* extract compared with wildtype (data not shown). This would suggest that *snu114-60* causes the NTC to be stalled either on a catalytic or post-catalytic spliceosome. I repeated the experiment, this time also shifting cultures to 16°C and 37°C, with the idea that stalled complexes might accumulate at the non-permissive temperatures. This time, both Ntc85 and Isy1 (Dix et al. 1999; Chen et al. 2001) co-precipitated similar amounts of all snRNAs from snu114-60 and SNU114 extracts, and from all temperatures tested (data not shown). Thus, the results are inconclusive but worth repeating.

In order to determine the composition of U5 snRNP in *snu114-60*, one could attempt to purify the snRNP. Following Stevens' (2001) strategy of separating U5 from tri-snRNP by glycerol gradient would be difficult, since there is minimal separation between the complexes in the mutant extract. Another strategy would be to create a strain in which a core-component of U5 snRNP, such as Brr2, is TAP-tagged and a component of U4/U6, such as Prp4, is Protein A tagged. U5-, di-, and tri-snRNPs could be purified on IgG resin; cleavage with TEV would cause release specifically of U5

[redacted]

snRNP. However, *snu114-60* is synthetically sick with many tagged proteins, including TAP-tagged Brr2, Prp8, and Prp4. Another method would be to purify U5 snRNP through a tag within U5 snRNA (O'Keefe et al. 1996).

Since *snu114-60* is cold-sensitive for growth, but displays minimal *in vitro* splicing defects in the cold, it seems likely that this mutation affects processes that occur within the cell but are not assayed during *in vitro* splicing. Attractive candidate processes are snRNP biogenesis or recycling of spliceosomes between rounds of splicing. It would be interesting to make splicing extract from cells grown at 16°C and analyze the snRNPs by native gel to determine whether the aberrant U5 snRNP, or any other aberrant complexes, increases in abundance. Performing *in vitro* recycling assays with *snu114-60*—potentially at 16° in addition to permissive temperature—would also be worthwhile.

CONCLUSION

By native gel analysis and glycerol gradient centrifugation, the characteristics of U5 snRNP in *snu114-60* are different from *SNU114* extract. Most notably, the snRNP appears to be larger, causing slower mobility during electrophoresis and faster mobility during centrifugation. It will be interesting to determine the cause of the differences in snRNP composition, since this may contribute to the slow-growth phenotype of *snu114-60* and the many genetic interactions with mutations in other tri-snRNP proteins.

MATERIALS AND METHODS

Native gels. Native gels were run and analyzed as described (Raghunathan and Guthrie 1998a). Extracts were incubated with or without ATP in splicing buffer in a volume of 10μL for 30 minutes at 25°C. Samples were split in half, and 1 μL heparin mix (2.5 mM

$MgCl_2$, 60 mM KP pH 7.0, 3% PEG, 8% glycerol, and 4 mg/ml heparin) was added to 5 μL aliquots of extract.

Glycerol Gradients. 75 μL *SNU114* or *snu114-60* extract were incubated with 2 mM ATP, 2.5 mM MgCl2, and 60 mM KP pH 7.0 and then layered on top of 10-30% glycerol gradients containing 20 mM Hepes 7.9, 200 mM KCl, 1.5 mM $MgCl_2$, 0.2 mM EDTA, 0.5 mM DTT, and protease inhibitors. Gradients were spun at 29K rpm for 18 hours at 4°C in a Sw 40 Ti rotor. Twenty-nine 400 μL fractions were collected. RNA was phenol extracted from the even-numbered fractions and ethanol precipitated. RNA was electrophoresed on 6% denaturing polyacrylamide gels and transferred to N-Hybond. Blots were probed with kinased oligos.

snRNA co-IPs. The co-immunoprecipitations of snRNAs with Ntc85 and Isy1 were performed as described in Chapter 2. Ntc85 and Isy1 antisera were gifts from S.-C. Cheng.

Figure 1. *snu114-60* exhibits an aberrant U5 snRNP profile. **A:** *SNU114* and *snu114-60* extracts were incubated under splicing conditions, with or without ATP. snRNPs were resolved by native gel electrophoresis and transferred to N-Hybond. Northern blots were probed for U4 (right), U6 (middle), and U5 (right). The asterisk indicates the U5-snRNP species found in *snu114-60.* **B:** Native gel analysis was performed as in A, except that extracts were incubated with heparin prior to loading on the gel. U4/U6•U5 tri-snRNP and U4/U6 di-snRNP are labeled; free snRNPs are indicated by black bars to the left of each panel. The species identified as the tetra-snRNP of U4/U6•U5•U2 in B exhibited the same mobility when the blots were sequentially probed with U2, U4, U5, and U6 snRNAs.

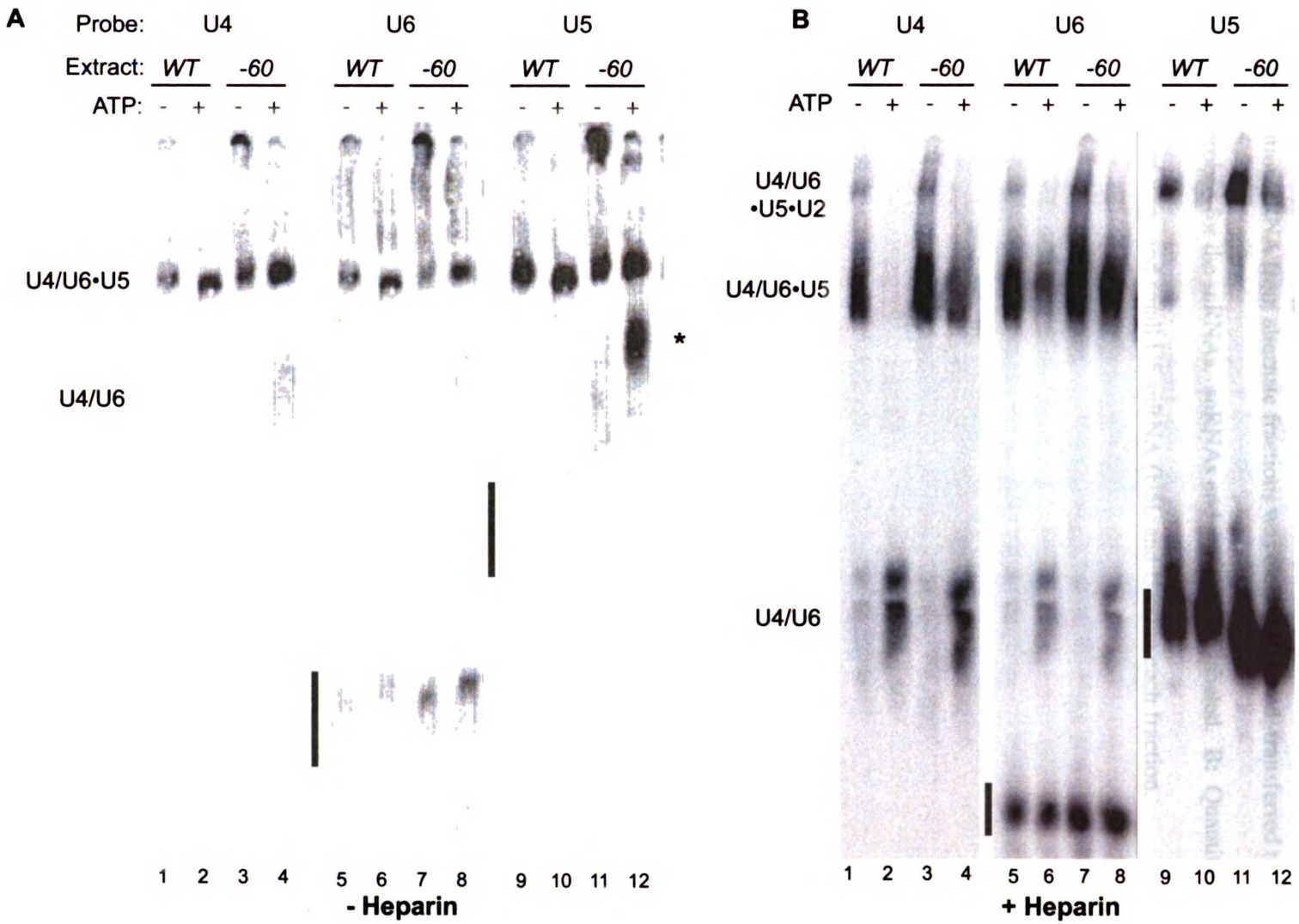
A
Probe: U4 U6 U5
Extract: WT -60 WT -60 WT -60
ATP: - + - + - + - + - + - +
U4/U6•U5
U4/U6
*
1 2 3 4 5 6 7 8 9 10 11 12
- Heparin
B
U4 U6 U5
WT -60 WT -60 WT -60
ATP - + - + - + - + - + - +
U4/U6 •U5•U2
U4/U6•U5
U4/U6
1 2 3 4 5 6 7 8 9 10 11 12
+ Heparin

Figure 2. Glycerol gradients show that U5 snRNP differs between *SNU114* and *snu114-60*. **A:** Extracts were layered on 10-30% glycerol gradients and separated by ultracentrifugation. RNA from alternate fractions was electrophoresed, transferred to Hybond, and probed for the snRNAs. snRNAs and snRNPs are labeled. **B:** Quantitation of the intensity of large and small U5 snRNA (U5L and U5S) in each fraction.

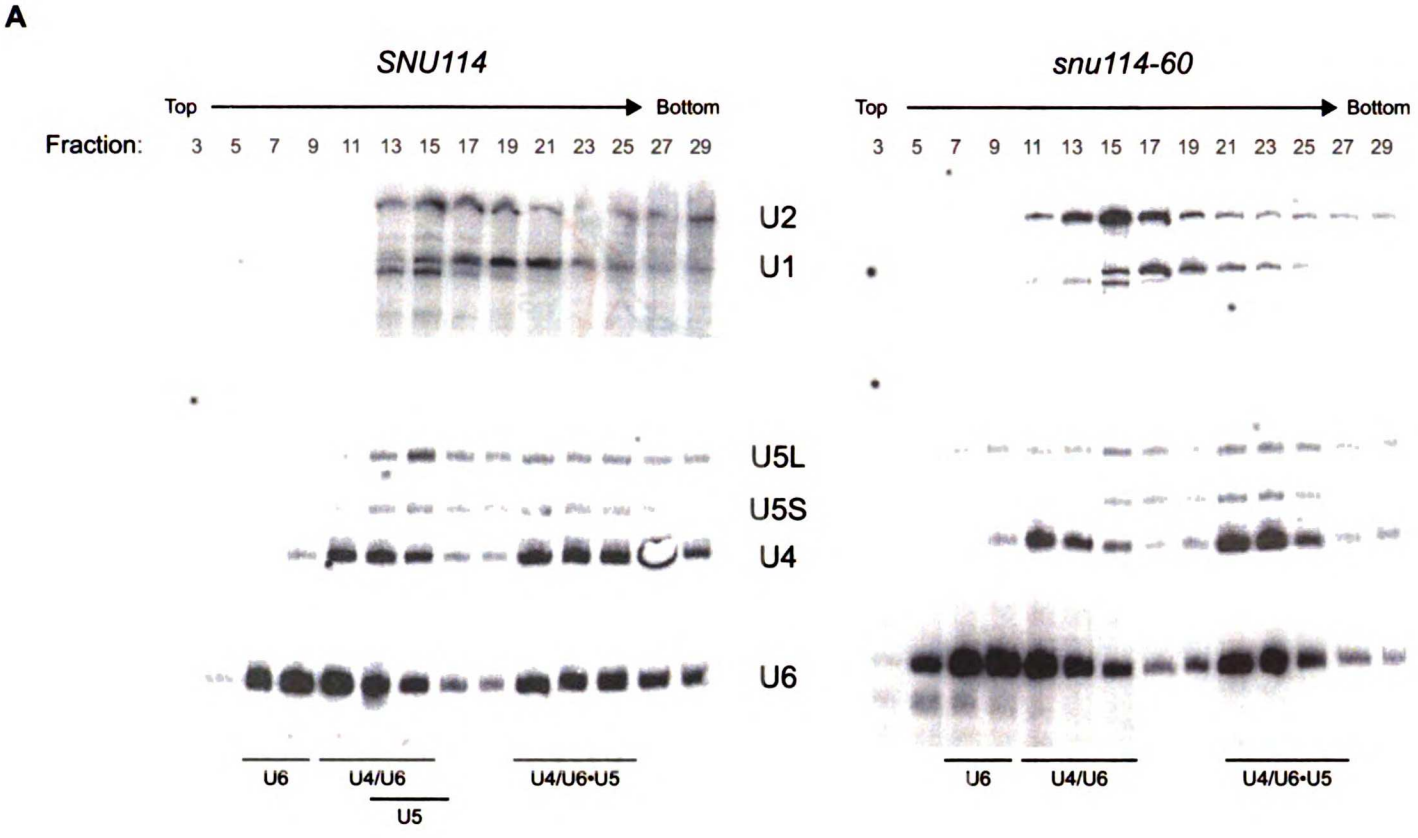
A
SNU114
snu114-60
Top
Bottom
Fraction:
3 5 7 9 11 13 15 17 19 21 23 25 27 29
U2
U1
U5L
U5S
U4
U6
U6
U4/U6
U5
U4/U6•U5

B

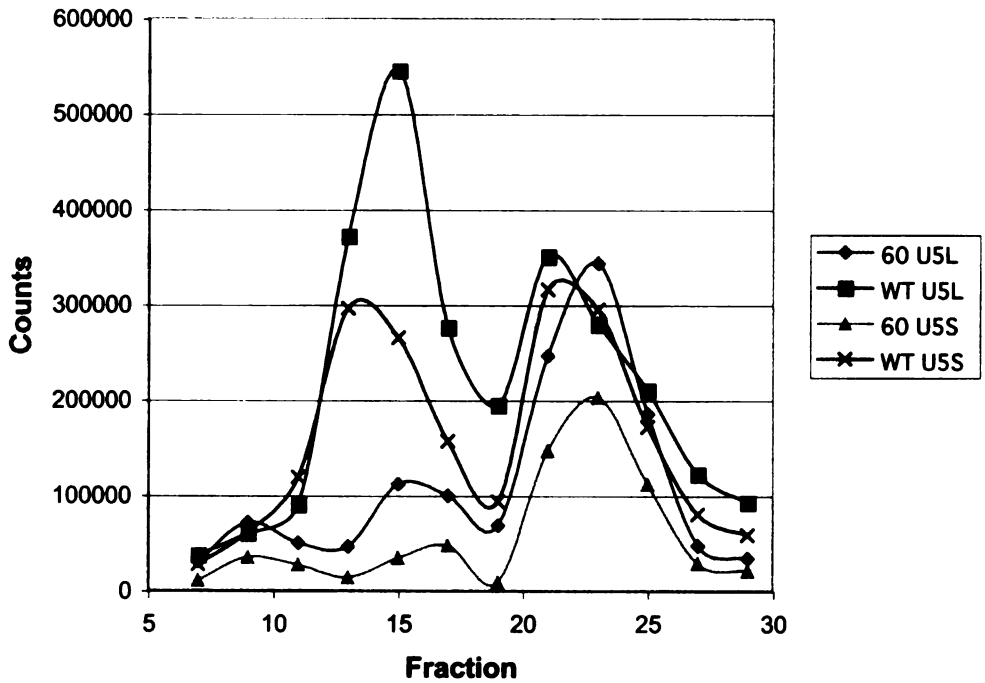
600000
500000
400000
300000
200000
100000
0
Counts
5
10
15
20
25
30
Fraction
60 U5L
WT U5L
60 U5S
WT U5S

REFERENCES

REFERENCES

Achsel, T., Ahrens, K., Brahms, H., Teigelkamp, S., and Luhrmann, R. 1998. The human U5-220kD protein (hPrp8) forms a stable RNA-free complex with several U5-specific proteins, including an RNA unwindase, a homologue of ribosomal elongation factor EF-2, and a novel WD-40 protein. *Mol Cell Biol* **18**(11): 6756-6766.

AEvarsson, A., Brazhnikov, E., Garber, M., Zheltonosova, J., Chirgadze, Y., al-Karadaghi, S., Svensson, L.A., and Liljas, A. 1994. Three-dimensional structure of the ribosomal translocase: elongation factor G from Thermus thermophilus. *Embo J* **13**(16): 3669-3677.

Agrawal, R.K., Penczek, P., Grassucci, R.A., and Frank, J. 1998. Visualization of elongation factor G on the Escherichia coli 70S ribosome: the mechanism of translocation. *Proc Natl Acad Sci U S A* **95**(11): 6134-6138.

Algire, M.A., Maag, D., and Lorsch, J.R. 2005. Pi release from eIF2, not GTP hydrolysis, is the step controlled by start-site selection during eukaryotic translation initiation. *Mol Cell* **20**(2): 251-262.

Andersen, G.R., Nissen, P., and Nyborg, J. 2003. Elongation factors in protein biosynthesis. *Trends Biochem Sci* **28**(8): 434-441.

Arenas, J.E. and Abelson, J.N. 1997. Prp43: An RNA helicase-like factor involved in spliceosome disassembly. *Proc Natl Acad Sci U S A* **94**(22): 11798-11802.

Ares, M., Jr., Grate, L., and Pauling, M.H. 1999. A handful of intron-containing genes produces the lion's share of yeast mRNA. *Rna* **5**(9): 1138-1139.

Ayadi, L., Miller, M., and Banroques, J. 1997. Mutations within the yeast U4/U6 snRNP protein Prp4 affect a late stage of spliceosome assembly. *Rna* **3**(2): 197-209.

Baca, O.G., Rohrbach, M.S., and Bodley, J.W. 1976. Equilibrium measurements of the interactions of guanine nucleotides with Escherichia coli elongation factor G and the ribosome. *Biochemistry* **15**(21): 4570-4574.

Bartels, C., Klatt, C., Luhrmann, R., and Fabrizio, P. 2002. The ribosomal translocase homologue Snu114p is involved in unwinding U4/U6 RNA during activation of the spliceosome. *EMBO Rep* **3**(9): 875-880.

Bartels, C., Urlaub, H., Luhrmann, R., and Fabrizio, P. 2003. Mutagenesis suggests several roles of Snu114p in pre-mRNA splicing. *J Biol Chem* **278**(30): 28324-28334.

Becam, A.M., Nasr, F., Racki, W.J., Zagulski, M., and Herbert, C.J. 2001. Ria1p (Ynl163c), a protein similar to elongation factors 2, is involved in the biogenesis of the 60S subunit of the ribosome in Saccharomyces cerevisiae. *Mol Genet Genomics* **266**(3): 454-462.

Bellare, P., Kutach, A.K., Rines, A.K., Guthrie, C., and Sontheimer, E.J. 2005. Ubiquitin binding by a variant Jab1/MPN domain in the essential pre-mRNA splicing factor Prp8. *RNA* **In press**.

Berchtold, H., Reshetnikova, L., Reiser, C.O., Schirmer, N.K., Sprinzl, M., and Hilgenfeld, R. 1993. Crystal structure of active elongation factor Tu reveals major domain rearrangements. *Nature* **365**(6442): 126-132.

Boehringer, D., Makarov, E.M., Sander, B., Makarova, O.V., Kastner, B., Luhrmann, R., and Stark, H. 2004. Three-dimensional structure of a pre-catalytic human spliceosomal complex B. *Nat Struct Mol Biol* **11**(5): 463-468.

Bourne, H.R. 1995. GTPases: a family of molecular switches and clocks. *Philos Trans R Soc Lond B Biol Sci* **349**(1329): 283-289.

Bourne, H.R., Sanders, D.A., and McCormick, F. 1990. The GTPase superfamily: a conserved switch for diverse cell functions. *Nature* **348**(6297): 125-132.

-. 1991. The GTPase superfamily: conserved structure and molecular mechanism. *Nature* **349**(6305): 117-127.

Brodersen, D.E. and Ramakrishnan, V. 2003. Shape can be seductive. *Nat Struct Biol* **10**(2): 78-80.

Brow, D.A. 2002. Allosteric cascade of spliceosome activation. *Annu Rev Genet* **36**: 333-360.

Burge, C.B., Tuschl, T.H., and Sharp, P.A. 1998. Splicing of precursors to mRNAs by the spliceosomes. in *RNA World II* (ed. R.F. Gesteland, T.R. Cech, and J.F. Atkins), pp. 525-560. Cold Spring Harbor Laboratory Press, Cold Spring Harbor, NY.

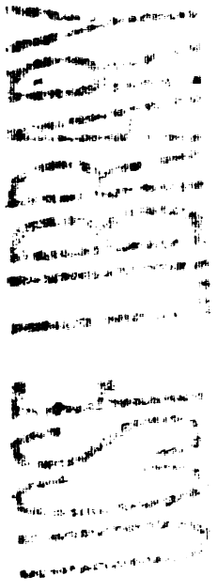

Caldon, C.E., Yoong, P., and March, P.E. 2001. Evolution of a molecular switch: universal bacterial GTPases regulate ribosome function. *Mol Microbiol* **41**(2): 289-297.

Chen, C.H., Tsai, W.Y., Chen, H.R., Wang, C.H., and Cheng, S.C. 2001. Identification and characterization of two novel components of the Prp19p-associated complex, Ntc30p and Ntc20p. *J Biol Chem* **276**(1): 488-494.

Chiara, M.D., Palandjian, L., Feld Kramer, R., and Reed, R. 1997. Evidence that U5 snRNP recognizes the 3' splice site for catalytic step II in mammals. *Embo J* **16**(15): 4746-4759.

Collins, C.A. and Guthrie, C. 2000. The question remains: is the spliceosome a ribozyme? *Nat Struct Biol* **7**(10): 850-854.

Cortes, J.J., Sontheimer, E.J., Seiwert, S.D., and Steitz, J.A. 1993. Mutations in the conserved loop of human U5 snRNA generate use of novel cryptic 5' splice sites in vivo. *Embo J* **12**(13): 5181-5189.

Czworkowski, J., Wang, J., Steitz, T.A., and Moore, P.B. 1994. The crystal structure of elongation factor G complexed with GDP, at 2.7 A resolution. *Embo J* **13**(16): 3661-3668.

Dix, I., Russell, C., Yehuda, S.B., Kupiec, M., and Beggs, J.D. 1999. The identification and characterization of a novel splicing protein, Isy1p, of Saccharomyces cerevisiae. *Rna* **5**(3): 360-368.

Dix, I., Russell, C.S., O'Keefe, R.T., Newman, A.J., and Beggs, J.D. 1998. Protein-RNA interactions in the U5 snRNP of *Saccharomyces cerevisiae*. *RNA* **4**(10): 1239-1250.

Fabrizio, P., Laggerbauer, B., Lauber, J., Lane, W.S., and Luhrmann, R. 1997. An evolutionarily conserved U5 snRNP-specific protein is a GTP-binding factor closely related to the ribosomal translocase EF-2. *Embo J* **16**(13): 4092-4106.

Field, D.J. and Friesen, J.D. 1996. Functionally redundant interactions between U2 and U6 spliceosomal snRNAs. *Genes Dev* **10**(4): 489-501.

Ghaemmaghami, S., Huh, W.K., Bower, K., Howson, R.W., Belle, A., Dephoure, N., O'Shea, E.K., and Weissman, J.S. 2003. Global analysis of protein expression in yeast. *Nature* **425**(6959): 737-741.

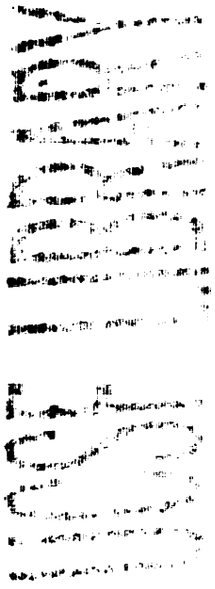

Gottschalk, A., Kastner, B., Luhrmann, R., and Fabrizio, P. 2001. The yeast U5 snRNP coisolated with the U1 snRNP has an unexpected protein composition and includes the splicing factor Aar2p. *Rna* **7**(11): 1554-1565.

Gottschalk, A., Neubauer, G., Banroques, J., Mann, M., Luhrmann, R., and Fabrizio, P. 1999. Identification by mass spectrometry and functional analysis of novel proteins of the yeast [U4/U6.U5] tri-snRNP. *Embo J* **18**(16): 4535-4548.

Grainger, R.J. and Beggs, J.D. 2005. Prp8 protein: at the heart of the spliceosome. *Rna* **11**(5): 533-557.

Gromadski, K.B. and Rodnina, M.V. 2004. Kinetic determinants of high-fidelity tRNA discrimination on the ribosome. *Mol Cell* **13**(2): 191-200.

Inada, M. 2004. Genetic, biochemical and genomic analyses of RNP biogenesis in *S. cerevisiae*. In *Department of Biochemistry and Biophysics*, pp. 124. University of California, San Francisco, San Francisco.

Jorgensen, R., Ortiz, P.A., Carr-Schmid, A., Nissen, P., Kinzy, T.G., and Andersen, G.R. 2003. Two crystal structures demonstrate large conformational changes in the eukaryotic ribosomal translocase. *Nat Struct Biol* **10**(5): 379-385.

Jurica, M.S. and Moore, M.J. 2003. Pre-mRNA splicing: awash in a sea of proteins. *Mol Cell* **12**(1): 5-14.

Jurica, M.S., Sousa, D., Moore, M.J., and Grigorieff, N. 2004. Three-dimensional structure of C complex spliceosomes by electron microscopy. *Nat Struct Mol Biol* **11**(3): 265-269.

Kapp, L.D. and Lorsch, J.R. 2004. The molecular mechanics of eukaryotic translation. *Annu Rev Biochem* **73**: 657-704.

Kaziro, Y. 1978. The role of guanosine 5'-triphosphate in polypeptide chain elongation. *Biochim Biophys Acta* **505**(1): 95-127.

Kim, S.H., Smith, J., Claude, A., and Lin, R.J. 1992. The purified yeast pre-mRNA splicing factor PRP2 is an RNA-dependent NTPase. *Embo J* **11**(6): 2319-2326.

Kjeldgaard, M., Nissen, P., Thirup, S., and Nyborg, J. 1993. The crystal structure of elongation factor EF-Tu from Thermus aquaticus in the GTP conformation. *Structure* **1**(1): 35-50.

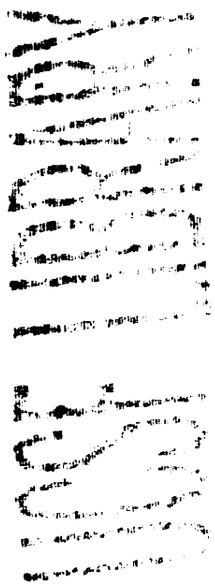

Klaholz, B.P., Pape, T., Zavialov, A.V., Myasnikov, A.G., Orlova, E.V., Vestergaard, B., Ehrenberg, M., and van Heel, M. 2003. Structure of the Escherichia coli ribosomal termination complex with release factor 2. *Nature* **421**(6918): 90-94.

Kuhn, A.N. and Brow, D.A. 2000. Suppressors of a cold-sensitive mutation in yeast U4 RNA define five domains in the splicing factor Prp8 that influence spliceosome activation. *Genetics* **155**(4): 1667-1682.

Kuhn, A.N., Li, Z., and Brow, D.A. 1999. Splicing factor Prp8 governs U4/U6 RNA unwinding during activation of the spliceosome. *Mol Cell* **3**(1): 65-75.

Kuhn, A.N., Reichl, E.M., and Brow, D.A. 2002. Distinct domains of splicing factor Prp8 mediate different aspects of spliceosome activation. *Proc Natl Acad Sci U S A* **99**(14): 9145-9149.

Laggerbauer, B., Achsel, T., and Luhrmann, R. 1998. The human U5-200kD DEXH-box protein unwinds U4/U6 RNA duplices in vitro. *Proc Natl Acad Sci U S A* **95**(8): 4188-4192.

Lancaster, L., Kiel, M.C., Kaji, A., and Noller, H.F. 2002. Orienation of Ribosome Recycling Factor in the ribosome from directed hydroxyl radical probing. *Cell* **111**: 129-140.

Li, Z. and Brow, D.A. 1996. A spontaneous duplication in U6 spliceosomal RNA uncouples the early and late functions of the ACAGA element in vivo. *Rna* **2**(9): 879-894.

Lin, R.J., Newman, A.J., Cheng, S.C., and Abelson, J. 1985. Yeast mRNA splicing in vitro. *J Biol Chem* **260**(27): 14780-14792.

Liu, Z.R., Laggerbauer, B., Luhrmann, R., and Smith, C.W. 1997. Crosslinking of the U5 snRNP-specific 116-kDa protein to RNA hairpins that block step 2 of splicing. *Rna* **3**(11): 1207-1219.

Lygerou, Z., Christophides, G., and Seraphin, B. 1999. A novel genetic screen for snRNP assembly factors in yeast identifies a conserved protein, Sad1p, also required for pre-mRNA splicing. *Mol Cell Biol* **19**(3): 2008-2020.

Madhani, H.D. and Guthrie, C. 1992. A novel base-pairing interaction between U2 and U6 snRNAs suggests a mechanism for the catalytic activation of the spliceosome. *Cell* **71**(5): 803-817.

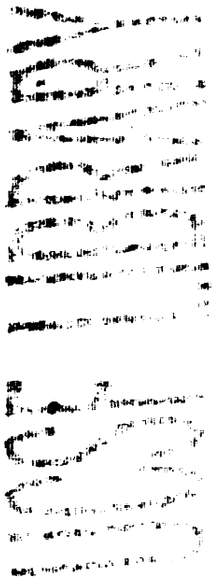

Makarov, E.M., Makarova, O.V., Urlaub, H., Gentzel, M., Will, C.L., Wilm, M., and Luhrmann, R. 2002. Small nuclear ribonucleoprotein remodeling during catalytic activation of the spliceosome. *Science* **298**(5601): 2205-2208.

Makarova, O.V., Makarov, E.M., and Luhrmann, R. 2001. The 65 and 110 kDa SR-related proteins of the U4/U6.U5 tri-snRNP are essential for the assembly of mature spliceosomes. *Embo J* **20**(10): 2553-2563.

Martin, A., Schneider, S., and Schwer, B. 2002. Prp43 is an essential RNA-dependent ATPase required for release of lariat-intron from the spliceosome. *J Biol Chem* **277**(20): 17743-17750.

Maytal-Kivity, V., Reis, N., Hofmann, K., and Glickman, M.H. 2002. MPN+, a putative catalytic motif found in a subset of MPN domain proteins from eukaryotes and prokaryotes, is critical for Rpn11 function. *BMC Biochem* **3**(1): 28.

Mohr, D., Wintermeyer, W., and Rodnina, M.V. 2000. Arginines 29 and 59 of elongation factor G are important for GTP hydrolysis or translocation on the ribosome. *Embo J* **19**(13): 3458-3464.

-. 2002. GTPase activation of elongation factors Tu and G on the ribosome. *Biochemistry* **41**(41): 12520-12528.

Moore, M.J., Query, C.C., and Sharp, P.A. 1993. Splicing of precursors to mRNA by the spliceosome. in *The RNA World* (ed. R.F. Gesteland and J.F. Atkins), pp. 303-357. Cold Spring Harbor Laboratory Press, Cold Spring Harbor, NY.

Nakamura, Y. 2001. Molecular mimicry between protein and tRNA. *J Mol Evol* **53**(4-5): 282-289.

Newman, A.J. 1997. The role of U5 snRNP in pre-mRNA splicing. *Embo J* **16**(19): 5797-5800.

Newman, A.J. and Norman, C. 1992. U5 snRNA interacts with exon sequences at 5' and 3' splice sites. *Cell* **68**(4): 743-754.

Newman, A.J., Teigelkamp, S., and Beggs, J.D. 1995. snRNA interactions at 5' and 3' splice sites monitored by photoactivated crosslinking in yeast spliceosomes. *Rna* **1**(9): 968-980.

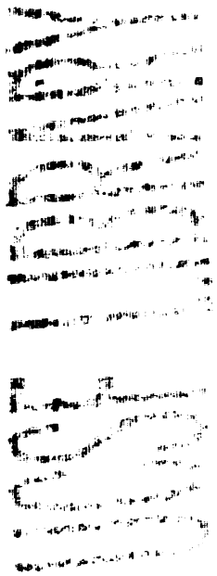

Nilsen, T.W. 1998. RNA-RNA interactions in nuclear pre-mRNA splicing. in *RNA Structure and Function* (ed. R. Simons and M. Grunberg-Manago), pp. 279-307. Cold Spring Harbor Laboratory Press, Cold Spring Harbor, NY.

Nissen, P., Kjeldgaard, M., and Nyborg, J. 2000. Macromolecular mimicry. *Embo J* **19**(4): 489-495.

Nissen, P., Kjeldgaard, M., Thirup, S., Polekhina, G., Reshetnikova, L., Clark, B.F., and Nyborg, J. 1995. Crystal structure of the ternary complex of Phe-tRNAPhe, EF-Tu, and a GTP analog. *Science* **270**(5241): 1464-1472.

Noble, S.M. and Guthrie, C. 1996. Transcriptional pulse-chase analysis reveals a role for a novel snRNP-associated protein in the manufacture of spliceosomal snRNPs. *Embo J* **15**(16): 4368-4379.

O'Keefe, R.T., Norman, C., and Newman, A.J. 1996. The invariant U5 snRNA loop 1 sequence is dispensable for the first catalytic step of pre-mRNA splicing in yeast. *Cell* **86**(4): 679-689.

Pape, T., Wintermeyer, W., and Rodnina, M.V. 1998. Complete kinetic mechanism of elongation factor Tu-dependent binding of aminoacyl-tRNA to the A site of the E. coli ribosome. *Embo J* **17**(24): 7490-7497.

Peske, F., Matassova, N.B., Savelsbergh, A., Rodnina, M.V., and Wintermeyer, W. 2000. Conformationally restricted elongation factor G retains GTPase activity but is inactive in translocation on the ribosome. *Mol Cell* **6**(2): 501-505.

Raghunathan, P.L. and Guthrie, C. 1998a. RNA unwinding in U4/U6 snRNPs requires ATP hydrolysis and the DEIH-box splicing factor Brr2. *Curr Biol* **8**(15): 847-855.

-. 1998b. A spliceosomal recycling factor that reanneals U4 and U6 small nuclear ribonucleoprotein particles. *Science* **279**(5352): 857-860.

Rawat, U.B., Zavialov, A.V., Sengupta, J., Valle, M., Grassucci, R.A., Linde, J., Vestergaard, B., Ehrenberg, M., and Frank, J. 2003. A cryo-electron microscopic study of ribosome-bound termination factor RF2. *Nature* **421**(6918): 87-90.

Rocak, S. and Linder, P. 2004. DEAD-box proteins: the driving forces behind RNA metabolism. *Nat Rev Mol Cell Biol* **5**(3): 232-241.

Rodnina, M.V., Gromadski, K.B., Kothe, U., and Wieden, H.J. 2005. Recognition and selection of tRNA in translation. *FEBS Lett* **579**(4): 938-942.s

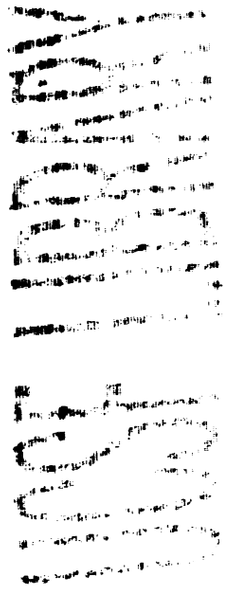

Rodnina, M.V., Savelsbergh, A., Katunin, V.I., and Wintermeyer, W. 1997. Hydrolysis of GTP by elongation factor G drives tRNA movement on the ribosome. *Nature* **385**(6611): 37-41.

Rodnina, M.V., Stark, H., Savelsbergh, A., Wieden, H.J., Mohr, D., Matassova, N.B., Peske, F., Daviter, T., Gualerzi, C.O., and Wintermeyer, W. 2000. GTPases mechanisms and functions of translation factors on the ribosome. *Biol Chem* **381**(5-6): 377-387.

Savelsbergh, A., Katunin, V.I., Mohr, D., Peske, F., Rodnina, M.V., and Wintermeyer, W. 2003. An elongation factor G-induced ribosome rearrangement precedes tRNA-mRNA translocation. *Mol Cell* **11**(6): 1517-1523.

Savelsbergh, A., Matassova, N.B., Rodnina, M.V., and Wintermeyer, W. 2000. Role of domains 4 and 5 in elongation factor G functions on the ribosome. *J Mol Biol* **300**(4): 951-961.

Savelsbergh, A., Mohr, D., Kothe, U., Wintermeyer, W., and Rodnina, M.V. 2005. Control of phosphate release from elongation factor G by ribosomal protein L7/12. *Embo J.*

Scheffzek, K., Ahmadian, M.R., and Wittinghofer, A. 1998. GTPase-activating proteins: helping hands to complement an active site. *Trends Biochem Sci* **23**(7): 257-262.

Schwer, B. and Guthrie, C. 1992. A conformational rearrangement in the spliceosome is dependent on PRP16 and ATP hydrolysis. *Embo J* **11**(13): 5033-5039.

Senger, B., Lafontaine, D.L., Graindorge, J.S., Gadal, O., Camasses, A., Sanni, A., Garnier, J.M., Breitenbach, M., Hurt, E., and Fasiolo, F. 2001. The nucle(ol)ar Tif6p and Efl1p are required for a late cytoplasmic step of ribosome synthesis. *Mol Cell* **8**(6): 1363-1373.

Siliciano, P.G. and Guthrie, C. 1988. 5' splice site selection in yeast: genetic alterations in base-pairing with U1 reveal additional requirements. *Genes Dev* **2**(10): 1258-1267.

Sontheimer, E.J. and Steitz, J.A. 1993. The U5 and U6 small nuclear RNAs as active site components of the spliceosome. *Science* **262**(5142): 1989-1996.

Sprang, S.R. 1997. G protein mechanisms: insights from structural analysis. *Annu Rev Biochem* **66**(639): 639-678.

Sprang, S.R. and Coleman, D.E. 1998. Invasion of the nucleotide snatchers: structural insights into the mechanism of G protein GEFs. *Cell* **95**(2): 155-158.

Sprinzl, M., Brock, S., Huang, Y., Milovnik, P., Nanninga, M., Nesper-Brock, M., Rutthard, H., and Szkaradkiewicz, K. 2000. Regulation of GTPases in the bacterial translation machinery. *Biol Chem* **381**(5-6): 367-375.

Staley, J.P. and Guthrie, C. 1998. Mechanical devices of the spliceosome: motors, clocks, springs, and things. *Cell* **92**(3): 315-326.

-. 1999. An RNA switch at the 5' splice site requires ATP and the DEAD box protein Prp28p. *Mol Cell* **3**(1): 55-64.

Stark, H., Rodnina, M.V., Rinke-Appel, J., Brimacombe, R., Wintermeyer, W., and van Heel, M. 1997. Visualization of elongation factor Tu on the Escherichia coli ribosome. *Nature* **389**(6649): 403-406.

Stark, H., Rodnina, M.V., Wieden, H.J., van Heel, M., and Wintermeyer, W. 2000. Large-scale movement of elongation factor G and extensive conformational change of the ribosome during translocation. *Cell* **100**(3): 301-309.

Stevens, S.W. and Abelson, J. 1999. Purification of the yeast U4/U6.U5 small nuclear ribonucleoprotein particle and identification of its proteins. *Proc Natl Acad Sci U S A* **96**(13): 7226-7231.

Stevens, S.W., Barta, I., Ge, H.Y., Moore, R.E., Young, M.K., Lee, T.D., and Abelson, J. 2001. Biochemical and genetic analyses of the U5, U6, and U4/U6 x U5 small nuclear ribonucleoproteins from Saccharomyces cerevisiae. *Rna* **7**(11): 1543-1553.

Stevens, S.W., Ryan, D.E., Ge, H.Y., Moore, R.E., Young, M.K., Lee, T.D., and Abelson, J. 2002. Composition and functional characterization of the yeast spliceosomal penta-snRNP. *Mol Cell* **9**(1): 31-44.

Takai, Y., Sasaki, T., and Matozaki, T. 2001. Small GTP-binding proteins. *Physiol Rev* **81**(1): 153-208.

Tanner, N.K. and Linder, P. 2001. DExD/H box RNA helicases: from generic motors to specific dissociation functions. *Mol Cell* **8**(2): 251-262.

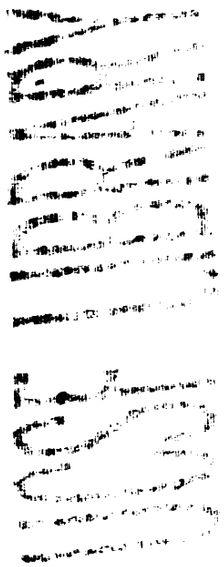

Tarn, W.Y., Lee, K.R., and Cheng, S.C. 1993. Yeast precursor mRNA processing protein PRP19 associates with the spliceosome concomitant with or just after dissociation of U4 small nuclear RNA. *Proc Natl Acad Sci U S A* **90**(22): 10821-10825.

Tsai, W.Y., Chow, Y.T., Chen, H.R., Huang, K.T., Hong, R.I., Jan, S.P., Kuo, N.Y., Tsao, T.Y., Chen, C.H., and Cheng, S.C. 1999. Cef1p is a component of the Prp19p-associated complex and essential for pre-mRNA splicing. *J Biol Chem* **274**(14): 9455-9462.

Umen, J.G. and Guthrie, C. 1995. A novel role for a U5 snRNP protein in 3' splice site selection. *Genes Dev* **9**(7): 855-868.

Urlaub, H., Hartmuth, K., Kostka, S., Grelle, G., and Luhrmann, R. 2000. A general approach for identification of RNA-protein cross-linking sites within native human spliceosomal small nuclear ribonucleoproteins (snRNPs). Analysis of RNA-protein contacts in native U1 and U4/U6.U5 snRNPs. *J Biol Chem* **275**(52): 41458-41468.

van Nues, R.W. and Beggs, J.D. 2001. Functional contacts with a range of splicing proteins suggest a central role for Brr2p in the dynamic control of the order of events in spliceosomes of Saccharomyces cerevisiae. *Genetics* **157**(4): 1451-1467.

Verma, R., Aravind, L., Oania, R., McDonald, W.H., Yates, J.R., 3rd, Koonin, E.V., and Deshaies, R.J. 2002. Role of Rpn11 metalloprotease in deubiquitination and degradation by the 26S proteasome. *Science* **298**(5593): 611-615.

Vetter, I.R. and Wittinghofer, A. 2001. The guanine nucleotide-binding switch in three dimensions. *Science* **294**(5545): 1299-1304.

Wilson, K.S. and Noller, H.F. 1998. Mapping the position of translational elongation factor EF-G in the ribosome by directed hydroxyl radical probing. *Cell* **92**(1): 131-139.

Wyatt, J.R., Sontheimer, E.J., and Steitz, J.A. 1992. Site-specific cross-linking of mammalian U5 snRNP to the 5' splice site before the first step of pre-mRNA splicing. *Genes Dev* **6**(12B): 2542-2553.

Zavialov, A.V., Buckingham, R.H., and Ehrenberg, M. 2001. A posttermination ribosomal complex is the guanine nucleotide exchange factor for peptide release factor RF3. *Cell* **107**(1): 115-124.

Zavialov, A.V., Hauryliuk, V.V., and Ehrenberg, M. 2005. Guanine-nucleotide exchange on ribosome-bound elongation factor G initiates the translocation of tRNAs. *J Biol* **4**(2): 9.

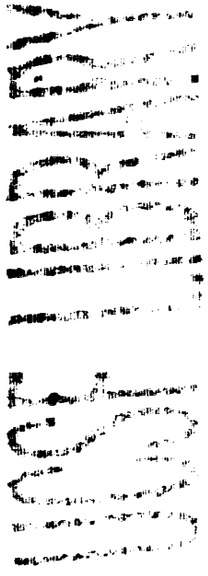

For reference

Not to be taken from the room.